

SAND81-8184
Unlimited Release
UC-62d

CEND - 389


CONCEPTUAL DESIGN SELECTION AND DEVELOPMENT OF A LATENT-HEAT THERMAL ENERGY STORAGE SUBSYSTEM FOR A SATURATED-STEAM SOLAR RECEIVER AND LOAD

Prepared for SANDIA NATIONAL LABORATORIES - LIVERMORE
Under CONTRACT No. 20-2990B
for U.S. DEPARTMENT OF ENERGY,
DIVISION OF ENERGY STORAGE SUBSYSTEMS

February 1981

When printing a copy of any digitized SAND Report, you are required to update the markings to current standards.

ADVANCED DEVELOPMENT DEPARTMENT

 **POWER
SYSTEMS**
COMBUSTION ENGINEERING, INC.

Issued by Sandia National Laboratories, operated for the United States
Department of Energy by Sandia Corporation.

NOTICE

This report was prepared as an account of work sponsored by the United States Government. Neither the United States nor the United States Department of Energy, nor any of their employees, makes any warranty, express or implied, or assumes any legal liability to responsibility for the accuracy, completeness or usefulness of any information, apparatus, product or process disclosed, or represents that its use would not infringe privately owned rights.

Printed in the United States of America
Available from
National Technical Information Service
U. S. Department of Commerce
5285 Port Royal Road
Springfield, VA 22161
Price: Printed Copy \$11.00; Microfiche \$3.00

CONCEPTUAL DESIGN SELECTION AND DEVELOPMENT OF
A LATENT-HEAT THERMAL ENERGY STORAGE SUBSYSTEM
FOR A SATURATED-STEAM SOLAR RECEIVER AND LOAD

Prepared For Sandia Laboratories, Livermore, California
 Under Contract No. 20-2990B

For The U. S. Department of Energy,
 Division of Energy Storage Systems

FEBRUARY 1981

By COMBUSTION ENGINEERING, INC.
 Advanced Development Department
 Windsor, Connecticut

 COMSTOCK & WESCOTT, INC.
 Cambridge, Massachusetts

NOTICE

This report was prepared as an account of work sponsored by the United States Government. Neither the United States nor the United States Department of Energy, nor any of their employees, makes any warranty, express or implied, or assumes any legal liability to responsibility for the accuracy, completeness or usefulness of any information, apparatus, product or process disclosed, or represents that its use would not infringe privately owned rights.

PATENT STATUS

This document, transmitted in advance of patent clearance, is made available in confidence solely for use in performance of work under contracts with the U.S. Department of Energy (DOE). It is not to be published nor its contents otherwise disseminated or used for purposes other than specified above before patent approval for such release or use has been secured from the cognizant assigned DOE patent group.

CONTRIBUTIONS TO THIS REPORT WERE MADE BY:

Ronald J. Calkins (C-E)
Gerald F. di Lauro (C-E)
Kurt W. Fretz (C-E)
Douglas N. Majors (C-E)
Devendra D. Mehta (C-E)
Richard C. Noyes (C-E)
Richard E. Rice (C&W)

The efforts by Barry M. Cohen for modifications on computer program TESST for the current application are gratefully acknowledged.

The diligent efforts by Carol Morrison in coordinating, assembling, and editing this report are also gratefully acknowledged.

TABLE OF CONTENTS

	<u>Page No.</u>
Title Page	i
Table of Contents	iv
List of Tables	vii
List of Figures	ix
List of Sketches and Drawings	xi
1.0 Summary	1
2.0 Introduction	6
3.0 Analysis of Alternative Concepts	8
3.1 Introduction	8
3.2 Alternate Phase Change Media	13
3.3 Survey of Thermal Energy Storage Concepts	23
3.4 Candidate TES Concepts	32
3.4.1 Passive Tube Intensive Concept	32
3.4.2 Heat Transfer Enhancement of Tube Intensive System	37
3.4.3 Chubb Boiler Tank Concept	42
3.4.4 Macroencapsulation of PCM Concept	47
3.4.5 Microencapsulation of PCM in a Porous Carrier	50
3.4.6 Direct Contact Systems with PCM Drop Intermediate Heat Exchanger	55
3.4.7 Direct Contact Systems Using an Oil Intermediate Heat Transfer Fluid	59
3.4.8 Mechanical Scraper: Rotating Drum	63
3.4.9 Mechanical Scraper: Rotating Auger	66
3.5 Rock Bed with Oil Intermediate	69
4.0 Selection of Preferred System	74
4.1 Selection Process	74
4.2 Selection Criteria	76
4.3 Unit Cost Data	78
4.4 Selection Results	82

	<u>Page No.</u>
5.0 Conceptual Design and Cost/Performance Estimates	93
5.1 Introduction	93
5.2 Subsystem Requirements	93
5.3 Major Configuration Choices	94
5.3.1 Modularization	94
5.3.2 Tank Design	97
5.3.3 Heat Transfer Enhancement	98
5.4 Design Description	101
5.4.1 TES Module	102
5.4.2 Instrumentation and Controls	103
5.5 Operational Characteristics	108
5.5.1 Charge/Discharge Operation	108
5.5.2 Storage Losses	114
5.5.3 Hydraulics	116
5.5.4 Maintenance	121
5.5.5 Safety	122
5.6 Cost Estimate	123
5.7 Evaluation of Final Design and Comparison with Oil/Rock Storage	126
5.7.1 Discussion of the Final Design	126
5.7.2 Comparison with the Oil/Rock System	130
6.0 Assessment of Commercial Scale TES	134
6.1 Potential Improvements	134
6.1.1 Performance Improvements	134
6.1.2 Large Field-Erected Units	135
6.1.3 Cost Improvements	136
6.1.4 Scaling	138
6.2 Potential Limitations	140
7.0 Application to Alternate Operating Conditions	144
7.1 Higher Temperatures	144
7.2 Secondary Fluid Charging	149

	<u>Page No.</u>
8.0 Development	154
8.1 Materials Testing	154
8.2 Heat Transfer Testing	155
8.3 Development of Performance Prediction Methods	155
References*	157
Glossary	162
Appendices	
I. Sketches, Drawings, and Final Design Characteristics	163
II. Phase Change Materials	175
III. A Simplified Procedure for Preliminary Sizing of the Tube Intensive TES Heat Transfer Surface	178
IV. A Preliminary Optimization of the Tube Intensive Concept	183
V. Computer Program TESST	196
VI. Heat Transfer Enhancement	199
VII. Preliminary Sizing of the Chubb Boiler Tank	233
VIII. Preliminary Sizing of Macroencapsulation of PCM Concept	239
IX. Direct Contact Systems Using PCM-Drop Intermediate Heat Exchanger	241
X. Direct Contact Systems Using an Intermediate Heat Transfer Fluid	261
XI. Mechanical Scraper Systems	271
XII. Oil/Rock Sensible Heat Storage Benchmark	276

* References appear in the text as underlined numbers in parentheses:
(3-7).

LIST OF TABLES

	<u>Page No.</u>	
3.1-1	Design Requirements	9
3.3-1	Listing of PCM-TES Concepts	25
3.3-2	The Most Promising PCM-TES Concepts	31
3.4.1-1	Major Components of the Tube Intensive Concept	35
3.4.1-2	Advantages, Disadvantages, and Design Uncertainties of the Tube Intensive Concept	36
3.4.3-1	Major Components of the Chubb Boiler Tank Concept	43
3.4.3-2	Advantages, Disadvantages, and Design Uncertainties of the Chubb Boiler Tank Concept	45
3.4.4-1	Major Components of the Macroencapsulation Concept	48
3.4.4-2	Advantages, Disadvantages, and Design Uncertainties of the Macroencapsulation Concept	49
3.4.6-1	Characteristics of PCM Drop System Using Liquid Metal and Oil as Heat Transfer Fluids	58
3.4.7-1	Characteristics of Direct Contact Systems Using Biphenyl as Intermediate Heat Transfer Fluid	62
3.4.8-1	Major Component Design Data, Mechanical Scraper-Rotating Drum Concept	64
3.4.9.1	Major Components Design Data, Mechanical Scraper-Rotating Auger Concept	67
3.5-1	Oil/Rock Storage System Component Description	71
4-1	Selection Criteria	77
4.3-1	Unit Cost Data for Concept Cost Estimates	79
4.4-1	Designs Cost Summaries of the Tube Intensive Concepts	83
4.4-2	Designs Cost Summaries of the Encapsulation Concepts	85
4.4-3(a)	Designs Cost Summaries for Direct Contact Heat Exchange PCM Drop Concepts	86
4.4-3(b)	Designs Cost Summaries for Direct Contact Heat Exchange Oil Intermediary	87
4.4-4	Designs Cost Summaries of Mechanical Scraper Concepts	89
4.4-5	Designs Cost Summaries of Oil/Rock Benchmark	90

		<u>Page No.</u>
4.4-6	Final Concept Selection	91
5.6-1	Thermal Energy Storage System Budgetary Cost Estimate	125
5.7.1-1	Cost Estimates for the Improved Design	128
5.7.2-1	Latent Heat vs. Oil/Rock Sensible Heat Storage	132
7.1-1	Approximate Total TESS Cost for Other PCM	148

TABLES IN APPENDICES

I-1	Final Design Characteristics	173
VI-1	Characteristics of Heat Transfer Enhancement Methods at the Design Point	204
VI-2	Results of Sizing Calculations for Double Finned Tubes	208
VI-3	Summary of Results - Channel Concept	212
VII-1	Preliminary Tank Sizing	236
IX-1	Properties of Pb-Bi Eutectic Alloy and Biphenyl at 500°F	242
IX-2	Pb-Bi - PCM Drop Heat Exchanger Summary	248
IX-3	Oil - PCM Drop Heat Exchanger Summary	249
IX-4	Tank Design for PCM Drop Concepts	254
IX-5	Discharge Heat Exchanger Characteristics for PCM Drop Systems	259
IX-6	Heat Transfer Fluid Inventory	260
X-1	Properties of Biphenyl at 500°F	267
XII-1	Oil/Rock Design Data	279
XII-2	Heat Exchanger and Storage Volume Size as a Function of Pinch Point	280
XII-3	Oil/Rock Containment Tank	281

LIST OF FIGURES

	<u>Page No.</u>	
3.1-1	Daily Duty Cycle	10
3.1-2	Basic Subsystem Configuration	11
3.2-1	Modified Phase Diagram - NaOH·NaNO ₃	18
3.4.2-1	Heat Transfer Enhancement Extended Surface Concept	39
3.4.3-1	Vapor Pressures of Biphenyl Water Mixtures	46
3.4.5-1	Porous PCM Carrier Fluid Bed Heat Exchanger System	51
3.4.5-2	Fluidized Bed Heat Exchanger	52
3.5-1	Oil/Rock Thermal Storage System	70
3.5-2	Oil/Steam, Shell and Tube Heat Exchanger Temperature Profile	72
5.3.3-1	Reference Heat Transfer Enhancement Concept	100
5.4.2-1	Control Concept for Tube Intensive TES Module	105
5.5.1-1	Variation of Charge/Discharge Flow Rate with Time	110
5.5.1-2	Variation of Inlet/Outlet, Water/Steam Temperature with Time	111
5.5.1-3	Vertical Temperature Profile of Storage Medium	112
5.5.3-1	A Typical Flow Instability Region in Two-Phase Flow System	117
5.5.3-2	Static Flow Stability Curve	120
6.1-1	830 MWh Field-Erected Thermal Storage Unit	137
7.1-1	Candidate PCMs for Range 200-400°C	146
7.2-1	System Options for Secondary Fluid Charging	150
7.2-2	Dual Coil Arrangement - Secondary Fluid Charging	152
III-1	Required Heat Transfer Length and Area as Function of Tube O.D.	180
IV-1	Schematic Explanation of Terms Used in TES Optimization	184
IV-2	Variation of Total Solar Energy Input with Amount of PCM	187
IV-3	Variation of Total Solar Energy Input with Number of Tubes	188
IV-4	Variation of Total Cost of Major Components with Charging Capacity and Amount of PCM	189

		<u>Page No.</u>
IV-5	Variation of Total Cost of Major Components with Charging Capacity and Number of Tubes	190
IV-6	Variation of Figure of Merit (FOM) with Amount of PCM	191
IV-7	Variation of Figure of Merit (FOM) with Number of Tubes	192
IV-8	Variation of Total Cost of Major Components with Figure of Merit (FOM) and Amount of PCM	193
IV-9	Variation of Total Cost of Major Components with Figure of Merit (FOM) and Number of Tubes	194
VI-1	Freeze Front Progression	201
VI-2	Tube Linear Heat Rate During Discharge	202
VI-3	Effect of Tube Diameter on TES Size for Bare Tubes	207
VI-4	Reference Heat Transfer Enhancement Concept	210
VI-5	Model of Heat Transfer Enhancement Concept	211
VI-6	Alternate Enhancement Concept	215
VI-7	Example of FREEZE Model Setup	217
VI-8	Example of Different Regions in Model	218
IX-1	Direct Contact with Pb-Bi or Oil PCM Droplet Intermediate Heat Exchanger	243
IX-2	Time to Solidify PCM Drop vs. PCM Drop Diameter	250
IX-3	Heat Exchanger Volume vs. PCM Drop Diameter	251
IX-4	Two-Phase Heat Transfer Coefficient	256
X-1	Direct Contact Reflux Oil Intermediate Heat Exchanger	264
X-2	Vapor Pressure of Biphenyl	265

LIST OF SKETCHES AND DRAWINGS IN APPENDIX I

		<u>Page No.</u>
<u>Sketches:</u>		
1	TES Concept - Modified Tube Intensive SD-13780-800-003	164
2	TES Concept - Encapsulation Schemes SD-13780-800-004	165
3	TES Concept - Direct Contact, PCM Drop SD-13780-800-005	166
4	TES Concept - Direct Contact-Oil Intermediary SD-13780-800-006	167
5	TES Concept - Horizontal, Rotating Drum Mechanical Scraper SE-13780-800-002	168
6	TES Concept - Vertical, Rotating Auger Mechanical Scraper SE-13780-800-001	169

Drawings:

1	Finned Serpentine Coil Module SE-13780-800-007	170
2	Containment Tank SE-13780-800-008	171
3	System Arrangement SE-13780-800-009	172

1.0 SUMMARY

The conceptual design of a tube intensive latent heat thermal energy storage (TES) subsystem utilizing a eutectic mixture of sodium hydroxide and sodium nitrate as the phase change material (PCM) has been developed. The charging and discharging of the unit is accomplished by the same serpentine tube bundle heat exchanger in which heat transfer is augmented by aluminum channels acting as fins. Every tenth channel is made of steel to provide tube support. A tube bundle is composed of 15 rows of 15.9 mm (0.625 in) O.D. tubes 15.2 cm (6.0 in) apart. Each row is a single tube approximately 78 m (255 ft) long formed into a vertically oriented serpentine. The horizontal runs of the tube are 15.2 cm (6.0 in) apart. The aluminum channels are inserted between the horizontal runs and connect all the tube rows. This assembly is strapped together and the tubes connect to the steam and condensate headers. Five of these bundles are contained in a single rectangular tank which is nominally 4 m x 4 m x 11.6 m (13'x13'x38'). Eight tanks are required to achieve the 148 MWh capacity and 30 MW peak charge and discharge rate established for this study.

The augmented heat transfer design resulted from an analytical effort which examined the freezing of salt over the discharge process in a unit cell surrounding a heat transfer tube. The two-dimensional, finite-difference calculations were performed by computer program FREEZE written for this effort. The study included the determination of the effects of conductivity enhancement and extended heat transfer surfaces of various configurations. Tube diameter and spacing were parametrically varied to assess geometric impact. Both steel and aluminum fins were considered. The final design configuration was simulated in the FREEZE model. The spacing of the heat transfer tubes was determined by finding when the target capacity, the peak discharge heat transfer rate, and virtually complete freezing of the PCM occurred simultaneously.

Performance characteristics for the TES unit were obtained with a modified version of the computer program TESST (1) which calculates the PCM temperatures, and the charging and discharging steam temperature distribution

and pressure drop over the daily duty cycle. The effect of the fins was simulated by an enhanced value for the PCM thermal conductivity. The value was selected by matching the results from the FREEZE code. At beginning of discharge the PCM is virtually all liquid with 28°C (50°F) of superheat at the top of the unit. As discharge proceeds the salt superheat at the top begins to reduce, and the salt starts to freeze at the bottom. Towards the end of discharge the bottom of the unit is subcooled solid and the top is at the melting point of the PCM. There is thus a thermocline which provides some sensible heat storage in addition to latent heat storage.

During discharge saturated water enters the bottom of the unit, boils uphill and emerges at the top. During the early stages of discharge the unit produces steam with 45-50°C (80-90°F) of superheat and, towards the end of discharge, steam with quality as low as 88-90%. For service applications in which a high degree of superheat is undesirable, a desuperheater can be used to reduce the level of superheat using subcooled water from the process. Alternatively, some of the saturated water entering the TESS could be bypassed and mixed with the effluent, and thereby bring the temperature within the desired range.

The stability of the boiling process was examined. At various stages during the discharge process the flow through the tubes was varied from 10% to 200% of the maximum flow, and the pressure drop through the two-phase and superheat regions was calculated. The total pressure drop including friction, acceleration, and elevation components shows a positive, monotonic variation with flow rate. The Ledinegg static stability criterion was thereby easily satisfied, so flow maldistribution of the discharging steam is not expected.

A budgetary cost estimate for the final design is $\$3.878 \times 10^6$ for the sell price of the total TES island. This includes the cost of materials and fabrication of the hardware; shipping to the site (using Chattanooga, TN to Barstow, CA as representative); site preparation and foundation; tank unloading from rail cars, moving, and installation; and installing piping, insulation, and lagging. The sell price reflects standard contingency, G&A and margin mark up on the shop door costs. A total shop door cost of

$\$2.93 \times 10^6$ is indicated. The estimate does not include engineering costs, sales tax, or cost of money. It does include the material cost of the salt eutectic but not the filling of the tanks. Cost for the tank fill was not available at the completion of this effort, but it is expected to be relatively small.

Based on preliminary calculations, a bare-tube version of the final design was estimated. More than 5 times the finned-tubing length was required for the 15.9 cm (0.625") O.D. tube. The shop door cost and sell price of the tubes are $\$1.36 \times 10^6$ and $\$1.89 \times 10^6$, respectively. These are $\$2.67 \times 10^5$ and $\$3.71 \times 10^5$ more than the corresponding costs of the tubing and fins in the final design. Thus, the use of fins to augment heat transfer is a definite cost improvement.

Close examination of the final calculation results from FREEZE and TESST indicated areas of conservatism in the component sizes of the final design. Taking advantage of thermocline formed in the PCM, which yields substantial solid subcooling and liquid superheat, approximately 4.5×10^5 kg (100×10^6 lb) of PCM can be saved. This reduces the number of containment tanks and the associated shipping costs. The heat transfer length is largely the same as estimated by the results of FREEZE; however, the spacing must be reduced because of the small volume of PCM. Savings in the amount of fins and tube bundle supports are realized. Additional savings can be obtained by increasing the fin spacing to 2.5 cm (1.0"). The reduced heat flux necessitates a 12% increase in tube length, but this increase is far outweighed by the reduced cost of the fins. These design improvements can reduce the shop door costs and sell price of the reference final design by as much as $\$5.31 \times 10^5$ and $\$8.35 \times 10^5$, respectively.

The main objective of this study is to develop a latent heat TESS which shows a cost advantage over the oil/rock sensible heat storage. For comparison during the selection process, an oil/rock benchmark was developed in which the major components were sized and costed. These costs amounted to $\$2.10 \times 10^6$ to $\$2.46 \times 10^6$ for volume utilization factors in the range of 80% to 60%, respectively. A 3½% loss of oil per year was estimated for the service condition under consideration. In addition, foundation costs

were scaled based on the latent heat cost estimate for a foundation design like that of the Barstow plant. The sum of the component costs and capitalized operation and maintenance costs is between $\$2.38 \times 10^6$ to $\$2.81 \times 10^6$ for the range of utilization factor values. In order to compare the latent heat TESS to the oil/rock system, the shop door cost of the major components (containment tanks, PCM, tubes and fins, and foundation) was determined. For the reference design, this is $\$2.34 \times 10^6$; and $\$1.85 \times 10^6$, for the improved design. The shop door cost of the improved design is 22-34% less than the corresponding cost of the oil/rock sensible heat TES.

The passive tube-intensive concept was selected from a large variety of candidate concepts. Selection criteria based on costs for the major components, and the state-of-the-art and reliability of the unit were established. The most promising concepts in the literature were roughly sized, and costs estimated. The designs considered were: (1) the tube-intensive concept with and without conductivity enhancement; (2) macro-encapsulation of the PCM with direct charging and discharging by steam, and indirect charging and discharging using oil as an intermediate (Chubb concept); (3) direct contact heat exchange using oil (e.g., biphenyl) or liquid metal (Pb·Bi) as the intermediary fluid between discharging steam and the PCM; and (4) mechanical devices to scrape the solid PCM from the heat transfer surface during discharge. An oil/rock sensible heat TESS was established for benchmark comparisons.

The encapsulation concepts were immediately eliminated due to high component costs. The Chubb boiler tank had an estimated cost of $\$3.5 \times 10^6$ to $\$6.1 \times 10^6$. This was high, compared to the tube intensive concept cost estimate $\$2.0 \times 10^6$ to $\$2.5 \times 10^6$, and the oil/rock system estimate, $\$2.1 \times 10^6$ to $\$2.5 \times 10^6$. The direct charging/discharging macroencapsulation concept required costly pressure vessels and had an estimated cost between $\$11.6 \times 10^6$ and $\$12.7 \times 10^6$. The mechanical scraper concepts were estimated to cost in the range of $\$1.8 \times 10^6$ to $\$2.4 \times 10^6$. The direct contact heat exchange concept using lead·bismuth initially showed higher cost than the oil systems. Further effort showed comparable cost in the area of $\$2.5 - \3.0×10^6 , with the oil system showing about a 15% lower cost.

Based on these costs the candidates were narrowed down to the tube intensive design, the direct contact concept and the vertical mechanical scraper. These concepts all showed comparable costs within the limits of the sizing and cost assumptions. The passive tube intensive design was selected since potential for cost improvements was still possible using augmented heat transfer methods, the design required little in the way of development program support, and it had the inherent reliability of a purely passive system.

2.0 INTRODUCTION

The effort described in this report is part of Phase I of a three-phase program. The objective of the initial phase is the development of conceptual designs of commercial scale thermal energy storage subsystems which exhibit cost/performance improvements over the existing, first-generation subsystems. The selection of a preferred concept will lead into the second phase which consists of the design, construction, testing, and evaluation of a subsystem research experiment (SRE). Upon successful completion of the SRE, the third phase, the final design, construction and implementation of a commercial TES unit, will be conducted.

2.1 Objectives

The primary objective of this effort is to develop the conceptual design of a TES subsystem utilizing latent heat storage in the mid-temperature range (200-320°C, 400-600°F) for use with water/steam cooled receivers producing saturated steam, and for the production of saturated steam for industrial process heat applications. An important aspect of this objective is that the selected concept show cost/performance advantages over the current, first-generation storage systems using oil or oil/rock sensible heat storage. For this purpose, an oil/rock system was sized on the same basis as the candidate concepts.

A secondary objective is to assess the applicability of the selected concept to other receiver steam conditions, in particular, higher charging-steam pressures and temperatures than those in the basic study. The effect of marrying the selected TES subsystem concept with an organic fluid- or silicone oil-cooled receiver also requires assessment. These assessments will enable judgements to be made on the range of TES applications, particularly in selecting a candidate retrofit service for the full scale subsystem.

2.2 Technical Approach

The approach has been to consider the wide range of concepts assembled

from the literature and new ideas that can take advantage of latent heat to store energy. Using selection criteria reflecting the objective of the study and the overall program plan, the most promising concepts were selected. A set of groundrules to size the major components of each concept was established in order to maintain the selected subsystems on comparable bases. Rough sizing and cost estimates eliminated unsuitable candidate concepts. Further evaluation of the reduced list of candidates allowed selection of the preferred concept.

A conceptual design was then developed in sufficient detail so that technical feasibility could be definitively assessed. Performance evaluation of the design was conducted. A cost estimate of the entire subsystem was made, and potential performance and cost improvements assessed. Design limitations and development activities required to support the concept were identified.

2.3 Technical Team

The effort was conducted by technical staffs at Combustion Engineering (C-E) Power Systems Division, and Comstock and Wescott (C&W). The technical manager is a senior engineer with the Advanced Development Department of C-E's Nuclear Power Systems Division. Engineering staff was drawn mostly from the Advanced Development Department. The final cost estimate was provided by the Business Development Department of the Nuclear Power Systems Division. Manufacturing engineering and cost estimating support were provided by C-E's Fossil and Nuclear Power Systems Divisions; these sources were drawn upon throughout the study.

Comstock and Wescott provided engineering service on a subcontractor basis and participated in virtually all activities. C&W has experience with latent heat storage systems used for thermal storage and for water heaters, and with the sodium hydroxide-sodium nitrate salt selected for the phase change material. This expertise was brought to bear on the problems of the design development.

3.0 ANALYSES OF ALTERNATIVE CONCEPTS

The development of the candidate concept is described in this section. The basic groundrules for making concept comparisons are set forth. A master list of all considered concepts is offered, from which the most promising were selected and developed. The major features of each of these concepts are described in this section, and the details of the design process are presented in corresponding appendices. By the nature of the multi-step selection process which is described in Section 4, these candidate concepts are developed, analyzed and evaluated to varying depths. After an initial evaluation the candidate concepts were reduced to: (1) the tube intensive concept with and without augmented heat transfer, (2) the direct contact system using an oil intermediary, and (3) the mechanical scraper system using a rotating auger. Finally, an oil/rock TES subsystem modeled on the Barstow system was sized in order to provide a benchmark representing the first generation storage system.

3.1 Introduction

The selected concepts have been sized for a specific duty cycle established for this effort: (1) a capacity of 148 MWh, (2) a maximum charge rate of 30 MW, and (3) a maximum discharge rate of 30 MW. The design requirements are listed on Table 3.1-1. A specific solar heat rate which reflects some average day for the Albuquerque, NM area was selected as a representative daily duty cycle. The heat rate curve presented in Reference (1) was scaled to a peak value of 60 MW. This is shown in Figure 3.1-1. A uniform process demand of 30 MW was imposed on the system. The charging of the storage subsystem begins when the insolation heat rate exceeds the process demands. When the insolation again falls below the demand, the storage subsystem switches to the discharge mode of operation. The total energy charged into storage with this duty cycle is the capacity specified above.

The basic system configuration and its interfaces with the receiver subsystem and the process are shown on Figure 3.1-2. When the receiver output exceeds the demand, saturated steam at 288°C (550°F) and 7.2 MPa

TABLE 3.1-1

DESIGN REQUIREMENTS

STORAGE CAPACITY	148 MWh
MAXIMUM CHARGE RATE	30 MW
CHARGING STEAM	1045 psia/550°F saturated vapor at storage inlet. Saturated liquid at storage outlet.
MAXIMUM FLOW RATE	20.1 kg/s (159600 lbm/hr)
MAXIMUM DISCHARGE RATE	30 MW
DISCHARGING STEAM	423 psia/450°F saturated vapor at storage outlet. Saturated liquid at storage inlet.
MAXIMUM FLOW RATE	16.6 kg/s (132100 lbm/hr)

Figure 3.1-1
DAILY DUTY CYCLE

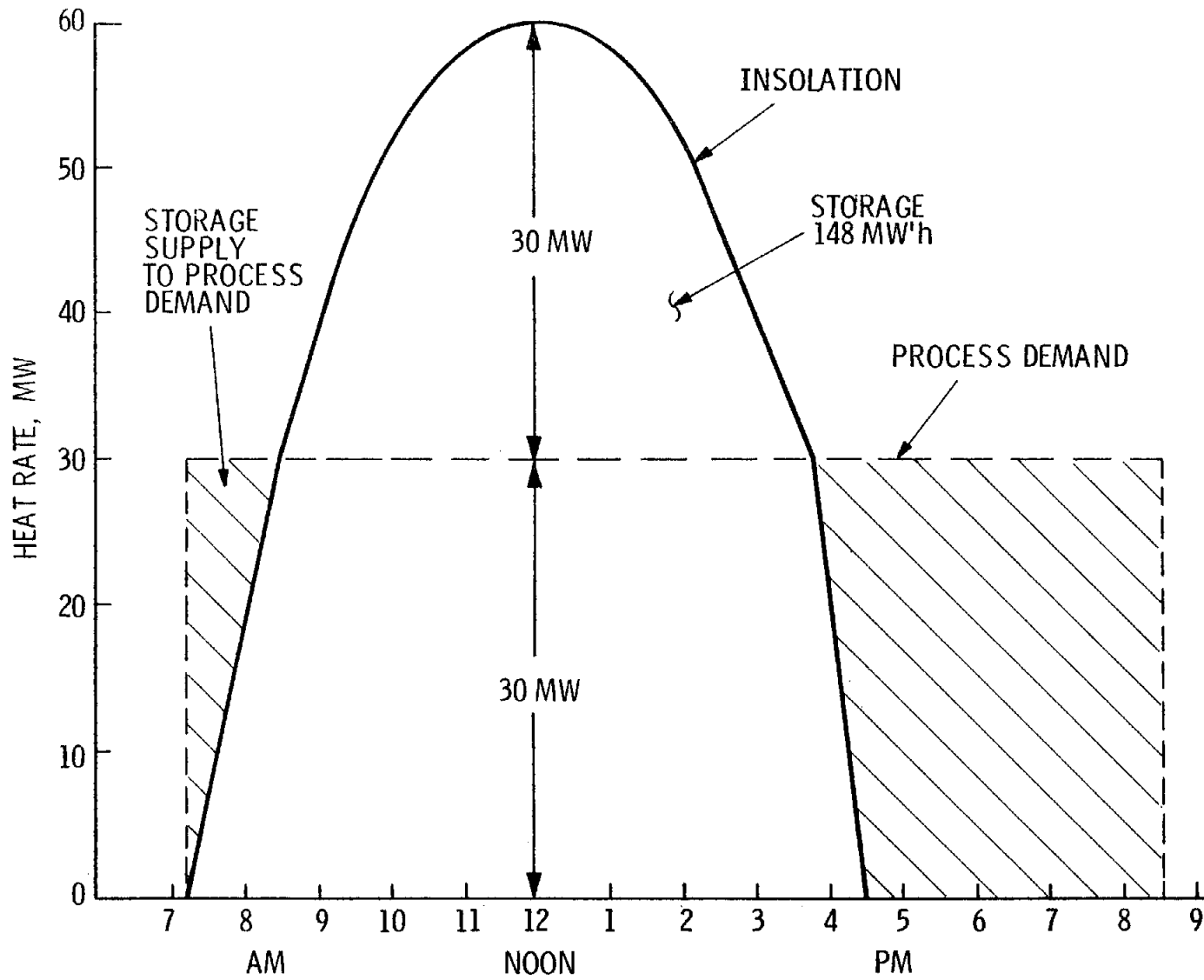
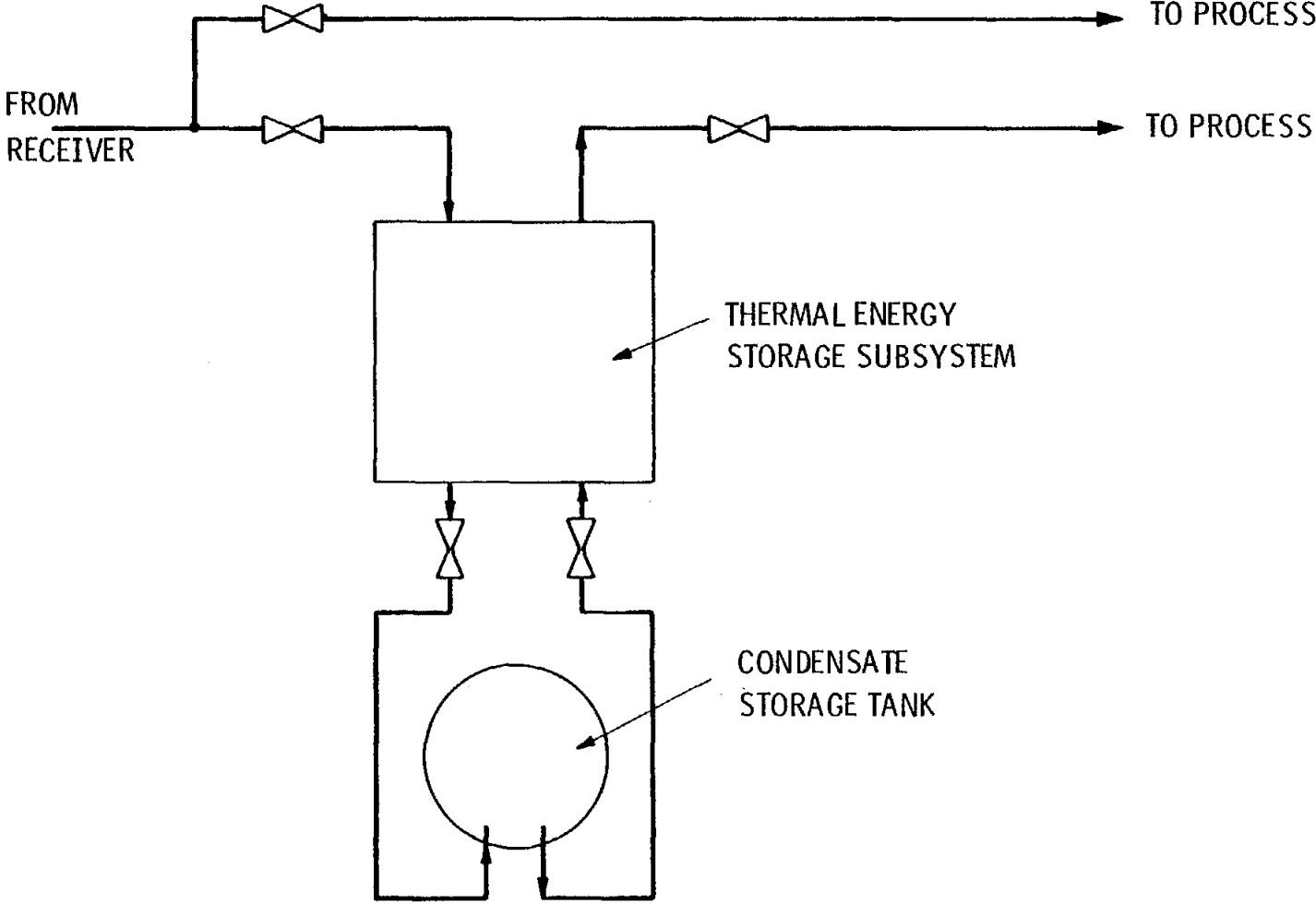


Figure 3.1-2
BASIC SUBSYSTEM CONFIGURATION



(1045 psia) is directed to the TES subsystem. The peak steam flow rate of 20.1 kg/s (15900 lbm/hr) at the peak heat rate of 30 MW over and above the process demand must be accommodated. During discharge, saturated water is provided at the inlet of the storage unit, and saturated vapor at 232°C (450°F) and 2.9 MPa (423 psia) is produced and sent to the process. The bulk of the discharge time is at the peak discharge rate, which requires a steam flow rate of 16.6 kg/s (132100 lbm/hr). Approximately 3.7 hours after the end of insolation, the demand from storage is stopped. Sufficient energy remains in storage to supplement the insolation at the start-up of the next day.

The system configuration shows a condensate storage tank in series with the latent heat TES subsystem. This is one possible system configuration in which the saturated liquid is stored in a pressure vessel. When the TES enters the discharge mode, liquid is drawn off from the accumulator, the pressure is reduced to the operating level of the unit, and energy is claimed from the storage to produce the target 232°C (450°F) saturated vapor. In this manner both the heat of vaporization and sensible heat of the charging steam are stored, and the sensible heat and a small portion of the latent heat of vaporization of the discharging steam are provided.

In order to minimize the cost of the storage tank, storage at pressure levels near that of the discharging steam should be employed. A tank peak pressure at 3.8 MPa (550 psia) is most appropriate for the storage design conditions. At full charge, saturated water at the peak pressure will fill 90% of the tank, the balance being a reasonable ullage with sufficient surface area to flash steam. During discharge, saturated water is drawn off and sent to storage through a pressure-reducing valve which reduces it to the discharge steam operating level. The water volume reduces and some of the water flashes to steam to maintain equilibrium pressure. At the end of discharge, the water has been reduced to 10% of the tank volume, and the pressure falls to approximately 3.10 MPa (450 psia). Since the charging steam has a lower heat of vaporization than the discharging steam, approximately 85% of the total charging mass is retained for ultimate discharge. The balance of the mass would be sent directly to the process for use.

The design and evaluation activities of the effort described in this report are concerned with the thermal energy storage subsystem (TESS) shown schematically on Figure 3.1-2. In order to make the design study more tractable, basic design groundrules were established. Specifically, shop-fabricated, rail-shippable containment tanks were considered for all concepts, except where this modularization does not lead to a sensible design (e.g., the Chubb Boiler Tank). In the direct-contact-heat-transfer designs, modular tanks were initially used. Later, as the design evolved, the large single tank was employed.

From the information supplied by C-E departments in the Fossil and Nuclear Power Systems Divisions, the limit on a rail-shippable unit is approximately 4 m (13 ft). The length of the unit depends on the specific site to which the unit is shipped; however a 12 m (40 ft) length will be shippable to virtually all sites. Based on this, two reference modular tanks were established: a rectangular tank 4 m x 4 m x 12 m (13'x13'x40') for unpressurized systems such as the tube intensive design; and a vessel 4 m (13') in diameter, 12 m (40') long for pressurized systems such as the macroencapsulation system.

Preliminary sizing of each concept is based largely on the data and design features presented in the literature. These designs are adapted to the current application. Each concept is developed with a sketch to scale to permit cost estimates of the major components. In addition, design problem and concerns can be identified along with advantages and disadvantages of each concept.

3.2 Alternate Phase Change Media

The phase change thermal storage media (PCM) adopted for the study were selected from a survey of available alkali metal salts, hydroxides, and their mixtures and eutectics. In order to meet the requirements of the present study and to be suitable for the subsequent phases of subsystem research experiment and commercial scale demonstration, potential PCMs must meet several criteria and, if possible, exhibit other desirable characteristics.

3.2.1 Selection Criteria

The design conditions for the study require that the TES be thermally charged with saturated steam at 288°C (550°F), and that the heat withdrawn from storage be used to generate saturated steam at 232°C (450°F). This requirement sets the fusion temperature of the PCM not only within this range, but also within a smaller range which provides temperature differences for charging and discharging. The greatest temperature differences are provided by single-component PCMs, eutectics, or congruent melting mixtures which have melting points near 260°C (500°F). Particularly in the case of concepts which employ an intermediate heat transfer fluid between the PCM and the discharge heat exchanger (HX), the melting point of the PCM should be close to the mid-temperature.

An incongruent melting PCM has been used (1) in a TESS similar in many respects to the tube intensive system discussed in Section 3.4.1 and selected for the conceptual design. In this type of TESS, the daily cycling normally leaves a small fraction of the PCM permanently solid at the bottom of the storage tank. In the cited work, chemical analysis of the PCM following repeated cycling showed segregation of the components of the PCM in a narrow zone just above the permanently solid zone. In this type of system a congruent melting PCM should be used if possible. In other systems in which the PCM is fully melted during each cycle, incongruent melting PCMs might be satisfactory if the melting range is small.

Successful commercialization of the selected concept would require large quantities of the PCM, and therefore only those materials which are presently available as, or can be easily derived from, industrial chemicals were considered as candidates. The cost analyses of the candidate TES systems of Section 3.4 have shown the PCM cost is a major element of the TESS cost. Therefore, its price is a determining factor in the practicality of the system.

In order to move confidently to the next phase of commercial development without costly and time-consuming research, the PCM should be one for

which there is a background of large scale use and experience, including containment in non-alloy steel at temperatures at least as high as those of the present study. While there is not yet any such experience in thermal storage systems, there has been extensive use of fused salts in metal heat treating and metal cleaning, and in the use of molten salts as heat transfer fluids.

The PCM must be chemically stable in contact with non-alloy steel, which must be used for containment vessels and internal structural elements; and in contact with low alloy steels, which may be used for heat exchanger elements in the steam systems. Compatibility with aluminum, which may be used in the PCM in order to enhance its thermal conductivity, is desirable.

In systems which operate at atmospheric pressure, by allowing ambient air to flow in and out of the ullage in the PCM tank, chemical stability in contact with air and atmospheric moisture is desirable to avoid the need for driers or inert cover gas systems. The PCM must be incapable of any violent chemical or heat-producing reaction with air or water, in case of an accidental spill.

The PCM must not release any environmentally harmful or toxic vapor, or thermal degradation product.

3.2.2 PCM Candidates

Candidate PCMs have been reviewed in several recently published studies (2-7). In addition, several extensive compendia of data on salts and salt eutectics are available (8-14). These were reviewed for candidate PCMs. Those which meet the criteria and whose melting points lie within a usable range of $\pm 14^{\circ}\text{C}$ ($\pm 25^{\circ}\text{F}$) of the mid-temperature between the charging and discharging saturated steam temperatures are as follows:

<u>Eutectics*</u> , mole % composition	<u>°C</u>	<u>°F</u>
4.2 NaCl - 40 NaNO ₃ - NaOH	247	477
18.5 NaNO ₃ - NaOH	258	497
15 NaBO ₂ - NaOH	260	500
45.5 Na ₂ Cr ₂ O ₇ - NaNO ₃	262	504

* No single salts were found.

Two PCMs were selected from this list, viz., the NaOH-NaNO₃ eutectic and the NaOH-NaBO₂ eutectic. Both have melting points which are very close to the midpoint of the operating temperature range. The bichromate nitrate eutectic was rejected because of price.

Nitrate Eutectic

The nitrate eutectic is within a range of compositions which have been widely used for many years in industrial metal cleaning and de-scaling operations. These are as follows (15):

Sodium hydroxide	60 to 90 weight %
Sodium nitrate	7 to 32 weight %
Sodium chloride	1.5 to 6 weight %

The operating temperatures of these baths may range from 427°C (800°F) to 538°C (1000°F), the preferred operating temperature being near 482°C (900°F). The salt is commonly contained in open carbon-steel tanks which have operating lifetimes of many years. The salt is heated by gas-fired or electric heaters. This experience demonstrates the acceptance of this salt on an industrial scale.

The constituents of the eutectic PCM are readily available industrial chemicals. The eutectic composition by weight is 68.5% NaOH and 31.5% NaNO₃. The cost of the mixture, assuming the NaOH is packed in steel drums to protect it from atmospheric moisture and carbon dioxide, is \$0.364/kg (\$0.165/lb).

No reliable data has been found on the thermophysical properties of the eutectic. However, the properties of the components are well known and are quite similar so that the properties can be taken as proportional to the mole fractions, except for the latent heat of fusion which was calculated by the Kirchoff method (4) as shown in Appendix II. If this PCM were to be used in a subscale research experiment or a commercial scale demonstration, it would be necessary first to determine the thermal and physical properties more precisely. For the purposes of this conceptual design study, the thermal conductivity, specific heat, and density of the eutectic are taken to be the same as those of "Thermkeep" (91.8% NaOH, 8% NaNO₃, 0.2% MnO₂) (1). These are listed in Appendix I.

The phase diagram for the NaOH-NaNO₃ system is shown on Figure 3.2-1 (16). The eutectic composition prepared from commercial chemicals is expected to deviate slightly from this diagram as a result of impurities, especially in the NaOH, which typically includes 2-3% of sodium chloride and sodium carbonate.

The chemical stability of the NaOH-NaNO₃ in the absence of air was investigated by Comstock & Wescott, Inc., during the development of the Thermbank Electric Water Heater, which uses "Thermkeep", and operates at a maximum PCM temperature of 455°C (850°F), with maximum heater surface temperature of 482°C (900°F).

Tests were made at 482°C (900°F), in steel containers which were hermetically sealed to prevent entrance of air, in which the pressure was monitored. It was observed that such a system at this temperature level initially develops a subatmospheric pressure which remains stable for about 5 days, after which it rises abruptly. The rise in pressure was found to be due to the generation of ammonia, from the sequential reduction of NaNO₃ -- first to NaNO₂, then to NH₃, according to the following net reaction:

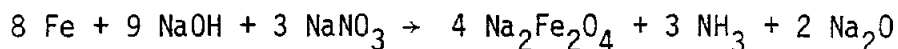
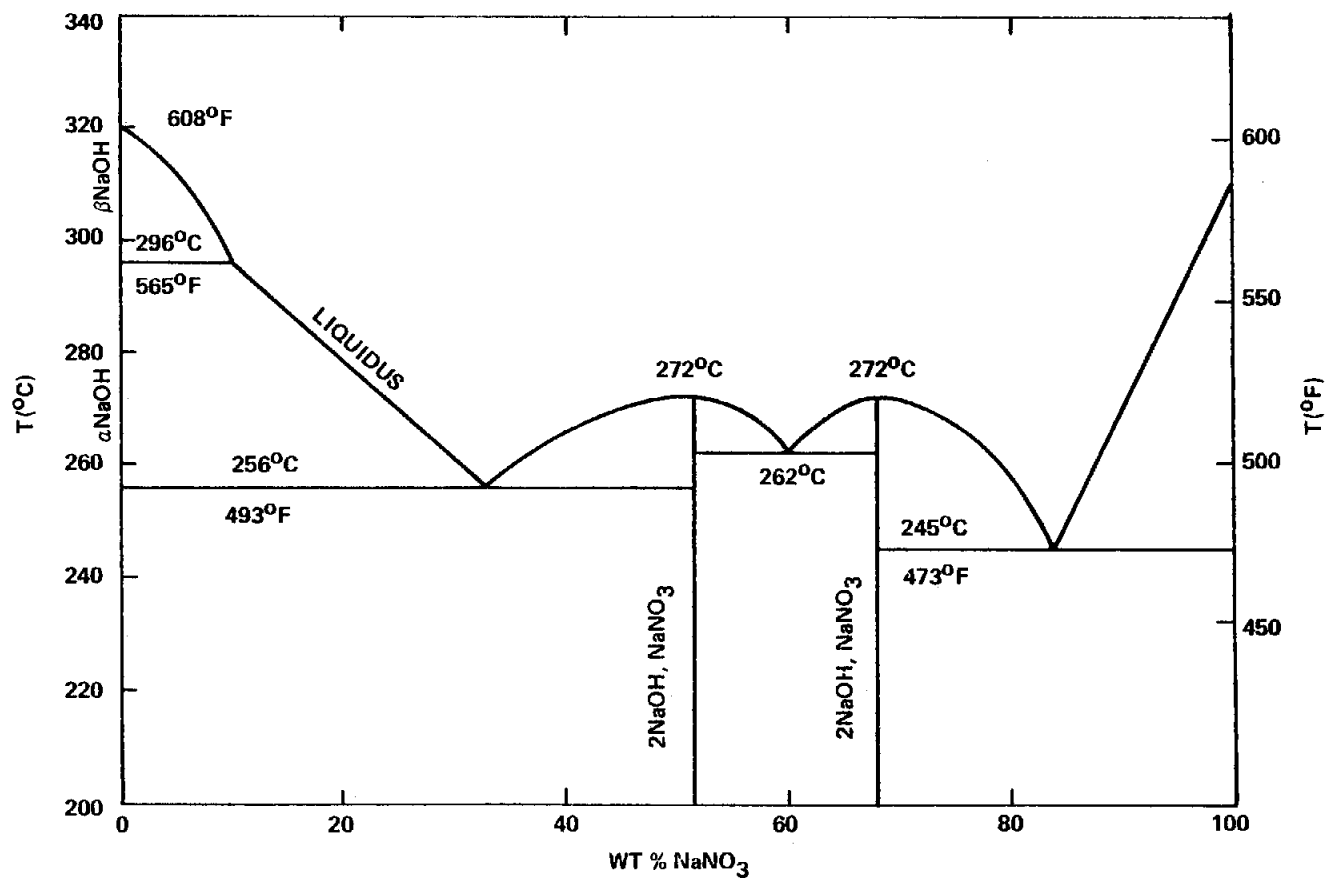
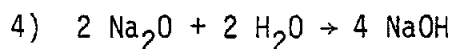
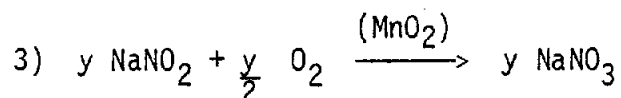
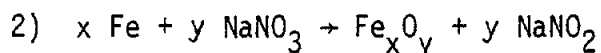
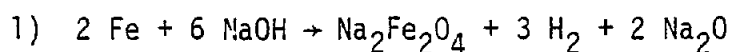


Figure 3.2-1
 MODIFIED PHASE DIAGRAM
 NaOH · NaNO₃

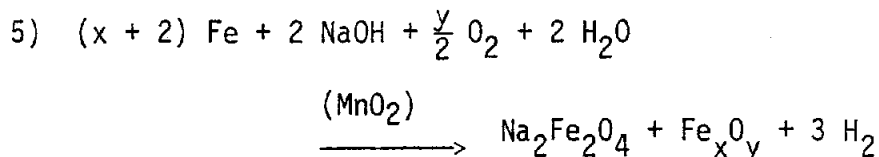


While these tests were at a substantially higher temperature than in the present case, these reactions might proceed at a rate which would be significant over the life of the equipment. Therefore, in those concepts where the system must operate in the absence of air, the borate eutectic is recommended.

In the presence of air admitted to the PCM tank through a breather pipe open to the atmosphere, the following reactions occur:



The net reaction is:



Eq. (1) is the "corrosion reaction." $\text{Na}_2\text{Fe}_2\text{O}_4$ is the principal corrosion product, and has been identified by x-ray diffraction tests. The presence of hydrogen has been confirmed.

Eq. (2) represents the formation of iron oxide of unidentified composition, by reduction of NaNO_3 .

Eq. (3) represents the oxidation of NaNO_2 to NaNO_3 by oxygen from the air. This reaction is catalyzed by MnO_2 .

Eq. (4) represents the reaction of the Na_2O formed by Eq. (1) with moisture introduced by the "breathing" of humid air.

Experimental work with an air-breathing subscale TES module by Comstock & Wescott, Inc. (1) at maximum temperatures of 316°C (600°F) with the 8% NaNO₃ - 92% NaOH PCM included chemical analyses of the PCM after a period of daily thermal cycling. This showed that no sodium nitrite was produced, and it was concluded that the system was chemically stable.

Corrosion rates were measured during the Thermbank Water Heater development referred to above. It was found that the corrosion penetration rate of the 8% NaNO₃ mixture at 482°C (900°F) on steel test samples, and on steel-sheathed heater surfaces of prototype water heaters, was less than 0.025 mm/year (0.001 inches/year). This indicates that corrosion rates in the present temperature range of 232 to 288°C (450 to 550°F) will be insignificant.

This study also included corrosion rate tests on a number of different materials, including aluminum, which was found to be even more resistant to corrosion in the 92% hydroxide, 8% nitrate mixture than steel, at 482°C (900°F). This is attributed to the fact that the anhydrous mixture is oxidizing and maintains an oxide film on the metal surface.

Metaborate Eutectic

The eutectic of sodium metaborate, NaBO₂, with sodium hydroxide, NaOH, has the following composition:

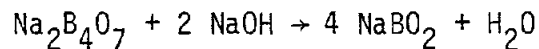
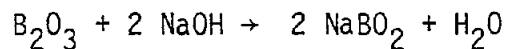
NaOH	85% mole %; 77.5 weight %
NaBO ₂	15 mole %; 22.5 weight %

The eutectic melting point (8) is 260°C (500°F). No technical literature on the thermophysical properties of the eutectic has been found. Data are also lacking on the specific heat of liquid NaBO₂, needed for calculation of the latent heat of fusion of the eutectic by the Kirchoff method, as was done for the nitrate eutectic. The latent heat of fusion of NaBO₂ is 551 kJ/kg (237 Btu/lb) at 966°C (1770°F) as compared with NaNO₃, whose latent heat of fusion is 181 kJ/kg (78 Btu/lb) at 307°C (585°F). In the absence of data, the latent heat of the metaborate

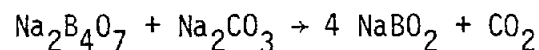
eutectic was assumed to be 274 kJ/kg (118 Btu/lb), the same as that of the nitrate eutectic. The thermal conductivity, specific heat, and density were also taken to be the same as the nitrate eutectic. Sodium metaborate is chemically very stable, having a melting point of 966°C (1770°F) and a boiling point of 1130°C (2060°F). It is hygroscopic at ambient temperatures and must be protected from atmospheric moisture, as does sodium hydroxide.

Sodium metaborate is not produced in commercial quantities in anhydrous form, but is available as a hydrate, $\text{Na}_2\text{B}_2\text{O}_4 \cdot 4 \text{H}_2\text{O}$, which is not hygroscopic, and which can be dehydrated by heating to 982°C (1800°F). It can also be produced by heating a saturated solution of the hydrate under moderate pressure at 105°C.

The metaborate can also be produced from anhydrous boric acid or from anhydrous borax by reaction with sodium hydroxide:



Another reaction which might be used is that of anhydrous borax with sodium carbonate:



Boric acid, borax, and the hydrated forms of sodium metaborate are industrial chemicals, available from United States Borax and Chemical Corporation. For purposes of the present study, a price of \$0.639/kg (\$0.29/lb) was used, which was derived from the cost of NaBO_2 as $\text{Na}_2\text{B}_2\text{O}_4 \cdot 4 \text{H}_2\text{O}$, plus an estimated cost for conversion (See Appendix II).

The metaborate eutectic was used in the analysis of those concepts with anaerobic conditions in which the nitrate eutectic is chemically unstable. It is believed that the metaborate would be stable under these

conditions. However, no prior experience in such an application was found in a literature search.

If a concept requiring the metaborate eutectic were to be selected for development, a preliminary development program would be necessary. This would include determination of the most cost-effective method of preparation of the anhydrous metaborate and the cost of product, a determination of the thermal and physical properties of the eutectic, and a study of the compatibility of the PCM with metals used for containment and with any intermediate heat transfer fluid with which it might be in contact.

3.2.3 Utilization Factor of PCM

The utilization factor (UF) of the PCM is the fraction from which the latent heat (and in some cases, sensible heat) is charged and discharged during cycling. In the direct contact and mechanical scraper concepts discussed in Section 3.4, a single tank may be used to hold both liquid and solid PCM. In some cases, the solid PCM formed near the top falls through the liquid to the charging heat exchanger at the bottom. The solid is in the form of particles which may have different shapes and sizes depending on the process. The particles form a porous mass, the interstices of which are filled with liquid. When solid reaches the top, this interstitial liquid cannot be brought into contact with the discharge heat exchanger or the intermediate heat transfer fluid and is a non-utilized fraction of the PCM.

No information has been found for the porosity of PCM particles falling through liquid. There is, however, information on the porosity of metallic and other powders (17):

... Equal-size spheres, most densely packed, have porosity of 26%.

... Powders of random sizes randomly packed have porosity of about 33%.

... Fine particles have greater porosity, e.g., 50%.

... Flake-shaped particles such as mica may have porosities over 90%.

If the above applies to the PCM, the UF of a system might vary from 0.75 as a maximum to as low as 0.1, depending on the shape and size of the solid PCM particles.

The shape and size of the solid PCM particles formed at the oil-PCM interface in the direct contact system described in Section 3.4.7 and in the scraper systems of Sections 3.4.8 and 3.4.9, cannot be reliably predicted. It is thought that the UF could be no greater than .65, but if the particles should be flake- or needle-shaped, it might be as low as .10. A utilization factor of 0.58 was estimated as reasonable for the direct contact systems.

In systems in which the solid PCM is separated from a liquid heat transfer fluid and stored in a separate tank, such as the PCM drop direct contact systems of Section 3.4.6, the UF is not affected by the porosity of the solid PCM drops and it can be as high as 0.95.

This uncertainty in the UF introduces an uncertainty in the cost estimate of the oil-PCM direct contact concept because the PCM cost is a large part of the total.

The UF must be studied experimentally as a part of any on-going development program of systems such as those described in Sections 3.4.7, 3.4.8 and 3.4.9.

3.3 Survey of Thermal Energy Storage Concepts

A broad-based literature survey (1, 3-7, 18-33) of TESS using the latent heat of fusion was conducted. The review of existing literature and further brainstorming of C-E/C&W ideas resulted in a comprehensive catalogue of latent heat TES systems.

The listing of more than forty PCM-TES concepts is shown in Table 3.3-1. The concepts were divided in the following major categories.

- I. Tube-Intensive (Passive)
- II. Encapsulation
- III. Direct Contact
- IV. Active Heat Exchange (Mechanical)
- V. Active Heat Exchange (Hydraulic)
- VI. Use of PCM Physical Property

The results of the published studies and analyses were qualitatively normalized to facilitate preliminary comparisons of the concepts. Along with the listing, Table 3.3-1 also shows technical status and some remarks for each concept. The technical status reflects the required effort to bring the concept to the commercial stage. Very few of the concepts are at the engineering state of development; in fact, more than half are still at the conceptual development stage.

Concepts which promise to achieve the objectives within the overall program schedule were selected. The initial selections were judged primarily on current operating experience, and concept risk and uncertainty. The selection criteria are discussed in more detail in Section 4.0. The concepts still requiring large developmental work were eliminated. Based on this initial selection, the list was reduced to nine most promising concepts as shown in Table 3.3-2.

Among the on-going development programs, the two concepts under development at Honeywell (the reflux boiler and the coated-tube-and-shell-flow-by system) were dropped due to disappointing test results. The rolling cylinders concept under development at GE was dropped since it seemed to be oriented towards the low temperature Glauber's salt application. Although the concept using the microencapsulation of the PCM in a porous carrier (e.g. Alumina, Zeolite) is still in the conceptual design state of development, it was selected since initial reflections indicated a good potential.

TABLE 3.3-1 LISTING OF PCM - TES CONCEPTS

	DESCRIPTION	DEVELOPING ORGANIZATION	TECHNICAL STATUS	REMARKS
I	<u>TUBE INTENSIVE - PASSIVE</u>			
	*1. COILED TUBE - REFERENCE	C&W	ED	<ul style="list-style-type: none"> ● EXTENSIVE EXPERIENCE ● EASY OPERATION AND MAINTENANCE
	*2. STRAIGHT /U TUBE		ED	<ul style="list-style-type: none"> ● TOO MANY TUBES ● EASY FABRICATION ● NEEDS DETAILED COMPARISON WITH COILED TUBE
	3. PCM CONDUCTIVITY	IGT	ED	<ul style="list-style-type: none"> ● SELECTION BASED ON COST OPTIMIZATION
	4. COATED TUBES TO AVOID OR DELAY PCM ADHESION TO TUBE	H	ED	<ul style="list-style-type: none"> ● LIMITED TESTS ARE DISCOURAGING
	5. HEAT PIPE CONDUCTOR BETWEEN CHARGING FLUID AND PCM	G	CD	<ul style="list-style-type: none"> ● HEAT PIPE MEDIA NOT FOUND ● ONLY MARGINAL PERFORMANCE IMPROVEMENT EXPECTED

KEY:

ED - Engineering Development, 2-3 yrs. (near term)
 AD - Advanced Development, 3-5 yrs.
 CD - Conceptual Development, 7-5 yrs.

C-E Combustion Engineering
 C&W Comstock & Wescott
 G Grumman
 GE General Electric
 H Honeywell

IGT Inst. of Gas Technology
 NRL Naval Research Laboratory
 SERI Solar Energy Res. Inst.
 SLL Sandia-Livermore Lab.

* SELECTED CONCEPTS

TABLE 3.3-1 LISTING OF PCM - TES CONCEPTS

	DESCRIPTION	DEVELOPING ORGANIZATION	TECHNICAL STATUS	REMARKS
II	<p>ENCAPSULATION (USE OF EXPENSIVE SODIUM METABORATE SALT NECESSARY)</p> <p>*1. BOILER TANK (CHUBB)</p> <p>*2. MACROENCAPSULATION - PLANK SHAPED FLEXIBLE BLOCK OF PCM</p> <p>*3. MICROENCAPSULATION OF PCM IN A POROUS CARRIER MATERIAL</p> <p>4. MICROENCAPSULATION - FLUIDIZED ENCAPSULATED PCM IN FLOW</p>	<p>NRL</p> <p>G</p> <p>C&W</p> <p>G</p>	<p>AD</p> <p>CD</p> <p>CD</p> <p>CD</p>	<ul style="list-style-type: none"> ● 4 PINCH POINTS ● PRESSURE VESSEL TANK ● DEMONSTRATION TEST IN PROGRESS ● PRESSURE VESSEL REQUIRED ● NO KNOWN TECHNIQUE ● PRESSURE VESSEL REQUIRED

TABLE 3.3-1 LISTING OF PCM - TES CONCEPTS

	DESCRIPTION	DEVELOPING ORGANIZATION	TECHNICAL STATUS	REMARKS
III	<u>DIRECT CONTACT</u> (NO SALT AVAILABLE FOR DIRECT CONTACT WITH STEAM)			
	*1. INTERMEDIATE LIQUID METAL (Pb-Bi) LOOP	G	AD	<ul style="list-style-type: none"> ● DEMONSTRATION TEST IN PROGRESS ● EXPENSIVE LIQUID METAL LOOP
	2. REFLUX BOILER	H	AD	<ul style="list-style-type: none"> ● DISAPPOINTING TEST RESULTS ● IMMISCIBLE STEAM/PCM SALT NOT YET FOUND ● PRESSURE VESSEL REQUIRED ● IRREVERSIBLE CHEMICAL REACTIONS AT LONG TERM
	*3. TERPHENYL/SALT (IMMISCIBLE SALTS)	C&W	CD	<ul style="list-style-type: none"> ● LIMITED FEASIBILITY STUDY ● LONG TERM STABILITY DATA NOT AVAILABLE ● TEMPERATURE LIMITATIONS OF TERPHENYL
	4. SUSPENDED PCM PARTICLES IN FLOW	SERI	CD	<ul style="list-style-type: none"> ● LIMITED TEST CONDUCTED
	5. SHOT TOWER (LEAD SHOT MANUFACTURING)	SLL	CD	<ul style="list-style-type: none"> ● NO INDUSTRIAL EXPERIENCE RELATED TO STORAGE
	6. PRILLING TOWER CRYSTALLIZATION (SPRAY FREEZING)	H	AD	<ul style="list-style-type: none"> ● CHEMICAL INDUSTRY EXPERIENCE

TABLE 3.3-1 LISTING OF PCM - TES CONCEPTS

	DESCRIPTION	DEVELOPING ORGANIZATION	TECHNICAL STATUS	REMARKS
IV	<u>ACTIVE HEAT EXCHANGE - MECHANICAL</u>			
	1. SCRAPERS - FIXED WITH ROTATING *DRUM	G	AD	<ul style="list-style-type: none"> ● DEMONSTRATION TEST CONSTRUCTED ● COMPLICATED HIGH PRESSURE ROTATING COUPLING
	*AUGER INTERNAL	C-E	CD AD	<ul style="list-style-type: none"> ● ONLY INCONGRUENT SALTS ● PRESSURE VESSEL REQUIRED ● REQUIRES EXCESSIVE POWER ● COMPLEX MOVING PART SYSTEM
	EXTERNAL		AD	<ul style="list-style-type: none"> ● FAST SCRAPING NECESSARY
	TRANSLATING	G	AD	<ul style="list-style-type: none"> ● HEAT EXCHANGE SURFACE MAY BE REDUCED BY FACTOR OF 5 to 7.
	2. ROLLING CYLINDER	GE	ED	<ul style="list-style-type: none"> ● MAY BE LIMITED TO GLAUBER'S SALT
	3. AGITATION	H	AD	<ul style="list-style-type: none"> ● ADDITIONAL REQUIREMENT OF COATED TUBES AND INCONGRUENT PCM

TABLE 3.3-1 LISTING OF PCM - TES CONCEPTS

	DESCRIPTION	DEVELOPING ORGANIZATION	TECHNICAL STATUS	REMARKS
IV	4. VIBRATION - PNEUMATIC HAMMER SHAKER TUBE TORSION	H G G	AD CD CD	<ul style="list-style-type: none"> ● LIMITED EXPERIENCE ● NO EXPERIENCE ● NO EXPERIENCE
	5. ULTRASONICS - AS IN CLEANING		AD	<ul style="list-style-type: none"> ● EXCESSIVE POWER REQUIREMENT PARTICULARLY FOR LARGE UNITS
	6. MECHANICAL FLEXING OF TUBES	H	CD	<ul style="list-style-type: none"> ● NO INDUSTRIAL EXPERIENCE
	7. TUMBLING ABRASIVE SOLIDS	H	CD	<ul style="list-style-type: none"> ● NO INDUSTRIAL EXPERIENCE
	8. FLUIDIZED BED ABRASION ON TUBES	H	CD	<ul style="list-style-type: none"> ● NO INDUSTRIAL EXPERIENCE
V	<u>ACTIVE HEAT EXCHANGE - HYDRAULIC</u>			
	1. COATED TUBE AND SHELL FLOWBY SYSTEM	H	AD	<ul style="list-style-type: none"> ● LIMITED LABORATORY TEST SHOWED NO ADVANTAGE ● SUITABLE COATING NOT YET FOUND
	2. FLOW PULSING	H	CD	<ul style="list-style-type: none"> ● LITTLE PRIOR EXPERIENCE

TABLE 3.3-1 LISTING OF PCM - TES CONCEPTS

	DESCRIPTION	DEVELOPING ORGANIZATION	TECHNICAL STATUS	REMARKS
V	3. FLOW VARIATION (STIRRER)	G	CD	● LITTLE PRIOR EXPERIENCE
	4. JET IMPINGEMENT	H	CD	● LITTLE PRIOR EXPERIENCE
	5. FREEZE - THAW (FROST FREE CYCLING)	H	ED	● EXTREMELY INEFFICIENT
	6. GAS BUBBLE TURBULATION	G	CD	● REQUIRES NON-STICK TUBES ● LABORATORY TEST SHOWED VERY LITTLE BENEFIT
VI	<u>USE OF PCM PHYSICAL PROPERTY</u>			
	1. CRYSTAL VOLUME CHANGE	H	CD	} LITTLE EXPERIENCE
	2. CRYSTAL WEAKENING ADDITIVES	H	CD	
	3. CONDUCTIVITY ENHANCING ADDITIVES	H	CD	
	4. MAGNETIC SUCEPTIBILITY	H	CD	
	5. ELECTROSTATIC SEPARATION	H	CD	
6. DELAYED NUCLEATION AND SUPER-COOLING (FOREIGN PARTICLES IN MELT)	H	CD		

TABLE 3.3-2 THE MOST PROMISING PCM - TES CONCEPTS

TYPE	CATEGORY	DESCRIPTION	DEVELOPING ORGANIZATION
PASSIVE	TUBE INTENSIVE	COILED TUBE - REFERENCE	C&W
PASSIVE	TUBE INTENSIVE	PCM CONDUCTIVITY ENHANCEMENT	
PASSIVE	ENCAPSULATION	BOILER TANK (CHUBB)	NRL
PASSIVE	ENCAPSULATION	POROUS CARRIER	C&W
PASSIVE	ENCAPSULATION	MACROENCAPSULATION	
ACTIVE	DIRECT CONTACT	INTERMEDIATE Pb - Bi LOOP	G
ACTIVE	DIRECT CONTACT	TERPHENYL/SALT (OR IMMISCIBLE SALTS)	C&W
ACTIVE	MECHANICAL	FIXED SCRAPER WITH ROTATING DRUM	G
ACTIVE	MECHANICAL	AUGER	C-E

3.4 Candidate TES Concepts

3.4.1 Passive Tube Intensive Concept

The passive tube-intensive PCM-TES concept is basically a conventional shell-and-tube heat exchanger in which the stationary PCM is allowed to freeze/melt on the outer tube surface. The charging/discharging heat transfer media may flow either in separate coils or in the single coil system (in sequence).

Comstock and Wescott has considerable operating experience of this concept, in work with media based upon anhydrous sodium-hydroxide - sodium nitrate mixtures. The specific experience worth noting includes:

- The use of a NaOH (92% wt)-NaNO₃ mixture in domestic space heating equipment (air heating), which was developed to the point of a successful two-year field test in ten homes by the Philadelphia Electric Company.
- The use of the same medium in the "Thermbank" electric water heater, which has been developed to the point of a one-year field test in five commercial locations by the Hydroelectric Power Commission of Ontario.
- The testing of a "Thermbank" water heater supplied to the NASA Lewis Research Center under Contract DEN3-105 by Comstock and Wescott, Inc.
- The development of a phase change thermal energy storage unit utilizing modified anhydrous sodium hydroxide for solar electric power generation under Contract NAS3-20615.
- A program of experimentation and analysis completing the development of a "Thermkeep" (NaOH 92%-NaNO₃) module for a large scale intermittent heat-source power generating system, under Contract DEN3-105. This also includes the development of a computer model for charging and discharging by phase-change fluids, which can be applied to the proposed conceptual design.
- Advanced development of "Thermbank" storage unit under Contract DEN3-162.

The initial design of this concept was developed using a single tube to both charge and discharge the unit in order to keep costs down. The

charging steam enters the top of the unit, condenses downhill, and emerges as saturated water. During discharge the saturated water enters the bottom of the unit, boils as it flows in a general upward direction, and emerges as saturated steam. The sodium hydroxide - sodium nitrate eutectic is employed since the unit can be vented to the atmosphere. Sketch 1 in Appendix I shows a schematic of the design which employs the rectangular tank module for a shop-fabricated, rail-shippable version of this concept. Both serpentine and helical coils are shown for the heat transfer tube configuration. The coil tube has been successfully used by C&W and an effective utilization factor of 0.8 has been found experimentally. The serpentine tube has the potential for better and more uniform distribution in the PCM with consequent improved utilization. The initial mechanical design shows a modularization of the tube bundle within the tank. The serpentine tube assembly is a nesting of eight serpentine tubes 5.1 cm (2.0") apart. Ten of the tube assemblies are headered together for ease of fabrication and maintenance. Assembly configurations that allow for drainage and removal of the tubes have been selected. The tank design is identical to the one used in the mechanical scraper concept and is discussed there. Design improvements were incorporated into this concept in the later stages and are discussed in Section 5.0.

A simplified procedure for preliminary calculation of heat transfer surface requirements is described in Appendix III. This procedure is based on a worst-case condition of the maximum discharge rate at a fully discharged storage state. The calculation model yields the total heat transfer length and surface area required. The required mass of PCM is estimated from the latent heat only, with no credit for any sensible heat storage.

The results of these calculations indicate that the required heat transfer length decreases with increasing tube diameter. However, it does not decrease as fast as the tube diameter increases, so that required heat transfer area increases with increasing tube diameter. Since preliminary costing is based on heat transfer area, the smallest tube diameter under consideration, 6.35 mm (0.25"), was selected. Similar results were obtained

by C&W from a detailed optimization study of latent heat TES (1). The successful operational experience of the C&W designs also supports this selection. The amount of PCM frozen requires a 5.1 cm (2.0") tube spacing. The results of the sizing calculations are summarized on Table 3.4-1-1.

To assess the extent to which this design can be improved, a preliminary optimization of the design concept was attempted with the computer TESST. This program, which calculates the spatial and temporal temperatures of the PCM, and the charging and discharging fluid over the daily duty cycle, is a C&W code (1) modified to handle charging by condensing steam. A series of calculations for a range in tube length and amount of PCM were performed; the details are described in Appendix IV. A relative cost optimum was selected which satisfied the performance requirements; the results are summarized on Table 3.4.1-1 as the improved design. A considerable reduction in the amount of PCM and required tube length was achieved. This is mainly due to the sensible heat storage in the liquid and solid phases that the conservative model did not reflect. In addition, towards the end of discharge, the unit produces wet steam rather than saturated steam. Auxiliary heating must be supplied in order to achieve the target design conditions. The total energy requirement is approximately 4% of the rated capacity. This is estimated to cost \$4.90 per million Btu, reflecting a cost of \$30 per barrel of oil and capitalization at 15%.

The advantages, disadvantages, and design uncertainties of the tube-intensive concept are listed on Table 3.4.1-2. This concept has a good deal of operating experience to support it. It has the inherent reliability of a purely passive device. The large number of tubes required, however, increases the probability of tube leaks and the potential for flow maldistribution due to boiling instability. The stability issue is a major concern addressed in the conceptual design described in Section 5.5.3. The reduction in the number of tubes is also a major issue addressed.

TABLE 3.4.1-1
MAJOR COMPONENTS OF THE TUBE-INTENSIVE CONCEPT

	<u>CONSERVATIVE</u>	<u>IMPROVED</u>
... PCM INVENTORY		
NaOH-NaNO ₃ Eutectic		
Latent Heat, Btu/lb	118	118
Utilization Factor	0.8	> 1.0*
Quantity, lb	5.35x10 ⁶	3.53x10 ⁶
... PCM TANK		
Modular Tanks		
Number	7.7	5.15
Cross Section, Length, ft	13x13x40	13x13x40
Thickness, in	0.25-0.50	0.25-0.50
... CHARGING/DISCHARGING HX		
U - Charging, Btu/hr·ft ² ·°F	150	150
U - Discharging	Variable	Variable
Δ T, °F	50	Variable
Surface, ft ²	96552	73304
... AUXILIARY HEATING	0	~ 4%

* With Sensible Heat

TABLE 3.4.1-2

ADVANTAGES, DISADVANTAGES, AND DESIGN UNCERTAINTIES
OF THE TUBE-INTENSIVE CONCEPT

ADVANTAGES

- EXTENSIVE EXPERIENCE WITH CONCEPT AND SALT
- COMPLETELY PASSIVE: - NO MOVING PARTS, NO SALT TRANSPORT, NO INTERMEDIATE MEDIUM
- NO TANK PRESSURIZATION
- SINGLE HEAT EXCHANGER
- POTENTIAL FOR HEAT TRANSFER ENHANCEMENT
- SENSIBLE HEAT ADVANTAGE DUE TO THERMOCLINE

DISADVANTAGES

- INCREASED PROBABILITY OF TUBE LEAKAGE
- POTENTIAL FLOW MALDISTRIBUTION DUE TO LARGE NUMBER OF PARALLEL PATHS

DESIGN UNCERTAINTIES

- LONG TERM CORROSION RATE DUE TO EFFECTS OF LEAKS
- FLOW MALDISTRIBUTION PARTICULARLY AT LOW FLOWS
- LONG TERM CYCLIC EFFECT ON NaOH-NaNO₃ MIXTURE
- CHARGING MODE HEAT TRANSFER COEFFICIENT

3.4.2 Heat Transfer Enhancement of Tube Intensive System

The initial sizing effort has indicated that approximately 12000 tubes are required for a tube-intensive TESS to satisfy the performance requirements. Cost estimates indicate that the tube bundle represents about 48% of the cost of the major components. These represent a great incentive to reduce the number of tubes and consequently tube surface area by means of heat transfer augmentation. Efficient methods must reduce the tubing required to the extent that cost savings outweigh the cost incurred by the augmentation method. A concomitant benefit is an increase in reliability obtained by a large reduction in pressure tubes and welded joints.

A study was conducted into possible methods of enhancing the heat transfer characteristics of the tube and the PCM during discharge. The latter is the design limiting condition since the solidifying layers of PCM insulate the remaining PCM from the discharge steam. High conductance paths must be provided to promote the heat interaction between the remote regions of the PCM and the tubes. Various methods of augmenting the heat transfer characteristics were considered (6,7) including enhancing the PCM conductivity and extended heat transfer surfaces.

A simple two-dimensional model was developed for this analysis and incorporated into a computer program FREEZE. FREEZE is a finite difference, time marching program which considers the freezing characteristics in a unit cell around the tube during discharge. The model includes the effects of latent heat and sensible heat contributions in the solid. Liquid superheat is precluded by the initial condition of uniform liquid at the melt temperature. Uniform conductivity enhancement and extended surfaces are possible. The FREEZE model is described in greater detail in Appendix VI.

The calculations using the FREEZE model, and the results of the calculations leading to the current evaluation are described in Appendix VI. The results from the model are the propagation of a freeze (solid-liquid

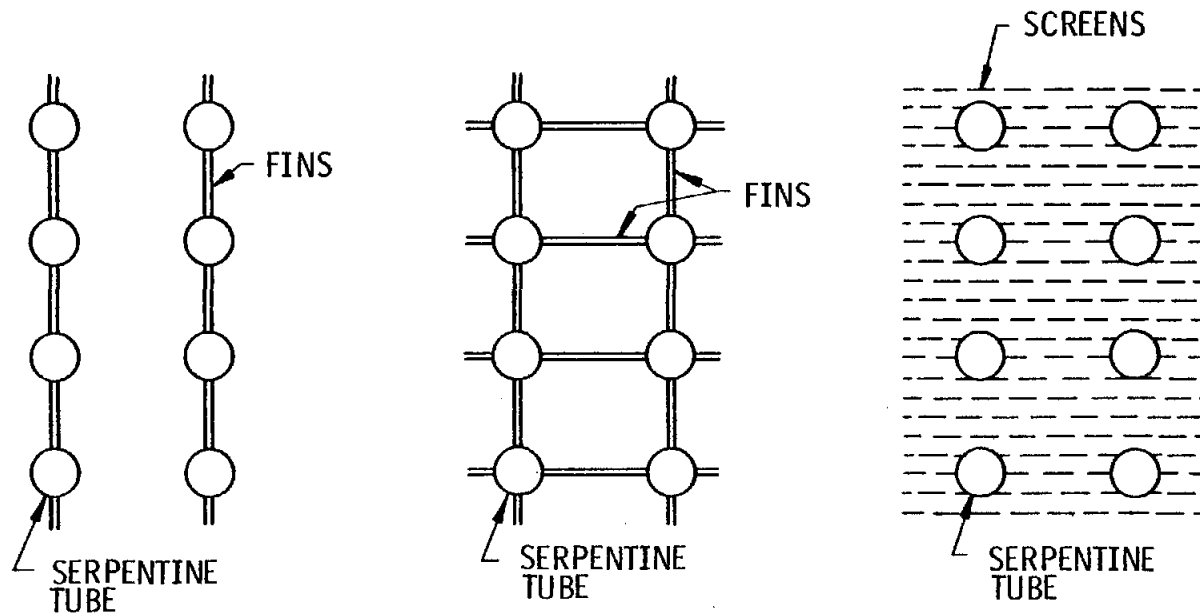
boundary) wave through the PCM, the fraction of PCM frozen and the heat rate per unit length of tube over the discharge process. A design point is established where both the target thermal capacity and discharge rate are simultaneously satisfied. This yields the required heat transfer length. The fraction of PCM frozen at the design point indicates the extent to which the tube spacing can be improved to minimize the PCM inventory. Ideally the freeze fraction should be near unity.

PCM conductivity enhancement has been considered analytically and experimentally using steel and aluminum wools and a honeycombed aluminum (Duocel) which adheres to the tube wall. The results of these efforts, reported in References (6) and (7) indicate best performance with the Duocel. Values for a uniform conductivity enhancement were obtained from Reference (7) and used in the FREEZE calculations for a 6.35 mm (0.25") O.D. tube. The results (see Appendix VI) show that 5 volume % of Duocel reduces the heat transfer requirements by a factor of 4.7 over the bare tubes. The effect of a contact resistance, equivalent to 0.24 mm (10 mils) of PCM, is relatively small: the required heat transfer area is reduced by a factor of 4.3 over the bare tubes. A major uncertainty is the fabrication cost of emplacing the aluminum matrix in the tube bundle. Also, the effect of tube leaks on the Duocel is uncertain.

A variety of fin concepts, shown on Figure 3.4.2-1, has been considered. The two- and four-fin configurations are tubes with radial fins 180° and 90° apart, respectively. The two-fin configuration is very much like the water walls used in fossil-fuel-fired boilers. Screens or thin plates have also been considered with and without the water walls. A series of calculations with FREEZE was performed for 6.35 mm (0.25") to 25.4 mm (1.0") O.D. tubes. The results indicate a reduction in required heat transfer area by a factor of 2.7 for a 6.35 mm (0.25") O.D. tube with a four-fin configuration over the bare tube case.

For bare tubes, the required heat transfer length is a strong function of tube O.D. However, the required length with the four-fin configuration is very weakly dependent on tube diameter. The two-fin configuration

Figure 3.4.2-1
HEAT TRANSFER ENHANCEMENT EXTENDED SURFACE CONCEPTS

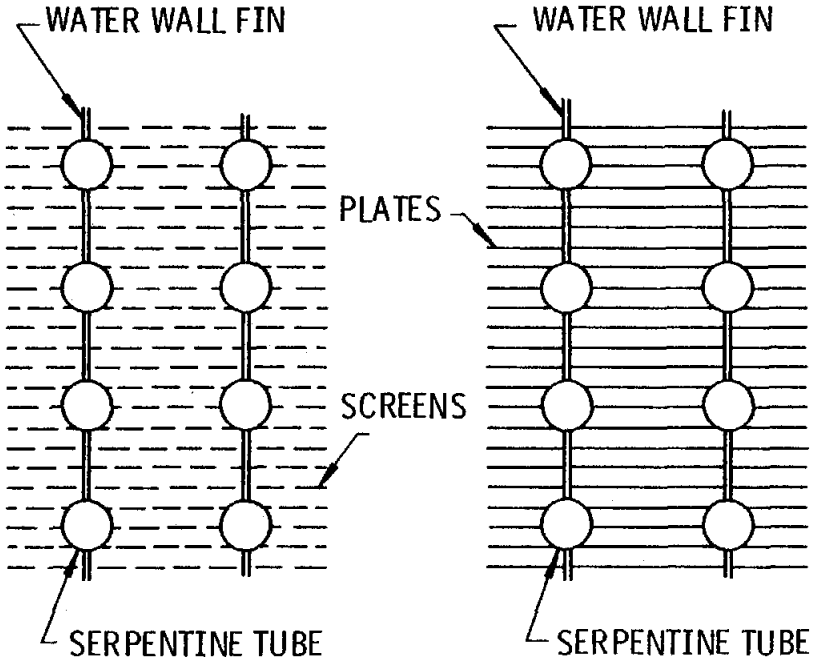


A. WATER-WALL OR TWO-FIN
CONFIGURATION

B. FOUR-FIN
CONFIGURATION

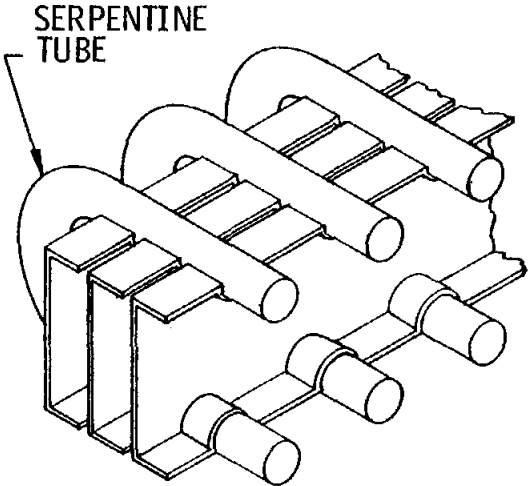
C. SCREENS

Figure 3.4.2-1 (Cont'd)
HEAT TRANSFER ENHANCEMENT EXTENDED SURFACE CONCEPTS



D. SCREEN ADDED TO WATER WALL

E. WATER WALLS WITH HORIZONTAL FINNS



F. CHANNEL SECTIONS

shows a large reduction in heat transfer length over the bare tube, and the four-fin configuration shows a smaller but significant reduction over the two-fin case.

The major deviation from standard finned-tube and water-wall technologies is that the fin height is on the order of 10 times the diameter of the tube. For water walls, the welding of the fin to the tubes is done by automatic machinery and could represent an inexpensive tube bundle. Current experience in the C-E shops are with a minimum tube O.D. of 19 mm (0.75"), and a wall thickness of 4.2 mm (0.165"). The tube-fin combinations come in lengths that are between 6 m to 19 m (20' to 63'). The minimum fin thickness is 4.2 mm (0.165") and a fin width (same as the fin height described above) is in the range 2.5 cm to 10.2 cm (1.0" to 4.0"). The extremes would take some minor tooling. Manufacturing development could extend the range on these parameters, but it would require further investigation. The cost estimate, however, was approximately \$5 to \$6 per linear foot.

Spiral fins were also briefly examined due to potential cost savings that automated manufacturing could provide. However, the minimum tube O.D. is 24 mm (1.0") and minimum height is in the range of 6.38 mm to 32 mm (0.25" to 1.25"). The costs are in the range of \$2-\$3 per linear foot. This concept did not appear attractive enough to pursue further.

Screens or thin plates running parallel to the tubes showed a large reduction in the required heat transfer length, approximately a factor of 3 over the bare tubes. These is a significant additional effect with the inclusion of a path perpendicular to the plates short-circuiting the heat to the tubes. The water walls connected by plates or screens show significant improvement over the four-fin configuration.

The major heat transfer benefits are obtained with fins extending in two directions: high frequency of fins in one direction with connecting plates to the tube in the other direction. Based on this physical picture a simple, easily-fabricated fin was developed as the reference concept for the final design. The concept is shown on Figure 3.4.2-1 and is described and discussed in Section 5.3.3.

3.4.3 Chubb Boiler Tank Concepts

The energy storage boiler tank concept is shown schematically in Sketch 2 of Appendix I. The high pressure steam passing through charging coils at the bottom of the unit evaporates the biphenyl intermediate heat transfer fluid. The biphenyl vapor rises, condenses on the outside of PCM cans, and returns back to the biphenyl pool at the bottom. This completes the charging cycle. For discharging, the biphenyl from the pool is sprayed on the top of the PCM cans. The biphenyl evaporates, rises, condenses on discharging coils at the top of the unit, and returns back to the PCM cans and biphenyl pool. This completes the discharge cycle. The system operates at two different pressure levels corresponding to the boiling temperatures of biphenyl for charging and discharging.

The major components of this concept were sized as described in Appendix VII. Table 3.4.3-1 shows the major components of this concept for specific duty cycle (Section 3.1). The advantages, disadvantages, and design uncertainties of this concept are described in Table 3.4.3-2.

One of the major points of concern for this concept is the operating properties of biphenyl (43) in the presence of water/steam leakage. Figure 3.4.3-1 shows the vapor pressure of biphenyl-water mixtures. From Table 3.4.3-1 it is quite evident that both charging and discharging heat exchangers would require a fairly large amount of heat transfer area. Therefore, small leaks in this type of heat exchanger system are unavoidable. From Figure 3.4.3-1, even a minute quantity (< 1000 PPM) of water concentration in biphenyl could alter the boiling temperature of biphenyl. Stable operation is possible, however, if the mixture is operated at 100 psig for a boiling temperature of 500°F.

The preliminary sizing of this concept has been based on optimistic values such as operation at, or near, atmospheric pressure. If the unit has to operate at higher pressure as above, the required field-fabricated pressure vessel would be one of the major (overwhelming) cost items of this concept.

TABLE 3.4.3-1

MAJOR COMPONENTS OF THE CHUBB BOILER TANK CONCEPT

PCM INVENTORY	
(NaOH-NaBO ₂ EUTECTIC)	
LATENT HEAT	118 Btu/lb
UTILIZATION FACTOR	1.00
QUANTITY	4.28x10 ⁶ lb
HEAT TRANSFER FLUID	
(BIPHENYL)	
QUANTITY	50,000 gal
PRESSURE	VACUUM - 150 psi*
PCM ENCAPSULATION	
(THIN SEAM SPOT WELDED CANS)	
NUMBER	289,550
DIAMETER, LENGTH	4.0 Dia. x 18.2 in
THICKNESS	0.012 - 0.06 in*
SURFACE	4.6x10 ⁵ ft ² .
CHARGING HX	
SURFACE COEFFICIENT	150 Btu/hr·ft ² ·°F
ΔT	25°F
SURFACE	2.73x10 ⁴ ft ²
DISCHARGING HX	
SURFACE COEFFICIENT	300 Btu/hr·ft ² ·°F
ΔT	25°F
SURFACE	1.36x10 ⁴ ft ²

* QUESTIONABLE BIPHENYL OPERATING PROPERTIES REQUIRE FURTHER STUDY.
OPTIMISTIC VALUES USED FOR COST ESTIMATION.

TABLE 3.4.3-1 (Continued)

TANK

DIAMETER, LENGTH	50-ft. Dia., 35-ft. length
PRESSURE	VACUUM - 150 psi*
THICKNESS	0.625 - 3.25 in

OTHER COMPONENTS

BIPHENYL PURIFICATION SYSTEM
GLYCOL START-UP LOOP
BIPHENYL SPRAY PUMP
HEXAGONAL CAGES TO HOLD CANS

* QUESTIONABLE BIPHENYL OPERATING PROPERTIES REQUIRE FURTHER STUDY.
OPTIMISTIC VALUES USED FOR COST ESTIMATION.

TABLE 3.4.3-2

ADVANTAGES, DISADVANTAGES AND DESIGN UNCERTAINTIES OF
THE CHUBB BOILER TANK CONCEPT

ADVANTAGES

- DEMONSTRATION TESTS SCHEDULED
- LARGE HEAT TRANSFER AREA BETWEEN BIPHENYL AND PCM

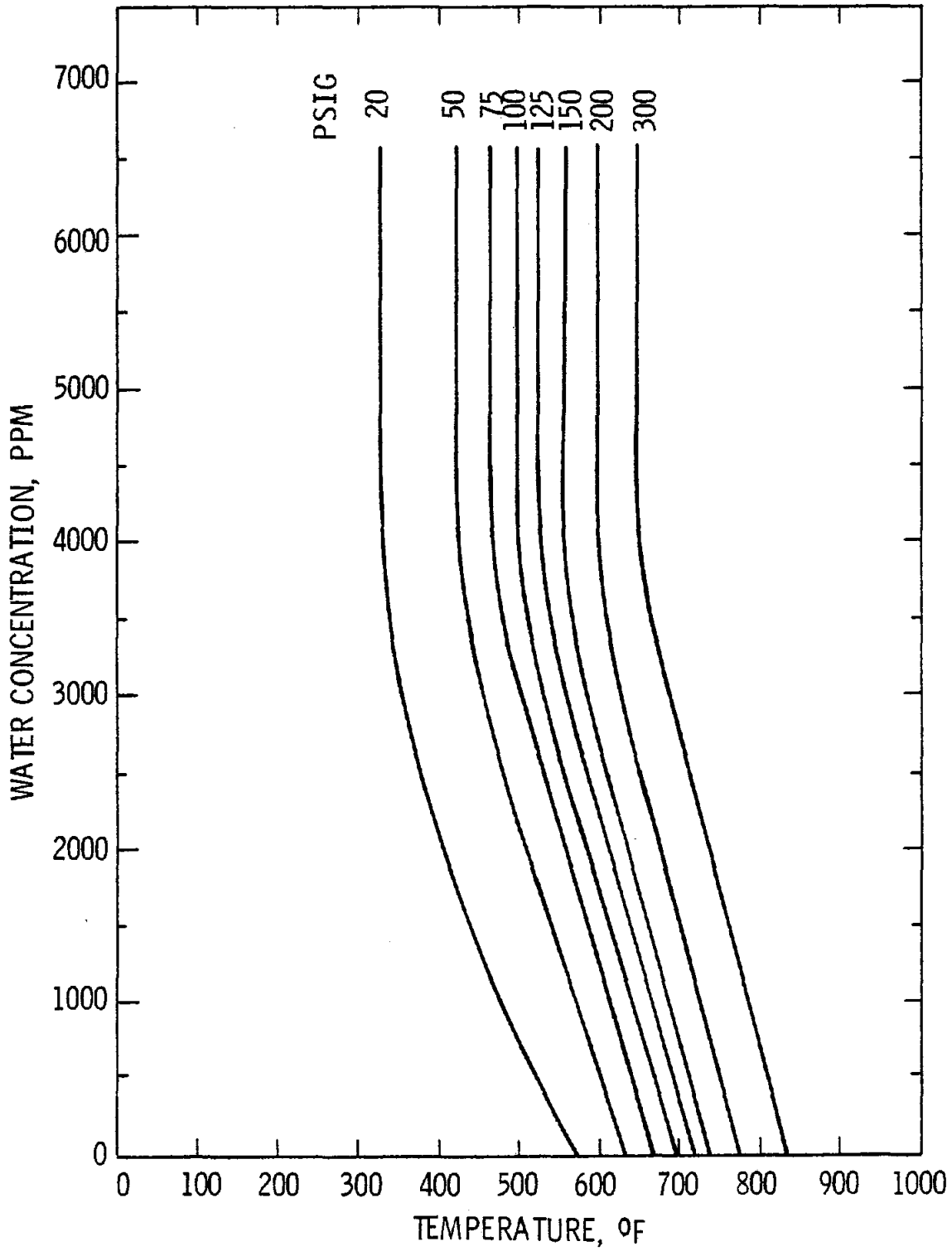
DISADVANTAGES

- FOUR PINCH POINTS
- SEPARATE CHARGING AND DISCHARGING HEAT EXCHANGERS REQUIRED
- DIFFICULT MAINTENANCE, PARTICULARLY CHARGING COILS AND PCM CANISTERS
- BIPHENYL FLASH POINT AND FIRE POINT REQUIRE CLOSE AIR LEAKAGE CONTROL
- CONTINUOUS BIPHENYL PURIFICATION SYSTEM NECESSARY
- GLYCOL START UP LOOP AND TRACE HEATING REQUIRED

DESIGN UNCERTAINTIES

- BIPHENYL OPERATING PROPERTIES IN PRESENCE OF WATER/STEAM LEAKAGE
- PROPERTIES AND EXPERIENCE WITH SODIUM METABORATE
- LIFE OF PCM CANISTER
- BIPHENYL FOULING AND DECOMPOSITION WITH LONG TERM CYCLING

Figure 3.4.3-1
VAPOR PRESSURES OF BIPHENYL-WATER MIXTURES Ref (p)



3.4.4 Macroencapsulation of PCM - Concept

The PCM macroencapsulation concept in its simplest version is basically a containment tank packed with long tubes containing PCM and hermetically sealed at two ends. The stationary PCM is allowed to freeze/melt in the tubes. The charging/discharging heat transfer medium would flow on the shell side. This basic scheme is shown in Sketch 2.

The major drawback in using this concept for current study is high operating pressures of charging and discharging steam/water. It was realized very early in the preliminary sizing of this concept that the major (overwhelming) cost item of this concept would be the pressure vessels designed for operating pressure of about 1200 psi. The cost of these pressure vessels was estimated to be almost order of magnitude higher than total cost of any other concepts. Therefore, this concept was dropped from further consideration.

The preliminary sizing calculations of this concept are explained in Appendix VIII. Table 3.4.4-1 shows major components of this concept for specific duty cycle (Section 3.1). The advantages, disadvantages, and design uncertainties of this concept are described in Table 3.4.4-2.

TABLE 3.4.4-1

MAJOR COMPONENTS OF MACROENCAPSULATION CONCEPT

PCM INVENTORY

NaOH·NaBO₂ EUTECTIC

LATENT HEAT

118 Btu/lb

UTILIZATION FACTOR

1.0

QUANTITY

4.28x10⁶ lb

PCM ENCAPSULATION

LONG, THICK PIPES CLOSED AT ENDS

NUMBER

12250

DIAMETER, LENGTH

4.0 in Dia. x 38 ft

THICKNESS

0.25 in

SURFACE

4.87 x 10⁵ ft²

PRESSURE (MAX. EXTERNAL)

800 psi

PRESSURE VESSEL

MODULAR TANKS

NUMBER

13.3

DIAMETER, LENGTH

13 Dia. x 40 ft

THICKNESS

7 in

PRESSURE

1200 psi

TABLE 3.4.4-2

ADVANTAGES, DISADVANTAGES AND DESIGN UNCERTAINTIES
OF THE MACROENCAPSULATION CONCEPT

ADVANTAGE

- LARGE HEAT TRANSFER AREA BETWEEN PCM AND CHARGING AND DISCHARGING STREAMS

DISADVANTAGE

- PRESSURE VESSEL NECESSARY
- PRESSURIZED PCM CONTAINER
- DIFFICULT MAINTENANCE DUE TO PRESSURE VESSEL AND PACKED PCM CANISTERS

DESIGN UNCERTAINTIES

- MAINTENANCE PROCEDURE FOR LEAKAGE OF PCM
- PROPERTIES AND EXPERIENCE WITH SODIUM METABORATE

3.4.5 Microencapsulation of PCM in a Porous Carrier

Microencapsulation of the PCM has several attractive features. Therefore, a concept utilizing the PCM in this form was developed to the point where its economics relative to those of other concepts could be assessed.

Microencapsulation of low temperature PCMs such as paraffin waxes in shells of an inert material, which can be circulated as a slurry in water, have been proposed. Experience with this type of microencapsulated PCMs has shown, however, that the shells rupture and release the PCM when the slurry is circulated by pumping.

The alternative is to absorb the PCM in the pores of a carrier in particulate form suitable for fluidizing. Experimentation has shown that the pores of powdered silica gel, activated alumina, and zeolites can be almost completely filled with liquid paraffin waxes while the powders remain free-flowing and suitable for fluidization. The advantages of the porous carrier result from the fact that the liquid PCM is held in the pores of the carrier by capillarity and is not dependent on the integrity of a coating to prevent leakage. Even when particles are ruptured, the liquid is held in the pores of the fragments.

Heat transfer to and from the PCM benefits from the relatively high heat transfer coefficients which are obtainable between small fluidized particles and heat exchange surfaces in the fluidized bed, and the absence of solid PCM accumulations on the surfaces. The change of volume at the phase change is accommodated within the pores rather than affecting the total volume.

The concept is illustrated by Figure 3.4.5-1 and Figure 3.4.5-2. The principal elements of the system are a fluidized bed containing a single heat exchanger which is used for charging and discharging, a "cold" storage tank for the discharged PCM, a "hot" storage tank for

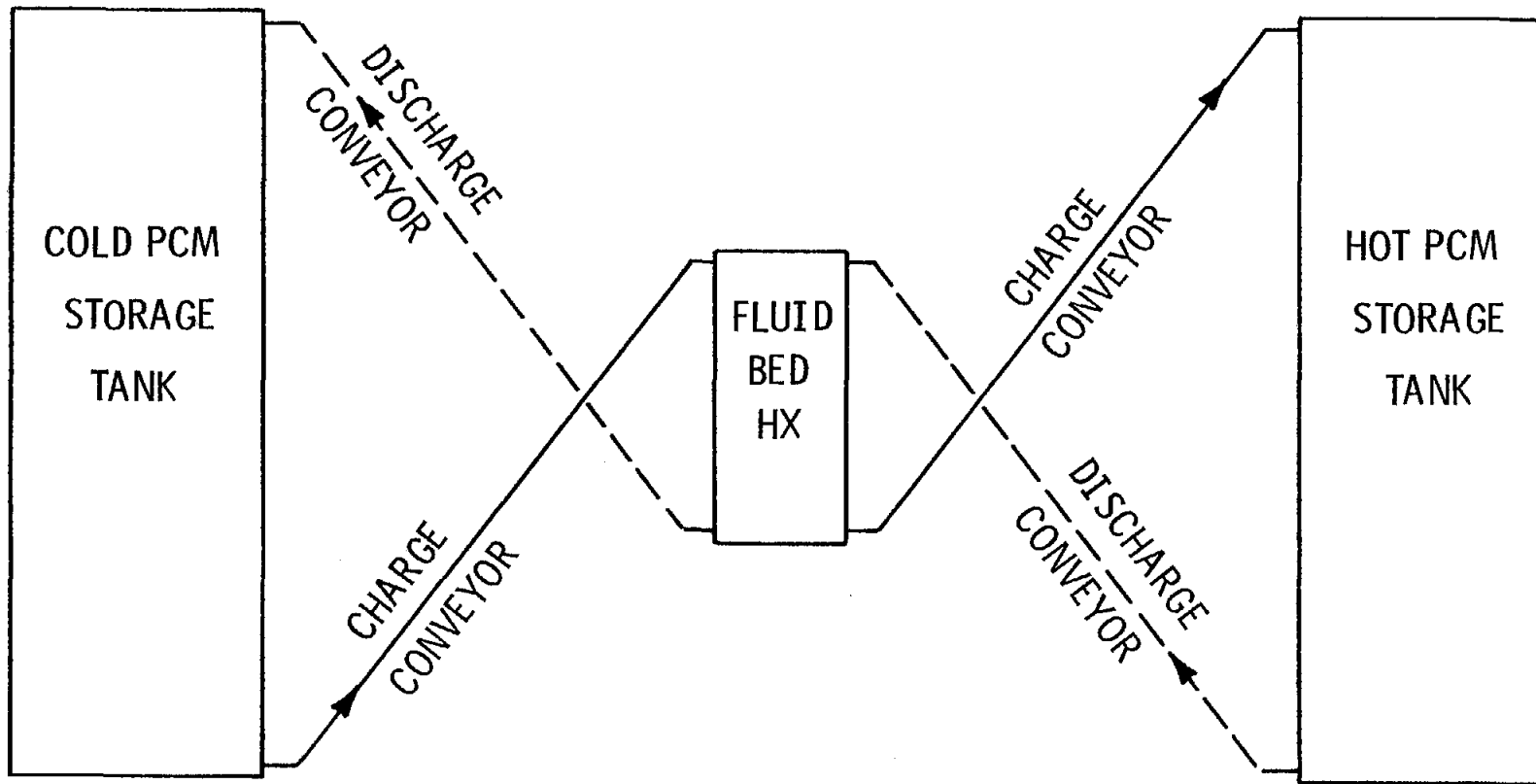


Figure 3.4.5-1
POROUS PCM CARRIER
FLUID BED HX SYSTEM

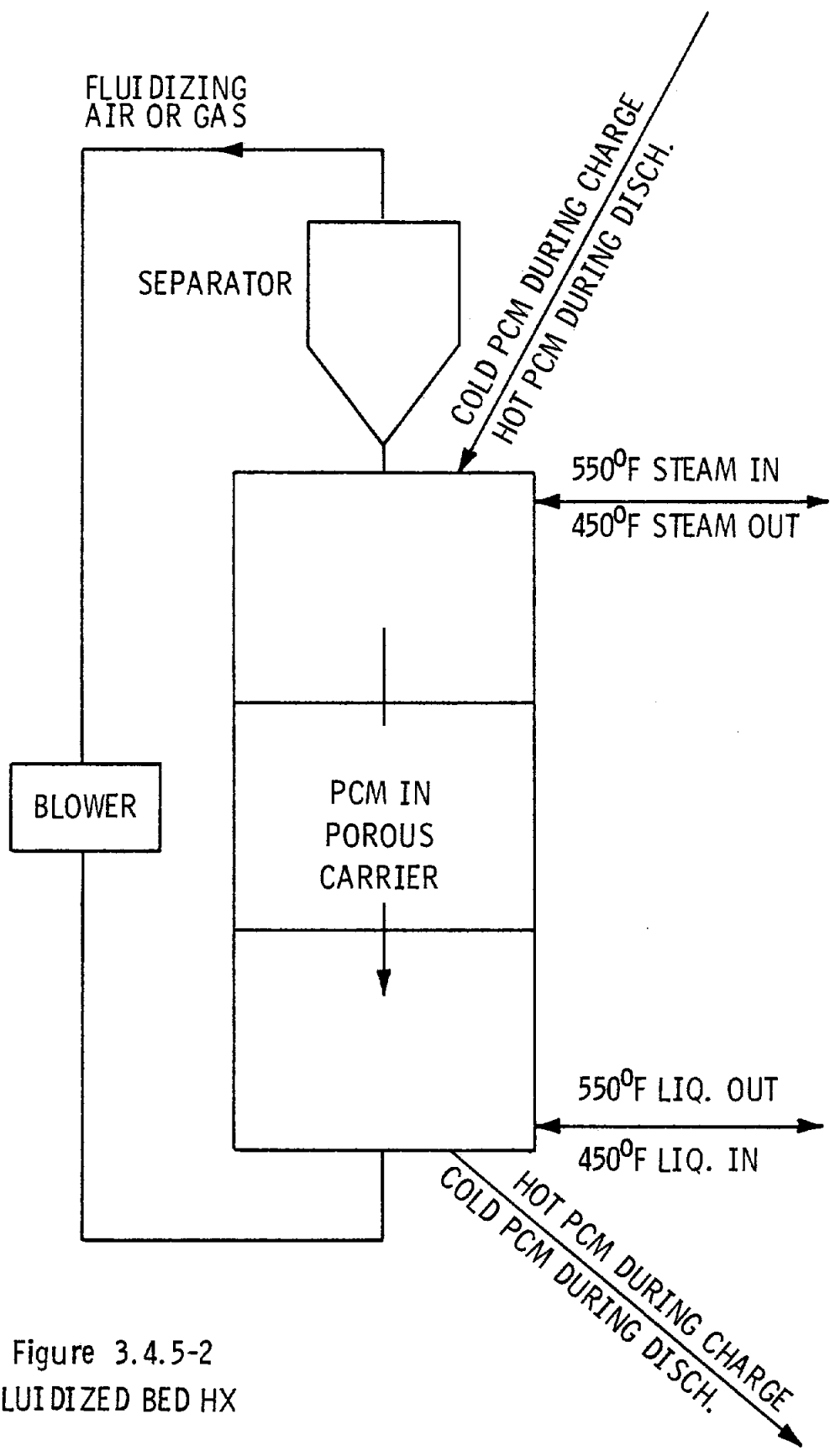


Figure 3.4.5-2
FLUIDIZED BED HX

the charged PCM, and four conveyors which move the PCM between the fluid bed and the storage tanks. The power to fluidize the PCM is a significant parasitic loss; therefore the size of the bed must be kept at the practical minimum.

The fluid bed consists of a conventional fluidizing system. The PCM in its porous carrier moves through the bed from top to bottom, in contact with a tubular heat exchanger which carries the 228°C (550°F) steam during charging, and the 232°C (450°F) saturated water during discharging. The PCM is fluidized by air or by another gas, such as hydrogen or helium, which might be chosen for improved heat transfer characteristics.

During charging, PCM from the bottom of the cold tank is conveyed to the top of the fluid bed, charged by the 228°C (550°F) condensing steam in the submerged heat exchanger, and conveyed from the bottom of the fluid bed to the top of the hot storage tank.

During discharging, charged PCM from the hot tank moves through the fluid bed and is conveyed to the top of the cold tank. Because the heat transfer is principally between the latent heats of the PCM and the steam, it makes little difference whether the flows are parallel or counter.

Separate tanks for the charged and discharged PCM appear to be required because it does not appear feasible to introduce the PCM into the bottom of a tank, nor to remove it from the top. If this were the case, there is no way to store and remove both charged and discharged PCM from a single tank without mixing.

The tankage requirement was estimated on the basis of a porous carrier having a PCM available pore volume of 50% and a packing density of 70%. A total of 36 tanks of rail-shippable size 4 m x 4 m x 4 m (13' x 13' x 40') are required, at an estimated cost of \$2,270,000.

The PCM can be used at a very high utilization factor, estimated at 0.95, and the lower priced NaOH-NaNO₃ eutectic can be used if the system is fluidized with air or helium. The cost of the PCM is estimated at \$743,000. However, the PCM carriers suitable for fluidization and for PCM impregnation are priced in excess of \$1.10/kg (\$0.50/lb), and a total of approximately 2.04×10^6 kg (4.5×10^6 lb) is required, costing in excess of \$2,250,000. The total cost of tanks, PCM, and carrier is in excess of \$5,200,000 to which must be added the costs of the fluid bed, fluidizing gas blower, separator, conveyors, and thermal protection to keep losses from this very large system within acceptable limits. Some saving might be made by use of large field erected tanks, but not enough to outweigh the other high costs. Thus, the fluidized bed system is not cost competitive in this application, and further analysis was not required.

3.4.6 Direct Contact Systems with PCM Drop Intermediate Heat Exchanger

This direct contact system is based upon the release of small drops of liquid PCM into an intermediate heat transfer fluid, where they solidify delivering the heat of fusion and a smaller amount of sensible heat. The intermediate fluid is required due to the incompatibility of the PCM and the charging and discharging steam. Schematics of two such systems, one using a liquid metal and the other an oil, are shown on Sketch 3 in Appendix I.

The PCM is melted by a charging heat exchanger, and the generation of the discharge steam requires a second heat exchanger, both of which are small relative to the single heat exchanger required in the tube intensive systems described in Sections 3.4.1. The principal advantages of the PCM drop systems are the avoidance of the thermal resistance of solid PCM accumulations on heat transfer surfaces, and a high utilization factor of the PCM.

Two pumps are required, one for the liquid PCM and another for the intermediate heat transfer fluid. A separator is needed to remove the solidified PCM drops from the fluid. The liquid PCM must be maintained somewhat above its melting point at all points in the pumping circuit to prevent solidification in the piping and pump due to insulation heat loss.

The intermediate fluid, whether liquid metal or oil, must be protected from oxidation by air or by the PCM. This required the use of a cover gas and the use of the NaOH/NaBO₂ eutectic, rather than the NaOH/NaOH₃ eutectic since the latter requires contact with air for chemical stability as described in Section 3.2.

Liquid Metal Heat Transfer Fluid

The PCM Drop concept using a liquid metal as the intermediate heat

transfer fluid is exemplified by the lead-bismuth eutectic alloy containing 44.5 wt % of Pb and 55.5 wt % of Bi (2), the properties of this alloy are shown in Appendix IX along with the sizing of the major components.

The system concept is illustrated schematically in Sketch 3 in Appendix I. The solid PCM is stored in a tank which contains a high temperature heat exchanger (HHX) at the bottom which receives 228°C (550°F) saturated steam for charging heat into the PCM. Most of the HHX surface is concentrated at the bottom, but several vertical elements extend to the top to provide molten PCM channels for the flow of expanding liquid to the top during melting.

Liquid PCM is pumped from the tank into the intermediate heat exchanger (IHX), which also receives the flow of the Pb-Bi alloy. The alloy flows upward rather than downward in order to minimize circulation resulting from expansion as it is heated. The liquid PCM is introduced into the bottom of the IHX through a disperser that releases substantially uniform drops, which rise through the cooler alloy, solidify, and heat the alloy. At the top of the IHX, the solidified PCM is separated from the alloy and returned to the storage tank.

The heated alloy leaving the IHX is pumped through the low temperature heat exchanger where it transfers heat to 232°C (450°F) saturated water to generate steam.

Oil Heat Transfer Fluid

The system using oil (biphenyl) as the intermediate heat transfer fluid is essentially the same as that using the liquid metal, with the exception of the intermediate heat exchanger and the method of separating the solid PCM drops from the fluid. The density of the PCM being greater than that of the oil, the drops sink relative to the oil. The oil, being heated, is flowed upward in the IHX in order to minimize thermal circulation. As the upward velocity of the oil is

greater than the sinking velocity of the PCM drops, the oil carries the drops from the IHX into a centrifugal separator, as shown by Sketch 3. The PCM goes to the storage tank, while the oil is pumped to the low temperature heat exchanger. The solid PCM storage tank and the charging heat exchanger are the same as for the system using the liquid metal heat transfer fluid.

Characteristics of Pb-Bi Alloy and Oil PCM Drop Systems

These systems were compared on the basis that a single field-erected tank is used in order to gain the cost advantage of a single PCM drop heat exchanger for each system. Physical characteristics of the two systems are given on Table 3.4.6-1. More details on these systems are to be found in Appendix IX.

If this concept were to be carried to the demonstration stage, several elements of the system would require development. The NaOH/NaBO₂ eutectic has not yet been well characterized. The most economical method of preparation from commercially available chemicals such as borax, boric acid, or the hydrated forms of sodium metaborate must be determined. Thermo-physical properties of the eutectic are lacking, as well as data on compatibility with the intermediate heat transfer fluids. A design for the PCM drop-intermediate heat transfer fluid heat exchanger must be developed and tested, including the device which separates the solid PCM drops from the liquid metal intermediate heat transfer fluid.

TABLE 3.4.6-1
CHARACTERISTICS OF PCM DROP SYSTEM USING LIQUID METAL AND OIL AS HEAT TRANSFER FLUIDS

	Units	Liquid Metal		Oil	
Heat Transfer fluid circulation Rate	kg/s (lb/hr)	15.1×10^3	(120×10^6)	857	(6.8×10^6)
	m^3/s (gal/min)	1.44	(22.8×10^3)	1.04	(16.4×10^3)
Heat Transfer Fluid Inventory					
Intermediate HX	kg (lb)	97.5×10^3	(215×10^3)	3.04×10^3	(6.70×10^3)
Discharge steam HX	kg (lb)	54.9×10^3	(121×10^3)	5.94×10^3	(13.1×10^3)
Other	kg (lb)	74.8×10^3	(165×10^3)	4.26×10^3	(9.4×10^3)
Total	kg (lb)	22.7×10^3	(501×10^3)	13.2×10^3	(29.2×10^3)
PCM (utilization factor .95)	kg (lb)	2.04×10^6	4.506×10^6	2.04×10^6	4.506×10^6
PCM storage tank, diameter & height	m (ft ²)	12.65	(41.5)	12.65	(41.5)
Charge HX surface	m ² (ft ²)	3.99×10^3	(42.9×10^3)	3.99×10^3	(42.9×10^3)
Discharge HX surface	m ² (ft ²)	678	(7.3×10^3)	2.17×10^3	(23.4×10^3)
Intermediate HX volume	m ³ (ft ³)	3.54	(125)	2.83	(100)

3.4.7 Direct Contact Systems Using an Intermediate Heat Transfer Fluid

The basic concept involved in the direct contact systems is the use of an intermediate heat transfer fluid which is brought into contact with the free surface of the liquid PCM in a storage tank. The fluid cools and solidifies the PCM at the contact surface, the solid falling to the bottom of the tank. The heated fluid is circulated over the surface of the discharge heat exchanger to produce 232°C (450°F) saturated steam. The charging heat exchanger is located at the bottom of the tank where 288°C (550°F) saturated steam is used to melt the PCM; this is the same as the corresponding component described in Section 3.4.6. A schematic of the system using this concept is shown on Sketch 4 in Appendix I.

A major advantage of the concept is the fact that the entire system, with the exception of the heat transfer fluid pump and purification system, is inside the PCM containment tank, and the PCM circulates by thermal convection rather than by pumping. The concept thus lends itself to a mechanically simple design.

The concept analysis was carried out for two methods by which the heat transfer fluid might be applied. In the first, the fluid is vaporized by the PCM and condensed on the tubes of the discharge heat exchanger, using the reflux condenser or heat pipe principle. In the second, the space containing the discharge heat exchanger is flooded with the fluid, which is circulated by pumping from the PCM interface to the heat exchanger.

Both the reflux and the circulating systems must be operated without contact with air in order to protect the oil from oxidation, which would cause rapid deterioration. The reflux system operates at a pressure only slightly below atmospheric if biphenyl is used as the heat transfer fluid. The non-oxidizing NaOH/NaBO₂ eutectic is required, which entails the research noted in Section 3.2 before system development could be undertaken.

Reflux Oil Intermediate Heat Exchanger

The reflux system is shown on Sketch 4. The PCM tank represents one of 10 modular elements of square cross-section, $3.96 \times 3.96 \text{ m}^2$ ($13 \times 13 \text{ ft}^2$) and height 1.274 m (41.8 ft), which can be prefabricated and moved by rail to the site. The charging heat exchanger located at the bottom of the tank is the same as that used in the PCM drop concepts described in Section 3.4.6.

The oil (biphenyl) is pumped through a set of nozzles which produce jets of oil directed at the liquid surface of the PCM. The pressure in the space occupied by the discharge heat exchanger tubes is maintained at a value corresponding to a boiling temperature of 264°C (475°F). In the case of biphenyl, the vapor pressure corresponding to this temperature is 82.7 kPa (12 psia). This pressure can be influenced by the formation of thermal degradation products of the oil, or by small amounts of water which might find their way into the system and which must be removed by the purification system. A thin layer of oil maintained on the PCM surface, boils, extracting heat from the PCM as it solidifies. Solid particles of the PCM form and fall to the bottom of the tank. The oil vapor flows upward and condenses on the surfaces of the discharge heat exchanger. The condensate is collected, and flows to a pump which returns the oil under pressure to the jets. The oil pumping rate must be controlled and matched to the demand for heat from storage, to avoid flooding or starving the system.

An oil purifying system operates continuously or intermittently to prevent the accumulation of high or low boiling materials which would affect the boiling point of the oil and the pressure in the system, or impede heat transfer.

The discharge heat exchanger consists of tube banks through which flows the 232°C (450°F) saturated water for generation of saturated steam. The characteristics of this system are summarized on Table 3.4.7-1. The sizing of the major components is described in Appendix X.

Circulating Oil Intermediate Heat Exchanger

The circulating oil system, Sketch 4, is similar to the reflux system except that the space between the PCM and the discharge heat exchanger is filled with liquid oil which is pumped from the PCM interface to the discharge heat exchanger tube banks. Using biphenyl, whose vapor pressure at 246°C (475°F) is 82.7 kPa (12 psia), the system can be operated at atmospheric pressure.

The PCM expansion during the phase change substantially increases the volume of the oil-filled space so an external oil reservoir is required. The reservoir requires a non-oxidizing gas cover to protect the oil.

The characteristics of the circulating oil system are given on Table 3.4.7-1. Further details of both concepts are given in Appendix X.

TABLE 3.4.7-1
CHARACTERISTICS OF DIRECT CONTACT SYSTEMS USING BIPHENYL AS INTERMEDIATE HEAT TRANSFER FLUID

	Units		Reflux Oil System		Circulating Oil System	
Biphenyl circulation rate	kg/s	(lb /hr)	123	(975 x 10 ³)	857	(6.8 x 10 ⁶)
	m ³ /sec	(gal/min)	0.148	(2.35 x 10 ³)	1.04	(16.4 x 10 ³)
Biphenyl inventory	kg	(lb)	1.81 x 10 ³	(4,000)	201 x 10 ³	(443 x 10 ³)
	m ³	(gal)	2.2	(578)	242	(64 x 10 ³)
Pumping power	kW	(hp)	113	(150)	790	(1.1 x 10 ³)
PCM (Utilization factor = .58)	kg	(lb)	3.35 x 10 ⁶	(7.38 x 10 ⁶)	3.35 x 10 ⁶	(7.38 x 10 ⁶)
Tanks						
Dimensions	m	(ft)	3.96 x 3.96 x 12.74	(13 x 13 x x 41.8)	3.96 x 3.96 x 12.74	(13 x 13 x x 41.8)
TES tanks, number			10		10	
Biphenyl expansion, Number			None		1	
Charge heat exchanger surface	m ²	(ft ²)	3.99 x 10 ³	(42.9 x 10 ³)	3.99 x 10 ³	(42.9 x 10 ³)
Discharge heat exchanger surface	m ²	(ft ²)	2.43 x 10 ³	(26.2 x 10 ³)	2.17 x 10 ³	(23.4 x 10 ³)

3.4.8 Mechanical Scraper: Rotating Drum

The rotating drum-fixed scraper TES concept employs horizontal drums across the top of the PCM containment tank. This is shown schematically in Sketch 5 in Appendix I. Fixed scrapers suspended from the top cover of the tank remove the solidified PCM from the drum surfaces. During discharge, saturated water is headered into the drum modules. Hot liquid PCM is pumped from the tank onto the drum surfaces and solidifies, thereby boiling the water within the drums. The removed PCM drops into the tank and eventually settles on the bottom. During the charging process, saturated steam from the solar receiver is passed through the finned-tube charging heat exchanger, thereby melting the PCM. Most of the charging heat transfer tubes are located at the bottom of the containment tank, but there are some vertical runs to insure that the heated liquid can freely expand without stressing the containment tank.

An off-eutectic sodium hydroxide/sodium nitrate mixture is selected for the PCM based on the experience in Reference (34). The off-eutectic salt forms a slush as it freezes, and this slush is much easier to remove than the strong crystalline structures of the eutectic or pure material. An effective utilization factor (heat recovery factor) of 60% is reported in Reference (34). This reflects a volume utilization and the operation with an off-eutectic salt. The 60% value is used in the current study. The initial sizing calculations employed a very optimistic 90% utilization factor. A more realistic target for improvement is 75%; however, the initial estimate serves as a very optimistic upper bound. For this range of utilization factor, $4.7-7.3 \times 10^6$ lb of PCM, contained in seven to ten rectangular tanks, are required.

The sizes of the major components are listed on Table 3.4.8-1 and the calculations are described in Appendix XI. A total of 300 scraping modules are required, and these span the top of the containment tanks.

TABLE 3.4.8-1

MAJOR COMPONENT DESIGN DATA, MECHANICAL SCRAPER-ROTATING DRUM CONCEPT

		<u>OPTIMISTIC ESTIMATE</u>
PCM INVENTORY		
NaOH/NaNO ₃ Off-Eutectic	20-30% NaNO ₃	
Latent Heat	118 Btu/lb	
Utilization Factor	.60	0.90
Quantity	7.13x10 ⁶ lb	4.7x10 ⁶ lb
Cost	14¢/lb	
PCM TANK		
Number	10	7
Size	13'x13'x40'	
Structural Code	ASME Section VIII	
Plate Thickness	1/2 in	
Usable Volume	6420 ft ³	
LIQUID PUMP		
Pump Size (Total)	5.8 Hp	
DISCHARGE HEAT EXCHANGER		
Number of Scraper Modules	300	
Heat Transfer Area	5100 ft ²	
Overall Heat Transfer Coefficient	400 Btu/hr·ft ² ·°F	
Drum Size	1/4"Thick x 6" Dia.	
Scraper Power	.21 Hp/ft ²	
Code	ASME Section VIII	
CHARGING HEAT EXCHANGER		
Heat Transfer Surface	Finned Tube 1/8 x 1/2 Fin 1" Tube	
Heat Flux	2379 Btu/hr·ft	
Length	42,900 ft	
Heat Transfer Area	41,300 ft ²	

Rotating couplings are provided in the steam and feed lines to each drum unit. Each drum is provided with a scraper, a PCM metering edge, and liquid PCM. A pump supplies liquid PCM to the drum through a piping system. One motor of about 29.8 kW (40 Hp) with a controller is used for each group of heat exchangers (11 per group). A speed controller varies the motor RPM to prevent excessive PCM from freezing on the drums.

An advantage of the rotating drum heat exchanger is that the chemical industry has extensive experience with similar heat exchangers, and test results are available. The discharge rotating drum heat exchanger is accessible for service and is replaceable. Also, a single tank is used for the liquid and solid PCM.

There are various disadvantages associated with this concept. Servicing of the charging heat exchanger will require draining the storage tank. More heat transfer area is required because the discharge heat exchanger cannot be used for charging. The rotating drum concept also has the disadvantage of the high cost of the rotating couplings for the condensate and steam lines. Additionally, the overall unit efficiency is reduced by the power required by the rotating drum and the liquid PCM pump. This turn around efficiency reduction is expected to be in the order of .068% for the PCM pump, and 1 to 6% for the rotating drum.

There are uncertainties associated with this concept. It is possible for the drum to freeze up during operation, and the freeze up may be difficult to control. The heat recovery factor may vary considerably from the 60% figure. Also, there is no experience with operating these systems with the off-eutectic selected.

3.4.9 Mechanical Scraper: Rotating Auger

The rotating auger mechanical scraper TES system consists of tanks which contain PCM, and heat exchangers which transfer heat from the steam or condensate to and from the PCM. This system is shown on Sketch 6 in Appendix I.

The module consists of a fixed vertical drum (bayonet type heat exchanger) with a helical rotating scraper. The scraper transports the liquid PCM to the drum surface and removes the solidified PCM from the drum surface. Stand-pipes allow the liquid PCM to be drawn down to the auger well located at the leading edge of auger. A 2.2-kW (3-hp) variable speed motor rotates the auger/scraper and a speed control on the motor increases the motor speed when freezing of the scrapers starts to occur. This will increase the flow of liquid PCM to the heat exchanger drum and reduce the freezing effect. A finned coil at the bottom of each tank provides the bulk heat transfer area for charging and is supplemented by the scraper modules.

As discussed in the previous section and in the appendices, an off-eutectic mixture of sodium hydroxide/sodium nitrate is used to insure the scraper does not freeze onto the drum. A utilization factor of 60% is appropriate, but an upper bound of 90% was also employed in the initial sizing effort. The results of the rough sizing of components, discussed in Appendix XI, are presented on Table 3.4.9-1. For the range of utilization factors, $4.7 - 7.13 \times 10^6$ lbm of PCM contained in 7 to 10 tanks are required. A total of 300 scraping modules are required to provide the peak 30-MW discharge rate. In addition, the scraper provides about 17% of the charging rate and supplements the charging heat exchanger at the bottom of the tank. It also provides a direct path for the liquid PCM to the free level, and thereby insures that the expansion of the heat liquid during charging does not overstress the containment tank walls.

TABLE 3.4.9-1

MAJOR COMPONENT DESIGN DATA

MECHANICAL SCRAPER-ROTATING AUGER CONCEPT

PCM INVENTORY:

OPTIMISTIC ESTIMATE

NaOH-NaNO ₃ Off Eutectic	20-30%	
Latent Heat	118 BTU/lbm	
Utilization Factor	.60	0.90 ⁶
Quantity	7.13x10 ⁶ lb	4.7x10 ⁶ lbm.
Cost	14¢/lbm	

PCM TANK:

Number	10	7
Size	13'x13'x40'	
Structural Code	ASME SECTION VIII	
Plate Thickness	1/2 in	
Usable Volume	6,420 ft ³	

DISCHARGE HEAT EXCHANGER:

Number of Scraper Modules	300
Heat Transfer Area	5,100 ft ²
Overall Heat Transfer Coefficient	400 Btu/nr.ft ² .°F
Drum Size	1/4" thick, 6" dia.
Scraper Power	0.21 hp/ft ²
Code	ASME SECTION XIII

CHARGING HEAT EXCHANGER:

Heat Transfer Surface	Finned Tube
	1/8"x1/2" Fin 1" Tube
Heat Flux	2379 Btu/hr.ft
Length	35,500 ft ²
Heat Transfer Area	34,300 ft ²

Many advantages are associated with this mechanical scraper concept. The modules may be removed by disconnecting the steam and condensate lines, and lifting from position for optimum servicing. The PCM need not to be drained from the tank to perform this operation. Only one tank is needed to contain the PCM, as compared to other systems which require separate tanks for the liquid and solid PCM. Also, the modules supplement the charging heat exchangers.

A major disadvantage is that the overall unit efficiency is reduced by the power required to rotate the scrapers/augers. This value is expected to vary from 1 to 6% of the rated capacity. Also, the unit must be drained to service the charging heat exchanger.

There are uncertainties associated with this concept. The performance of the scrapers with regard to freeze up remains uncertain. The heat recovery factor and operation with an off-eutectic also remain uncertain.

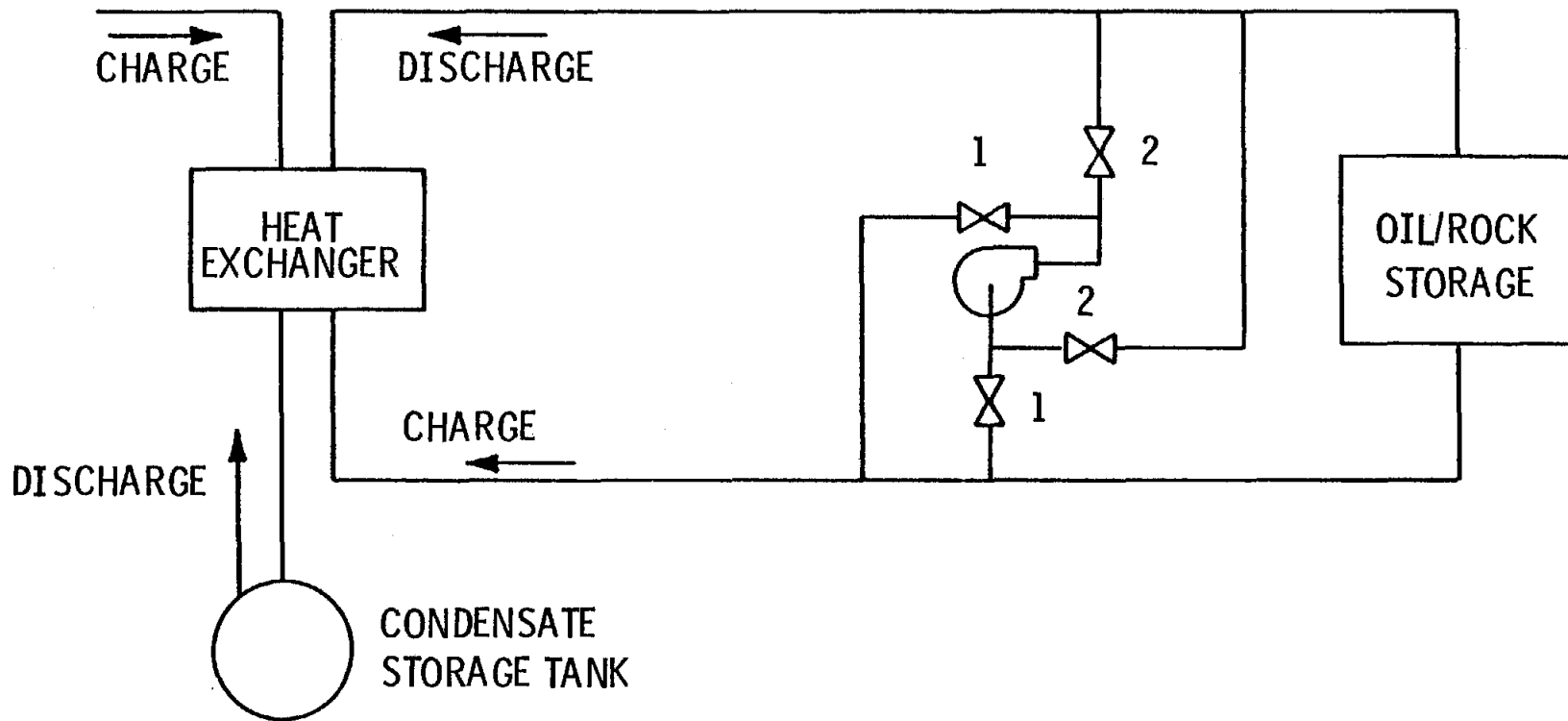
3.5 Rock Bed with Oil Intermediate

A rock-bed-with-oil-intermediate-heat-transfer-fluid (Caloria HT43) storage system serves as the cost benchmark for the various latent heat concepts being considered in this study. This system is designed to have the same storage characteristics and charge/discharge rates as the latent heat concepts (see Section 3.1) and to fit into the same basic system configuration. As with the tube-intensive latent heat system, a single heat exchanger is employed for charging and discharging processes.

The storage system is shown on Figure 3.5-1. During charging of the system, Caloria is taken from the bottom of the storage tank, pumped through the shell-and-tube heat exchanger, where it receives heat from the solar receiver coolant, and returned to the top of the storage tank. During discharge, the hot Caloria is taken from the top of the storage tank, run through the heat exchanger producing steam for the process, and returned to the bottom of the storage tank. The heat exchanger is operated in counterflow mode, with steam flowing downhill during charging and uphill during discharging. Operation of the steam side of the heat exchanger is the same as for the latent heat concepts described earlier. The heat exchanger, storage tank, pump, and piping were sized as part of the oil/rock storage evaluation. A summary description of these components is given in Table 3.5-1. The efficiency of oil/rock as a storage medium has been taken into account by considering two utilization factors. The utilization factor (UF) for the oil/rock system is the ratio of the theoretical storage volume needed to the actual storage volume needed. Utilization factors of 0.6 and 0.8 are considered here: 0.8 is considered optimistic; 0.6 is considered to be conservative.

The oil/steam, shell-and-tube heat exchanger temperature profile is shown on Figure 3.5-2. Pinch points of 5.6, 8.3, and 13.9°C (10, 15, and 25°F) were considered in sizing the system. As the pinch point increases, the heat transfer surface area required decreases; but, the

Figure 3.5-1
OIL/ROCK THERMAL STORAGE SYSTEM



VALVES	1	OPEN DURING CHARGE; CLOSE DURING DISCHARGE
	2	CLOSE DURING CHARGE; OPEN DURING DISCHARGE

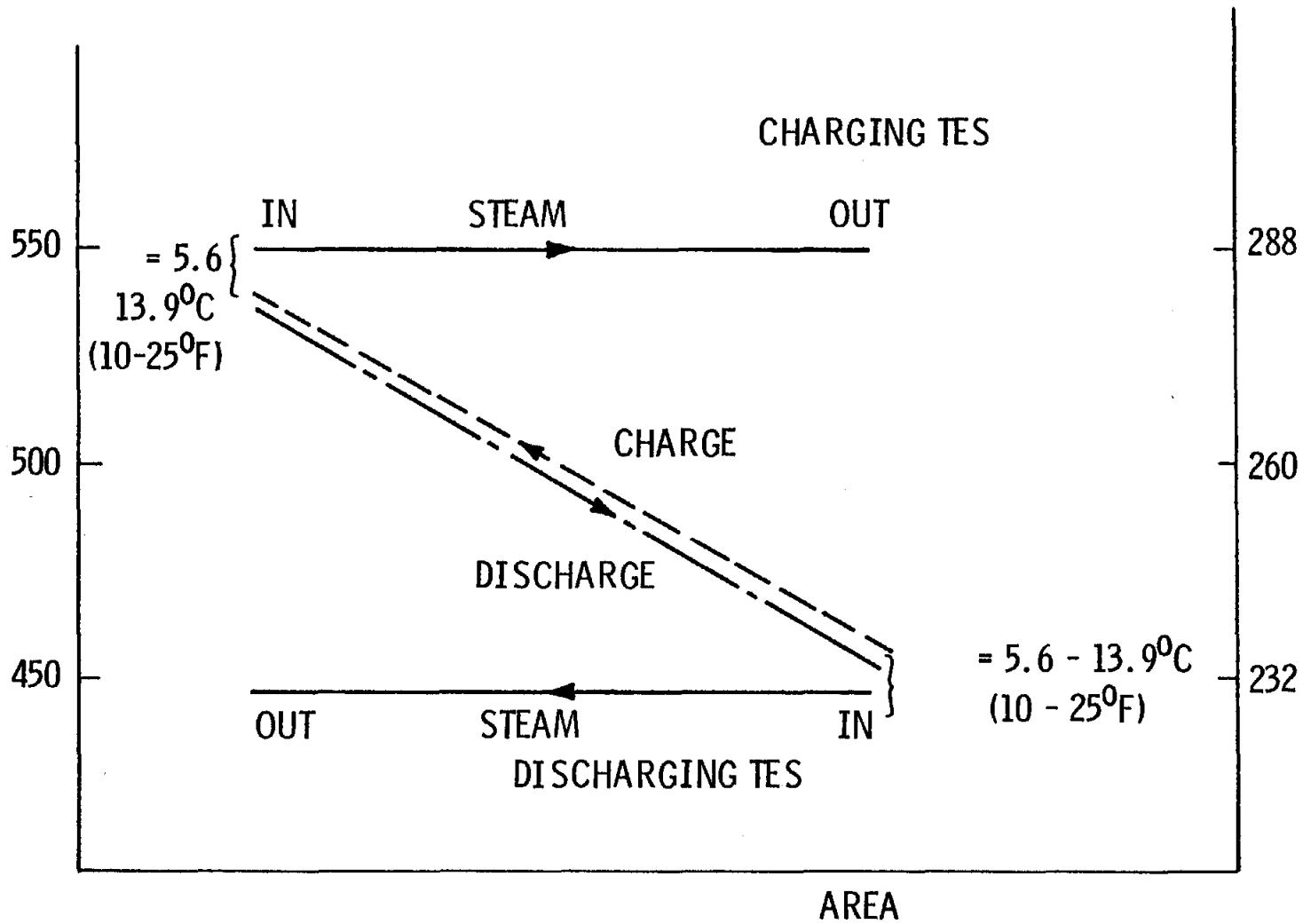
TABLE 3.5-1

OIL/ROCK STORAGE SYSTEM
COMPONENT DESCRIPTION[†]

TANK: UF=60%	Diameter	24.69 m (81 ft)
	Height	16.76 m (55 ft)
	Thickness	.635-3.8 cm (1/4 - 1-1/2 in) Varies as a function of height
	Caloria	.2013.83 m ³ (532,000 gal)
	Rock	1605.7 Mg (17,700 sh. ton)
	UF-80%	Diameter
	Height	15.24 m (50 ft)
	Thickness	.635-3.18 cm (1/4 - 1-1/4 in) Varies as a function of height
	Caloria	1521.73 m ³ (402,000 gal)
	Rock	12156.2 Mg (13,400 sh. ton)
HEAT EXCHANGER:	Shell-and-tube	
	Heat transfer area	2612.4 m ² (28120 ft ²)
PUMP:	Single 101 kW (135hp) centrifugal pump/motor	
PIPING:	40.64 cm (16 in) schedule 40	
	122 m (400 ft) assumed	

[†]For 5.6°C (10°F) Pinch Point

Figure 3.5-2
 OIL/STEAM, SHELL AND TUBE HEAT EXCHANGER
 TEMPERATURE PROFILE



storage volume required increases. Based on cost considerations (see Appendix XII) it was found that the system with the smaller pinch point is more desirable.

The storage tank is assumed to be field erected and designed to API650 as modified by the ASME Boiler Code Section VIII. Only the major components of this system have been sized. Others, such as the ullage maintenance units and instrumentation and controls were not considered for the cost comparison of the concept selection phase of this effort. A more detailed description of the sizing calculations is given in Appendix XII.

4.0 SELECTION OF PREFERRED SYSTEM

In the previous section the variety of concepts for using the latent heat for thermal energy storage was presented. Designs which were developed for the more promising concepts were described. In this section the process used to narrow down the list of candidates is described along with the selection criteria. Since the most important criterion is cost, the unit cost data are presented. In the final part, costs estimates based on the major component sizes developed in Section 3 are presented, and the selection of the preferred concept described.

4.1 Selection Process

The selection process was a three-step process in which the number of candidate designs was systematically reduced to the preferred concept. A literature survey of thermal energy storage systems using latent heat of fusion of the storage medium was conducted. Based on the published studies and C-E/C&W ideas, a list of more than 40 concepts was prepared. The designs were segregated into several broad categories: passive systems, encapsulated PCM concepts, direct contact heat exchange designs, active systems using mechanical and hydraulic assistance for heat exchange, and concepts taking advantage of characteristics of the PCM. The list is presented in Section 3.3.

The selection criteria established were costs, state-of-the-art evaluation, and reliability. The criteria were applied to the master list of candidates, and the initial selections were based mainly on judgement on current operating experience and concept risk and uncertainty. Concepts which are still in their infant conceptual design stage and would require large development programs were eliminated. The concepts selected for further development were:

- (1) Tube intensive concepts using various tube configurations and with and without heat transfer enhancement,

- (2) Macroencapsulation of PCM with and without direct charging and discharging by steam,
- (3) Microencapsulation using a powered, porous carrier to contain the PCM (Heat exchange with the carrier material is accomplished in a fluidized bed heat exchanger.),
- (4) Direct contact heat exchange using an oil or liquid metal as an intermediary fluid between the PCM and the discharging steam,
- (5) Mechanical devices to scrape the solid PCM from the heat transfer surface during the discharge process.

The design of each of the selected concepts was developed to the point where the major components were sized and rough costs developed. Sketches of each design were developed to scale to aid the sizing effort and to help identify design and operating problems. Unit costs were obtained for tanks, piping, pumps, heat exchangers, and PCM from the C-E cost estimating department and from the Stearns-Roger (35) input to SERI. Finally, advantages, disadvantages and design uncertainties of each concept were identified based on the design development effort and experience described in the literature.

Three designs were selected based on the initial component cost estimates. The selected designs were developed further in the next phase. Design uncertainties and problem areas identified in the initial sizing effort were addressed. In addition, an oil/rock system modeled on the Barstow system was sized and a cost of major components estimated. This provided a benchmark for comparison. A final design comparison was made and the preferred concept selected. Since the costs were comparable for the various designs, judgements on the design, the potential for improvement and the ability to meet the near term schedule of the potential follow-on SRE were used as further discriminators.

4.2 Selection Criteria

The criteria established for the concept selection process are listed on Table 4-1. The single most important criterion is the cost. To reduce the cost comparison to the essential level, only the major components of each storage subsystem concept were considered. This eliminated the need to cost components that are common to all concepts or that have minor or negligible effects on the cost comparison. The major components are the amount of PCM, containment tanks, heat exchangers, and, to a minor extent, pumps and piping. In addition, the active devices require power to operate and this must be included in the costs.

The state-of-the-art of the concept is another important criterion. Existing operating experience and experimental data indicate the best direction for the design development. They provide a basis of projecting the design behavior for the selected application. Consequently, the risk and uncertainty for each concept can be assessed. In addition, the requirement for development programs to support the design and reduce the risk and uncertainty to a reasonable level can be judged. As a backdrop to these considerations the overall schedule of the Advanced Solar Thermal Energy Storage project must also be considered. Phase II: The Subsystem Research Experiment may be a direct follow-on to this conceptual design effort. This is a 30-month effort in which the storage subsystem is designed, constructed and operated. Consequently those concepts requiring extensive and/or costly development programs to support the design must be viewed less favorably.

The reliability of a given concept must also be considered. The preferred concept will eventually be in long-term commercial service. The potential downtime costs for replacement power and maintenance will play a role in the economics of the TESS. Consideration of the reliability at the conceptual design stage will help minimize the possibility of incurring additional costs.

TABLE 4-1

SELECTION CRITERIA

- COSTS - MAJOR COMPONENTS
 - TANK VOLUMES
 - HEAT TRANSFER AREA
 - PUMPING POWER
 - TONNAGE OF SALT
 - POWER REQUIRED FOR ACTIVE DEVICES

- STATE-OF-THE-ART
 - REASONABLE RISK AND UNCERTAINTY
 - OPERATING EXPERIENCE
 - EXPERIMENTAL DATA

- RELIABILITY

4.3 Unit Cost Data

The unit costs for the major components in the several design concepts under consideration are listed in Table 4.3-1 along with information sources. C-E manufacturing resources were drawn upon to develop this cost data for the preliminary evaluation. In particular the Business Development Department in the Nuclear Power System Division gathered representative costs from various suppliers. Supplementary information was obtained from the Special Products Estimating Department of the Fossil Power System Division. A representative cost was selected after this data was compared with the Stearns-Roger data (35), some of which was used directly.

At the outset of the initial design effort a rectangular tank was sized within the 4 m x 4 m x 12 m (13'x13'x40') envelope established for rail-shippable units. Most of the candidate design concepts were able to use this design. An estimated sell price of \$63,000 per tank or \$0.96/lb for the estimated 65800 lb weight was obtained.

Field fabricated tanks made most sense for the Chubb boiler tank, the oil/rock system, and the later stages of the direct contact heat exchange systems using the PCM drop heat exchanger. The material cost of \$0.75/lb was provided by Reference (35). The cost was then doubled to account for the cost of installation. The multiplier is based on Guthrie's module costing approach described in Reference (36).

The macroencapsulation concept requires pressure vessel to contain the condensing and boiling steam. The shop-fabricable, rail-shippable groundrules results in a 4 m (13 ft) diameter vessel, 12 m (40 ft) long. C-E's Special Products Estimating Department provided a cost of \$1.50/lb for a carbon steel vessel designed to ASME B&PV Code, Section VIII.

Several heat-exchanger tube bundles were roughly sized based on the Barstow plant components. These included straight-tube and "U"-tube superheaters, boilers, reboilers and preheaters. Preliminary estimated selling prices for carbon steel units were estimated in the range

TABLE 4.3-1
UNIT COST DATA FOR CONCEPT COST ESTIMATING

<u>COMPONENT</u>	<u>UNIT COST</u>	<u>SOURCE/DESCRIPTION</u>
● TANKS		
- SHOP FAB.	\$63,000/TANK (\$0.96/lb)	C-E/13'x13'x40' RECTANGULAR TANK
- FIELD FAB.	\$1.50/lb	\$1.50 - APPROXIMATE INSTALLED COST BASED ON S-R* \$0.75 FOR MATERIAL COST ONLY
● PRESSURE VESSEL		
- SHOP FAB.	\$1.50/lb	C-E/VESSELS 2-1/2"-5" THICK, CS, DESIGNED TO ASME CODE SEC. VIII, DIV. I
● HEAT EXCHANGERS		
- SHELL & TUBE	\$20/ft ² \$25/ft ²	C-E & S-R/CARBON STEEL S-R/CHROME MOLY.
- TUBE BUNDLE ONLY	\$12/ft ²	C-E & S-R/CARBON STEEL
- FINNED TUBE	\$2.50/ft ²	S-R/FIN AREA INCLUDED
- COILED	\$12/ft ²	C&W/1977 PURCHASE PRICE ESCALATED TO 1980
● PIPING	\$0.77/lb	C-E/AVERAGE PRICE FOR CARBON STEEL SCH. 40 PIPE IN THE RANGE OF 2"-14" OD
● PUMPS	\$400/hp	C-E/BASED ON 250 hp CENTRIFUGAL PUMP PLUS MOTOR, SINGLE SPEED, CARBON STEEL

* S-R = STEARNS-ROGER SERVICES, INC., REFERENCE (35)

TABLE 4.3-1 (CONTINUED)

<u>COMPONENT</u>	<u>UNIT COST</u>	<u>SOURCE/DESCRIPTION</u>
● PCM		
- NaOH/NaNO ₃ EUTECTIC	\$0.165/lb	S-R* <u>AND CHEMICAL MARKETING REPORTER</u> (8/7/80)
- NaOH/NaBO ₂ EUTECTIC	\$0.29/lb	
● HEAT TRANSFER FLUIDS		
- CALORIA	\$1.50/gal	SANDIA
- BIPHENYL	\$1.45/lb	S-R
- Pb.Bi	\$1.70/lb	S-R
● SCRAPER UNITS	\$1500-\$2000/ea.	C-E/BASED ON COST OF MAJOR COMPONENTS
● PCM CANS	\$1 - \$4/ea.	CHUBB - \$1/ \$4 - ASSUMED UPPER BOUND
● ROCK	\$10 - \$15/ton	SANDIA/\$15 USED - INCLUDES TRANSPORTATION

* S-R =STEARNS-ROGER SERVICES, INC., REFERENCE (35)

\$13-18/ft² of heat transfer area. The data in Reference (35) indicates a \$20-25/ft² for shell and tube heat exchangers. Based on this input, \$20/ft² was elected as an appropriate and representative cost value. For heat exchangers using chrome moly steel, as in the case of the lead-bismuth direct contact system, a cost of \$25/ft² from Reference (35) was used. Some concepts require only the tube bundle since the heat exchanger is placed in the containment tank or vessel. Contact with both C-E Business Development Department and Stearns-Roger Services, Inc. indicated that the tube bundle cost is expected to be approximately 60% of the cost of a shell-and-tube heat exchanger. Therefore, a \$12/ft² cost was selected for the carbon steel tube bundle costs.

Reference (35) provides a cost of \$2.50/ft² for finned-tube heat exchangers. The heat transfer area includes the total fin area and the exposed tube area. The cost were based on air dump heat exchangers in which the cost of the enclosing shell is negligible. Consequently, the value can be applied to just the bundle. The direct contact heat exchange concepts and the mechanical scraper systems used the finned tube bundles in the PCM containment tank/or the charging process.

The unit cost for coiled tubing is based on Comstock and Wescott's experience with purchasing coiled tubing for a demonstration latent heat TES device. Unit cost data are given in Reference (1) for coiled tubing in 1977 Dollars. This cost was escalated 30% to get it in 1980 Dollars, and then increased approximately 50% to include the cost of headers and to add a degree of conservatism to the cost estimate.

A range of pipe sizes from 2" to 14" O.D., schedule 40, were provided to the Business Development Department. Prices for ASTM A106 Grade B carbon steel were obtained in 1980 Dollars. The variation on a price per pound basis was from \$0.85-0.56/lb. An average value of \$0.77/lb was adopted for the cost comparison.

The cost for the two salts considered in this design were based mainly on data provided in Reference (35). The details of the values for the mixtures are explained in Appendix II. The cost of the PCM can used

in the Chubb boiler tank and the macroencapsulation concepts were estimated at \$1.00/can by Chubb. A \$4/can value was used as an upper bound to the cost.

The cost estimate for the bayonet steam generator/scrapper unit in the mechanical scrapper concept was developed by considering the cost of the major components of the unit. The components considered were: motor and gear box, square cross-sectional scrapper spring, and heat exchange piping. Estimates for the motor and gear box and the scrapper spring are based on vendor quotes.* The cost for the heat exchanger piping is based on conversations with C-E cost estimators. The cost of these components is approximately \$1000.00. This cost was increased 50 to 100% to account for the cost of actually fabricating these units. Thus, a unit cost range of \$1500.00 to \$2000.00 is estimated for these units.

4.4 Selection Results

The unit cost data were applied to the most promising concepts described in Section 3. The results are summarized in Tables 4.4-1 through 4.4-4. The oil/rock storage system summary is provided on Table 4.4-5.

Two sizes for the tube intensive concept are shown on Table 4.4-1. The conservative design is based on a simple but very conservative sizing procedure. The more optimistic design results from a detailed performance evaluation of the unit through its daily duty cycle using the computer program TESST. Towards the end of discharge the steam conditions fall below the saturated steam target, resulting in a deficit that is 4.3% of rated capacity. The power supplied was costed at \$4.90 per MBtu and capitalized at 15%. The benefits that could be obtained with heat transfer enhancement was not factored in at the concept selection stage; however, further improvements in the design were still expected.

- * (1) Westinghouse Electric Corporation
- (2) General Electric Company, Industrial Sales Division
- (3) Associated Spring, Baines Group, Inc.

TABLE 4.4-1

DESIGN AND COST SUMMARY OF THE TUBE INTENSIVE CONCEPT

COMPONENT	CONSERVATIVE DESIGN		IMPROVED DESIGN	
	QUANTITY	COST	QUANTITY	COST
CONTAINMENT TANKS (13'x13'x40')	8	\$504,000	6	\$378,000
PCM (NaOH/NaNO ₃)	5.36x10 ⁶ lb	\$883,000	3.53x10 ⁶ lb	\$582,000
HEAT EXCHANGERS (COILED OR SERPENTINE TUBES 0.25" OD)	96,540 ft ²	\$1,158,000	73300 ft ²	\$888,000
OTHER EQUIPMENT	--		--	
DEFICIT POWER COSTS	--			\$150,000
TOTAL COST		\$2,545,000		\$1,998,000

The concepts which employ encapsulation of the PCM are summarized on Table 4.4-2. The Chubb boiler tank concept employed a single large containment tank which might operate under vacuum conditions or under pressure, depending on the required pressure for the biphenyl heat transfer fluid. The PCM is encapsulated in cans, thus requiring the sodium metaborate salt mixture. Due to the additional heat transfer fluid and heat exchangers, the resultant component costs are moderately high to high. The range in cost reflects an uncertainty about the cost of the encapsulation cans and the necessity of a vacuum or pressure vessel. The lower containment tank cost is for the vacuum tank. Further effort on this concept was stopped after the second step of the selection process.

The macroencapsulation concept also uses the sodium metaborate sealed in cans. However, the steam/water condenses and boils directly on the can surface, requiring a pressure vessel containment. Because of the operating pressure levels and the number of tanks required to enclose the PCM, a very high cost is incurred. No further effort was expended on this concept. It should be noted that this concept would not be so unattractive in application where low-pressure charging and discharging fluids are employed.

The microencapsulation of the PCM in a porous carrier is also listed on Table 4.4-2. Since both hot and cold containment tanks are required, a large cost is incurred. The porous material is also extremely costly. The initial rough sizing of this concept indicated the very high cost, and no further effort expended.

The various concepts using a direct contact heat exchanger are shown on Table 4.4-3. During the initial sizing effort, the reflux oil and the lead-bismuth system using the PCM drop heat exchanger were developed using modular tanks and high PCM utilization factors. Based on these costs further effort on direct contact was selected, but the lead-bismuth system was abandoned in favor of the oil intermediary. During the subsequent effort a circulating-oil version was developed paralleling the reflux system, and a PCM-drop/oil system patterned on the lead-bismuth

TABLE 4.4-2 DESIGN AND COST SUMMARIES OF ENCAPSULATION CONCEPTS

COMPONENT	CHUBB CONCEPT		MACROENCAPSULATION		FLUID BED POROUS CARRIER	
	QUANTITY	COST	QUANTITY	COST	QUANTITY	COST
CONTAINMENT TANKS	1 - 50' Dia. 35' Ht.	\$ 510,000 - 2,199,000	14 (13' dia., 40' length)	\$9,800,000	36 -13'x13'x40' Tanks	\$2,270,000
PCM (NaOH/NaBO ₂)	4.28x10 ⁶ lb	\$1,240,000	4.28x10 ⁶ lb	\$1,240,000	4.50x10 ⁶ lb NaOH/NaNO ₃	\$ 743,000
HEAT TRANSFER FLUID	Biphenyl ~ 50,000 gal	\$ 500,000			Carrier 4.5x10 ⁶ lb	\$ 2,250,000
HEAT EXCHANGERS						
CHARGE	27,300 ft ²	\$ 328,000				
DISCHARGE	13,600 ft ²	\$ 163,000				
OTHER EQUIPMENT						
	PCM Cans	\$ 290,000- \$1,160,000	PCM Cans	\$ 600,000- \$1,700,000		
	Hex Cage Sprayer Glycol Loop	\$ 500,000				
TOTAL COST		\$3,531,000- \$6,090,000		\$11,640,000 \$12,740,000		\$6,260,000

TABLE 4.4-3(a)

DESIGN AND COST SUMMARIES FOR DIRECT CONTACT HEAT EXCHANGE
PCM DROP CONCEPTS

Component	Oil (Biphenyl)		Liquid Metal (Pb-Bi)	
	Quantity	Cost	Quantity	Cost
Containment Tank 42' dia., 42' ht.	1	\$180,000	1	\$180,000
PCM (NaOH/NaBO ₂)	4.51x10 ⁶ lb	\$1,310,000	4.51x10 ⁶ lb	\$1,310,000
Heat Transfer Fluid	29,200 lb	\$ 42,400	501,000 lb	\$851,000
Heat Exchangers Charge (Finned tubes)	42900 ft ²	\$107,000	42,900 ft ²	\$107,000
Discharge (Shell & tube)	23400 ft ²	\$468,000	7,300 ft ²	\$183,000
Other Equipment				
Separator		\$250,000		\$100,000
Fluid Pump		\$100,000		\$200,000
PCM Pump		\$100,000		\$100,000
Piping		\$ 17,000		\$ 25,000
Lower Temperature Heat Exchanger		\$ 10,000		\$ 10,000
		-----		-----
TOTAL COST		\$2,584,000		\$3,070,000

TABLE 4.4-3 (b)

DESIGN AND COST SUMMARIES FOR DIRECT CONTACT HEAT EXCHANGE OIL INTERMEDIARY

Component	Reflux Oil		Circulating Oil	
	Quantity	Cost	Quantity	Cost
Containment Tanks (13'x13'x41.8')	10	\$630,000	10	\$630,000
PCM (NaOH/NaBO ₂)	7.38x10 ⁶ lb	\$2,140,000	7.38x10 ⁶ lb	\$2,140,000
Heat Transfer Fluid (Biphenyl)	4,000 lb	\$ 5,800	443,000	\$642,000
Heat Exchangers				
Charge (finned tubes)	42,900 ft ²	\$107,000	42,900 ft ²	\$107,000
Discharge (tube bundle)	26,200 ft ²	\$314,000	23,400 ft ²	\$281,000
Other Equipment				
Oil Expansion Tank		--	1 tank	\$ 63,000
Agitator Pumps		\$ 75,000		\$450,000
Oil Purifier		\$150,000		--
TOTAL COST		\$3,422,000		\$4,313,000

concept was also developed. A single large tank was elected for the latter for PCM containment over the modular rectangular tanks; this is reflected in the final designs and costs. The lead-bismuth design was also updated to insure proper comparison. The costs did improve but did not invalidate the original selection decision to drop the lead-bismuth concept. The PCM-drop/oil concept does show the best costs of all the direct contact concepts and was used in the final comparison for preferred-concept selection.

The two mechanical scraper concepts are listed on Table 4.4-4. The initial sizing effort was developed with an optimistic value for volume utilization. Both mechanical concepts displayed very good costs and were selected for further development. However, the vertical scraper design was selected for the follow-on stage as a generic representation of mechanical systems. During the subsequent effort the volume utilization uncertainty was examined and a more realistic value of 60% was employed, resulting in an increase in the cost estimate. The parasitic power cost is based on a \$4.90 per MBtu cost, reflecting \$30 per barrel oil and capitalized at 15%.

The oil/rock costs which were developed during the final stages of concept selection serve as a benchmark for the cost comparison. The literature indicated uncertainty in the volume utilization of the thermocline storage, so bounding values were assumed to define a representative range in the costs. The results are listed in Table 4.4-5.

The three selected concepts for final comparisons are shown on Table 4.4-6 along with the oil/rock benchmark. The costs for each concept are judged along a spectrum using the term expected to mean a reasonable representative cost. Optimistic cost implies a lower limit and an expectation that cost would increase as the design uncertainties are investigated. The conservative figures generally reflect conservative sizing and costing, and with further effort, the costs may be expected to decrease. It should be noted that the cost of foundations and bottom insulation is not included in these costs. In the case of the three PCM systems these costs will not differ greatly. The oil/rock system,

TABLE 4.4-4
DESIGN AND COST SUMMARY OF MECHANICAL SCRAPER CONCEPT

COMPONENT	VERTICAL SCRAPER		HORIZONTAL SCRAPER	
	QUANTITY	COST, \$	QUANTITY	COST, \$
CONTAINMENT TANKS (13'x13'x40')	7-10	\$441,000-\$630,000	7-10	\$441,000-\$630,000
PCM (NaOH/NaNO ₃)	4.7-7.1 x 10 ⁶ lb	\$658,000-\$994,000	4.7-7.6 x 10 ⁶ lb	\$658,000-\$994,000
HEAT EXCHANGERS CHARGE (FINNED TUBE)	35,500 ft ²	\$89,000	42900 ft ²	\$107,000
DISCHARGE-SCRAPER MODULES	300	\$450,000-\$600,000	300	\$450,000-\$600,000
PARASITIC POWER		\$100,000		\$100,000
TOTAL COST	90% UTILIZATION: 60% UTILIZATION:	\$1,738,000-\$1,888,000 \$2,263,000-\$2,413,000	90% UTILIZATION: 60% UTILIZATION:	\$1,756,000-\$1,906,000 \$2,281,000-\$2,431,000

TABLE 4.4-5

DESIGN AND COST SUMMARY OF THE OIL/ROCK BENCHMARK

COMPONENT	80% UTILIZATION		60% UTILIZATION	
	QUANTITY	COST	QUANTITY	COST
CONTAINMENT TANK	1 - 74' Dia. 50' Ht.	\$657,000	1 - 81.5' Dia. 55' Ht.	\$756,000
STORAGE MEDIUM (ROCKS)	13,400 tons	\$201,000	17,700 tons	\$266,000
HEAT TRANSFER FLUID (CALORIA)	402,200 gal	\$603,000	532,000 gal	\$798,000
HEAT EXCHANGER	28,120 ft ²	\$562,000	28,120 ft ²	\$562,000
OTHER EQUIPMENT PUMPS	1 - 135 hp	\$ 54,000	1 - 135 hp	\$ 54,000
PIPING (16" O.D., Sch 40)	400'	\$ 26,000	400'	\$ 26,000
TOTAL COST		\$2,104,000		\$2,462,000

TABLE 4.4-6
FINAL CONCEPT SELECTION

	<u>CONSERVATIVE COST</u>	<u>EXPECTED COST</u>	<u>OPTIMISTIC COST</u>
TUBE INTENSIVE	$\$2.55 \times 10^6$	$\$2.0 \times 10^6$	
MECHANICAL		$\$2.32 \times 10^6$	$\$1.8 \times 10^6$
DIRECT CONTACT			$\$2.58 \times 10^6$
OIL/ROCK		$\$2.1-2.5 \times 10^6$	

however, has a substantially higher bottom area and a higher bottom loading pressure, which will make its costs relatively higher.

The higher tube intensive costs were judged conservative, particularly since more detailed calculations on the unit indicated large reductions. The potential for further reductions exists because of the possibility of augmented heat transfer techniques. At the time of selection, the analysis of these methods were incomplete and would have been judged slightly on the optimistic side. The data indicated than an 60% utilization factor for the mechanical concept is conservative. However, this value is expected to be representative. The 90% utilization factor leads to a very optimistic cost for the system. The conservatism in the component cost may be in the details of the mechanical arrangement. Further design effort could reduce this cost somewhat. The direct contact system was judged to be representative (perhaps slightly optimistic), based on the design procedure and supporting data base.

The cost of the major components of these concepts is fairly comparable to the extent that uncertainties in the design process and the cost data base could outweigh differences. The tube intensive concept was selected since the cost trend was favorable and the potential for further improvements exists. The tube intensive is an existing technology requiring very little in the way of a development program. The reliability of a purely passive system is also extremely attractive. The latter two considerations are very important when the overall program schedule is considered. The possible follow-on to this concept selection is a 30-month effort on the SRE from design to testing. The selected tube intensive concept has the highest probability of meeting this schedule successfully.

Both the mechanical and the direct contact concepts still appear attractive. Base technology programs should still consider developing these concepts in order to reduce the fundamental design uncertainties. A more definitive assessment could then be made.

5.0 CONCEPTUAL DESIGN AND COST/PERFORMANCE ESTIMATES

5.1 Introduction

The final result of the conceptual design study for the selected tube intensive TESS is presented in this section. The concept selection was based on bare tube heat transfer tubes. The parallel task on augmented heat transfer indicated benefits in reducing the amount of heat transfer tubing. Based on these results, a design concept is developed which provides increased heat transfer and tube support. The mechanical design of the tube, tube bundle and containment tank is pursued. Some consideration of large, field fabricated vs. small, shop-fabricable, rail-shippable containment tanks is given. Tank design is developed to minimize the unavailable volume of PCM. The tube bundle is developed with consideration of cost and ease of fabrication, assembly and maintenance, particularly with regard to tube plugging or repairing.

The performance evaluation is conducted in parallel to the mechanical design. The major concern of this activity is flow distribution during discharge. This is assessed with calculations concerning the hydraulic stability using the Ledinegg static stability criterion. Following this, the detailed temperature profiles for the PCM and the charging and discharging steams are obtained. The extent to which the design conditions are met is assessed, and recommendations made.

Drawings and specifications are produced and a concept cost estimate is made. The cost includes an estimate for the foundation, thus giving a total TES subsystem island cost. The final drawings of the tube bundle module and containment tank are in Appendix I along with a tabulation of the design data.

5.2 Subsystem Requirements

The performance requirements for the conceptual design of the TESS are the same as those used for the preliminary sizing in the concept selection. These are described in Section 3.1 and listed in Table 3.1-1. The daily

solar duty cycle is shown on Figure 3.1-1. The subsystem was designed to satisfy these performance requirements. The TESS will handle the fully charging and discharging mode of operation and the transition between the modes. Since the TESS is coupled with a steam cooled receiver and produces saturated steam during discharge, a simultaneous charging/discharging mode of operation was deemed unnecessary. The same effect could be obtained by appropriate valving around the TESS and provide the process with its demand.

The major design requirements imposed on subsystem:

- 1) ability to drain the water in the heat transfer tubes
- 2) ability to drain the PCM
- 3) removable tube bundle for tube plugging or repairs
- 4) charging steam enters the unit at the top and condenses in a general downhill direction
- 5) discharging water enters the unit at the bottom and boils in a general uphill direction
- 6) heat losses in a 24-hour period will be limited to 2% of the heated capacity.

Further design requirements were not established at this conceptual design stage as a specific process heat application was not identified.

5.3 Major Configuration Choices

The major configuration choices considered tank configuration and size, tube size, and heat transfer enhancement. Complete optimization studies of these were not conducted, but some considerations were given in order to establish the best direction for the conceptual design.

5.3.1 Modularization

At the outset of the conceptual design effort the containment tank size and configuration was addressed. Both shop-fabricated, rail-shippable, and field-fabricated vessels were briefly considered. Since vertical

cylindrical tanks take advantage of the hoop stress, they provide potentially large cost savings. From a heat transfer point of view, the height-to-diameter ratio should be in the range 0.5 to 1.0. To contain the PCM and the heat exchanger a vessel with diameter in the range of 12 m to 15 m (38' to 50') and height in the range of 7 m to 12 m (24' to 40') is required. The placement of a regular pattern of serpentine tube bundles would leave pockets of PCM volume that are remote from the tube bundle. This unavailable volume could be minimized by keeping the horizontal runs of the serpentine tubes to a minimum: 1.2 m to 1.8 m (4' to 6').

The tube bundle height is another concern since the tube bundle support structure must bear the load of the entire tube and the PCM frozen onto the tube. Both these design concerns can be reduced by going to a wide, squat tank with a diameter approximately 18 m to 21 m (60' to 70') and height from 3.0 m to 4.6 m (10' to 15').

Small cylindrical tanks, 4 m (13') in diameter, in a horizontal orientation were considered. Very rough preliminary sizing calculations indicated a relatively thick-walled shell, 2.5 cm to 5.0 cm (1" to 2"). In addition, the level change of the PCM due to freezing only allows a bundle height approximately 2/3 of the diameter in order to keep the heat exchanger always submerged in the PCM. Furthermore, the horizontal runs of the serpentine depend on the height across the circular cross section. To improve the cross section within the rail-shippable groundrule of 4 m x 4 m (13' x 13'), the maximum utilization is obtained with a square cross section.

At this stage it was decided that the design development should be pursued with the shop-fabricable, rail-shippable module. The quality control with shop fabrication is much greater than field fabrication; this is most important for the early stages of the commercialization of a concept. On the other hand, the large field-fabricated tank would be more efficient in size and volume utilization for larger thermal capacities than that considered in this effort. Section 7 discusses this aspect and even offers a conceptual arrangement of modular tube bundles within a large tank.

A further step in modularization was made. To facilitate fabrication and potential tube plugging or replacement, the tank is divided into a number of individual tube bundles each with its own inlet and outlet headers. Five bundles were selected as a reasonable division of the 12 m (40') tank with tractable dimension for handling of the individual bundles.

Each tube bundle is an assembly of parallel serpentine tubes. The method of heat transfer enhancement employed, discussed in Section 5.3.3 below, requires that each tube assembly of the tube bundle is a single tube.

In steam generator trade-offs among heat transfer area, tube size, and number of tubes, the smallest required heat transfer area and the smallest tube sizes are favored. However, industrial experience has been that the cost of a large multitude of very small tubes begins to outweigh the savings of reduced heat transfer. A 15.9 cm (0.625") O.D. tube is generally the smallest used. This experience has been applied to the TES design. Contact with tubing suppliers through C-E purchasing organizations yielded that the 15.9 cm (0.625") O.D. tube is generally the smallest electric resistance welded (ERW) tube fabricated. At lower diameters the tubing is usually the much-more-expensive drawn tubing. Very small ERW tubes would require special tooling and equipment, thus leading to higher unit costs for the tubing.

Another aspect of the tube diameter is related to the quality of the feedwater. Very small diameter tubes, particularly when used in once-through steam generators, may be clogged by solids plating out. From this point of view, the selected tube may be considered a prudent minimum. Finally, the results of the heat transfer enhancement study presented in Section 3.4.2 and Appendix VI indicate that the required heat transfer length is fairly insensitive to tube diameter. Thus, the minimum cost of tubing would result from the minimum tube diameter.

The most important determination of the acceptability of tube diameter and number of tubes is the concern for flow distribution among parallel

paths through a steam generator, i.e., through the discharge portion of the daily cycle in the TES subsystem. This issue is addressed in Section 5.5.3.

5.3.2 Tank Design

The examination of the tank configuration resulted in the selection of the rectangular tank. The emplacement of the tube bundle inside the tank would result in a large amount of PCM in the region between the inside tees, but remote from the heat exchanger. This unavailable PCM added about \$100,000 to the cost. To reduce this cost, the support structure was moved so that it would be external to the tank. To maximize the internal dimensions of the tank within the rail-shippable envelope of 4 m (13'), the support tees were examined closely. The 20 cm (8") tee section in the initial design (see Appendix XI) were replaced with 10 cm (4") tees, 47 cm (22.5") on-centers around the tank periphery. This allows flat internal walls approximately 3.8 m (12.3') apart.

The tank walls were designed to resist the load imposed by the hydrostatic load of the PCM. ASME B&PV code allowables were obtained from Section VIII. There is no specific analytical procedure recommended by the code for rectangular tanks. The walls of the tank are formed of plate and structural tees which run vertically to reinforce the plate on the side walls. Gusset plates are run perpendicular to the plate and tees to additionally reinforce the plate in the opposite direction. Each section of tank wall was analyzed as an unequally wide flange beam. The maximum bending moment is given by Reference (37).

$$M_{\max} = 0.064 \omega L^2$$

where L is the beam length and ω is the hydrostatic load of the PCM at the bottom of the tank. The peak stress is obtained from the bending moment and the section modulus. The allowable bending stress is related to the allowable stress intensity given in Table UCS-23 of Section VIII of the ASME code by a shape factor. A value of 1.14 was obtained for this factor from Reference (38).

The plate at the lower section of the tank was evaluated against bending at the center. The maximum primary bending stress at the center of the plate is given by Reference (37).

$$s_b = \beta \frac{W b^2}{t^2}$$

where t = thickness
 b = side length
and β = is a geometric factor given in Reference (37).

The tank is set on Foamglas insulation which has a compressive strength of 690 kPa (100 psi) (39). The combined weight of the tanks including the weight of the salt and coils will exert a distributed load of 69 kPa (10 psi) on the insulation when the tank is evenly supported by the insulation as the design provides.

The side walls react the forces into the floor and roof of the tank. The roof of the tank is also designed to withstand a 2.9 kPa (60 lb/ft²) load per the AISC code.

5.3.3 Heat Transfer Enhancement

The analysis of enhanced heat transfer using extended surfaces indicates that large reductions in the required total tube length could be achieved. Preliminary calculations, described in Section 3.4.2 and discussed in detail in Appendix VI, considered radial fins (90° apart), water walls, and screening concepts. The calculations were performed for a 10 cm x 10 cm (4" x 4") tube spacing and extended surfaces of carbon steel. These results indicate that the use of fins extending in one direction, such as screens interspersed between the tubes or a 'water wall', give a significant reduction in tube length required, by as much as a factor of 2 or 3. The PCM is however, underutilized with a large fraction of the PCM left un-frozen. Further studies on radial fins and water walls, (or their equivalent), perpendicular to the walls showed additional significant benefits with respect to both tube length reduction

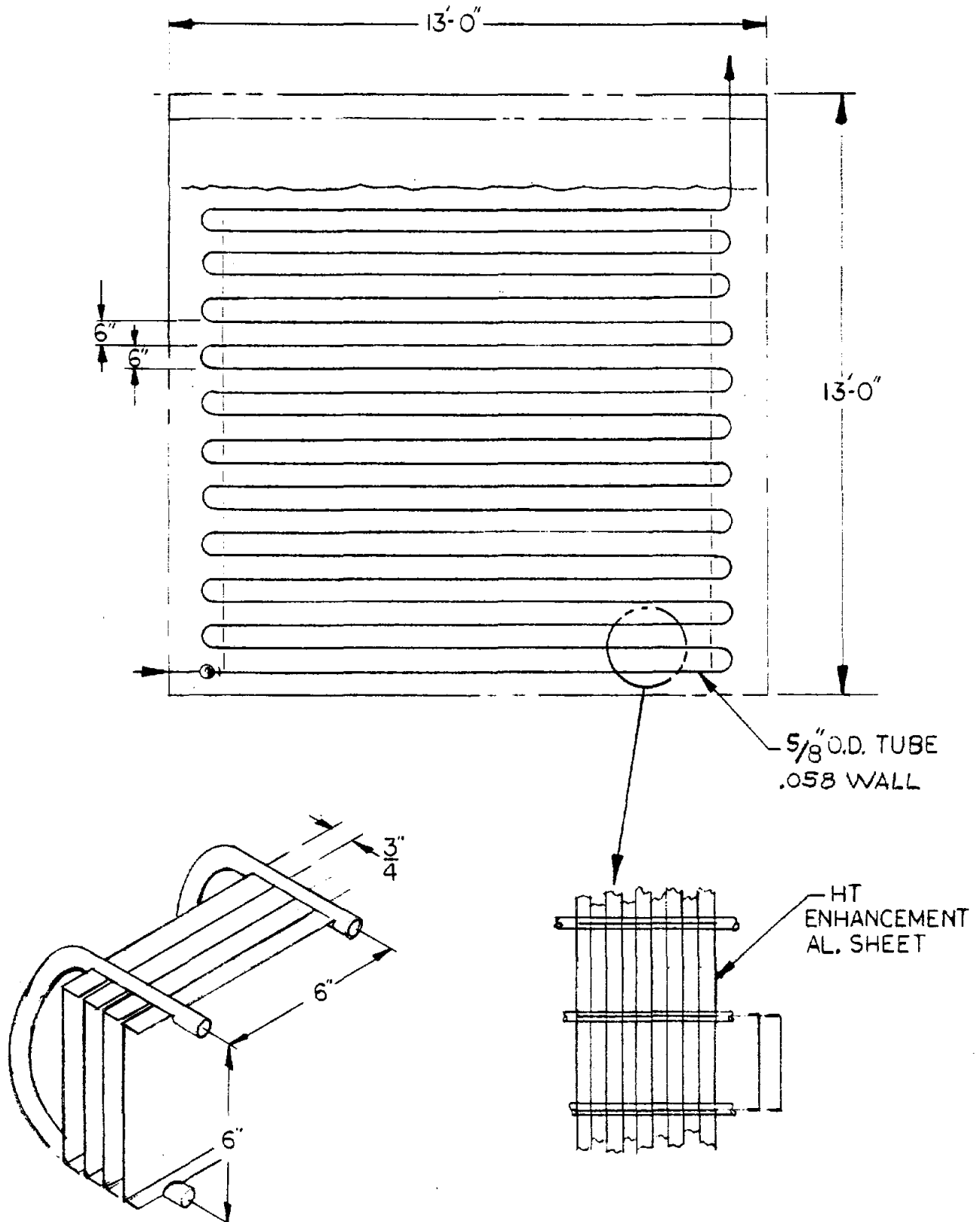
and increased PCM utilization. The calculations indicate that fins extending in two directions relative to the heat transfer tubes are required in order to communicate completely with the phase change material.

The specific configurations studied that could accomplish this are relatively complex and would be difficult or costly to fabricate. From the results discussed above and described in Appendix VI, an equivalently effective fin configuration in the form of channel sections was selected. These sections are inserted between two horizontal runs of a serpentine tube and connect a number of the tube banks in the horizontal direction. The configuration is shown in Figure 5.3.3.1. The channels are inserted every 19 mm (3/4"), the dimension of the flanges. This was found to be about optimum with respect to heat transfer benefits and materials requirements. A range of 12.7-24 mm (1/2" to 1") was considered. The heat transfer calculations indicate that steel channels with 10 cm (4") web (i.e., distance between the horizontal runs of the serpentine tube) and 10 cm (4") between tube tanks would provide the 148 MWh target capacity, the peak discharge rate of 30 MW at full discharge conditions, and freeze virtually all the PCM. The use of aluminum allows the dimensions to extend to 15.2 cm x 15.2 cm (6" x 6"), with a corresponding reduction in tube length requirements. These calculations are described in more detail in Appendix VI.

Use of all aluminum channels would require ~ 39,600 m (130,000 ft) of enhanced tubing. The structural abilities of aluminum in the 450-500°F temperature range are somewhat doubtful in providing tube support, so steel channels will be interspersed for tube support. Since the steel does not provide as efficient an enhancement medium as aluminum, the tube length requirements are increased somewhat. Employing steel for every tenth channel increases the tube length requirement by ~5% to 43,600 m (143,000 ft) of enhanced tubing.

The analysis of the freeze patterns around the channel is actually a three-dimensional problem. Since the FREEZE model is only two dimensional, estimates of the effectiveness of the selected concept were made in two

Figure 5.3.3-1
REFERENCE HEAT TRANSFER ENHANCEMENT CONCEPT



steps. The freezing patterns of the PCM around the surface joined by the tube plus the channel flanges were calculated. The freeze patterns around the webbing of the channel were analyzed separately. The calculations using FREEZE were performed for a variety of channel flange and web spacings and for aluminum and steel channels. The results of these calculations were married to obtain an effective linear heat input to the tubes. At the time when both the heat rate and integrated heat rate are proportional to the 30 MW discharge rate and 148 MWh capacity, the fraction of PCM frozen is checked. The tube spacing is adjusted to bring the fraction near unity at the time of the proper heat rate and integrated heat rate. It is then that the peak discharge rate is applied to the local heat rate and the total tube length is determined. The results of these calculations are discussed in Appendix VI.

5.4 Design Description

The total TES subsystem requires 8 rectangular containment tanks bearing the PCM and heat exchanger to provide the target 148 MWh capacity and the peak charge and discharge rates of 30 MW. These are shown in the three drawings in Appendix I. The eight tanks are installed next to each other in 4-tank by 2-tank array to minimize the heat loss surface, and consequently the amount of insulation required. Mineral fiber insulation is wrapped around the entire array with an aluminum-lagging outer covering at the sides and top. The tanks rest on Foamglas insulation which has a bearing strength of 100 psi.

The steam line from the solar receiver field enters the TESS and is headered into four lines, each of which penetrates a tank (see Drawing 3, Appendix I). The steam lines emerge from the first set of tanks and immediately enter the second set. The steam flows through the heat exchanger tube bundle, emerging as condensate. Five condensate lines penetrate each tank. These are collected in 3 main condensate lines which are headered together into a single condensate line. During discharge, saturated water enters the eight tanks through the condensate lines. The generated steam is collected in the four main steam headers and collected into the main steam line.

5.4.1 TES Module

The TES module is a single rectangular tank containing the PCM and the heat exchanger. The tank walls are made of 9.5 mm (0.375") carbon steel plates which are supported by tees (WT 4-29) spaced 57 cm (22.5") around the outer periphery of the tank (see Drawing 2, Appendix I). For additional support of the walls, gusset plates, 5 cm x 57 cm x 0.64 cm (2" x 22.5" x 0.25"), are run perpendicular to the wall and the tees. Four gusset plates are placed at regular intervals up the side walls. The gross dimensions of the tank including the support tees are 4 m x 4 m x 11.7 m (13' x 13' x 38'-4½").

Angle sections run around the outer periphery of the tank at the top; this provides a seating lip for the tank cover. The cover is composed of five 6.35 mm (0.25") thick plates which are welded to the support lip. Welded construction was selected since the C&W experience with sodium hydroxide/sodium nitrate mixtures is that surface tension causes the PCM to creep up along the walls and out bolted joints. There is a vent pipe in the cover to allow ambient air to fill the ullage during discharging and to be pushed out during charging. The moisture in the ambient air is also required for the chemical stability of the PCM (see Section 3.2).

The steam header penetrates the side of each tank near the top, runs the entire length of the tank, and emerges on the opposite end. The five condensate headers at the bottom of each tank penetrate the tank sides. These lines are externally headered.

Within each tank there are five tube bundles. This is shown in Drawing 2 in Appendix I and the tube bundle details are shown in Drawing 1. Each tube bundle is composed of a parallel array of 15 single serpentine tubes 15.2 cm (6") apart. Each tube is connected to the steam header running at the top of the tank and the condensate header at the bottom. The condensate header for the bundle penetrates the tank and merges with the header from the other four tube bundles outside the tank.

Each serpentine tube is a 1.6 cm (0.625") O.D. electric resistance welded tube, 1.5 mm (0.058") minimum wall, and it is formed from a 78 m (257') tube length. There are 21 horizontal runs 3.5 m (11.5') long and 20 bends on a 7.6 cm (3") radius. The horizontal runs are therefore separated by 15.2 cm (6"). Inserted between the horizontal runs and connecting laterally to all tubes within the bundle, are aluminum and steel channel sections. The aluminum channels have a 15.2 cm (6") web and 1.9 cm (0.75") flanges and serve as extended heat transfer surfaces. The top and bottom flanges have grooves rolled in for the seating of the tubes. Holes are also punched in the flanges to allow the movement of PCM during phase change and to allow the draining of the unit. Every tenth channel is made of steel to provide tube support. Elastic buckling calculations indicate that the steel fin could buckle, so dimples are rolled into the webbing to provide a strongback to the buckling load. The tube bundle rests on tee and angle sections, and the entire assembly is strapped together. The structure at the top of the bundle allows the bundle to be lifted and inserted into the tank during fabrication and maintenance operations that require removing the tube bundle. When the bundle sits in the tank, the top is 3.3 m (10.75') above the tank bottom so that it is totally below the minimum PCM level.

5.4.2 Instrumentation and Controls

Instrumentation and controls are required to monitor the rate of charge and discharge of the TESS, to control the state of the discharge steam, to match the discharge to the load demand, and to determine the state of charge of the TESS.

The present study has regarded the TESS as an independent element, without considering its interaction with the total system of which it is a part. The requirements for the study specified that the TESS is charged with dry saturated steam at 288°C (550°F) and discharged by introducing 232°C (450°F) saturated water. The stored heat is to be discharged as saturated steam at 232°C (450°F) that may contain up to 10% liquid. Heat from a fossil fuel burner may be used to bring the steam quality up to 1.0 or within a given specified tolerance range.

A complete control system and instrumentation to maintain output conditions and the state of the TESS under all conditions of operation including start-up, shut-down, and unusual transient conditions has not been designed. However, the basic control elements and instrumentation are shown schematically by Figure 5.4.2-1.

Charging Circuit

If the charging steam is delivered to the TESS at 288°C (550°F), dry and saturated, the rate of charge can be determined by measuring the flow rate and the temperature of the condensate discharged from the TESS. The total heat charged into the TESS during a daily cycle can be determined by the use of an integrating system.

The temperature of the condensate will vary as the TESS approaches the fully charged state, and can be used to control the rate of charging, or to terminate charging by means of a flow control, which can be located in the condensate discharge line to avoid throttling the steam entering the TESS.

Discharging Circuit

If the 232°C (450°F) liquid to the TESS during discharge is maintained at 2.91 MPa (422 psia) plus the pressure drop through the TESS, its entering enthalpy can be determined from pressure and temperature measurements. A pressure measurement may also be used to ensure that the inlet pressure is sufficient to provide for the ΔP through the TES module in addition to maintaining the saturation pressure at the outlet. It is assumed that this pressure is supplied by the receiver feed pump.

The enthalpy of the steam delivered to the load is also determined by its temperature and pressure. These, together with a flow measurement of the feed water, including that to the de-superheater, can be used to determine the rate of discharge and the total heat delivered over any time interval. Any auxiliary heating provided by a fossil fuel burner can be determined by fuel flow measurement and knowledge of the efficiency of the heater,

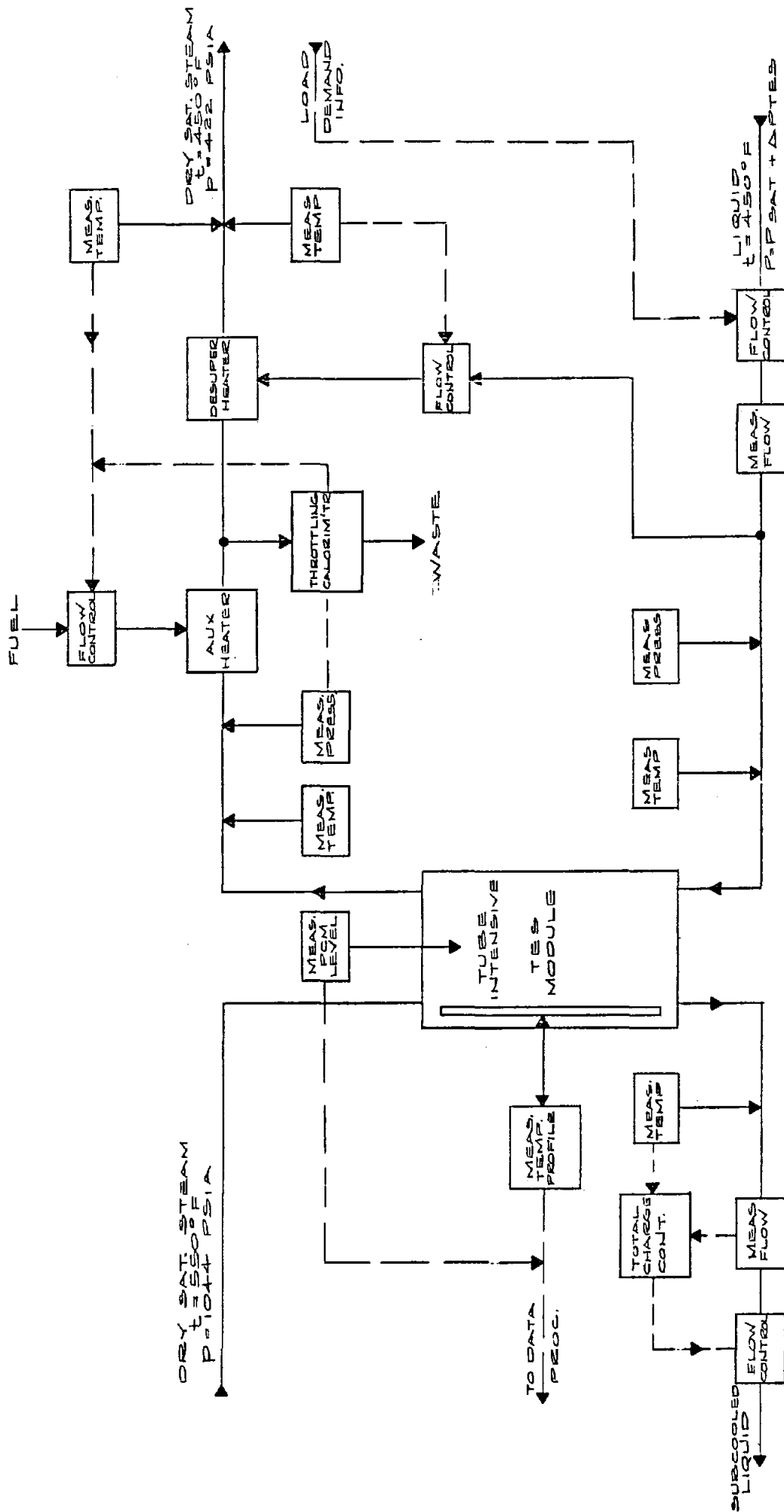


FIG 5.4.2-1
 CONTROL CONCEPT
 FOR
 DISTRIBUTED TUBE
 TESTS MODULE

and deducted from the total to determine the heat withdrawn from the TESS. Thermal losses must, of course, be taken into account.

At the start of the daily discharge period, the PCM in the upper part of the TES module will normally be liquid at a temperature between 288°C (550°F) and the fusion temperature of the PCM, 260°C (500°F) (see Figure 5.5.1-3), and the discharge steam will be superheated. To produce the 232°C (450°F) saturated state, a desuperheater can be used, which injects 232°C (450°F) saturated liquid from the feed line or feedwater from the process. The desuperheater is controlled by a temperature sensor located downstream from the injection point and a flow control valve. Pressure and temperature sensors at the outlet of the TESS are used to determine the point in the discharge cycle at which the temperature drops to the saturation value. From that point, a throttling calorimeter can be used to determine the percentage of moisture in the wet steam, and its output used to govern the firing rate of the auxiliary fossil fuel heater. (The throttling calorimeter, which expands the wet steam to a superheated vapor state at atmospheric pressure by a constant enthalpy process, is limited to a moisture content no greater than about 7%, and therefore cannot be used upstream of the heater.) As an alternative control of the auxiliary heater, a temperature sensor placed downstream of the heater would maintain a few degrees of superheat in the steam delivered to the load, which may be desirable to provide for downstream heat losses without producing condensation.

Leak Detection

Moisture entering the PCM (perhaps through small leaks in the heat exchanger) that could cause a significant corrosion rate might be detected by a hydrogen detector in the breather tube connecting the tank ullage with the ambient. As shown in Section 3.2, moisture that causes corrosion releases hydrogen in quantities which should be detectable. Alternatively, a periodic leak check could be made by introduction of a tracer gas such as helium into the steam and a detector in the ullage introduced through the breather tube.

If a leak is detected, it can be traced to a particular tank and tube bundle by means of the helium detector if provision is made for introducing helium into individual tube bundles.

TES Energy Content

The thermal energy content of the TES module is a necessary piece of operating information. This cannot be determined solely by measurement of energy input and output because of cumulative errors in measurement and inexact allowances for losses from the system. A method is required by which the energy content can be measured directly, continuously or periodically, so that the state of charge can be known with reasonable accuracy. A method which permits a measurement once during the daily cycle can provide a datum to which charge and discharge rates measured as described above can be referred to provide state-of-charge information at other times. Such a method is also needed to determine state-of-charge after non-operating periods.

Two methods have been considered for determining state-of-charge by measurements made on the TES module. The first is based on measurements of the volume of PCM in the tank. It is expected that the NaOH-NaNO₃ eutectic will undergo a density change from approximately $2.08 \times 10^3 \text{ kg/m}^3$ (130 lb/ft³) in the solid state to $1.76 \times 10^3 \text{ kg/m}^3$ (110 lb/ft³) in the liquid. The density change of the solid and liquid phases between 232°C (450°F) and the melting point and from the melting point to 288°C (550°F) total about 6% of that accompanying the phase change. The total volume of the PCM is related to the solid-liquid fraction and to the temperatures of the solid and liquid portions. The volume can be measured at a point in the daily cycle such as at the end of the charge period when the volume is maximum, and the top surface of the PCM is sure to be completely liquid. Volume can be measured by determining the position of the PCM surface, by means of a float, or by an optical or ultrasonic device operating through the air-breather opening at the top of the tank.

In order to take account of the volume changes of the solid and liquid portions of the PCM, if this should be necessary for the desired accuracy, the temperature of the upper surface of the liquid and of the solid at the bottom of the tank can be measured. The temperature of the solid-liquid interface is, of course, the melting point of the PCM. From these, the enthalpies of the solid and liquid can be estimated. The thermal expansions of the tank, the heat exchanger and other internal metal parts will affect the location of the PCM level, and must be taken into account.

The second method by which the energy content of the TESS can be determined would be useful in systems which are computer-controlled. In such cases, temperature measurements could be made on the TESS to obtain a temperature profile from top to bottom. Using the computer model of the system, the temperature profile data together with the data on charging and discharging steam flows, temperatures, and pressure, the state of charge of the TESS can be monitored continuously. The reference datum, determined by the PCM volume measurement described above, can be changed periodically, to prevent error accumulation.

5.5 Operational Characteristics

5.5.1 Charge/Discharge Operation

The TES subsystem is part of a complete solar energy system. Therefore, some of the operating conditions are fixed by the systems requirements, as described in Section 3.1. The flow from the solar collector field is set by a typical solar daily cycle (Figure 3.1-1), and the process demand. Part of the total flow from the collector field meets the constant demand of system, and the remaining goes to TES subsystem to charge the unit. During discharge the TESS supplements the solar field to maintain a constant supply to the process. After sundown the TESS supplies the total process demand for a period of approximately 3.7 hours.

Figure 5.5.1-1 shows the variation of TESS flow rate with time, during charging and discharging cycles for one of the eight modules. The TES subsystem consists of single coil heat transfer system having downflow during charging and upflow during discharging. The detailed daily duty cycle calculations were performed with the TESST code described in Appendix V. The heat transfer augmentation method was simulated in the TESST model as an enhanced PCM conductivity. A factor of 10 was required to match the results of the FREEZE code.

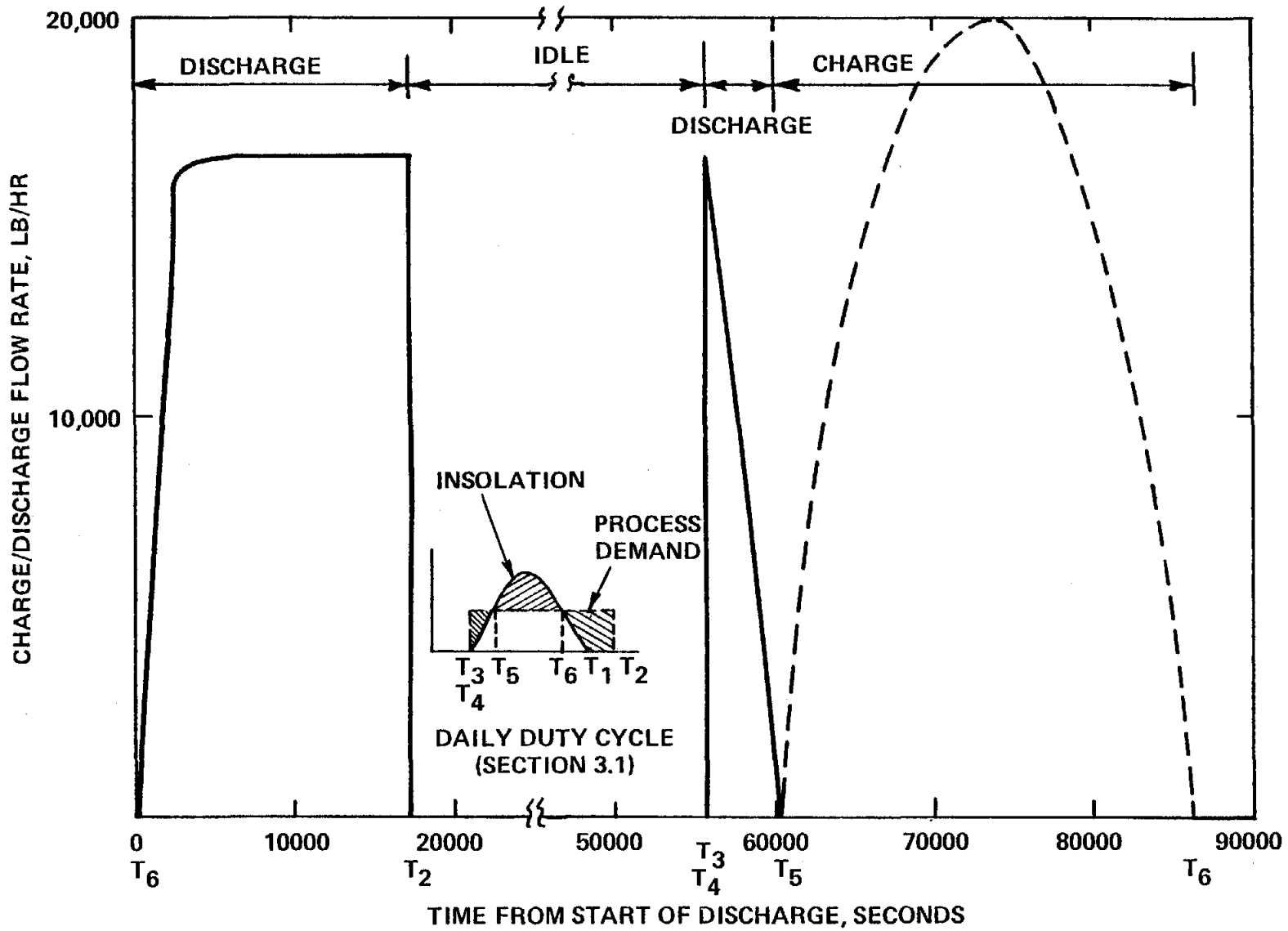
The TES subsystem operating conditions set by system requirements suggest constant inlet and outlet conditions during the entire daily duty cycle. However, the outlet conditions, both during charging and discharging of the unit, depend on the site and performance of the unit. Moreover, variable insolation makes it impractical to design the unit for constant outlet conditions.

Figure 5.5.1-2 shows the variation of water/steam conditions with time, both for charging and discharging cycles. Figure 5.5.1-3 shows the axial temperature profile of the PCM at the fully charged condition, at the beginning and end of the full discharge rate, and at the fully discharged condition.

The distinct thermocline nature of the operation is readily seen. Advantage is being taken of the PCM sensible heat in both the liquid and solid phases. It is worth noting here that in latent heat TES systems, a 100% utilization factor means all the PCM is used, accounting only for the latent heat. Consequently, the sensible heat contribution permits the effective utilization factor to exceed 100%.

Figure 5.5.1-2 shows that, at the beginning of discharge, superheated steam with approximately 44°C (80°F) of superheat is produced. This results from the large heat transfer area and the superheated liquid PCM at the steam outlet region. As discharging progresses, the superheat of the PCM at the steam exit plane decreases until the PCM hits its freezing temperature and begins to solidify. The steam outlet conditions

Figure 5.5.1-1
 VARIATION OF CHARGE/DISCHARGE FLOW RATE WITH TIME



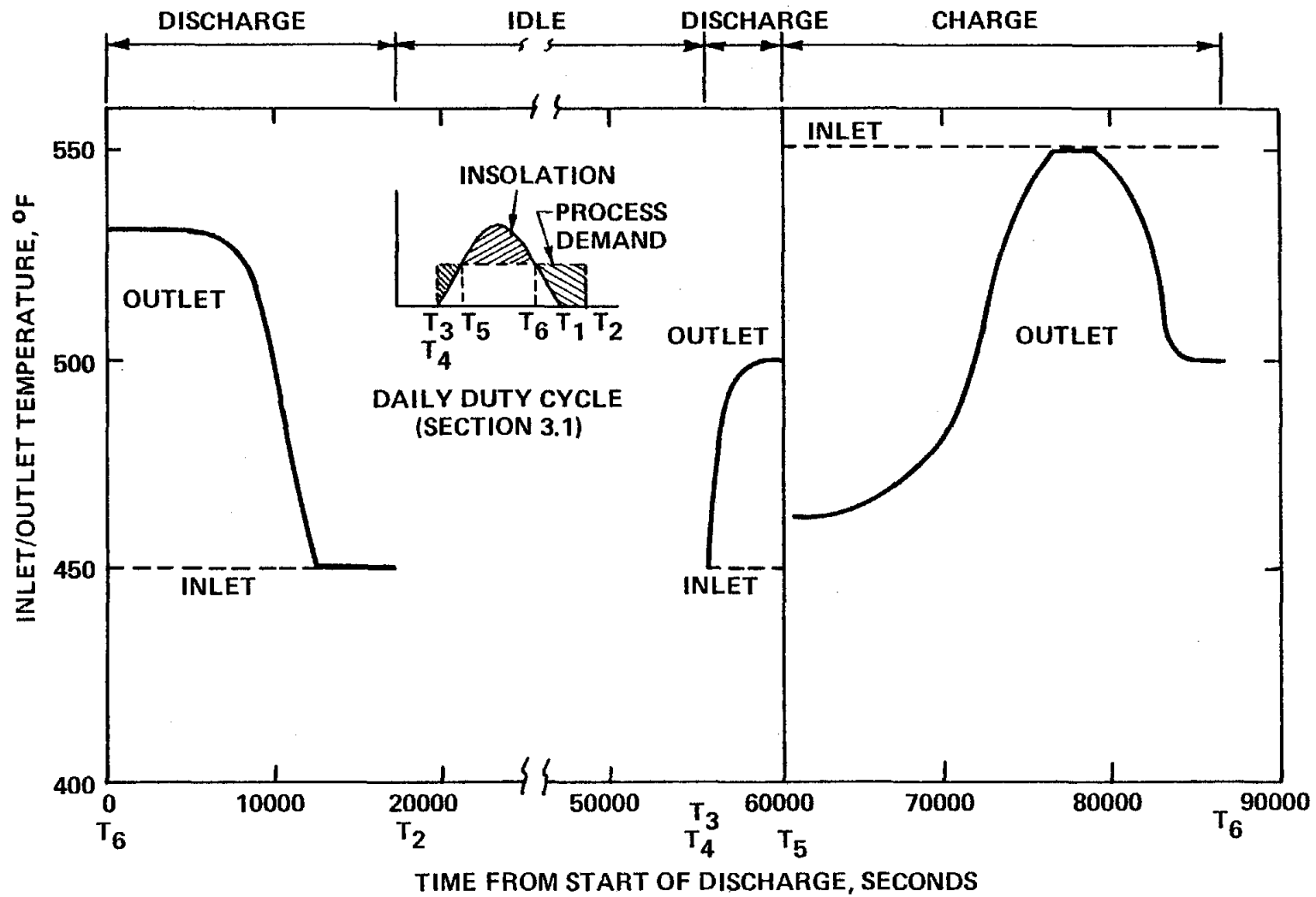


Figure 5.5.1-2
 VARIATION OF INLET /OUTLET, WATER/STEAM TEMPERATURE WITH TIME

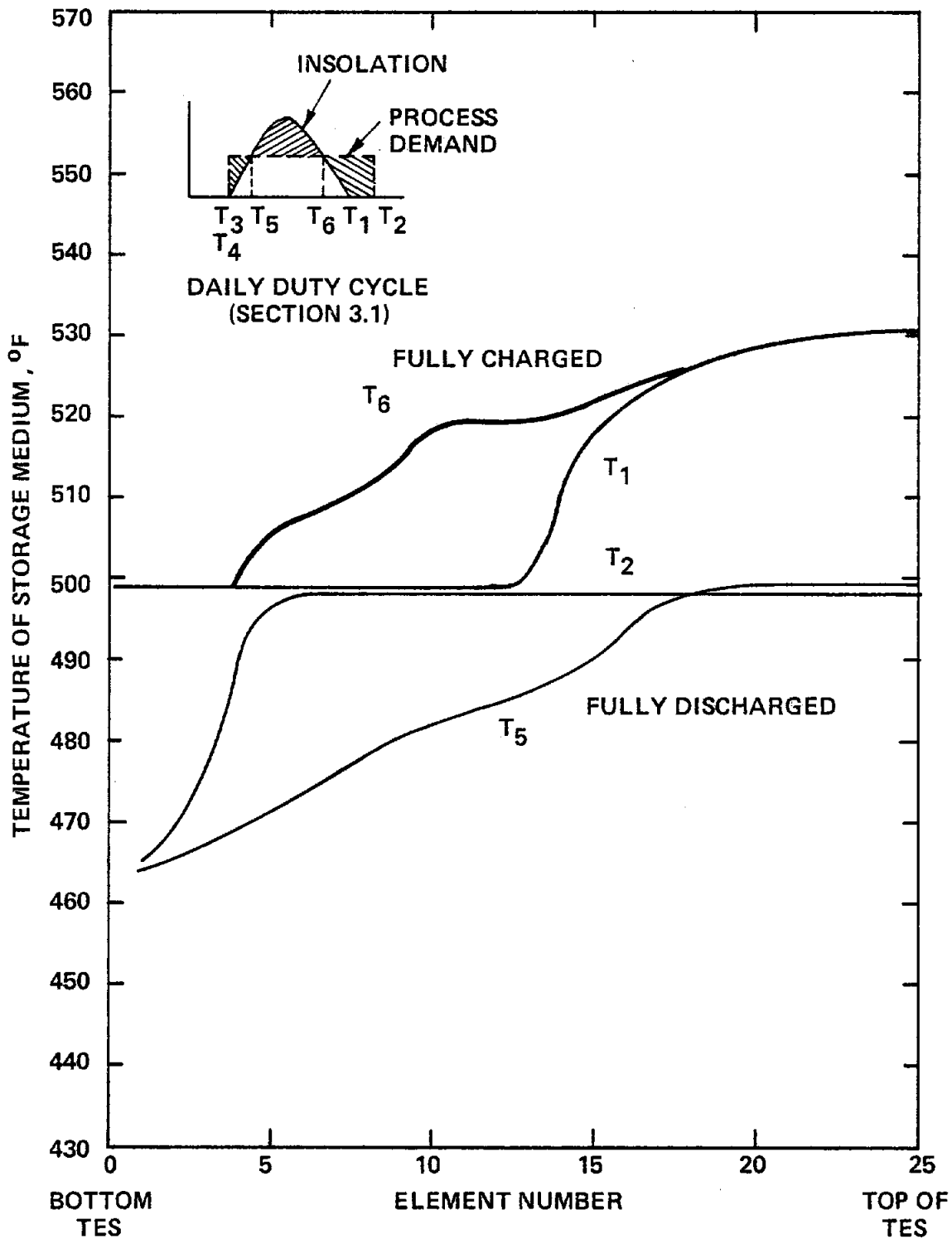


Figure 5.5.1-3
VERTICAL TEMPERATURE PROFILE OF STORAGE MEDIUM

produce less and less superheat and, near the end of the day, produce a wet steam mixture. In the morning the TESS discharge supplements the solar field output so the flow decreases over this discharge period. Initially wet steam is produced, but the steam superheats as the flow decreases. The PCM at full discharge includes considerable subcooled solid at the bottom of the unit and a two-phase mixture at the top.

If the process can accept and use the discharge steam, there are no penalties. However, if a tolerance range on the discharge output is imposed (for example, 6 to 8°C (10-15°F) of superheat to 85-90% quality or even tighter), then, clearly, additional handling of the steam on the TES island is required. A desuperheater using feedwater from the process island would be required on the discharge steam line to bring the steam within tolerance. An alternate approach would take some of the saturated water entering the TES unit, bypass it to the outlet, and mix it with the effluent from the TES unit. The effluent will have the same high degree of superheat as if the total discharge flow passed through the unit because of the PCM thermocline and the relatively large heat transfer area.

At the lower end of the tolerance range, wet steam mixtures below tolerance would require energy input from a heat source, such as a boiler, to bring the mixture to within tolerance. This deficit energy cost would have to be added to the cost of the TES island. The specific service considered here is within this tolerance range, and no deficit energy is added to the capital cost of the TES unit (See Section 5.6).

It should be noted that the final design is considered conservative since the basic heat exchange bundle and amount of PCM required were based on the results of the FREEZE model. This model involves the latent heat of the PCM and a small amount of solid sensible heat as compared to the FREEZE results. However, the results of the TESST calculations indicate that there is a substantial amount of liquid and solid sensible heat as compared to the FREEZE results. This should lower the required amount of PCM. The main barrier in trying to take credit for

the sensible heat is the appropriate value to use for conductivity enhancement. The procedure used on this design study was to benchmark TESST against FREEZE. Consequently, there is a strong incentive to develop a new heat transfer model in TESST or to perform analytical and/or experimental studies to obtain the appropriate enhanced conductivity value (see Section 8.0).

5.5.2 Storage Losses

The total parasitic heat losses from the TES subsystem consist of heat losses from storage tanks and pipes, and the pumping power required to charge and discharge the unit. These losses can be made arbitrarily small by adding extra insulation to reduce heat losses and by reducing the overall pressure drop of the subsystem.

Pumping Power

The peak pressure drops in the TES subsystem for charging and discharging operation modes are estimated to be less than 0.34 MPa (50 psi). This includes the tube bundle, headers, and piping losses. The total pump work over the daily duty cycle including the charging and discharging operation, as estimated from computer TESST, is small ($< 0.05\%$), compared to the TES capacity.

Heat Losses

The heat losses in the subsystem can be reduced by adding extra insulation. However, the law of diminishing return applies, and the point is reached when the added insulation would not have any cost benefit. The parametric study including the thermal insulation cost has been reported in Reference 1. The extensive work experience of Comstock and Wescott for latent heat TES systems and water heaters suggests that the insulation is one of the cheapest cost items in the latent heat TES system.

A representative heat loss requirement was established as a 2% loss per daily duty cycle, i.e., 2% of the 148 MWh capacity in a 24-hour period. The thermal insulation requirements were calculated for two island configurations: in one, each of the tanks stands alone; in the other, the tanks are grouped together. The latter configuration is shown on Drawing 3 in Appendix I. The calculations assumed an average containment tank temperature of 260°C (500°F).

The typical heat transfer coefficient of insulation were based on the following insulation characteristics:

- At bottom of tank:
Foamglas (Pittsburgh Corning) $K = 0.11 \text{ W/m}\cdot\text{°C} \left(0.74 \frac{\text{Btu}\cdot\text{in}}{\text{hr}\cdot\text{ft}^2\cdot\text{°F}} \right)$
- On sides of tank:
Fiberglas (Owens-Corning) $K = 0.088 \text{ W/m}\cdot\text{°C} \left(0.61 \frac{\text{Btu}\cdot\text{in}}{\text{hr}\cdot\text{ft}^2\cdot\text{°F}} \right)$

The loose fiberglass insulation on the sides of the tank is held in place by a thin aluminum sheet.

The total exposed area of the 8 stand-alone tanks is approximately 1800 m² (19000 ft²). For the eight tanks grouped together, the exposed area is approximately 1100 m² (12000 ft²). There is no insulation between the tanks within the outer insulation envelope. The total insulation requirement is summarized as follows:

<u>Arrangement</u>	<u>Bottom Foamglas</u>	<u>Sides and Top Fiberglass</u>
Individual Tanks	16"	14"
Grouped Tanks	11"	9"

In order to reduce the heat losses to 1% of capacity in a 24-hour period, the insulation must be doubled. The energy saving would be 1.48 MWh (5.1 MBtu). Costing this at \$4.90 per MBtu, reflecting \$30 per barrel of

oil and capitalizing at 15%, yields \$41,300. The sell price of this additional insulation is listed on Table 5.6-1 as \$101,600. There is no strong incentive to reduce the requirement to 1%.

5.5.3 Hydraulics

In general, a once-through steam generator in which feedwater is directly converted to saturated or superheated steam may undergo flow and pressure oscillations under certain operating conditions. The problem gets more severe as the number of parallel paths increases. The tube-intensive TESS by its very nature has an extremely large number of tubes and consequently may be prone to boiling instability during discharge. Condensation is an inherently stable process, so there are no flow distribution concerns during charging.

Static and dynamic flow instabilities are commonly studied in steam generator thermal-hydraulic analysis. The dynamic stability study, involving all the dynamic effects including fluid acceleration, thermal inertia and feedback between primary and secondary sides, requires a complex transient analysis. However, a reasonably good evaluation of the operation of such a TES unit can be made on the basis of static instability analysis. This involves evaluating the performance of one tube as a function of flow for a given heating condition.

The nature of the static flow stability problem is indicated by Figure 5.5.3-1, showing the variation of total pressure drop with flow rate in a typical unstable unit. The total pressure drop consists of components due to friction, acceleration, and elevation. The importance of each depends on operating conditions, geometry of the flow channel, and the direction of flow with respect to gravity. For given PCM thermal conditions, the following effects may be observed as the tube water flow during the discharge cycle increases:

- a) Steam quality, or superheat, may decrease at the tube outlet.
- b) The length of the preheat and boiling zones increases.

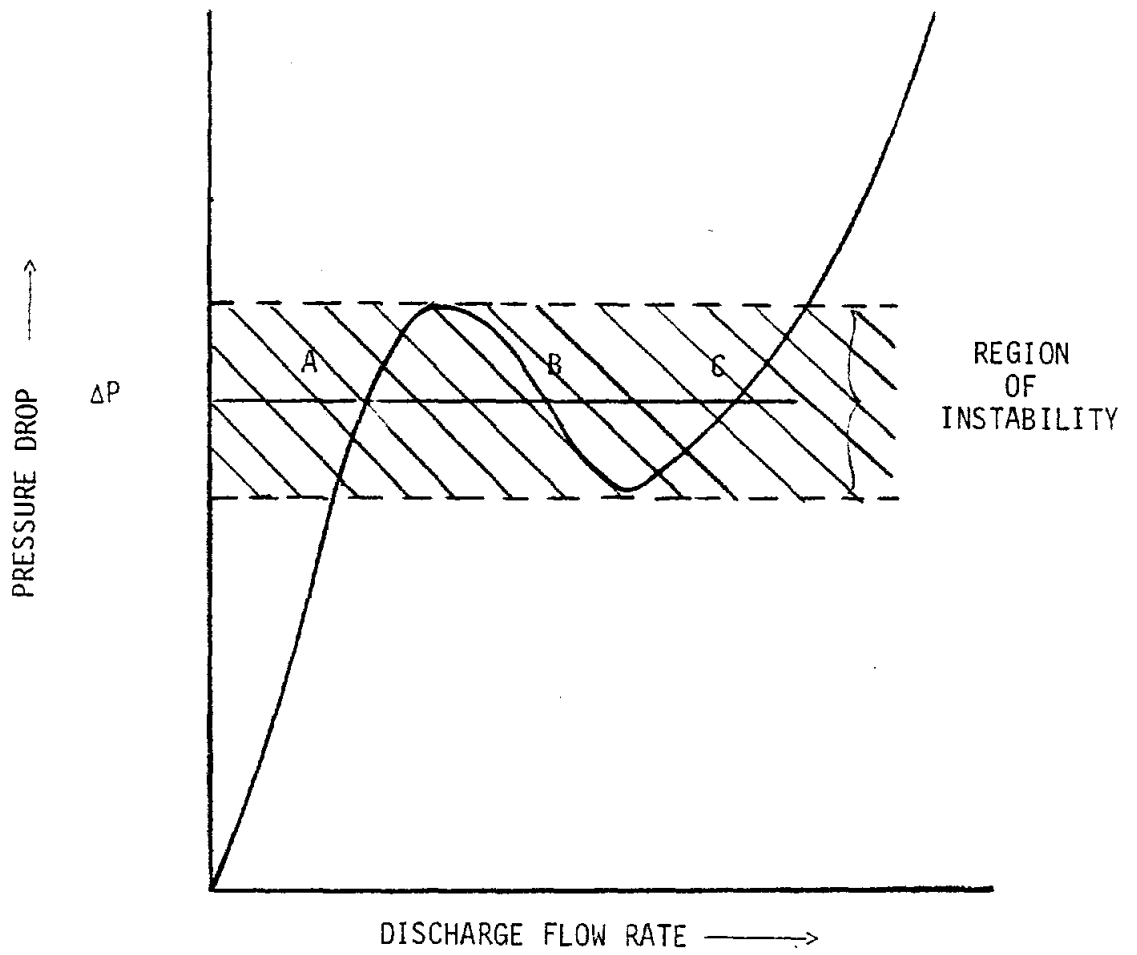


FIGURE 5.5.3-1 A TYPICAL FLOW INSTABILITY REGION IN TWO PHASE FLOW SYSTEM

- c) The length of the superheat section reduces.
- d) The average density of the mixture increases due to (b) and (c).
- e) The velocity of steam in the superheat section may decrease if the increase in mass velocity cannot compensate for decrease in specific volume.

In the upflow discharge system, the hydrostatic pressure drop may increase due to (d). For a given flow rate in a tube the frictional pressure drop per unit length is smallest for the single phase liquid, higher for a two phase flow, and highest for the superheat region, due to the specific volume of each region. Due to the effects (b), (c), and (e) above, the low-pressure-dropping zone increases and the high-pressure-dropping zone decreases. This could lead to a decrease in the frictional pressure drop.

The overall effect could therefore lead to a decrease in the total pressure drop with increasing flow rate. This is shown by shaded region in Figure 5.5.3-1.

Figure 5.5.3-1 also indicates that at a typical constant total pressure drop in the shaded region (constant pressure drop line), there are three different possible flow rates (points A, B, and C). The intermediate point, B, is in the unstable region because any slight disturbance tending to increase the flow leads to a decrease in pressure drop, which further increases the flow. Similarly, the effects of a slight reduction in flow are also cumulative. Flow conditions at points A and C are stable, but the flow may abruptly shift from point A to point C; or, vice versa, to a new stable point with overall heat exchanger mal-performance. The flow could oscillate continuously between the multi-stable states as well.

The above discussion leads to the static flow stability criterion suggested by Ledinegg. To obtain stable, predictable flow conditions, the curves for pressure drop as a function of flow rate should have a substantial positive slope throughout the range of operating conditions.

Figure 5.5.3-2 shows the static flow stability curve for the final conductivity-enhanced TES system. For three sets of thermal conditions at various times during the daily duty cycle, the curves clearly indicate that the pressure drop of discharging steam increases very positively with large variation in flow rate. The Ledinegg static stability criterion is easily satisfied as the frictional pressure drop variation is dominated by the change in flow rate, rather than the change in phase associated with this flow rate.

It should be noted here that during the preliminary sizing phase, using long tube lengths in the tube-intensive concept, similar results were obtained. The results indicate that for the operating conditions of this latent-heat TES, the flow stability is not critical. The additional orificing at the inlet of each of the parallel paths as in the case of once-through steam generation is, therefore, not necessary.

Figure 5.5.3-2 may also be used to envision three parallel channels having different heating rates, resulting in three sets of PCM thermal conditions (e.g., curves at T_2 , T_5 , and T_6). A criterion similar to that of Ledinegg can be applied, leading to the conclusion that if there were differences in heat addition to channels operating in parallel with the same pressure drop, there would be no difficulty with static-flow instability. Points A, B, and C in Figure 5.5.3-2 show one such set for the worst case. Imagine most of the channels operating at PCM thermal condition T_6 , while other parallel channels are operating at PCM thermal condition T_2 , or T_5 . Obviously, the thermal condition of steam at exit would be different in those channels. However, the flow would be stable, and, unlike fired boilers, the maximum tube temperature would be limited to the PCM temperature.

From the above discussions it can be concluded that, for the given set of operating conditions, a once-through discharge circuit in the TES system would not experience static flow instability.

The hydraulic calculations were performed with a special algorithm added

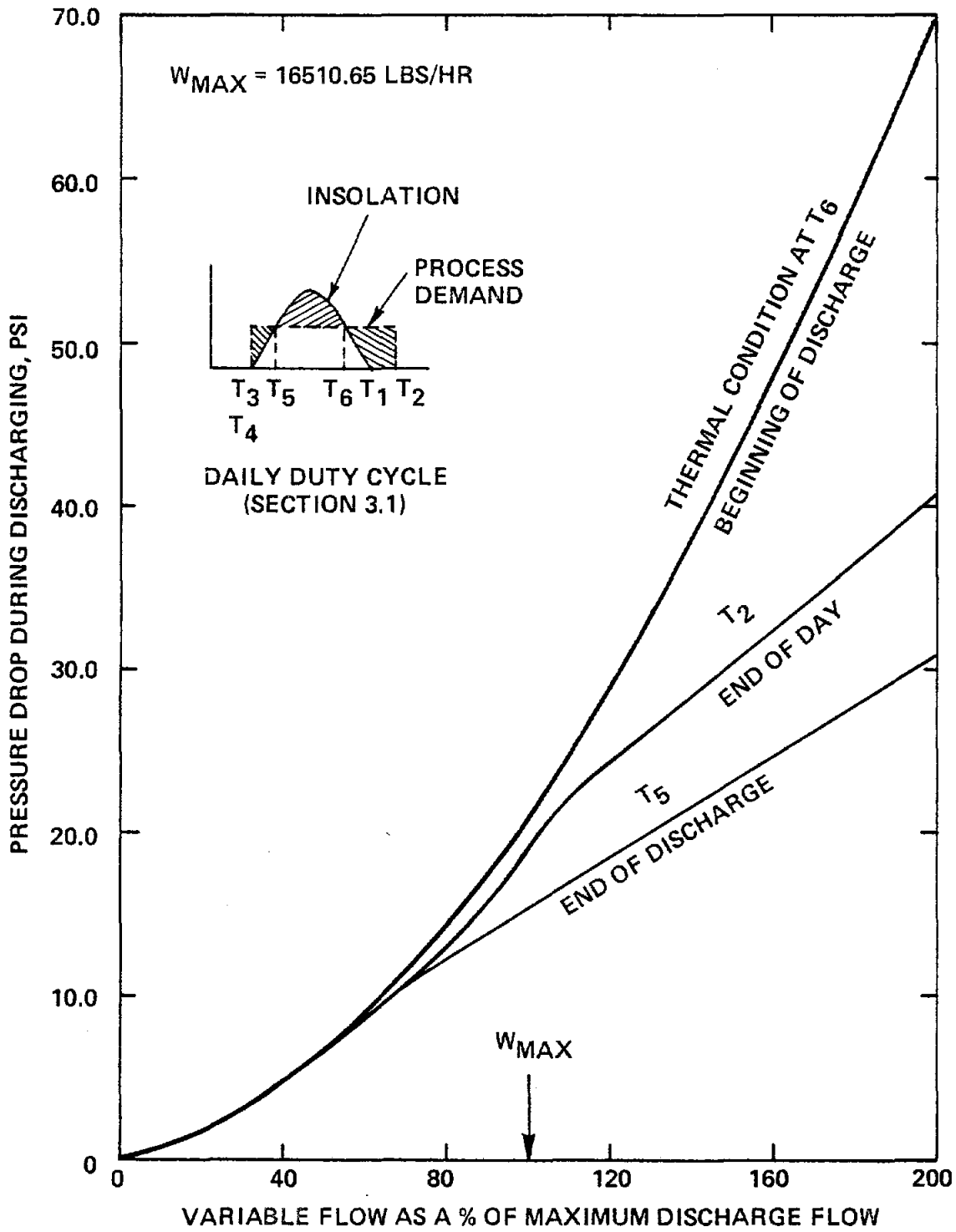


Figure 5.5.3-2
 STATIC FLOW STABILITY CURVE

into the computer program TESST, described in Appendix V. The program determined the PCM and steam/water axial temperature profile throughout the daily duty cycle. At various times during discharge, the program fixed the PCM temperature profile and calculated the steam temperature/quality profile and pressure drop for tube flow that varied from 10% to 200% of the maximum nominal flow. In the two-phase region, the program used a friction pressure drop multiplier based on a homogeneous model of the flow and McAdams expression for equivalent viscosity (40). The values from this expression integrated over a length fall between the data of Martinelli and Thom for boiling water.

5.5.4 Maintenance

The tube-intensive latent heat TES subsystem is designed on the assumption that the modules will have been tested and found highly reliable. However, if a module fails, it is possible to remove, and in most cases, repair and reuse it.

First, the tank will have to be drained. If the PCM is frozen, it will have to be melted by circulation of available steam, or by circulation of hot gases if the use of steam would be deleterious. Then drainage can proceed by means of a drain pipe. No valve is required on the drain line because the pipe must be heated to start the salt flowing. This could be accomplished by a strip heater wrapped around the drain pipe. The end cap may be cut and tanks rewelded after the tank is drained. Each cover plate (roughly 13' x 8') will have a fillet weld on the perimeter. One of these plates must be cut out and the roof structure on the tank must be unbolted from the sides of the tank. Of course the insulation on top of the tank must be removed locally for access. Once the cover is off the tank, the steam header is cut in one or two places depending on the module being removed. The condenser line is cut through the outside of the tank. The module can then be lifted by the four lifting eyes provided at the top of the module. A reverse procedure can be followed for insertion of a new or repaired module.

5.5.5 Safety

The Thermal Energy Storage equipment was designed with concern for personnel and structural safety requirements typically applied to similar industrial equipment. Applicable sections of the ASME code were implemented for the design of related equipment such as the storage tank and piping.

During normal operation of the TESS, a very low degree of hazard will exist to operating personnel when basic procedures are followed. Standard procedures for commercial operation of equipment with high-temperature heat transfer fluids in the chemical-processing industry and petroleum-processing industry may be applied to the operation and servicing of the TES unit.

Care must be taken to avoid external exposure to PCM as well as internal exposure (inhalation, ingestion). All hot surfaces on the heat transfer equipment and piping are insulated beyond the insulation thickness required to provide personnel protection. The hot fluids are totally enclosed in the system. During maintenance of the TESS, the PCM is drained and allowed to cool to ambient temperature. Salt baths of similar composition sold under several tradenames have been used industrially for many years at temperatures of 477°C (890°F) and higher for metal cleaning and descaling. These baths are contained in large steel tanks open to the atmosphere. The PCM used is chemically stable and has insignificant vapor pressure at temperatures up to 477°C (890°F). Its stability in air allows the containment vessel to be vented to the atmosphere. Experience has shown that small amounts of seepages through the tank walls are not harmful to operation of the unit because the PCM tends to solidify on the outside of the tank wall by conversion to NaCO₃, reducing the effect of the leak. A major leak of PCM due to rupture of the tank wall is not considered likely. The steam and condensate lines present another possibility for leakage, again small. Leak detection equipment will monitor the vent line exhaust.

5.6 Cost Estimate

The final drawings and specifications for the latent heat TESS were provided to the C-E Business Development Department, which coordinates all relevant purchasing, manufacturing and construction sections of the corporation. The design was put through the normal cost estimate procedure. An estimated total storage island cost was made; this includes materials, purchasing, equipment fabrication, transportation, site preparation, the foundation, and field installation costs. These are summarized on Table 5.6-1 where shop door costs and sell prices are listed. The mark-up for the hardware reflects standard guidance and administration (G&A) fees at 15%, and contingency and net margins at 10% each. The remaining items reflect a straight 26.5% mark-up. The sell price reflects minimum gross margins.

The rectangular PCM tanks would be shop assembled at the St. Louis works of the Fossil Power System Division and shipped to the Chattanooga facility. For the eight tanks, the total billing weight is approximately 489,000 lb for a total shop cost of \$347,000. Shipping to Chattanooga incurs an additional \$17,000 cost. The total shop door cost is \$364,000 for a total sell price of \$506,000.

The St. Louis works would also fabricate the retainer straps, and angle- and bottom-support tees for the tube bundle support structure. The horizontal bottom angles and tees would be assembled into one piece. The entire package weighing approximately 98,000 lb would be shipped to Chattanooga for the tube bundle assembly. The total shop door cost is \$77,000, including freight to Chattanooga.

The 40-tube bundles would be fabricated at Chattanooga and inserted into the eight containment tanks. The tubing and piping for the 40-tube bundles amounts to 50,000 lb. The cost of the tubing and formation of it into serpentine has a shop door cost of \$262,000. There are 161,920 pieces of aluminum and steel fins for heat transfer and tube support that must be formed from 230 miles of coil stock. The material cost is estimated

at \$359,000. The labor for making the dies and forming the material is estimated at \$73,000. Finally, the labor for actually assembling the tube bundles and tank modules is estimated at \$400,000. The total shop door cost is, therefore, \$832,000 with a sell price of 1.1583×10^6 .

Since no specific site was identified for this study, the Barstow, CA site was selected for characteristic shipping costs. Finally, general liability insurance at 31¢ per \$100 was added. The total hardware sell price amounts to 2.382×10^6 .

The installation costs were estimated by C-E Construction Services. The budgetary estimate includes site preparation, pouring the concrete pad, off-loading the tanks from the rail cars and moving them to the site, and installation of piping and insulation. The work was estimated to take an average composite crew of 10 men about 21-22 weeks from beginning site preparation to the finish of external lagging. The cost includes 7700 manhours of labor at \$28.35 per hour; fee, overhead, and profits on labor; 115 days of supervision at \$430 per day; and tool costs. These four items add to a sell cost of \$369,500.

The sodium hydroxide/sodium nitrate eutectic cost of \$0.165/lb presented in Appendix II was increased by 10% for a 1981 cost and the standard mark-up added, for a total cost 1.103×10^6 for the 4.8×10^6 lb required. The cost of actually filling the tanks was not included in this estimate, as this cost was not quantified at the completion of the effort.

Site preparation and foundation costs were estimated based on mean construction costs for 1981. These average values are representative of these costs. The costs are listed on Table 5.6-1 and amount to approximately \$20,000. With general liability insurance, the total sell price including installation is 1.496×10^6 .

The total cost of the TES island is 3.878×10^6 . This price does not include cost of engineering, sales tax or cost of money. For routine production of the TES subsystem where engineering includes project

TABLE 5.6-1
THERMAL ENERGY STORAGE SYSTEM BUDGETARY COST ESTIMATE
(Island Cost w/o Engr.)

<u>Hardware</u>	<u>Shop Door Cost</u>	<u>% Markup</u>	<u>Sell Price 2/81</u>
8 - Tanks @ \$45,500 ea. (incl'd prime coat)	\$364,000	10+15+10	\$ 506,500
40 - Tube bundle support structure @ \$1,925 ea.	77,000	10+15+10	107,200
50,000 lb tubing & piping	262,000	10+15+10	364,600
230 miles (161,920 pieces) aluminum & steel fins, fabrication and assembly	832,000	10+15+10	1,158,300
8 - Sets of tank insulation & aluminum jacket	73,000	10+15+10	101,600
Freight (rail) Chatt., TN to Barstow, CA	88,000	26.5	136,400
General liability insurance @ \$0.31/\$100	5,800	26.5	<u>7,400</u>
<u>Hardware Total</u>			<u>\$2,382,000</u>
 <u>Installation (Field Construction Cost)</u>			
Labor, 7,700 manhours @ \$28.35/hr			\$ 218,300
Fee, overhead & profit on labor			31,500
Supervision, 115 days @ \$430/day			49,500
Tools & equipment, owned & rental			70,200
Mat'ls, eutectic (NaOH-NaNO ₃), 4.8x10 ⁶ lb.	871,000	26.5	1,102,300
Concrete, 132 cu. yd (4,000 psi) @ \$50/yd.	6,600	26.5	8,400
Rebar, 3½ tons, with chairs & wires	2,800	26.5	3,500
Gravel base, 400 cu. yd @\$15/cu. yd	6,000	26.5	7,600
General liability insurance @\$0.31/\$100	3,700	26.5	<u>4,700</u>
<u>Installation Total</u>			<u>\$1,496,000</u>
Total present day budgetary sell price, delivered and erected, subject to escalation from 2/81, w/o engineering, sales tax & cost of money			<u><u>\$3,878,000</u></u>

management, and routine engineering and drafting (i.e., no development), a \$100,000 engineering cost is representative. A drain tank to hold the PCM from a single tank was not included in the cost of the TESS. In the event of maintenance requiring the draining of a tank, rental of a holding tank will be considered. This then becomes an unquantified maintenance cost.

5.7 Evaluation of the Final Design and Comparison with Oil/Rock Storage

5.7.1 Discussion of the Final Design

The use of extended surface heat transfer does indeed present a cost savings for the TESS. If the simplified tube-bundle sizing method (Appendix III) is calibrated against the results of the optimization study (Appendix IV) for the 6.35 mm (0.25") O.D. tube and the resulting equation applied to the 15.9 mm (0.625") O.D. tube selected for the final design, then a 229,400 m (752,600 ft) heat transfer length is obtained for a bare-tube bundle. The length is 5.2 times the required tubing for the final finned-tube design (reference design). The bare-tube cost can be estimated by scaling the \$262,000 cost listed in Table 5.6-1; a shop door cost of \$1,360,800 and a sell price of \$1,893,600 are obtained. These outweigh the costs of the tubing and fins listed on Table 5.6-1 by \$266,800 on a shop door cost basis and \$370,000 on a sell price basis. The selection of finned tubes is thus substantiated on a cost basis.

The sizes of the major components in the final (reference) design reflect inherent design conservatism. The tubing, fins, and PCM were all sized based on the results of FREEZE calculations. As noted previously, the FREEZE model considers no liquid superheat and very little solid sub-cooling. The results of the TES unit performance evaluation using TESST (see Section 5.5.1) show substantial liquid superheat for the fully discharged state. Additionally, a thermocline is established. Credit for these effects could not be taken since TESST had to be benchmarked against

the FREEZE results. This uncertainty in simulating the extended surface heat transfer in the TESST model inhibited a meaningful optimization study of the final design.

An examination of the preliminary analysis on the tube-intensive TESS using bare tubes proves useful for the evaluation of design trends. The optimization study of the design using 6.35 mm (0.25") O.D. bare tubes (see Appendix IV) showed that the thermocline with subcooled solid and superheated liquid could be translated into a substantial reduction in the required PCM. Defining a utilization factor on the basis of latent heat only, a value of 1.21 is indicated by the optimization study. Applying this to the simplified tube bundlesizing method, a heat transfer length of 3.40×10^6 m (1.116×10^6 ') is obtained. This is virtually the result of the optimization study. Thus, if the appropriate utilization factor is applied, a very good estimate of the heat transfer surface can be obtained from the simpler sizing procedures. This view is applied to the finned tube design: the utilization factor from the optimization study is adopted and the heat transfer area requirements are obtained from the FREEZE results.

The reduced amount of PCM, based on the high utilization factor, results in a reduction of tube length if the 15.2 cm x 15.2 cm (6" x 6") tube spacing is maintained. A total tube length of 35,330 m (115,920') is arranged into 30 tube bundles, each containing 16 tubes, and inserted into 6 tanks. The required PCM, is 1.76×10^6 kg (3.88×10^6 lb). The costs for the reference design in Table 5.6-1 are scaled for this design and the results are presented as Design Improvement 1 in Table 5.7.1-1. The tubing, fins, and tube supports costs were scaled on the basis of tube length. Tank, shipping, and foundation costs were scaled on the number of tanks. Any savings on insulation relative to the reference cost were ignored since reductions in the close-packed arrangement of tanks would be small. Installation labor was kept at the same level as in the reference. As noted on Table 5.7.1-1, a \$719,300 cost reduction would be achieved.

TABLE 5.7.1-1

COST ESTIMATES FOR IMPROVED DESIGN

<u>Hardware</u>	<u>DESIGN IMPROVEMENT 1</u>		<u>DESIGN IMPROVEMENT 2</u>	
	<u>Shop Door Costs</u>	<u>Sell Price</u>	<u>Shop Door Cost</u>	<u>Sell Price</u>
Tanks	\$ 273,000	\$ 379,900	\$ 273,000	\$ 379,900
Tube bundle support	61,500	85,600	61,500	85,600
Tubing	209,600	291,600	262,000	364,600
Fins	665,600	926,200	759,500	960,800
Insulation	73,000	101,600	73,000	101,600
Shipping	70,400	89,100	70,400	89,100
Insurance	<u>4,600</u>	<u>5,800</u>	<u>4,800</u>	<u>6,100</u>
TOTAL	\$1,357,700	\$1,879,800	\$1,504,200	\$1,987,700
 <u>Installation</u>				
Installation Labor	---	\$ 369,500	---	\$ 369,500
Salt	704,200	890,800	691,200	874,400
Foundation	11,600	14,600	11,600	14,600
Insurance	<u>3,200</u>	<u>4,000</u>	<u>3,100</u>	<u>3,900</u>
TOTAL		\$1,278,900		\$1,262,400
TOTAL HARDWARE AND INSTALLATION		\$3,158,700		\$3,250,100
COST RELATIVE TO REFERENCE COST (TABLE 5.6-1)		(-)\$ 719,300		(-)\$ 627,900

To substantiate this design, the equation for heat transfer length in the simplified size method was employed to determine an equivalent PCM conductivity enhancement factor. Values corresponding to the reference design and Design Improvement 1 were obtained, and the ratio of these values was applied to the factor of 10 required in the TESST analysis of the reference design. A value of 13 was obtained. The improved design was analyzed with TESST, using a conductivity enhancement of 13. The target capacity of 148 MWh and PCM and steam performance similar to the reference design were obtained. Stable hydraulic characteristics were also noted.

Alternatively, a second design improvement could also be obtained. The amount of PCM dictated by the utilization factor and the heat transfer length dictated by FREEZE are selected. To accommodate these selections, the local tube spacing must be changed. This was done by bringing the parallel serpentine tubes closer together for a 15.2 cm x 12.2 cm (6" x 4.8") tube spacing. The 44,170 m (144,900') of tube are arranged into 30 tube bundles, each containing 20 tubes, and inserted into 6 tanks. A total mass of 1.73×10^6 kg (3.81×10^6 lb) of PCM is required. The cost values for the reference design presented in Table 5.6-1 are again scaled as described above, and the results are presented in Table 5.7.1-1 as Design Improvement 2. The fin cost was scaled based on a detailed breakdown of the cost components. The shop door cost of the reference design fins breaks down to \$73,000 for dies and metal forming, \$359,000 for fin material, and \$400,000 for bundle assembly. The \$73,000 cost was adopted unchanged for this design improvement. The materials cost was scaled on the mass of fins which is lower due to the tighter tube spacing. The bundle assembly cost was adopted unchanged since the number of pieces for handling were the same as those of the reference. This results in a \$72,500 shop door cost reduction over the reference. Design Improvement 2 reflects a \$627,900 reduction in sell price over the reference design. Again, to substantiate this design the sizes were input to TESST and a PCM conductivity enhancement of 10 employed. The target capacity was achieved, and PCM and steam performance similar to the reference design were obtained. No hydraulic stability problems were

observed in the results.

A further improvement in the second design improvement can be achieved by decreasing the fin frequency with a 2.5 cm (1.0") fin spacing. Examining the results of the FREEZE calculation (see Appendix VI) an increase in the fin spacing from 1.9 cm (0.75") to 2.5 cm (1.0") results in a decrease in heat flux of approximately 12%, and consequently an increase in heat transfer length of 12%. The result obtained for steel fins is assumed applicable to aluminum fins. Placing the additional heat transfer length into the fixed amount of PCM requires a further reduction in tube spacing. This is again accomplished by moving the adjacent serpentine tubes together. A 15.2 cm x 10.8 cm (6" x 4.25") tube spacing results. The tube costs increase by 12%: \$31,400 on a shop door cost basis and \$43,800 on a sell price basis. The amount of fins decreases because of the fin frequency and tube spacing but increases because of the increased tube length. A \$170,400 cost of material is estimated. The assembly labor decreases because of the fin frequency and increases because of the tube length for a net cost of \$336,000. The die and metal forming cost of \$73,000 is assumed unchanged. The net cost is \$579,400 or \$180,100 less than the corresponding shop door cost in Design Improvement 2. The net reduction in shop door cost is \$148,700 and \$206,800 for the sell price. Consequently, Design Improvement 2 could have as much as a \$834,700 reduction in the sell price relative to the reference design.

The reduction of the fin frequency indicates a trade-off between tube cost and fin cost that can result in a cost optimum with even larger fin spacing than discussed above. The scope of the FREEZE calculation does not provide a sufficient data base to pursue this further. This consideration does indicate that the cost of the TESS can be improved further.

5.7.2 Comparison with Oil/Rock Benchmark

The main objective of this study is the development of a latent heat TESS with cost improvement over an oil/rock sensible heat system. For this purpose a benchmark oil/rock system modeled on the Barstow system was

developed during the selection process. The final design of the latent heat TESS is now compared with the benchmark. However, the cost results presented in this section must be appropriately selected to insure that the costs are comparable. The cost comparison will be accomplished on the basis of major components cost. For the latent heat, these are the shop door costs for the tanks, the PCM, and the tube bundle including tubes, fins, and tube bundle supports. These are shown on Table 5.7.2-1 for the reference design, whose costs are obtained from Table 5.6-1, and for Design Improvement 2 with the wider fin spacing. Foundation costs were also included since there is a significant difference with the oil/rock TESS.

The sizing effort for the oil/rock benchmark is discussed in Section 3.5 and Appendix XII. The component costs are presented in Table 4.4-5 for 80% and 60% volume utilizations; these costs are repeated on Table 5.7.2-1. The range of utilization factors was selected to bound the expected component costs. Several costs were not included in the initial sizing effort. These will be discussed here and added to the component costs.

Due to the large weight of the oil/rock tank, the foundation costs are significantly greater than those of the latent heat system. The foundation design for Barstow includes 60" of concrete, 24" of insulating concrete and 2" of fiberboard and sand for insulation. These dimensions were used to calculate the required volume of concrete for the storage tank of the benchmark design. The balance of the subsystem was not included. Both concrete and insulating concrete were costed at \$50 per cubic yard, as in the case of the latent heat TESS. The gravel and rebar costs were scaled from the shop door costs of the latent heat reference design presented in Table 5.6-1 on the basis of concrete volume. Total costs of \$114,600 and \$141,700 were obtained for the 80% and 60% utilization factor sizes, respectively.

The operating and maintenance costs include the pumping power and the annual Caloria make-up due to thermal degradation of the inventory. The peak pump power is 101 kW (135 hp) to provide for a maximum pressure drop of 241 kPa (35 psi) at a maximum flow rate of 8.80×10^5 kg/hr (1.94×10^6 lb/hr).

TABLE 5.7.2-1

LATENT HEAT VS. OIL/ROCK SENSIBLE HEAT STORAGELATENT HEAT

	<u>Reference Design</u>	<u>Improved Design</u>
Tanks	\$ 364,000	\$ 273,000
Tubes	262,000	293,000
Fins	832,000	579,400
Tube Bundle Supports	77,000	61,500
Salt	<u>792,000</u>	<u>628,300</u>
TOTAL COMPONENT COST	\$2,327,000	\$1,835,000
Foundation	<u>15,400</u>	<u>11,600</u>
TOTAL	\$2,342,000	\$1,847,200

OIL/ROCK SENSIBLE HEAT

	<u>80% Utilization</u>	<u>60% Utilization</u>
Tanks	\$ 657,000	\$ 756,000
Oil	603,000	798,000
Rocks	201,000	266,000
Heat Exchanger	562,000	562,000
Pumps	54,000	54,000
Piping	<u>26,000</u>	<u>26,000</u>
TOTAL COMPONENT COST	\$2,103,000	\$2,462,000
Foundation	114,600	141,700
Operating & Maintenance	<u>158,300</u>	<u>205,800</u>
TOTAL	\$2,375,900	\$2,809,500

The energy demand over the daily duty cycle is estimated to be 631 kW·h (2.15×10^6 Btu). Costing this at \$4.90 per million Btu reflecting \$30 per barrel of oil and assuming a 250-day year, an annual cost of \$2630 is obtained. Capitalizing this at 15%, a cost of \$17,600 is calculated.

The annual loss of Caloria for the conditions considered here is estimated by Sandia at $3\frac{1}{2}\%$. This comes to an annual cost of \$21,100 for the 80% design and \$27,900 for the 60% design. Capitalizing these, also at 15%, yields \$140,700 and \$186,200 for the two designs. The total operating and maintenance costs are listed on Table 5.7.2-1.

The latent heat TESS shows a definite cost advantage over the oil/rock system. The cost improvements reduce the reference latent heat TESS from $\$2.34 \times 10^6$ to $\$1.85 \times 10^6$. The oil/rock benchmark lies in the range $\$2.38 \times 10^6$ to $\$2.81 \times 10^6$. The improved design shows a 22% cost reduction over the lowest cost oil/rock system and a 34% improvement over the 60% utilization factor design.

6. ASSESSMENT OF COMMERCIAL SCALE TESS

6.1 Potential Improvements

The fundamental technology for thermal storage using sodium hydroxide based PCM and tube intensive heat transfer has been demonstrated by Comstock and Wescott in small units. Results of the current study indicate that high PCM utilization factors and relatively high charge/discharge rates can be achieved at relatively low cost by using efficient heat transfer enhancement. Some potential for performance improvement exists; however, more significant improvements will result from learning curve, scale, and volume effects associated with production of significant commercial quantities of TES units.

6.1.1 Performance Improvements

The principal performance parameters are:

- PCM Utilization Factor
- Charge Rate
- Discharge Rate
- Charge - Discharge Temperature Difference
- Heat Loss
- Steam Quality (or Superheat) at Discharge

The current design has a PCM utilization factor of 121%, defined in the basis of the latent heat, or a utilization factor of 86% defined on the basis of latent and sensible heat over the entire temperature range. Consequently, much further performance improvement cannot be expected.

Charge rates, discharge rates and the charge-discharge temperature difference are determined by heat transfer surface area and tube diameter. The present design does not challenge the physical limits of these parameters, so higher rates and/or lower temperature differences could be obtained by appropriate adjustments of tube spacing, tube diameter, and plate spacing. In this case, of course, greater performance would be achieved only at added cost.

Since the heat transfer efficiency of the design is not yet completely optimized, it is clear that the specified charge rates, discharge rates, and temperature differences can be achieved with less heat transfer surface at lower cost. This has been classified as a "cost improvement" rather than a "performance improvement" and is discussed further below. Heat losses are approximately 2%; there is not room for great improvement in this area. However, large field-fabricated units could achieve low losses at significantly reduced cost. (See below.)

It is an inherent characteristic of the tube intensive concept that the output steam superheat (or quality) is not directly controllable. Slightly superheated steam is produced most of the time and a desuperheater is required if saturated steam is a requirement. The desuperheater solution is relatively straightforward and not particularly costly. Nevertheless, this is an area for potential improvement if a better control method can be devised. One possibility that needs further evaluation is a design for the sequenced discharge of modules. Development of this concept might eliminate the need for the desuperheater and improve overall control of system output.

6.1.2 Large Field-Erected Units

Large field-erected tanks about 30 m (100') in diameter and 14 m (45') high are constructed routinely for storage of various chemicals, and have been designed for molten salts. Except for certain design problems associated with elevated temperatures in the foundation area, it is not expected that any special difficulties would be encountered in building such a large tank. Utilization of large tanks would reduce costs associated with salt containment and thermal insulation.

The general design approach envisioned for a large field-erected system would entail the use of heat transfer modules of a design very much like those employed in the shop-fabricated TES unit. These are 2.3 m x 3.3 m x 3.7 m (7'5" x 10'9" x 12') assemblies which include primary

heat transfer tubes, heat transfer enhancement method, structure and steam/water headers. (See Drawing 1 in Appendix I.) Such heat transfer modules could be stacked 3-high with additional structures to provide independent support of each module. Figure 6.1-1 shows the general arrangement for a tank 27.4 m (90') in diameter and 13.7 m (45') high. The thermal storage capacity of this unit would be 5.6 times that of 8 modules of the shop fabricated design. This single tank would have about 830 MWh of storage capacity and a maximum charge/discharge rate of 170 MW.

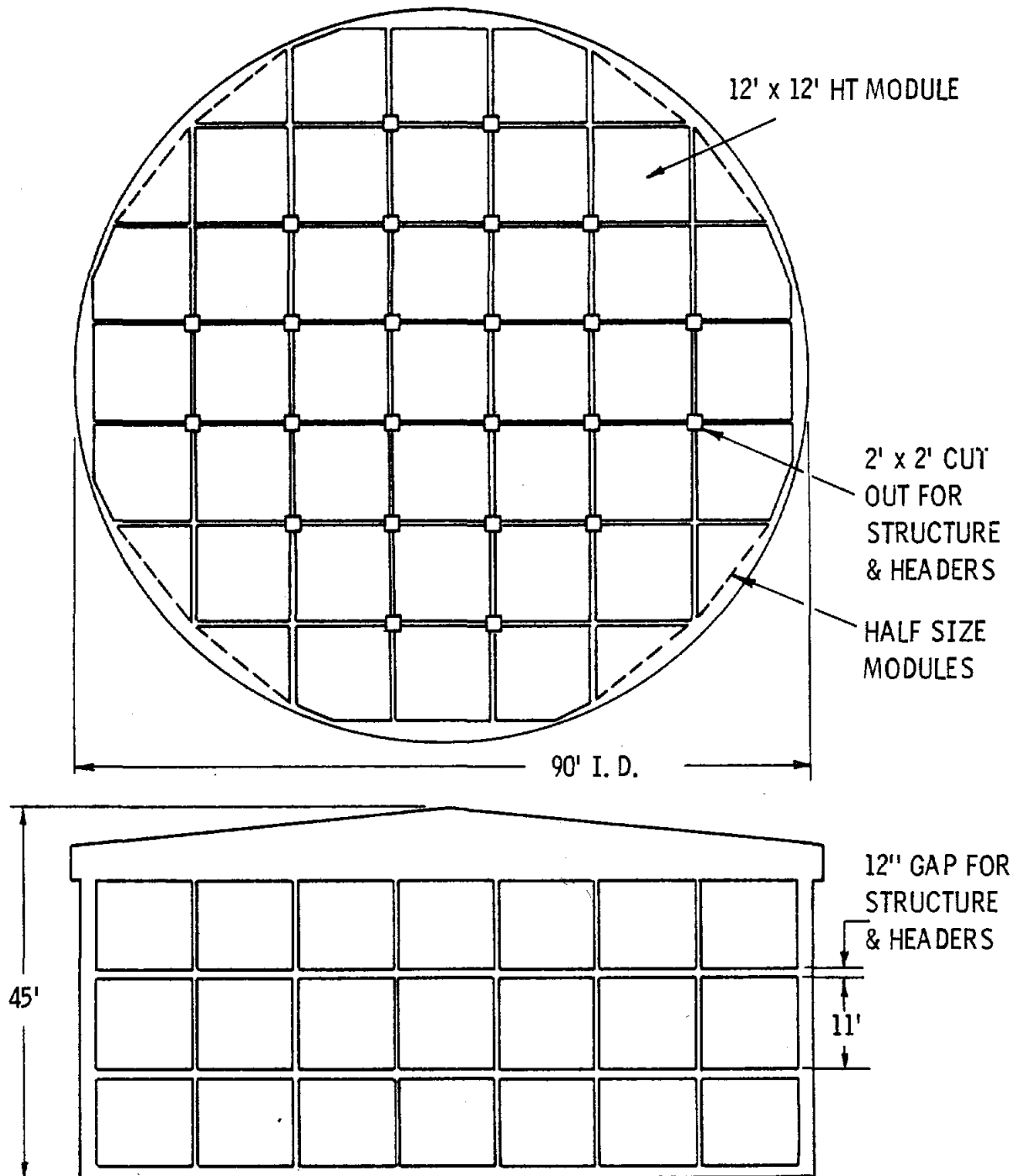
Compared to a system of equal capacity using rectangular, shop-fabricated modules, the large field erected unit requires much less land area, has lower PCM containment and insulation costs and would have less piping and valves. PCM costs would increase by 10% to 15% because of the reduced volumetric efficiency of the design. Maintenance of heat transfer modules would be more difficult. Drainage of the PCM would be difficult without a second large tank.

Detailed designs and cost comparisons are premature at this point. There appears to be no particular technological difficulties associated with scale-up to a large unit. There is also probably a significant cost advantage to doing this, provided the expected high reliability of the heat transfer modules is demonstrated satisfactorily.

6.1.3 Cost Improvements

The largest element of the basic cost of the tube intensive TES system is associated with the heat transfer modules. There have been designed to be of modest size and simple configuration. Since even a relatively small capacity installation would require a considerable number of these units, commercial development of the concept would lead to relatively high production rates. The design is such that quantity production methods would be expected to result from employment of mechanized production techniques.

Figure 6.1-1
830 MWh FIELD ERECTED THERMAL STORAGE UNIT



Mechanized production of heat transfer modules would result in equal cost advantages whether relatively small, shop-fabricated TES units were commercialized or whether large field-fabricated units proved more economical. Since the latter option leads to reduced costs for tanks and insulation, it is clear that this represents a significant potential area for cost reduction.

As discussed above, this option also has the potential for reduction of costs associated with occupied land area. However, this may not be very important for solar applications since solar installations tend to be placed at sites where the cost of land is low.

Improvements of design offer some further potential for cost improvement. By combining the results of tests with improved analytical techniques, it will be possible to optimize the design of heat transfer module. This will allow a reduction in the number of tubes and/or a reduction of the thickness and number of heat transfer plates (fins). This reduction in the amount of metal required to achieve a specified performance would reduce costs.

6.1.4 Scaling

The geometric configuration established for the final design is based directly on the FREEZE calculations for the time when both thermal capacity and peak discharge rate are simultaneously satisfied. This ratio is termed the storage time, and for this application it has a value of 4.93 hr. The tube bundle design can be used at higher or lower capacity, provided the peak discharge rate is proportionately higher or lower. Under these circumstances, more or fewer tube bundles are included in the system to achieve target conditions. One such case is discussed in Section 6.1.2.

For other storage times, the tube spacing and tube length required would change accordingly. As noted in Section 5.7.1, the PCM volume is largely dictated by the capacity and the utilization factor; and the heat transfer

length is determined by the peak discharge rate and FREEZE results for heat flux. Close examination of the FREEZE results for a storage time of 2.5 hr indicates that a 10.2 cm x 10.2 cm (4" x 4") pitch is appropriate with 0.76 mm (0.030") aluminum fins spaced 1.9 cm (0.75") apart. For a 30 MW peak discharge rate (and hence a 75 MWh capacity) a length very similar to the reference design is obtained. Consequently, tube costs would be very similar to the reference design. The fin cost would be less because of the material component of the cost of fins; metal forming and bundle assembly labor would be about the same as the reference. The PCM and tank costs would be less because of the reduction in the thermal capacity. At higher discharge rates and capacity, the cost would scale directly with the basic costs of the 2.5 hr design. Economies of scale with field-erected tank and automated procedures (discussed above) could also play a role in the ultimate costs.

For larger storage times, e.g. 15 hr, the tube spacing would get much wider. Spacing of 20 cm x 20 cm (8" x 8") or 25 cm x 25 cm (10" x 10") might be required. For a 30 MW peak discharge rate and a spacing that virtually freezes all the local PCM, a heat transfer length quite close to the reference design is expected. The amount of PCM and the number of containment tanks would be determined largely by the 450 MWh capacity and the effective PCM utilization factor. The fin costs would scale on the material cost basis, and the PCM and tanks on the basis of the thermal capacity.

Thus, in scaling to other capacities for a given discharge rate, there are economies of scale. The energy-related costs (PCM and containment tanks) go up with capacity. The power-related costs (tubes and fins) go up very slowly with additional fin-material requirements. For a given capacity, the energy-related costs will be virtually fixed. TESS cost would scale with power-related cost components as the peak discharge rate requirements are varied. Under these circumstances, tube length, fin material, and bundle assembly labor will vary strongly with the discharge rate requirements.

One possible area that needs further exploration is the effect of fin spacing and fin thickness on the tube bundle design. Large variation in fin spacing may be able to satisfy a wide variety of peak discharge rates. Consequently, the basic tube configuration, in terms of tube spacing between horizontal runs of the serpentine tube and spacing of adjacent tubes, could be fixed. The heat transfer capability of the bundle could be varied by the fin frequency and/or thickness. Capacity requirements would dictate the number of standardized tube bundles. The rate would dictate the fin frequency and thickness. Power-related costs on a per-bundle basis would scale with fin material and assembly labor. A variety of applications with different capacities, discharge ratios, and storage terms could be satisfied with relatively small adjustments on a basic design. This design standardization would set the stage for automated cost savings. However, parametric studies using FREEZE are required initially to evaluate this possibility.

6.2 Potential Limitations

Commercialization could be inhibited if unanticipated technological problems became apparent during development or during initial deployment of commercial units. The probability of unanticipated problems is strongly dependent upon the quantity and quality of past experience with the particular technology being commercialized.

Technology which is useful for a relatively narrow range of end uses will have difficulties in commercial competition with technology which has broad applicability, even when the broader technology has disadvantages for certain specific applications. Latent heat thermal storage tends to be more narrowly applicable than sensible heat thermal storage; consequently, it will have some disadvantage in competing with sensible heat systems. These factors are discussed further below.

6.2.1 Status of Technology

The development of phase change TESS using NaOH/NaNO₃ mixtures has advanced

to the point where a demonstration system can be designed and built as the next step toward commercialization. Subscale experimental units that are similar to those of the tube-intensive design presented here have been successfully operated (1) with a PCM and heat exchanger. In addition, commercial product designs have been carried through the first stages of field testing by a U.S. and a Canadian electric utility company (42). This background indicates that the technical, institutional, and environmental characteristics will be acceptable.

The two technological areas which are not completely proven are: (1) materials compatibility and (2) heat transfer in the plate(fin) region. SA-214, the tube material selected for this application, is a standard alloy approved by ASME for boiler application. It is used extensively in C-E boilers and is reliable. It is resistant to water-side corrosion over a wide range of feed water impurity levels. It is not the same alloy used by C&W for construction and testing of portotype TES units; however, it is sufficiently similar that it is very unlikely to behave significantly differently from the tested alloys. For these reasons, only a very low probability exists that serious materials compatibility problems will delay commercialization.

The reliability and the low cost of the reference design are quite dependent on successful implementation of the heat transfer enhancement methods developed in this study. The large reduction in the number of tubes required for extraction of heat during discharge reduces costs and also improves reliability by greatly reducing the number of weld joints in the pressure tubing and pipes.

The effectiveness of heat transfer via conduction in radially oriented plates was established primarily through calculations. Experiments done at the Institute of Gas Technology (6) have shown that similar (but less ideal) geometries are effective in improving performance. However, until appropriate small scale tests of the reference design are completed, there will remain some doubt as to exactly how much improvement is obtainable through these means. Nevertheless, it is felt that there is sufficient

conservatism in the analytical methods used for the reference design to assure a high probability of success in this area.

6.2.2 Range of Application

Such limitations to industrial commercialization as may exist are more likely to result from the inherent inflexibility of the phase-change TES system in meeting varying operating conditions. This tends to require a specific design to meet a specific set of performance requirements, rather than standardized components which can be used over a wide range of conditions.

For example, the TES concept presented herein could not be designed to operate if it were supplied with steam at 371°C (700°F) for charging, and required to deliver steam at 316°C (600°F), rather than at 288°C (550°F) and 232°C (450°F), respectively. It would require a PCM melting temperature of about 343°C (650°F), which is outside the range of possibilities for NaOH/NaNO₃ mixtures. For a PCM with different thermo-physical properties and materials compatibilities, appropriate changes would be required in the heat exchanger and possibly the tank designs.

A change of materials usually leads to new requirements for corrosion testing, property testing, and other development work. Such development work is costly and time consuming. In combination with added engineering costs these costs would significantly inhibit the commercialization of latent heat thermal storage systems.

6.2.3 Safety, Environment and Land Use

With respect to safety, environment, and land use, no significant inhibitions to commercialization are seen. The PCM is contained in sealed steel tanks and is not pumped from place to place during normal operation. Spills are quite unlikely.

There are no vapors or fumes given off by the molten NaOH/NaNO₃ eutectic

and it does not react chemically with air or water. These characteristics minimize the hazard of a spill if one should occur. Of course, it is necessary to provide a berm for containment of a spill. Once the material has cooled and solidified, cleanup would be straightforward.

Except for sulfuric acid, NaOH is the most commonly used industrial chemical in the United States. As the principal component of many oven and drain cleaners, it is a common chemical for home use. It is necessary to avoid skin contact and inhalation of NaOH dust. Methods for safe handling of this chemical are easy to apply and well established. Environmental safety or land use restrictions are not expected to limit the use of the TESS in a solar energy system.

7. APPLICATION TO ALTERNATE OPERATING CONDITIONS

The use of phase change to store thermal energy has the great advantage of a high energy storage density. However, this thermal storage method has the disadvantage of flexibility limitations related to the fixed melting point of the phase change material. These limitations tend to require some custom design of the storage unit for each application. Consequently the following discussion is concerned mainly with design changes required to make the system meet changed requirements. Cost projections for the TESS associated with saturated-steam-cooled receivers at higher pressure are presented, for several cases.

7.1 Higher Temperatures

As is apparent from its phase diagram (Figure 3.2-1), the NaNO_3 system can be adjusted to melt at a temperature as high as 320°C (608°F) (pure NaOH) and as low as 245°C (473°F). The practical upper limit on the melting temperature is about 316°C (600°F), which is obtainable with a mix of 95% NaOH, small quantities of NaNO_3 , MnO_2 , and impurities such as NaCl and Na_2CO_3 .

A TES unit using this salt mixture and designed for the reference design temperature differentials could be charged with saturated steam at 343°C (650°F), 15 MPa (2200 psi). The system would discharge steam at 288°C (550°F), 7.2 MPa (1050 psi).

The design of such a higher temperature unit would be similar to the design of the reference unit. Aluminum has sufficient strength at 343°C (650°F) to perform adequately. The principal change would be stronger heat transfer tubes and steam headers to handle the higher pressures involved.

Comstock and Wescott has considerable experience with thermal storage units using non-eutectic salt mixtures containing more than 90% NaOH operated at temperatures up to 482°C (900°F). That experience has shown

that elevated temperatures do not affect reliability. Salt-side corrosion rates are very low and carbon steel behaves very satisfactorily. Water-side corrosion considerations and high pressures may make it desirable to use a low alloy steel (e.g., 2½ Cr-1 Mo) for heat transfer tubes and piping. However, this is not likely.

As indicated above, an increase of about 56°C (100°F) in operating temperatures could be accomplished without changing the basic design, operating characteristics, or cost.

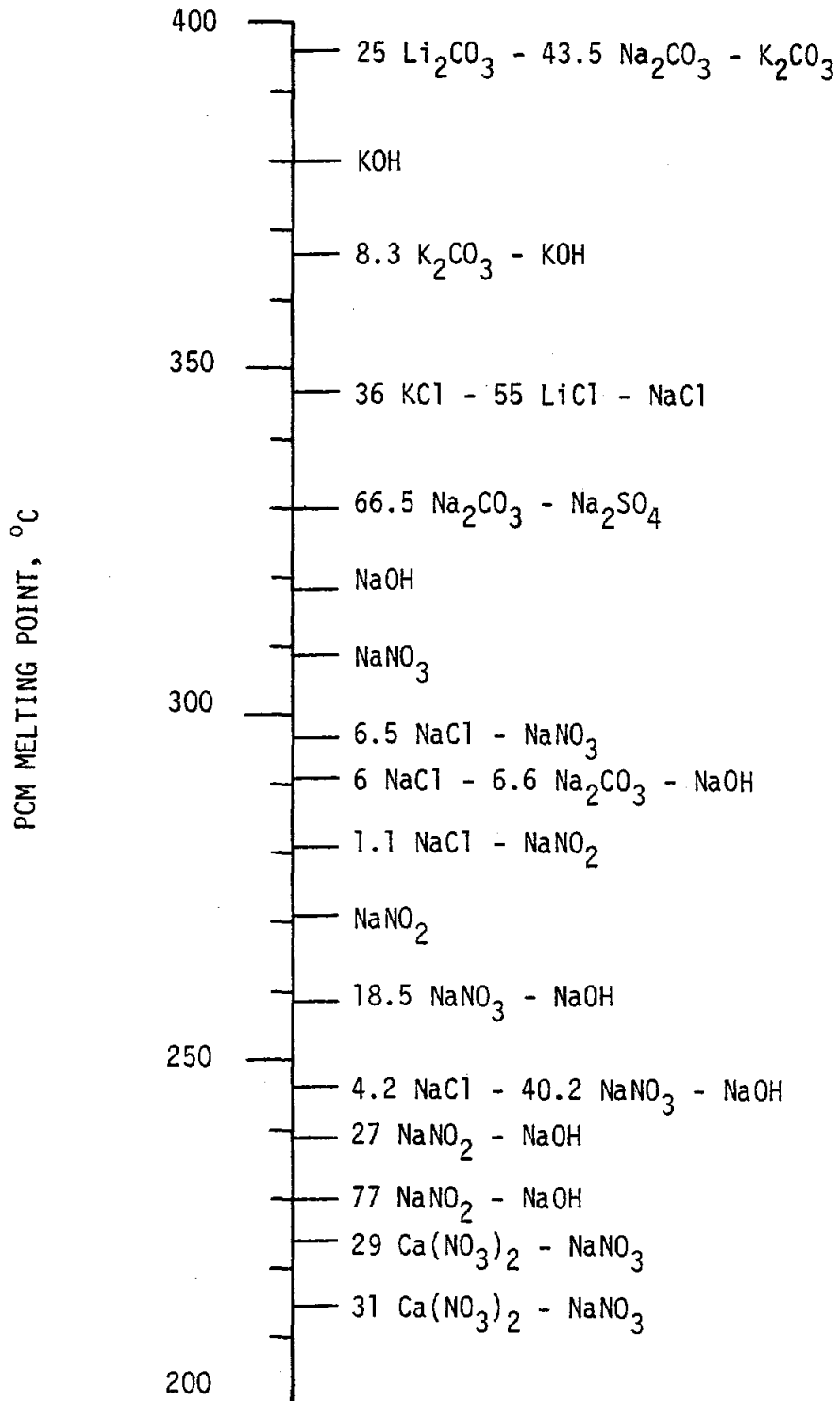
However, if it should be desirable to increase the operating temperature more than 56°C (100°F), it would be necessary to identify a new PCM salt mix. A carbonate eutectic might be appropriate. Other substantial design changes would also be required. For example, the high pressure and temperature of the steam would require the use of alloy steels. The compatibility of these steels with the salt would have to be established. The design concept resulting from these extensive changes is essentially different from the reference concept; therefore, the reference concept should be regarded as having an upper temperature limit of 343°C (650°F).

For TESS operating at temperatures other than that of the present study, eutectics and single salts having melting points in the range 200 to 400°C (392°F to 752°F) may be of interest. Reference (8) lists 62 eutectics that may be reasonable candidates and that are distributed quite uniformly over the temperature range.

Selections from this list are shown on Figure 7.1-1 against a temperature scale. In making the selection, preference was given to the salts of sodium and calcium because of availability and price. Preference was also given to the nitrates, nitrites, hydroxides, carbonates, and chlorides of these metals for reasons of chemical stability, availability, and price. A few eutectics containing the more costly salts of potassium and lithium were included where necessary to fill spaces in the temperature spectrum. Lithium salts, although more costly, tend to have high latent heats and chemical stability, and, therefore, are often worthy of consideration.

FIGURE 7.1-1

CANDIDATE PCMs FOR RANGE 200-400°C
 (Mole percentages shown for eutectics)



Although the PCMs were not investigated during this study, it is believed that several would be found suitable.

Three of the candidates in Figure 7.1-1, in addition to the NaOH-NaNO₃ eutectic used in the tube-intensive conceptual design, are compared on Table 7.1-1, to show the effect of the differences in thermal and physical properties of these PCMs on the total cost of the TESS.

The cost for the NaOH-NaNO₃ eutectic is the same as that shown on Table 5.6-1, except that the items making up the total are grouped to indicate the costs of tanks, heat exchanger, PCM, other hardware items, and installation.

The costs for the other PCMs were estimated by the following approximations. The tankage requirements are taken as inversely proportional to the energy densities of the PCMs (the product of the latent heat and liquid density). The heat exchanger costs consist of two parts, the quantity of tubing, which is assumed to be the same for all PCMs, and the number of fins, which is taken as proportional to total tank volumes. The PCM costs are all calculated on the same basis. The installation costs are assumed proportional to total tank volumes. In the case of the carbonate eutectic, the tanks and heat exchanger tubing costs are based on the price of stainless steel.

If a temperature difference of 28°C (50°F) is assumed for heat transfer between the melting point and the charge and discharge steam temperatures, then NaNO₃ could be charged and discharged with saturated steam at 13.8 MPa and 6.41 MPa (2000 and 930 psia), respectively.

The carbonate eutectic would be most useful for charging and discharging with superheated steam because of its high melting point. For such an application, the heat exchanger cost estimate is certainly optimistic because more surface would be required for vapor superheating than for the two-phase heat transfer for which it was designed.

TABLE 7.1-1
APPROXIMATE TOTAL TESS COST FOR OTHER PCM

	<u>NaOH NaNO₃</u> Eutectic	<u>NaNO₃</u>	<u>NaOH</u>	<u>(LiNaK)₂CO₃*</u> Eutectic
PCM Melting Point, °C, (°F)	260 (500)	308 (586)	318 (605)	397 (747)
PCM Heat-of-Fusion, kJ/kg, (Btu/lb)	274 (118)	181 (78)	325 (140)	277 (119)
PCM Price, Marked Up, \$/kg, (\$/lb)	.51 (.23)	.29 (.13)	.62 (.28)	1.04 (.47)
No. of Tanks	8	11.4	6.75	7.27
<u>TESS Component Costs</u>				
Tanks	\$ 506,500	\$ 721,000	\$ 427,400	\$ 804,600 **
Heat Exchanger	1,630,000	2,168,000	1,432,000	1,862,000 **
PCM	1,102,000	953,000	1,112,800	3,519,000
Other Hardware	245,000	350,000	207,000	223,000
Installation	394,000	531,000	343,000	364,000
TESS TOTAL COST	\$3,880,000	\$4,720,000	\$3,520,000	\$6,773,000

* 32-33-35%

** Stainless Steel

In the case of NaOH, the total latent heat of 325 kJ/kg (140 Btu/lb) is divided equally between the latent heat of fusion at 318°C (605°F) and the latent heat of a solid state transition at 293°C (560°F). In order to utilize the total latent heat with a difference of 56°C (100°F) between the charging and discharging steam temperatures, a somewhat larger heat exchanger would be required, resulting in a higher system cost. If the 28°C (50°F) differential for which the heat exchanger was designed were maintained, then the difference between the charge and discharge steam temperatures would be increased from 56°C (100°F) to about 80°C (145°F), which would reduce the thermodynamic efficiency of the storage and retrieval process.

With these limitations in mind, however, the effects of the PCM characteristics on costs can be seen on Table 7.1-1. Comparing the NaNO₃ with the NaOH-NaNO₃ eutectic shows that the price advantage of the former is more than outweighed by its lower latent heat, which results in higher tank and heat exchanger costs and significantly higher total cost. The NaOH, on the other hand, with its higher price and latent heat, has lower tank and heat exchanger costs, and slightly lower total cost (but lower thermodynamic efficiency).

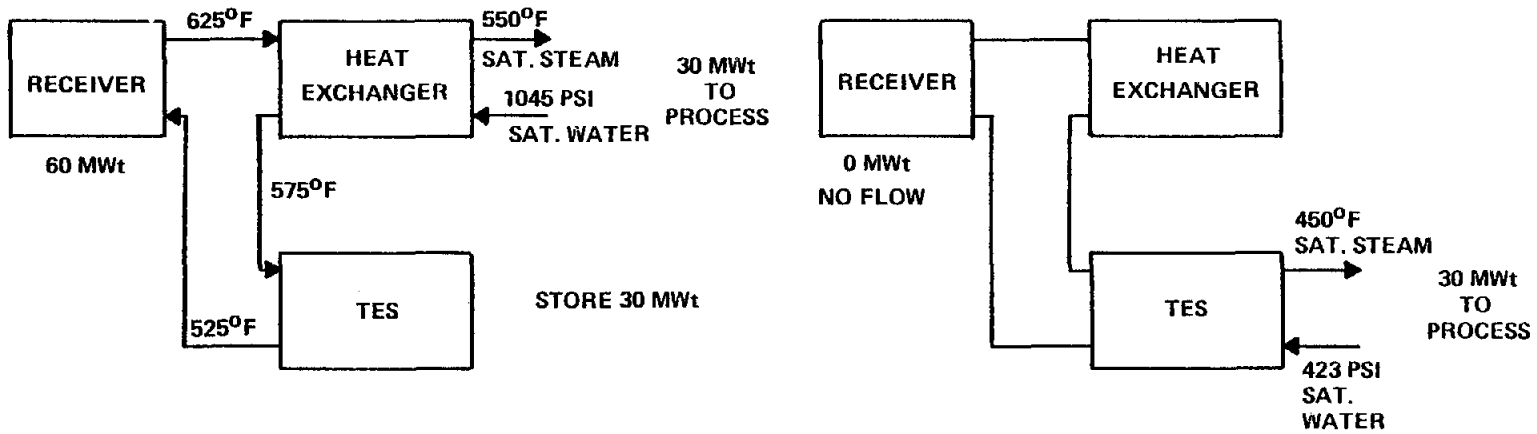
The very high total cost of the carbonate system reflects the high price of the PCM because of its high lithium content, in addition to the requirement for stainless steel for the tanks and heat exchanger tubing. Some improvements in cost could be made by substituting alloy steels for stainless.

7.2 Secondary Fluid Charging

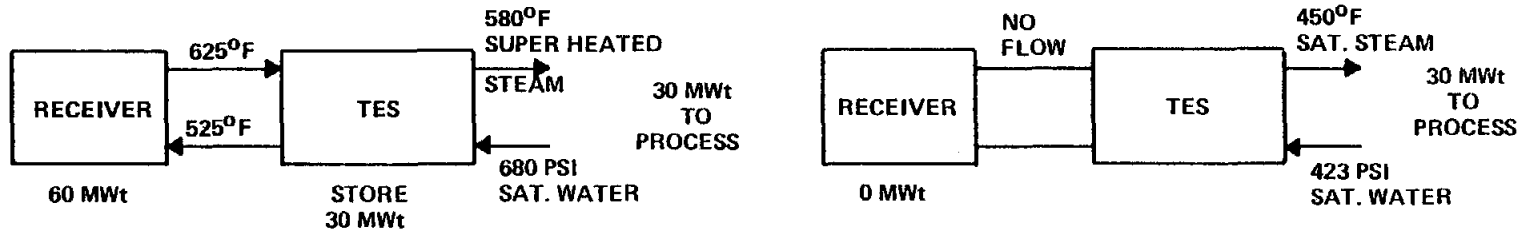
If the receiver is cooled with an organic or silicone sensible-heat working fluid instead of steam, there are several ways that the thermal system could be arranged. Two such arrangements are diagrammed in Figure 7.2-1. Option A puts the thermal storage unit in series with a 1858 m² (20,000 ft²) heat exchanger. This arrangement allows production of 30 Mwt of 7.2 MPa (1045 psi) saturated steam while charging the TES unit, thus duplicating the output of the reference system.

Figure 7.2-1
SYSTEM OPTIONS FOR SECONDARY FLUID CHARGING

OPTION A: DUPLICATES OUTPUT OF REFERENCE SYSTEM



OPTION B: ELIMINATES THE NEED FOR AN EXTERNAL HEAT EXCHANGER



CONDITION WHILE CHARGING TES AT NOON

CONDITION AT END OF DISCHARGING FROM STORAGE

Option B utilizes the TES unit as a heat exchanger as well as a storage unit. Here, process steam conditions at midday must be altered slightly to be compatible with operation of the system.

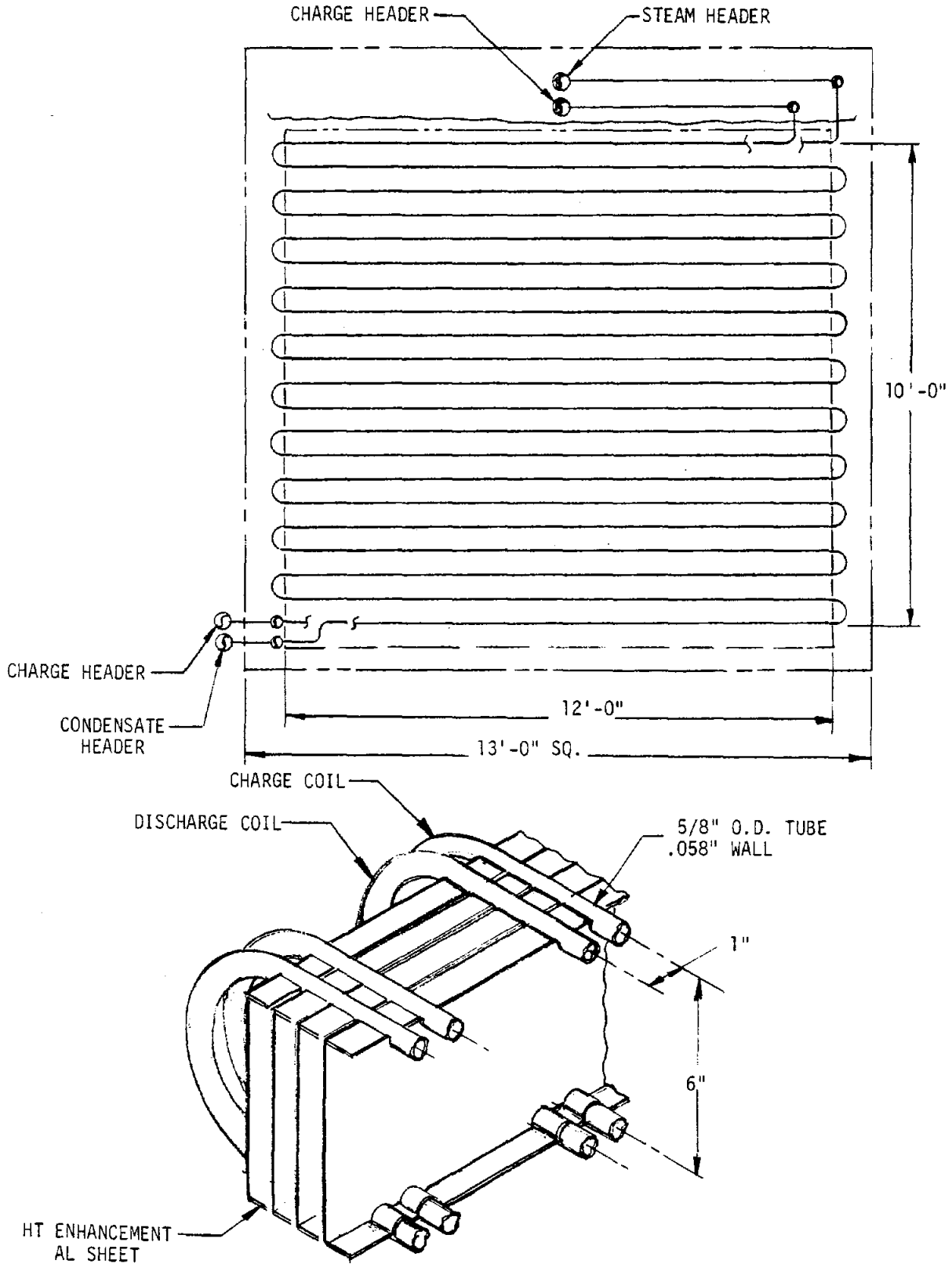
Reference (41) gives results of detailed, application-specific computer studies comparing Option B-type systems with systems utilizing a heat exchanger in parallel with the thermal storage unit (a third option not shown in Figure 7.2-1). For the cited application, it was shown that the use of the TES unit as a heat exchanger as well as a storage unit reduced net costs by 43% over a storage unit with an external discharge heat exchanger. It is generally true that the combined system is less costly because the modifications required to accomplish this are simple. Option B, therefore, should be significantly cheaper than Option A. Of course, the optimum arrangement could be determined within the context of a specific application.

Modification of the reference design to accommodate secondary fluid charging is very simple, as illustrated in Figure 7.2-2. Because of the wide spacing of the serpentine coils in the reference design, there is plenty of room to add a second set of charging coils without affecting the size of the unit or its basic arrangement. If the unit is to be used as a heat exchanger as well as a storage unit (Option B), the charging coil would completely duplicate the discharge coil. It is estimated that this would increase the conceptual design cost of the TES module by 15%.

If the second coil is for charging only (Option A), it need not duplicate the discharge coil. The cost of the TES module is estimated to increase only 5% for Option A over the conceptual design cost.

The aluminum fins provide excellent thermal coupling between the charge and discharge coils. Eight modules contain 2200 m^2 ($24,000 \text{ ft}^2$) of heat transfer area at the surface of the discharge coil. A conventional shell-and-tube heat exchanger would require about 1858 m^2 ($20,000 \text{ ft}^2$) to transfer 30 Mwt between hot oil and boiling water at an LMTD of 28°C (50°F). The principal thermal resistances are on the fluid side in these

FIGURE 7.2.2 DUAL COIL ARRANGEMENT - SECONDARY FLUID CHARGING



systems. Rough calculations indicate that the dual tube arrangement shown in Figure 7.2-2 would be adequate to handle the 30 MWt heat exchanger load while charging at the peak midday rate.

In summary, the reference TES design is easily modified to accommodate secondary fluid charging. This modification would increase the cost of the unit by 5% to 16% depending on overall system requirements. A new cost saving might be realized if the TES unit could also serve a heat exchanger function. This modification requires no new technology and presents no new safety or environmental constraints.

8. DEVELOPMENT

Development activities required to support the design and bring it to a state of readiness for final design and construction are discussed in this section. Passive, tube-intensive thermal energy storage using the latent heat of sodium hydroxide/sodium nitrate is a current technology. The PCM is composed of common industrial chemical ingredients found in household cleaners; there is a great deal of experience in handling the materials. Comstock and Wescott has developed and tested heat storage units with variants of the selected PCM for home heating and water heating since 1962. Much of their experience with the storage medium was described in Section 3.2. In the past few years C&W has been funded by Sandia Laboratories and NASA Lewis Research Center to analyse, design, construct, and test latent heat TESS for a variety of charging and discharging fluids and conditions. The current design is built on this foundation.

8.1 Materials Testing

A specific experimental data base for the selected commercial grade sodium hydroxide/sodium nitrate PCM eutectic should be developed. This includes the thermal conductivity and specific heat for the solid and liquid phases, the latent heat of fusion and the liquid phase viscosity. In addition, a phase diagram for a limited range around the eutectic point is needed.

The data used on the design development are based on the material properties of pure sodium hydroxide and pure sodium nitrate presented in Reference (1), since no information could be found for the specific eutectic. Thermal conductivity and specific heat for "Thermkeep" (91.8% sodium hydroxide, 8.0% sodium nitrate and 0.2% manganese dioxide) from Reference (1) were applied to the eutectic. During the conduct of this contract C&W obtained cooling curves for commercial grades of sodium hydroxide and sodium nitrate. In both cases the indicated melting points were about 6-7°C (10-12°F) less than the data in literature (8). This

was attributed to impurities in the commercial-grade samples. The eutectic mixture selected for the PCM was also tested. The melting temperature was approximately 5°C (9°F) higher than the phase diagram (1) showed. The materials testing will eliminate the uncertainties associated with commercial grade materials and give specific data for the specific mixture.

8.2 Heat Transfer Testing

Aluminum channels have been selected to augment the heat transfer from the PCM to the steam. The results of heat transfer calculations determined the sizing and spacing of these channels. The efficacy of this design needs to be demonstrated experimentally. This can be done on a laboratory scale with a small section of the serpentine tube bundle. A test bundle with 3 or 4 serpentine tubes with only 3 horizontal runs of sufficient length to allow about 10-15 channel sections could be tested. Condensing and boiling fluids would be run through the tubes to simulate the bulk of operating conditions expected. The heat removal capability, particularly near the end of discharge, can be determined. Parametric variations in channel spacing and size (i.e. tube spacing) can be included. In addition, the means of improving heat transfer, such as using punched-out tabs on the channel sections, could be investigated.

8.3 Development of Performance Prediction Methods

The performance characteristics of the TES unit were calculated using a modified version of the C&W TESST (1) computer program. The effect of augmented heat transfer had to be simulated by enhanced conductivity of the PCM. In the particular calculations performed, the conductivity was increased until the unit output matched that projected by local heat transfer study. An analytical effort is needed to develop an appropriate model of heat transfer for inclusion in a program, such as TESST, that performs detailed thermal analysis of the unit through charging and discharging of the daily duty cycle. The results of such a program can

be used as part of the data evaluation of the heat transfer tests described in Section 8.2.

An important aspect of storage design is the specific application for which the unit is selected. The interaction of the unit with the solar field may have a direct impact on storage economics and consequently the storage design decisions. A simple computer model of the solar collector field and a simple characterization of the process features should be married with the TES model discussed above. Overall system performance would be obtained, and the feedback of the storage system could then be assessed. The impact of the storage design would then be employed in the design decision process. Finally, a prediction of the operating unit performance in a SRE or a commercial system could be made.

REFERENCES

1. Cohen, B.M., Rice, R.E., and Rowny, P.E., Comstock and Wescott, Inc., "Development of a Phase-Change Thermal Storage System Using Modified Sodium Hydroxide for Solar Electric Power Generation," DOE/NASA/0615-79/1, December 1978.
2. Alario, J., Kosson, R., and Haslett, R., Grumman Aerospace Corporation, "Active Heat Exchanger System for Latent Heat Thermal Energy Storage," DOE/NASA/0039-79/1, January 1980.
3. Le Frois, R.T. and Mather, A.K., Honeywell, Inc., "Active Heat Exchanger System Development for Latent Heat Thermal Energy Storage," DOE/NASA/0038-80/2, April 1980.
4. Bramlette, T.T., et al., "Survey of High Temperature Thermal Energy Storage," Sandia Laboratories, Albuquerque, SAND 75-8063, March 1976.
5. Chubb, T.A., et al., "Energy Storage as Heat-of-Fusion in Containerized Salts," Naval Research Laboratory, Washington, Report 4267, June 27, 1980.
6. Maru, H.C., et al., "Molten Salt Thermal Energy Storage Systems," Institute of Gas Technology, Chicago, Illinois, Report UC-94a, March 1978.
7. Petri, R.J., et al., "High-Temperature Molten Salt Thermal Energy Storage Systems," U.S. Department of Energy, Washington, DOE/NASA/0806-79/1; NASA CR-159663, February 1980.
8. Janz, G.J., et al., "Eutectic Data," Molten Salts Data Center, Troy, New York, TID-27163-P1 & 2, July 1976.
9. Janz, G.J., et al., "Physical Properties Data Compilations Relevant to Energy Storage," Molten Salts Data Center, Troy, New York, April 1979.

10. Charlesworth, J.F., "Melting Points of Metallic Elements and Selected Compounds," Air Force Materials Laboratory, Air Force Systems Command, Ohio, Technical Report AFML-TR-70-137, October 1970.
11. Birchenall, C.E., "Heat Storage in Alloy Transformations," U.S. Department of Energy, Washington, DOE/NASA/3184-1; NASA CR-1599787, April 1980.
12. Birchenall, C.E., "Heat Storage Materials," U.S. Department of Energy, Washington, C00-4042-16, December 1977.
13. Eichelberger, J.L., "Investigation of Metal Fluoride Thermal Energy Storage Materials," Penwalt Corporation, Pennsylvania, C00-2990-6, December 1976.
14. Hale, D.V., et al., Lockheed Missiles and Space Company, Huntsville, AL, "Phase Change Materials Handbook," NASA CR-61363, September 1971.
15. Metals Handbook, 8th Edition, Volume 2, American Society for Metals, Ohio.
16. Mellor, J.W., Inorganic and Theoretical Chemistry, Volume 2, New York: John Wiley and Sons, Inc., 19.
17. Goetzel, C.G., Treatise on Powder Metallurgy, Volume 1, London: Interscience Publishers Ltd., 1949.
18. Calogeras, J.E., and Gordon, L.H., "Storage Systems for Solar Thermal Power," Proceedings of the 13th Intersociety Energy Conversion Engineering Conference, August 1978, Volume 2.
19. "Thermal Energy Storage, Fourth Annual Review Meeting," NASA Conference Publication 2125, DOE Publication Conf-791232, December 1979.

20. Hall, E.W., et al., General Electric, "Conceptual Design of Thermal Energy Storage Systems for Near-Term Electric Utility Applications," EPRI-EM-1218, November 1979.
21. Thornton, R.F., General Electric, "Thermal Energy Storage Subsystems for Solar Heating and Cooling Applications (Rolling Cylinder Thermal Storage)," Interim Report Contract No. DE-AC05-78OR05759, June 1979.
22. Dullea, J. and Mara, H.C., Institute of Gas Technology, "Molten Salt Thermal Energy Storage Systems," Report Prepared under Contract No. EY-76-C-02-2888 for ERDA, June 1976 - May 1977.
23. Alario, J., et al., Grumman Aerospace Corporation, "Active Heat Exchange System Development for Latent Heat Thermal Energy Storage," Topical Report No. DOE/NASA/0039-79/1, NASA CR 159726, January 1980.
24. Ferrara, A., et al., Grumman Aerospace Corporation, "Thermal Energy Storage Heat Exchanger," NASA CR-135244, October 1977.
25. "Solar Pilot Plant Preliminary Design Report," Conceptual Design Report, ERDA Contract No. E(04-3)-1109, Honeywell, Inc., May 1976.
26. "Life and Stability Testing of Packaged Low-Cost Energy Storage Materials," ORNL-Union Carbide, Report No. ORNL/SUB-7585/1, July 1980.
27. "Encapsulation of Phase Change Materials in Concrete Masonry Construction," Progress Report No. 3 (Final), Process Science Division, Brookhaven National Laboratory, Report No. BNL 51100, June 1978 - September 1978.
28. "Thermal Storage Applications Workshop," Plenary Session Analysis and Contributed Papers, NASA-CR-158643 and NASA-CR-158644, Jet Propulsion Laboratory, February 1979.
29. Lee, C., et al., "Solar Applications of Thermal Energy Storage," Report No. TID-29430, Hittman Associates, Inc., January 1979.

30. "Development of an Active Heat Exchanger System for Latent Heat Thermal Energy Storage Systems," Comstock and Wescott Internal Report, September 1977.
31. "Development of Thermkeep Thermal Energy Storage Module," Report to be published, Comstock and Wescott, Inc., January 1981.
32. "Thermal Energy Storage," Annual Report, DOE/NASA/1034-8, NASA TM-81514, NASA-LRC, January 1979 - March 1980.
33. Ramanathan, J., "Thermal Energy Storage Systems Using Fluidated Bed Heat Exchangers," NASA Conf. Publication No. 2125, page 47, Midwest Research Institute, 1979.
34. "Solar Pilot Plant: Phase I, Conceptual Design Report, Thermal Storage Subsystem Research Experiment," CRDL Item No. 5, Honeywell, Inc., Minneapolis, MN, May 19, 1976.
35. "Cost and Performance of Thermal Storage Concepts in Solar Thermal Systems, Conceptual Design Review," Prepared for SERI by Stearns-Roger Services, Inc., Denver, CO, September 3-4, 1980.
36. Popper, H., et al., Modern Cost Engineering Technique, New York: McGraw-Hill Book Company, 1970.
37. Roark, R.T., Formulas for Stress and Strain, 4th Ed., New York: McGraw-Hill Book Company, 1965.
38. Brockenbrough, R.L. and Johnston, B.G. USS Steel Design Manual, United States Steel Corporation, May 1974.
39. Telecommunication with G. Meyers, Pittsburg Corning Glass Works.
40. Tong, L.S., Boiling Heat Transfer and Two Phase Flow, New York: Robert C. Kreiger Publishing Company, Huntington, 1975.

41. Rice, R.E., Rowny, P.E. and Cohen, B.M., Comstock and Wescott, Inc., "Extended Development of a Sodium Hydroxide Thermal Energy Storage Module," DOE/NASA/0138-1; NASA CR-165206, February 1981.
42. Perdue, D.G., and Gordon, L., "Engineering Evaluation of a Sodium Hydroxide Thermal Energy Storage Module," DOE/NASA/1034-80/7; NASA Lewis Research Center, February 1980.
43. Mc Ewen, M. "Organic Coolant Databook," Monsanto Chemical Company, Technical Publication AT-1, July 1958.
44. Jordan, D.P., and Leppert, G. "Nucleate Boiling Characteristics of Organic Reactor Coolants," Nuclear Science and Engineering, Volume 5, No. 6, June 1959.
45. Handbook of Heat Transfer, Edited by Rohsenow, W.M. and Hartnett, J.P., New York: McGraw-Hill, 1973.
46. El-Wakil, M.M., Nuclear Power Engineering, Second Ed., New York: McGraw-Hill, 1962.
47. Perry, R.H. and Chilton, C.H., Chemical Engineers' Handbook, 5th ed., New York: McGraw-Hill, 1973.
48. McAdams, W.H., Heat Transmission, 3rd Ed., New York: McGraw-Hill, 1954.
49. Kreith, F., Principles of Heat Transfer, Second Ed., New York: International Textbook Co., 1967.
50. Hallet, R.W., and Gervais, R.L. "Central Receiver Solar Thermal Power System, Phase I, CDRL Item 2, Pilot Plant Preliminary Design Report," Volume V: Thermal Storage Subsystem, Prepared for U.S. DOE by Sandia Laboratories, October 1977, SAN/1108-8/5.

GLOSSARY

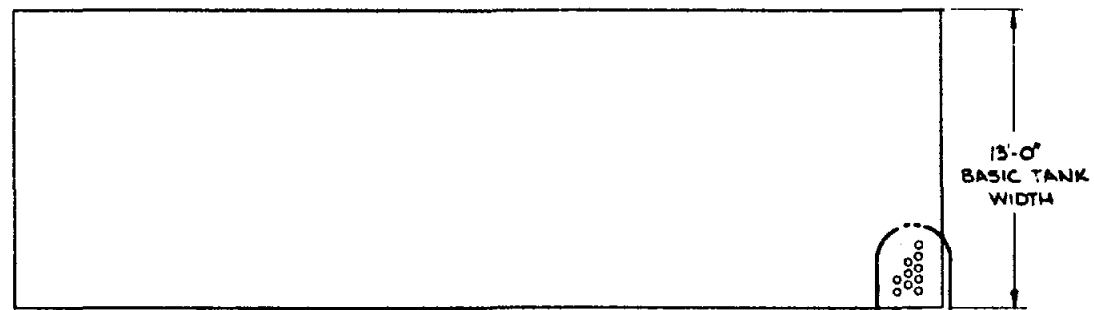
AISC	American Institute of Steel Construction
ASME B&PV	American Institute of Mechanical Engineers Boiler and Pressure Vessel Code
HHX	High Temperature Heat Exchanger
HX	Heat Exchanger
IHX	Intermediate Heat Exchanger
LHX	Low Temperature Heat Exchanger
PCM	Phase Change Material
SERI	Solar Energy Research Institute
SRE	Subsystem Research Experiment
TES	Thermal Energy Storage
TESS	Thermal Energy Storage System
UF	Utilization Factor

APPENDIX I

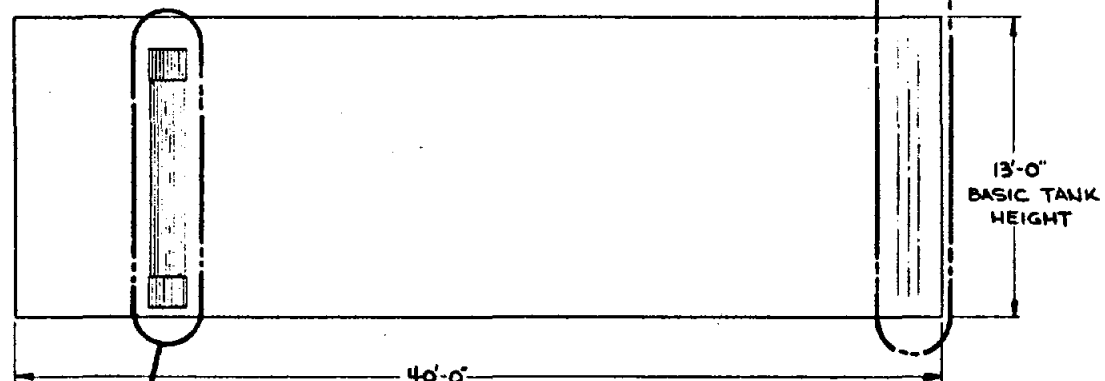
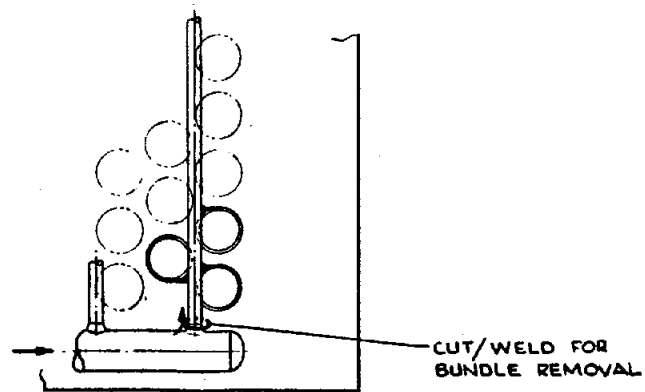
Sketches of TESS - Most Promising Concepts

Drawings of Final Concept

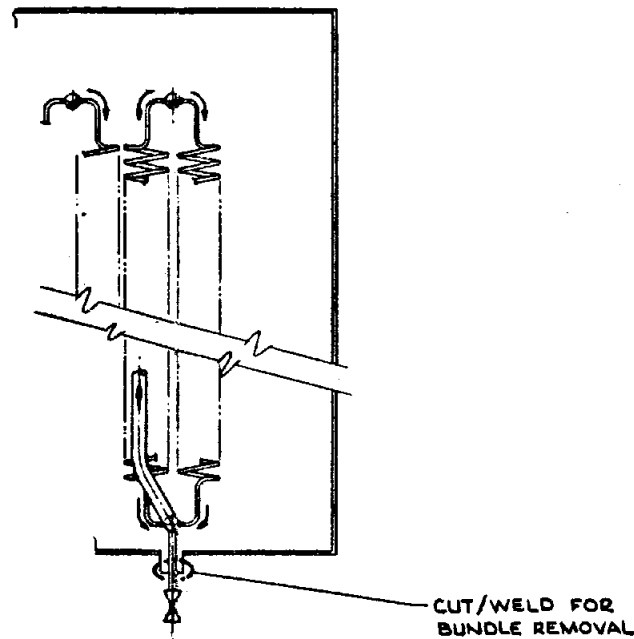
Design Characteristics of Final Concept



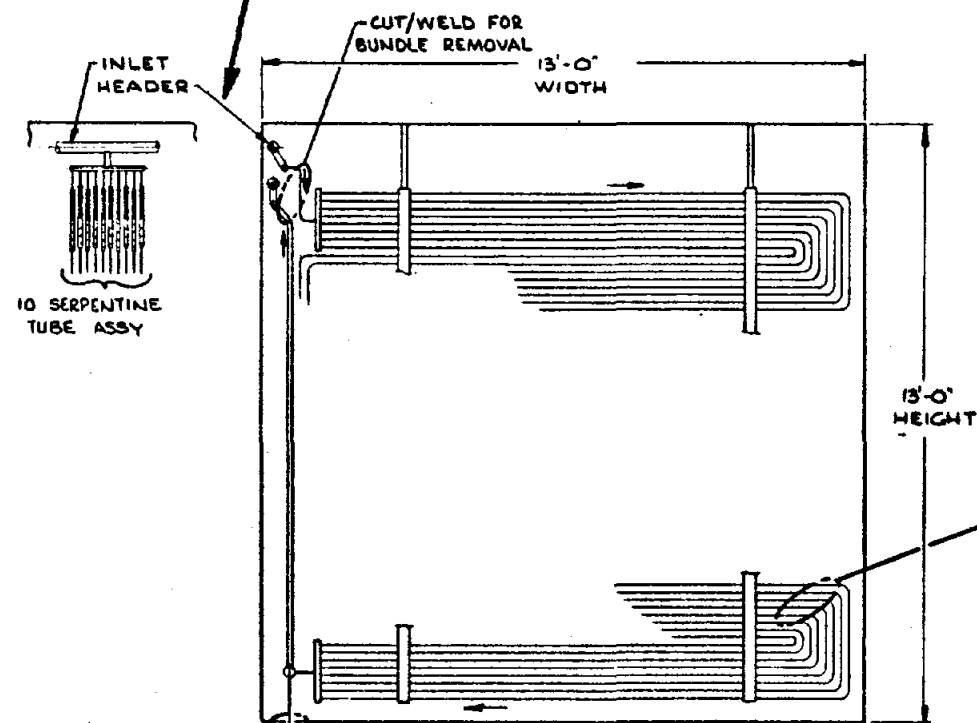
PLAN VIEW



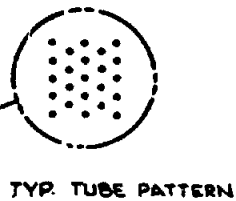
ELEVATION VIEW



COILED TUBE SCHEME



SERPENTINE TUBE SCHEME
SIDE ELEVATION



TYP. TUBE PATTERN

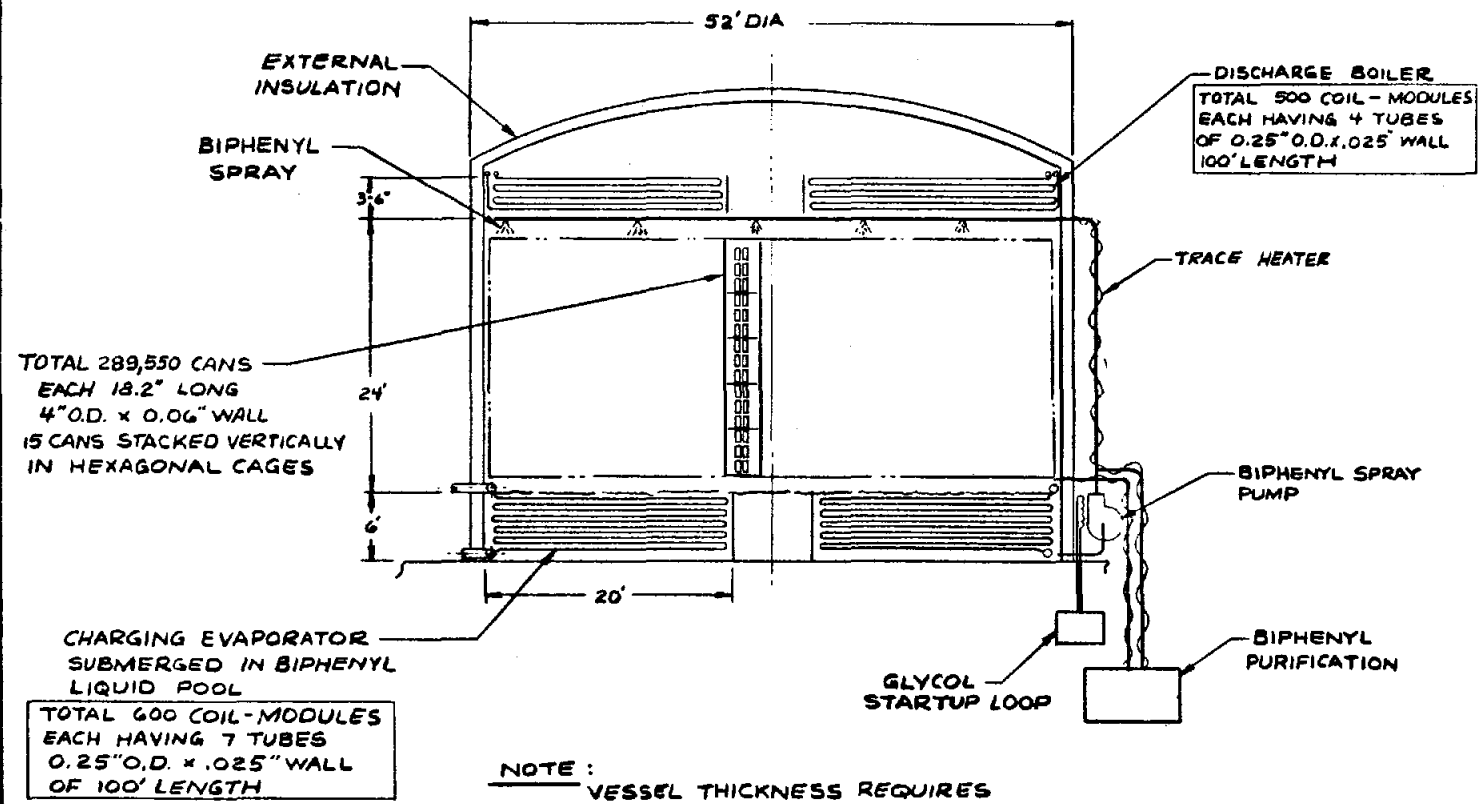
MODIFIED TUBE INTENSIVE CONCEPT

SD-13780-800-003

SKETCH 1

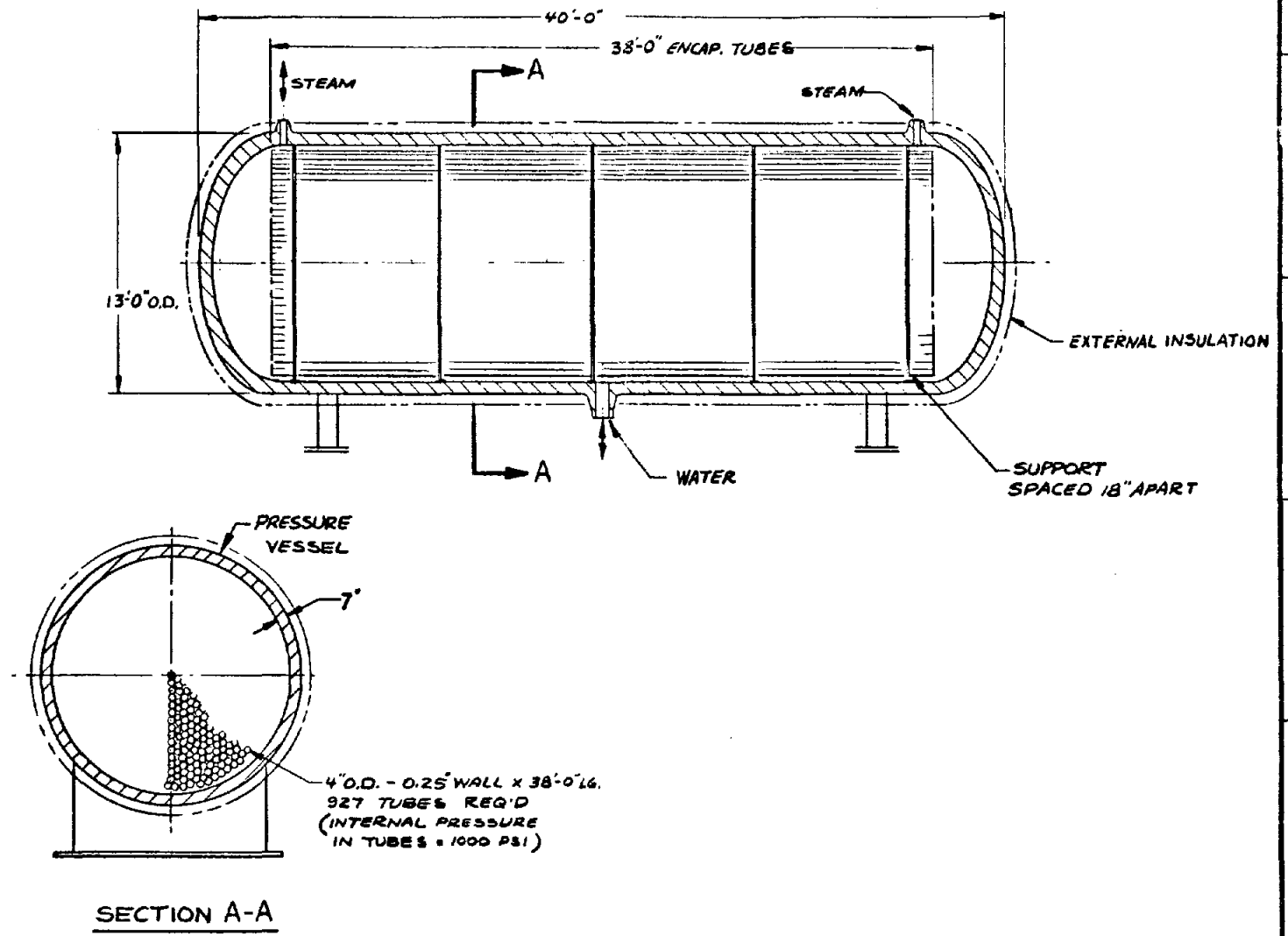
164

	<small>This drawing is the property of GE POWER SYSTEMS Combustion Engineering Inc. Windsor, Connecticut 06095 and is not to be reproduced or used to furnish any information for making of drawings or apparatus except where provided for by agreement with said company.</small>		DRAWN BY D.WEBB 10/1/80
	NUCLEAR POWER SYSTEMS		CHECKER APPROVALS
CUSTOMER		TITLE TES CONCEPT MODIFIED TUBE INTENSIVE	
NEXT ASSY	SUPERSEDES	DWG. NO. SD-13780-800-003	
P/B NO.	COMPONENT CODE	SCALE	



NOTE:
VESSEL THICKNESS REQUIRES
FURTHER EVALUATION OF BIPHENYL
OPERATING PROPERTIES WITH
SMALL WATER LEAKAGE. (0.5" - 3" THICK)
CAN THICKNESS ALSO MAY VARY FROM
0.012" TO 0.06".

BOILER TANK (CHUBB) SCHEME



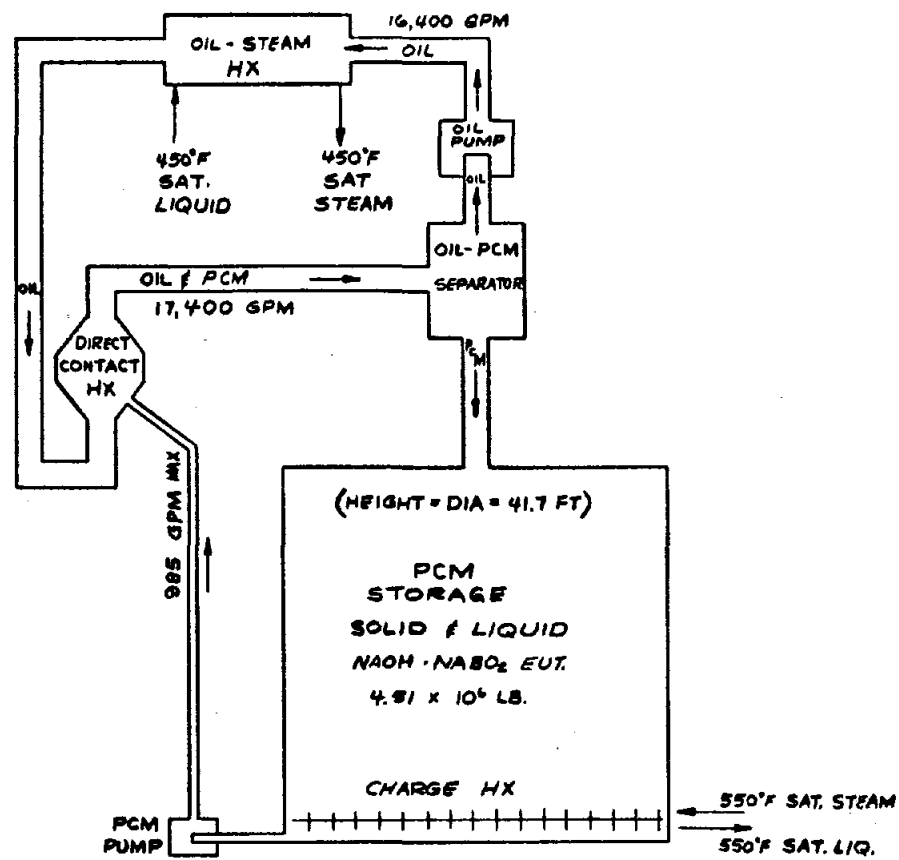
MACRO ENCAPSULATION SCHEME
TOTAL 14 MODULES REQ'D.

SD-13780-800-004

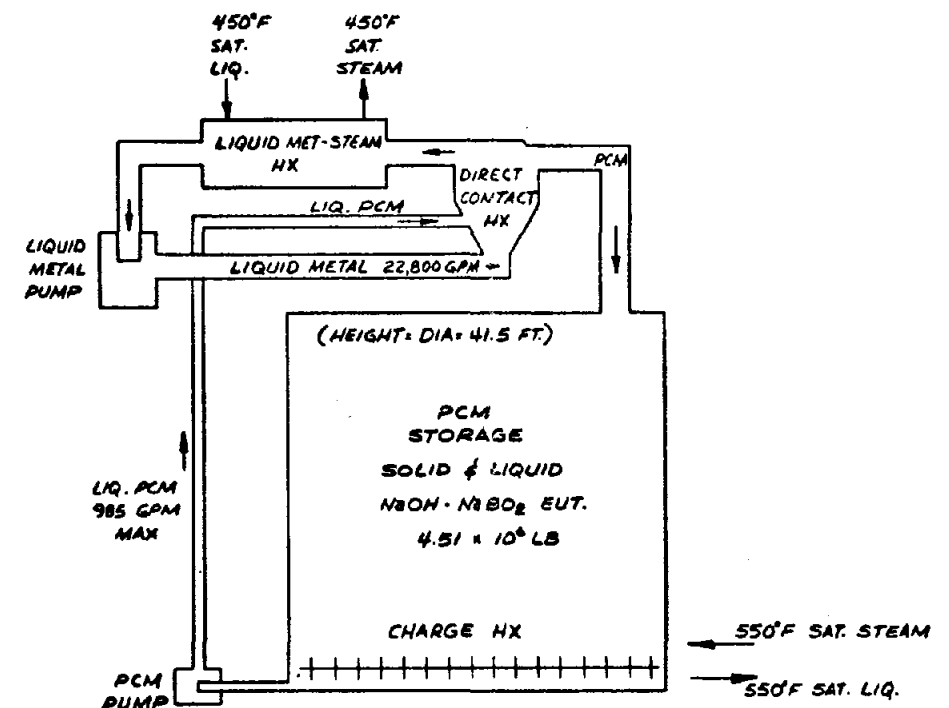
SKETCH 2

165

<p>POWER SYSTEMS COMBUSTION ENGINEERING INC. NUCLEAR POWER SYSTEMS</p>	<p>This drawing is the property of CE POWER SYSTEMS Combustion Engineering, Inc. Windsor, Connecticut 06095 and is not to be reproduced or used to furnish any information for making of drawings or spe- cimens except where provided for by agreement with said company.</p>	<p>DRAWN BY D. WEBB 01/780</p>
		<p>CHECKER</p>
<p>CUSTOMER</p>		<p>TITLE TES CONCEPT ENCAPSULATION SCHEMES</p>
<p>NEXT ASSY</p>	<p>SUPERSEDES</p>	<p>DWG NO. SD-13780-800-004</p>
<p>JOB NO. 682101</p>	<p>COMPONENT CODE</p>	<p>SCALE SHEET 01</p>



DIRECT CONTACT CONCEPT
USING
PCM DROP - OIL
INTERMEDIATE HEAT EXCHANGER

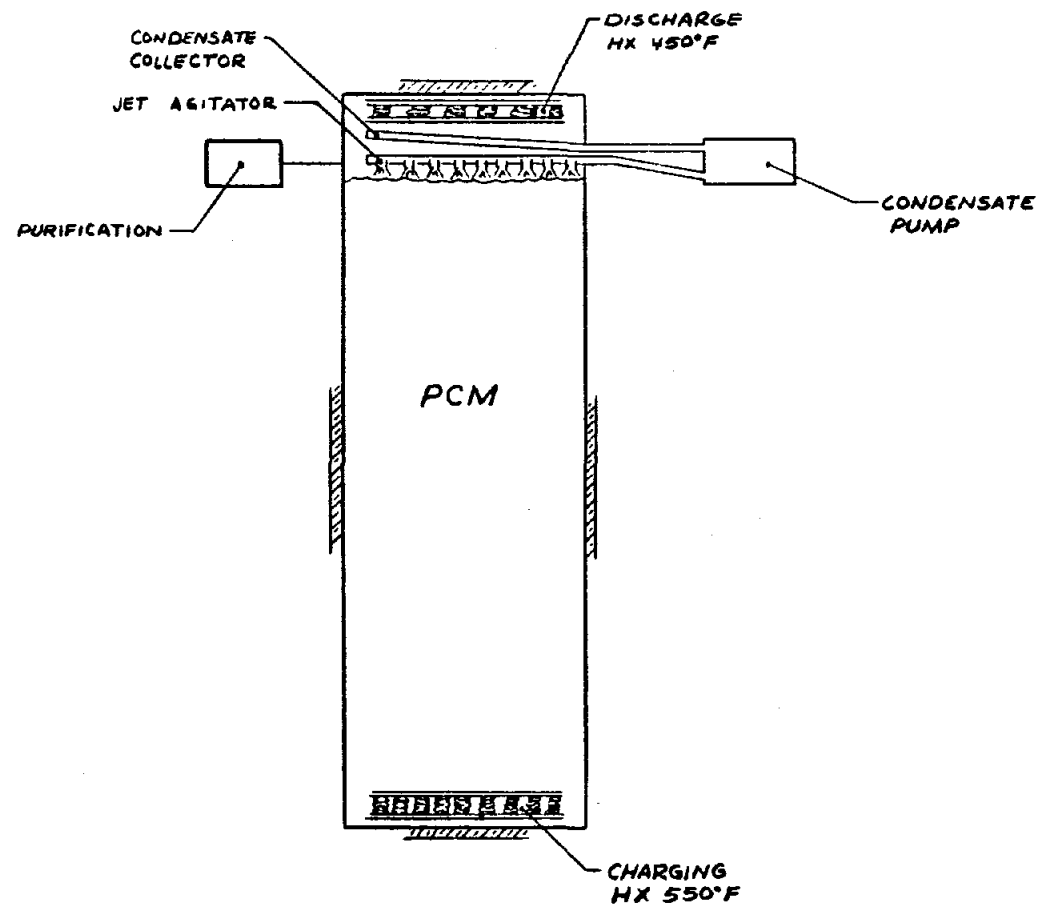


DIRECT CONTACT CONCEPT
USING
PCM DROP - LIQUID METAL
INTERMEDIATE HEAT EXCHANGER

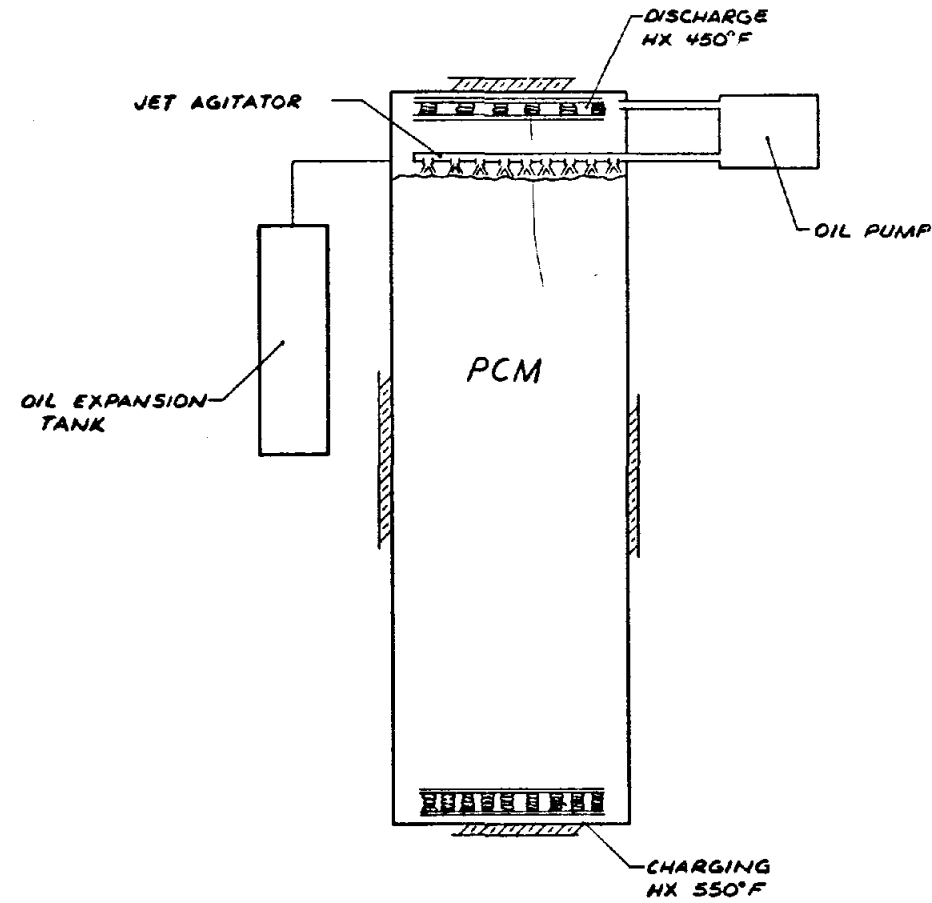
SD-13780-800-005

SKETCH 3

CE POWER SYSTEMS COMBUSTION ENGINEERING, INC. NUCLEAR POWER SYSTEMS	This drawing is the property of CE POWER SYSTEMS Combustion Engineering, Inc. Windsor, Connecticut 06095 and is not to be reproduced or used to furnish any information for making of drawings or spare parts, except where provided for by agreement with said company.	DRAWN BY J. COLTURE 11-13-80
		CHECKER APPROVALS
CUSTOMER	TITLE TES CONCEPTS DIRECT CONTACT, PCM DROP	DWG NO. SD-13780-800-005
NEXT ASSY	SUPERSEDES	SCALE
JOB NO. 682101	COMPONENT CODE	SHEET REV.



DIRECT CONTACT
REFLUX OIL
ONE 'MODULE'

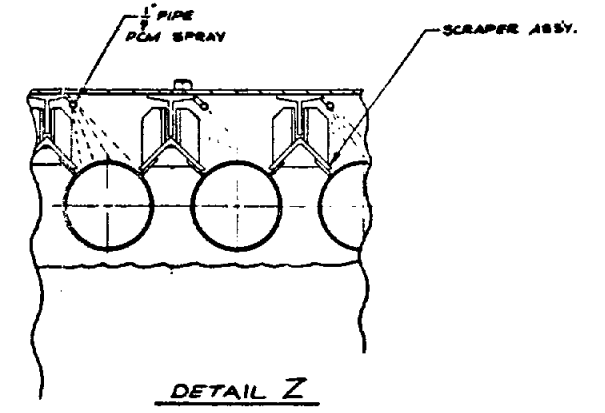
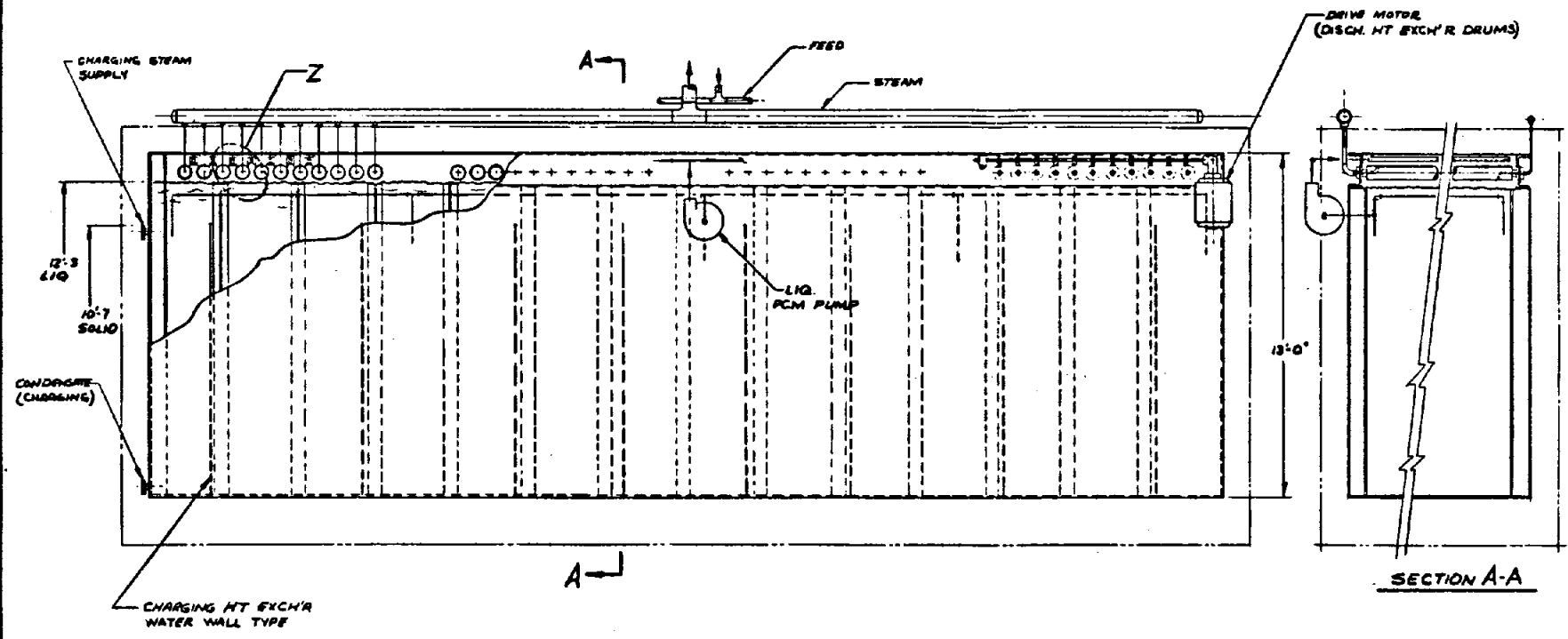
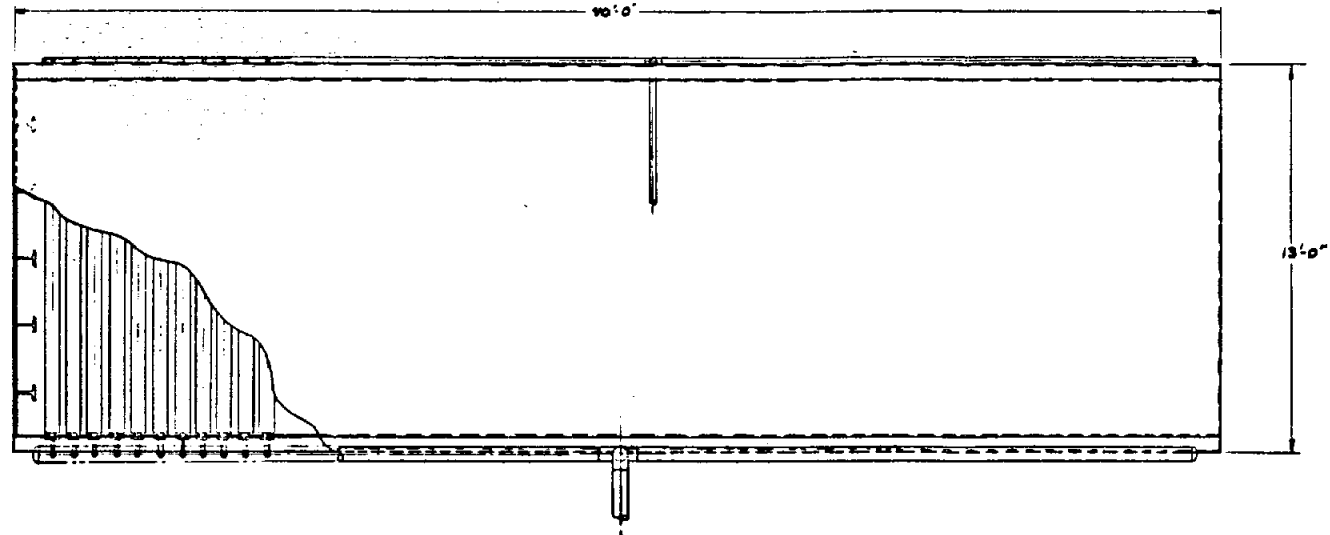


DIRECT CONTACT
CIRCULATING OIL
ONE 'MODULE'

SD-13780-800-006

SKETCH 4

POWER SYSTEMS COMBUSTION ENGINEERING INC. NUCLEAR POWER SYSTEMS	This drawing is the property of CE POWER SYSTEMS Combustion Engineering Inc., Windsor, Connecticut 06095 and is not to be reproduced or used to furnish any information for making of drawings or specifications except where provided for by agreement with said company.	DRAWN BY J. COLTURI 11-14-89
		CHECKER APPROVALS
CUSTOMER	TITLE TES CONCEPT DIRECT CONTACT-OIL INTERMEDIARY	DWG. NO. SD-13780-800-006
NEXT ASSY	SUPERSEDES	SCALE 1/2"=1'-0"
JOB NO.	COMPONENT CODE	SCALE



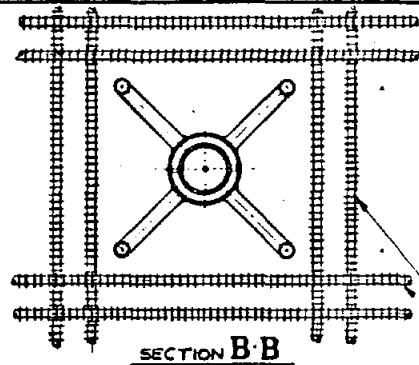
SE-13780-800-002

SKETCH 5

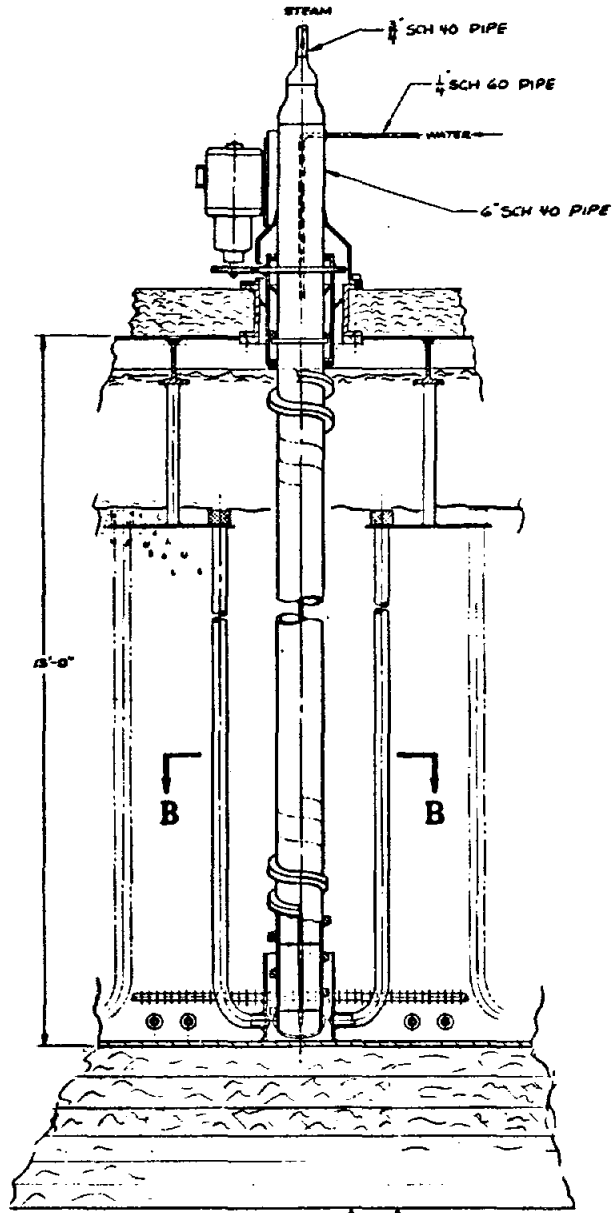
168

POWER SYSTEMS CONSULTING ENGINEERS	THE DESIGN OF THIS PROJECT IS THE PROPERTY OF POWER SYSTEMS CONSULTING ENGINEERS. NO PART OF THIS DESIGN IS TO BE REPRODUCED OR TRANSMITTED IN ANY FORM OR BY ANY MEANS, ELECTRONIC OR MECHANICAL, INCLUDING PHOTOCOPYING, RECORDING, OR BY ANY INFORMATION STORAGE AND RETRIEVAL SYSTEM.	DRAWN BY: V. CALYURI CHECKED: [] APPROVAL: []	10/2/80
	SANDIA LABS	TITLE: TES CONCEPT HORIZONTAL POTATING DRUM MECHANICAL SCRAPER PROJ. NO.: SE-13780-800-002	SHEET: 1 OF 1

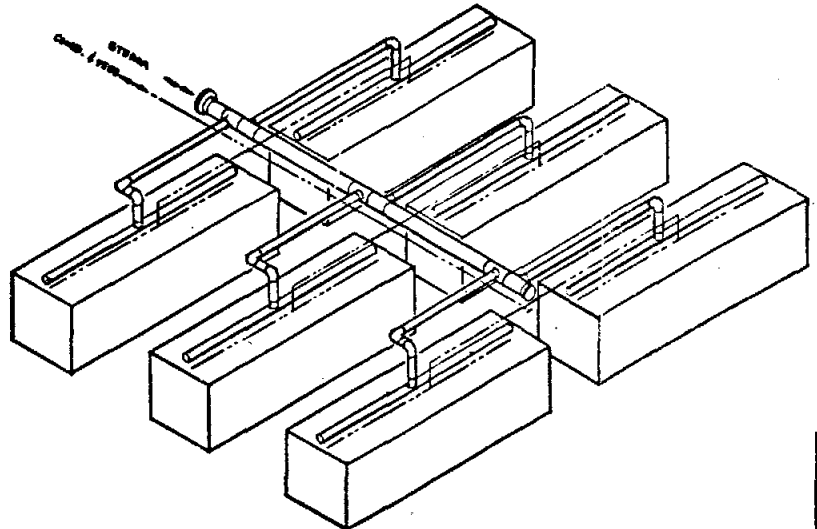
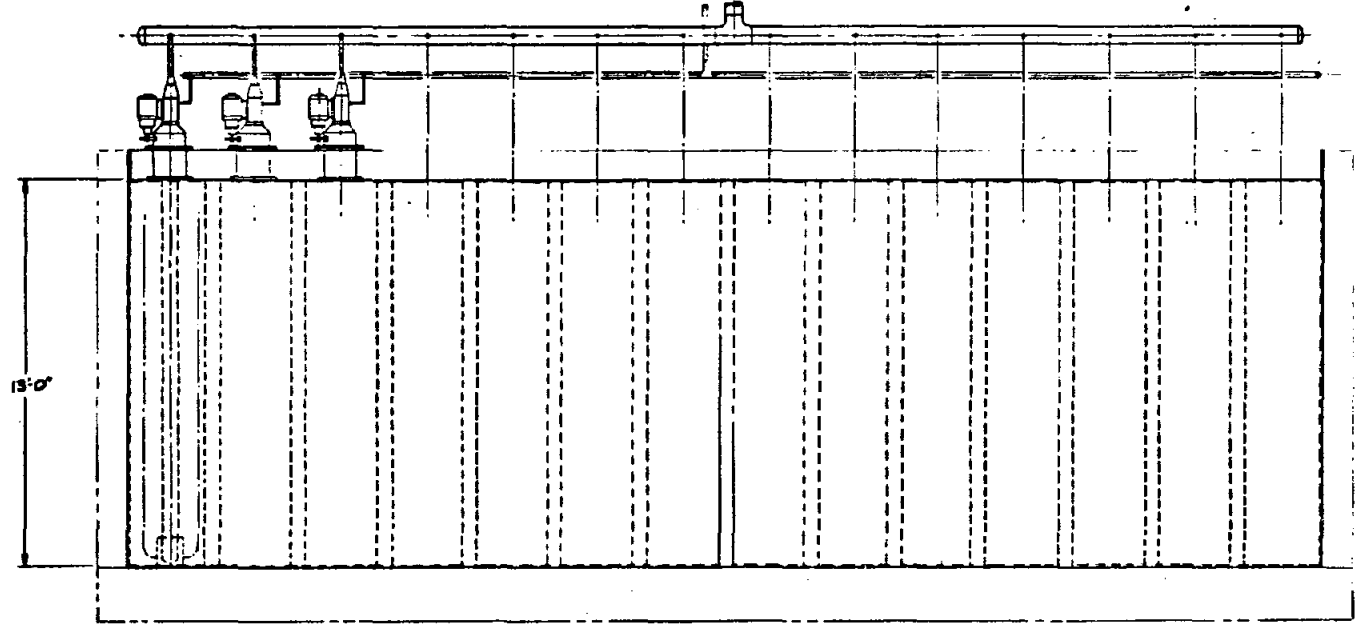
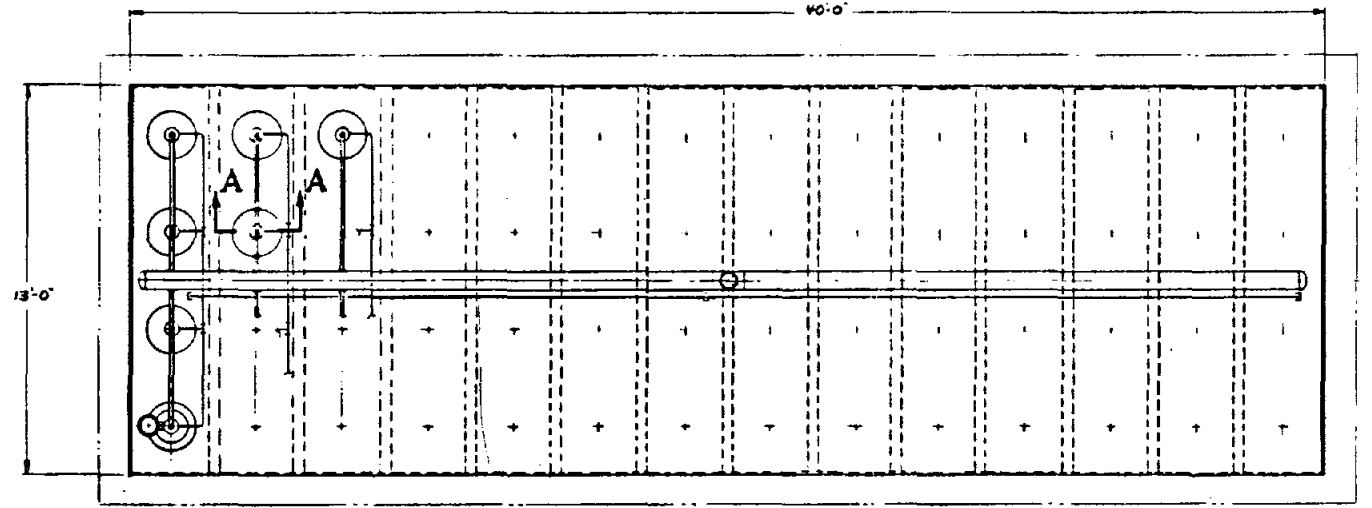
8 | 7 | 6 | 5 | 4 | 3 | 2 | 1



HEATING COILS
FINNED TUBE TYPE
1" O.D. TUBE 4 1/2" x 1/2" FINS



SECTION A-A
SCALE: 1/2" = 1'-0"



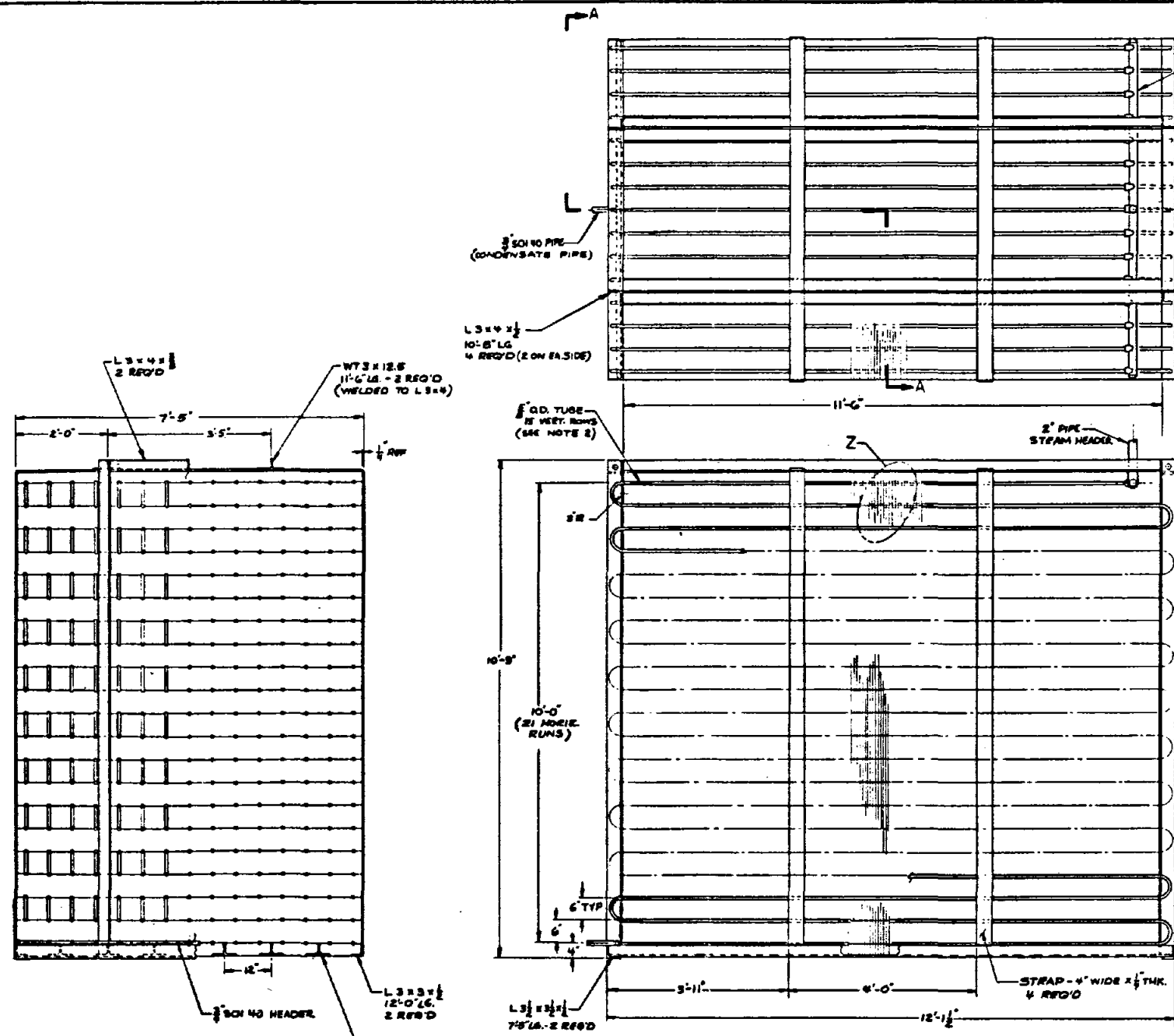
SE-13780-800-001

SKETCH 6

169

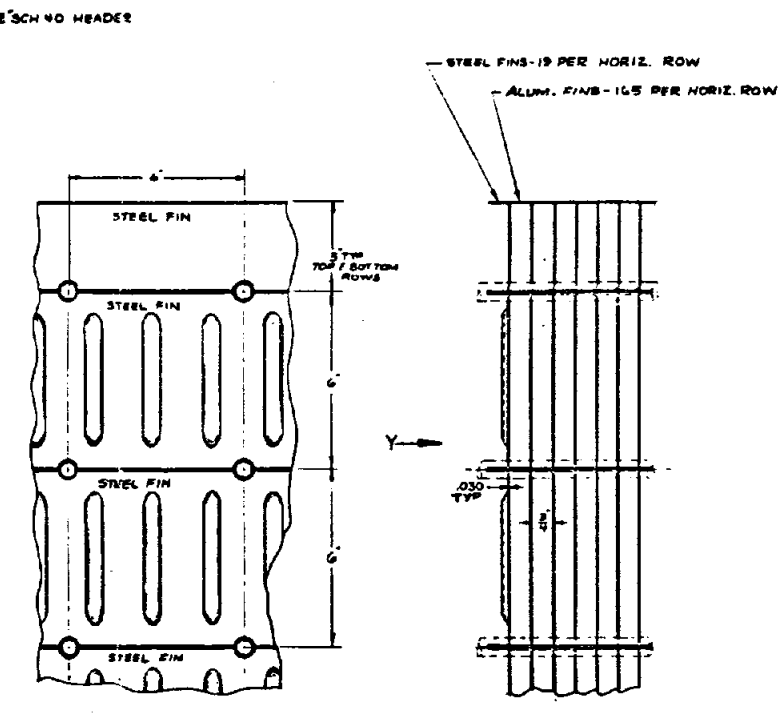
POWER SYSTEMS CONSULTING ENGINEERS, INC.		DESIGNED BY: V. COLYURI	
SHELLETT POWER SYSTEMS		CHECKED BY: []	
DATE: []		APPROVAL: []	
PROJECT NO. []		TITLE: TES CONCEPT VERTICAL ROTATING AUGER MECHANICAL SCRAPER	
DRAWN BY: []		SCALE: []	
PROJECT: []		NO. OF SHEETS: []	
SHEET: []		OF: []	

8 7 6 5 4 3 2 1



SECTION A-A

SCALE: 1"=1'-0"



VIEW Y

DETAIL Z

SCALE: HALF SIZE

2. $\sqrt{0}$ O. TUBING (.035" WALL) TO BE RESISTANCE WELDED TUBE
 1. ALL MATERIALS CARBON STEEL UNLESS OTHERWISE NOTED.

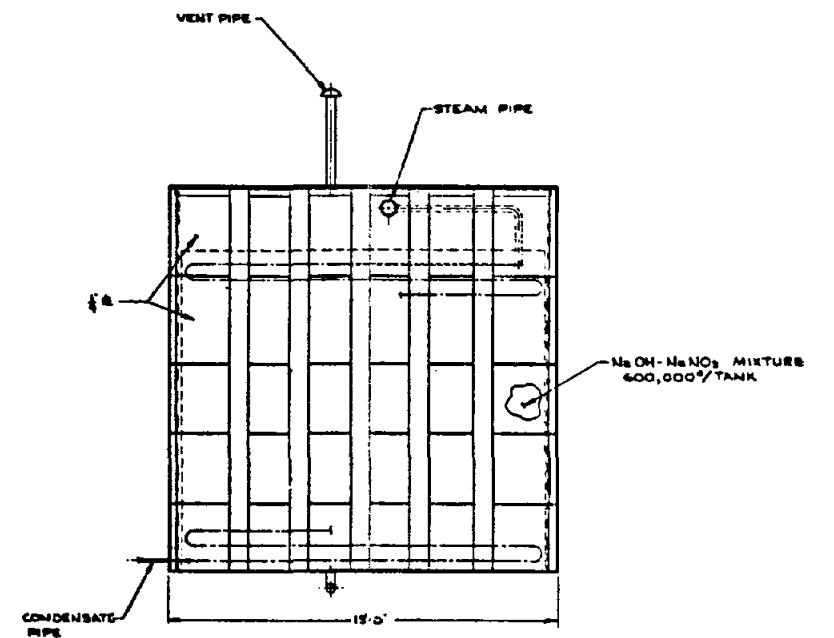
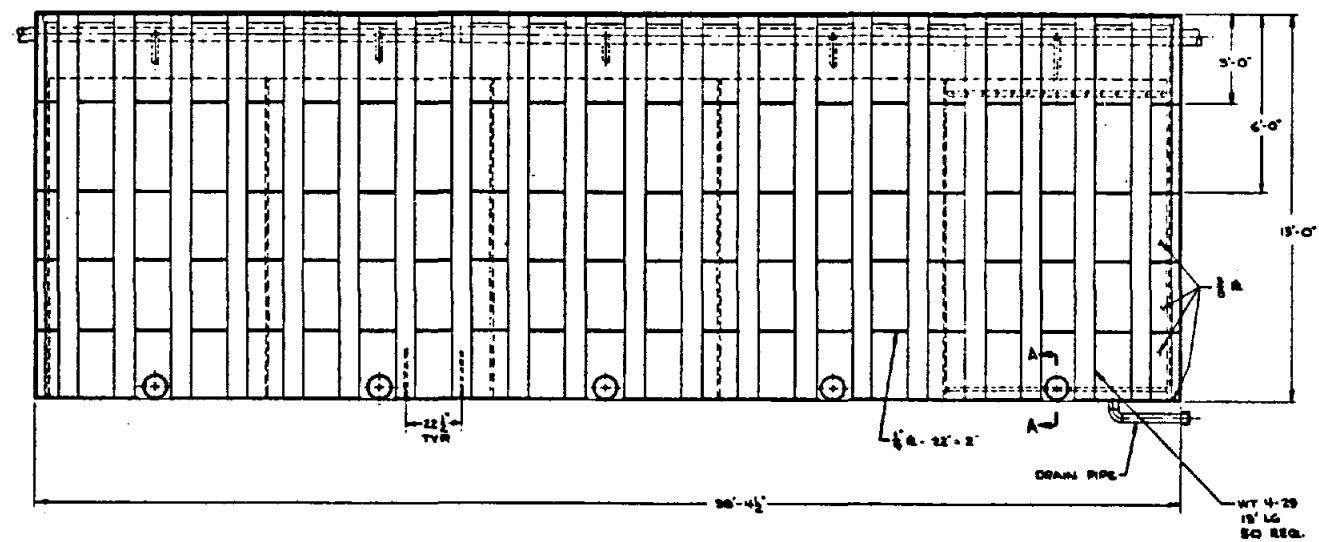
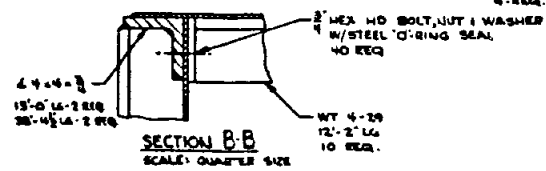
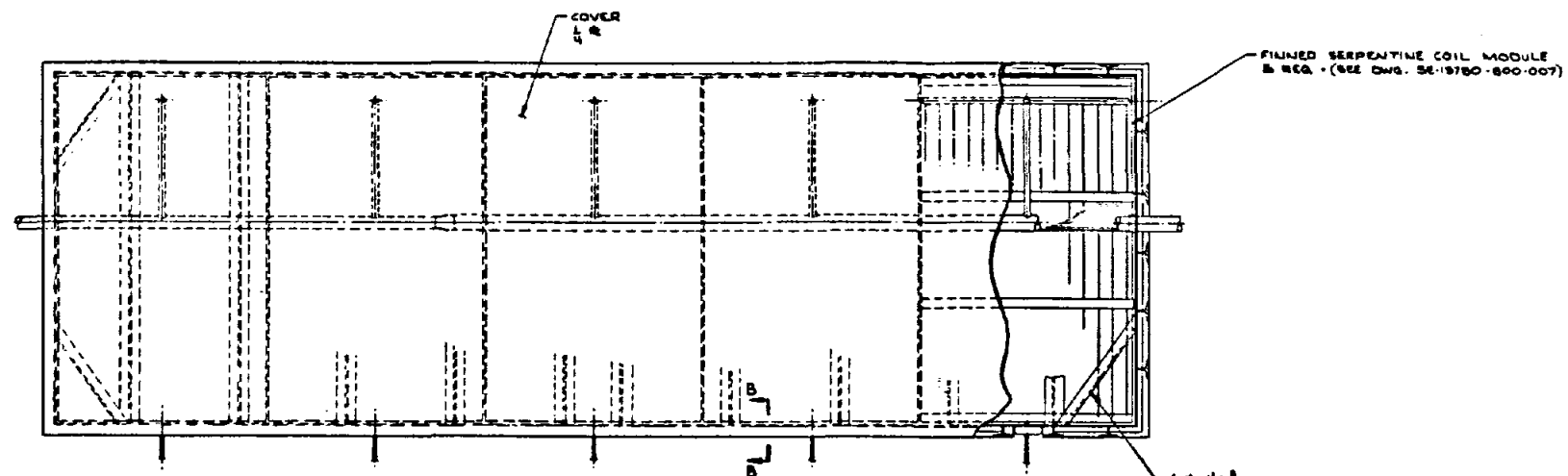
SE-13780-800-007

DRAWING 1

170

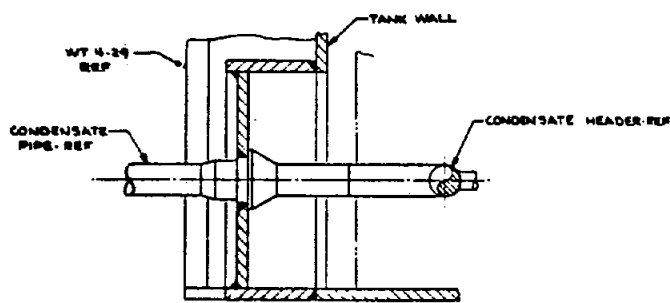
POWER SYSTEMS CONSULTING ENGINEERS, INC. 2175 W. BROADWAY SUITE 100 DENVER, CO 80202	PROJECT NO. SE-13780-800-007 DRAWING NO. 1	DATE: 10/25/80 SCALE: AS NOTED	TITLE: FINNED SERPENTINE COIL - MODULE THERMAL ENERGY STORAGE
	DESIGNED BY: [Signature] CHECKED BY: [Signature] APPROVED BY: [Signature]	DRAWN BY: [Signature] DATE: 10/25/80	PROJECT NO. SE-13780-800-007 DRAWING NO. 1

8 7 6 5 4 3 2 1



NOTE:
 1. ALL MATERIALS CARBON STEEL
 UNLESS OTHERWISE NOTED.

SE-13780-800-008

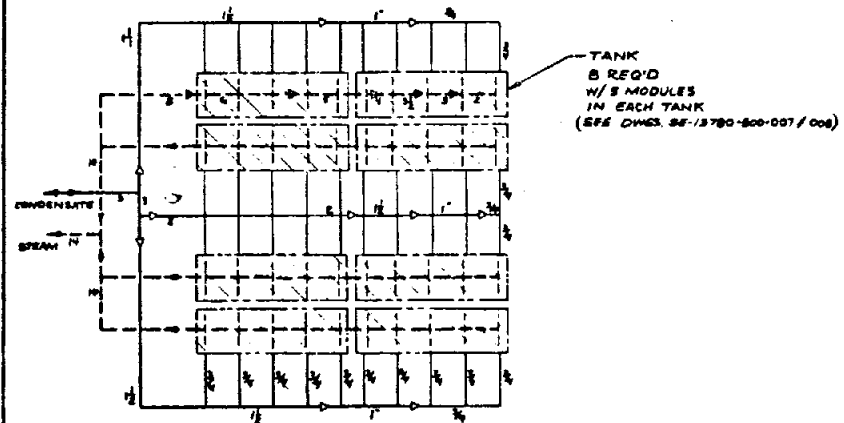


DRAWING 2

171

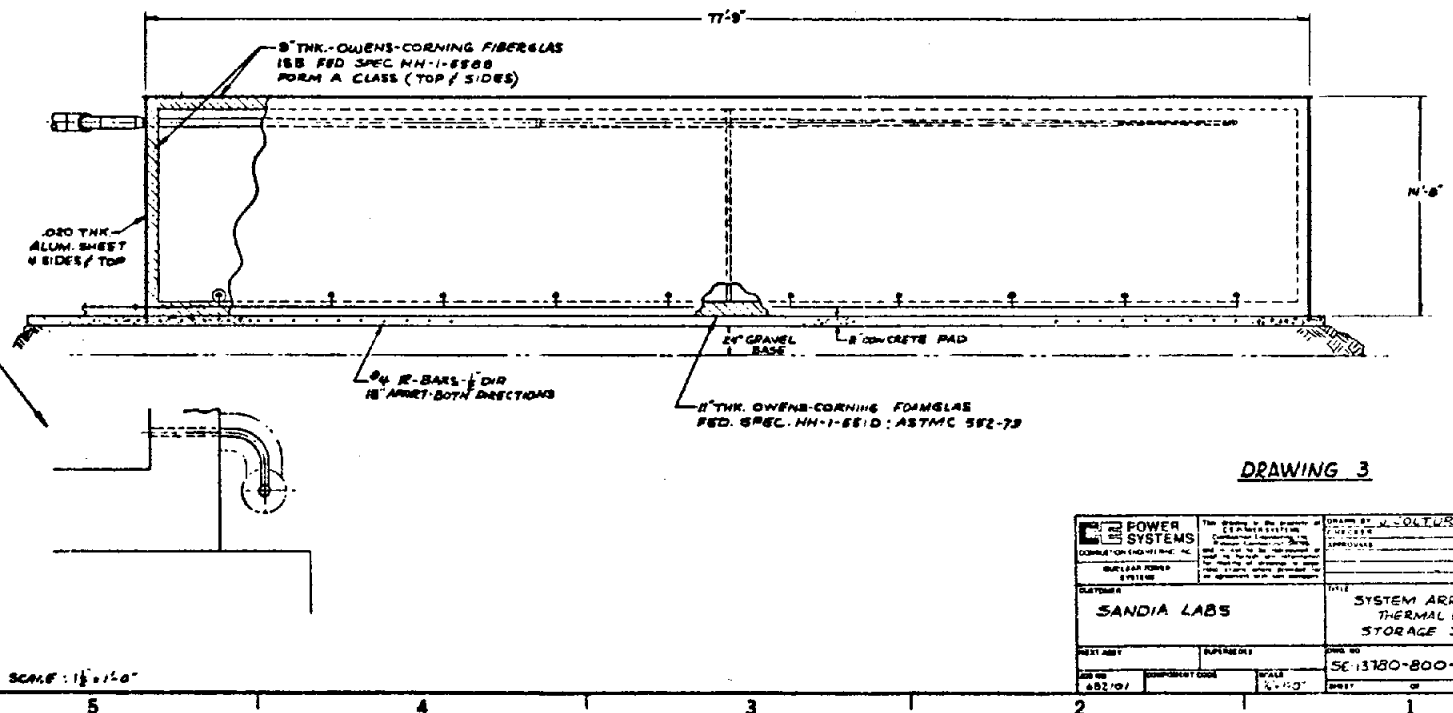
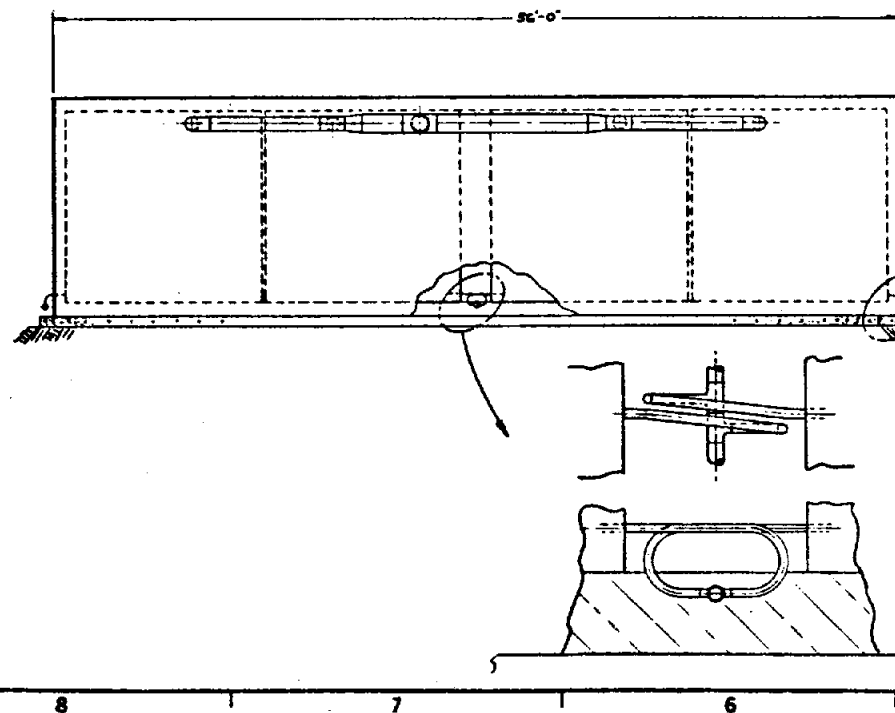
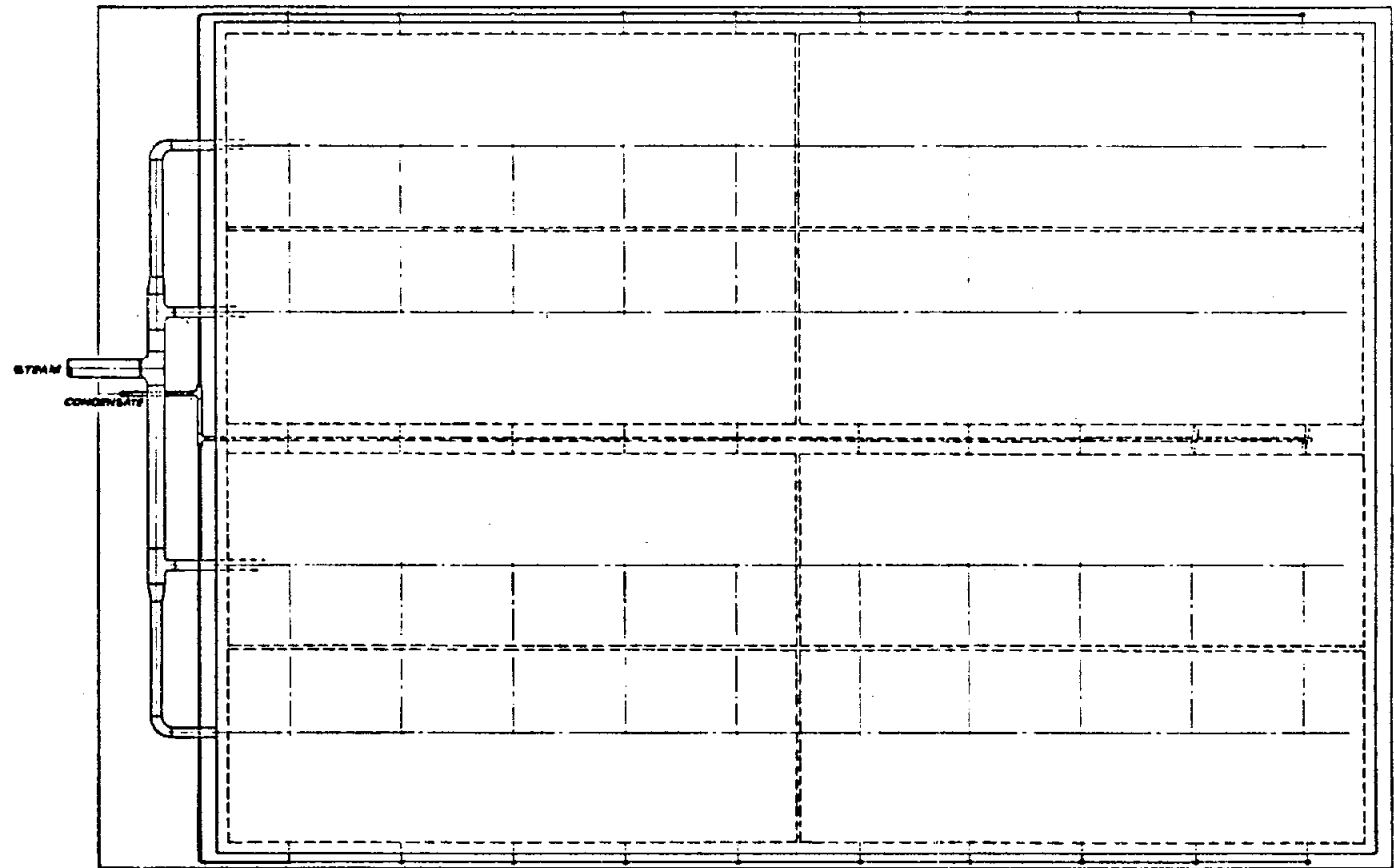
POWER SYSTEMS COMBUSTION ENGINEERING, INC.	DESIGNED BY C. WEBB	DATE 11/11/61
REVISIONS DATE BY	CHECKED BY DATE BY	APPROVED BY DATE BY
CUSTOMER SANDIA LABS	TITLE TANK - THERMAL ENERGY STORAGE	
PROJECT NO. SE-13780-800-008	SHEET NO. 1	DWG. NO. SE-13780-800-008
DATE 6-21-62	SCALE 1/2" = 1'-0"	BY CWB

8 7 6 5 4 3 2 1



SCHMATIC P/I DIAGRAM

1. ALL PIPING TO BE IPS
2. PIPES 3/4" TO 6" SCH 40
3. PIPES 6" TO 14" SCH 80
4. INSULATION PER C.E. STD 2V-65-9. MINERAL FIBER INSULATION OR SPEC 1-72 WITH ALUMINUM LAGGING CORRUGATED .016 THK. 3003 ALLOY WITH ATTACHED 30-30-30 DUPLEX WATERPROOF ASPHALT LAMINATED PAPER MOISTURE BARRIER. CHILDERS PROD. CO.
5. THE FOLLOWING PIPES HAVE INSULATION THICKNESS: 3/4" TO 2" PIPES HAVE 2" THK. 2" TO 10" PIPES HAVE 2 1/2" THK. 14" PIPE HAS 3 1/2" THK.



DRAWING 3

172

	THE SYSTEMS GROUP CONSULTING ENGINEERS 1000 W. BROADWAY SUITE 1000 DENVER, CO 80202	DRAWN BY: M. S. COLTURI CHECKED BY: APPROVED BY:
	CUSTOMER: SANDIA LABS	TITLE: SYSTEM ARRANGEMENT THERMAL ENERGY STORAGE SYSTEM
PROJECT NO: 94-13790	SHEET NO: 3 OF 3	DRAWING NO: 94-13790-800-009

TABLE I-1

FINAL DESIGN CHARACTERISTICS

A. DESIGN CHARACTERISTICS

1. Storage Media

Sodium hydroxide	81.5 mole %	67.5 wt %
Sodium nitrate	18.5 mole %	32.5 wt %

	<u>Solid</u>	<u>Liquid</u>
Specific heat kJ/kg·°C (Btu/lbm·°F)	2.00 (.478)	2.00 (.478)
Thermal conductivity kW/m·°C (Btu/hr·°F)	0.00108 (0.624)	0.0010207 (0.5)
Density kg/m ³ (lbm/ft ³)	2082 (130)	1794 (112)
Latent Heat of Fusion kJ/kg (Btu/lbm)	274(118)	

2. Storage Media Mass 2.18 x 10⁶ kg (4.8 x 10⁶ lbm)

3. Tank Characteristics

a. Number of storage tanks	8	
b. Tank geometry and dimension, m (ft)	3.96x3.96x11.7 (13x13x38.3)	
c. Tank volume, m ³ (ft ³) - total	1304	(46,048)
	- per tank	163 (5,756)
d. Tank material	CARBON STEEL	
e. Tank design temperature	315°C	(600°F)
f. Tank mass, kg(lb) - total	159,665	(352,000)
	- per tank	19,958 (44,000)

TABLE I-1 (Continued)

g. Tank surface area (Total-Combined)

top	m ² (ft ²)	386.1	(4156)
side	m ² (ft ²)	315.9	(3400)
bottom	m ² (ft ²)	386.1	(4156)

h. Tank insulation material (external) top & sides Fiberglass
 bottom Foamglas

i. Insulation thickness

top and side - cm (in)	22.9	(9)
bottom - cm (in)	27.9	(11)

j. Insulation mass

top and sides - kg (1b)	10,630	(23,436)
bottom - kg (1b)	2,897	(6,386)

4. Piping, Material, OD/ID/Wall/Lengths

See Drawing 3

5. Piping, Insulation, Material, Thickness

See Drawing 3

B. OPERATING CHARACTERISTICS

- | | |
|---------------------------------|--|
| 1. <u>Extractable Capacity</u> | 148 MWh (5.05 x 10 ⁸ Btu) |
| 2. <u>Peak Charging Rate</u> | 30 MW (1.02 x 10 ⁸ Btu/hr) |
| 3. <u>Peak Discharging Rate</u> | 30 MW (1.02 x 10 ⁸ Btu/hr) |
| 4. <u>Duration</u> | 3.7 hr at maximum discharge rate |
| 5. <u>Storage Media</u> | |
| <u>Operating Temperature</u> | 260°C (500°F) |
| 6. <u>Storage Tank</u> | |
| <u>Operating Pressure</u> | top: ullage at ambient pressure
bottom: 69 kPa gage (10 psig) |
| 7. <u>Design Heat Loss Rate</u> | 125 kW (4.27 x 10 ⁵ Btu/hr) |

APPENDIX II

PHASE CHANGE MATERIALS

Hydroxide-Nitrate Eutectic

The latent heat of fusion of the 81.5 mole % NaOH, 18.5 mole % NaNO₃ eutectic is calculated by the use of the Kirchoff equation (4).

$$\Delta H_{f,e} = X_A \cdot \Delta H_{f,A} + X_B \cdot \Delta H_{f,B} + (C_{pA}(s) - C_{pA}(l)) \cdot \Delta T_A \cdot X_A \\ + (C_{pB}(s) - C_{pB}(l)) \cdot \Delta T_B \cdot X_B;$$

$$\Delta T_A = T_{f,A} - T_{f,e}$$

$$\Delta T_B = T_{f,B} - T_{f,e}$$

where X_A and X_B are the mole fractions of A (NaNO₃) and B (NaOH) in the eutectic; $\Delta H_{f,e}$ is the molal heat of fusion of the eutectic; $\Delta H_{f,A}$ and $\Delta H_{f,B}$ are the molal heats of fusion of A and B; and $T_{f,A}$ and $T_{f,B}$ are the fusion temperatures of A and B. ΔT_A and ΔT_B are the temperature differences between the fusion temperatures of A and B, and the eutectic fusion temperature; and C_{pA} and C_{pB} are the specific heats of the solid and liquid phases of A and B.

The physical properties used are:

	<u>A = NaNO₃</u>	<u>B = NaOH</u>
X (mole fraction)	.185	.815
ΔH_f (fusion) Btu/lb·mole	6655	5600
C_p (s) Btu/lb·Mole·°F	38.2	19.2
C_p (l) Btu/lb Mole·°F	37.0	20.4
ΔT °F	585-493=92°	604-493=111°
Mole Wt.	84.99	40.0

The calculated value of $\Delta H_{f,e}$ is 5707 Btu/lb·mole.

The molecular weight of the eutectic is determined, from the molecular weights of the components and their mole fractions, to be 48.3, from which the latent heat of fusion of the eutectic is found to be 118 Btu/lb.

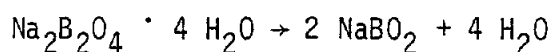
In this calculation, the latent heat of NaOH is taken to be the sum of the latent heat of fusion (604°F) and the latent heat of the $\beta \rightarrow \alpha$ transformation (565°F).

The price of the eutectic, based on prices given by Reference (35) for the constituents, is \$0.146/lb. Increased by 13% to cover the cost of packaging in steel drums and freight, the total price used in cost analyses is then \$0.165/lb.

Hydroxide-Metaborate Eutectic

The price of the metaborate eutectic, which is 85 mole % (77.5 wt %) NaOH, and 15 mole % (22.5 wt %) NaBO₂, is estimated in the following way.

The price of hydrated sodium metaborate, Na₂B₂O₄ · 4 H₂O from U.S. Borax, is quoted as \$635/ton, or \$0.318/lb. By dehydration,



The molecular weights of the hydrated and anhydrous forms are 202 and 65.8, from which the price of NaBO_2 is determined as

$$$.318 \times \frac{202}{2 \times 65.8} = $.488/\text{lb.}$$

The price of the eutectic is

$$(.775 \times .175) + (.225 \times .49) = $.245/\text{lb.}$$

Increased by 18% to cover costs of preparation, the price is \$0.29/lb.

APPENDIX III

A SIMPLIFIED PROCEDURE FOR PRELIMINARY SIZING OF THE TUBE INTENSIVE TES HEAT TRANSFER SURFACE

The preliminary sizing of the tube-intensive concept is based on the following simple model. At the fully discharged condition the maximum discharge rate is imposed. The solid PCM builds up radially around the tube, posing increasing thermal resistance to heat transfer. At the end of discharge the PCM layer is thickest, requiring the largest length of tube to achieve the required discharge rate. Heat is liberated by the PCM only through the latent heat of fusion; no credit for solid or liquid phase sensible heat is taken. The discharge fluid remains at the saturation condition. These conditions are uniform throughout the TESS.

Letting,

ρ	=	density of PCM
K_{PCM}	=	thermal conductivity of PCM
H_L	=	latent heat of PCM
x_s	=	thickness of PCM
r_i, r_o	=	tube inner and outer radii
L	=	length of tube
V	=	total PCM volume
A	=	reference heat transfer area
U	=	overall heat transfer coefficient
ΔT	=	$T_{PCM-fusion} - T_{steam}$
F_{PCM}	=	utilization factor of PCM
Q	=	TES capacity
q	=	maximum discharge rate

Then the total heat capacity is given by

$$Q = \pi (2 r_o + x_s) x_s L \rho H_L F_{PCM} \quad (1)$$

For the heat transfer rate at this time, the thermal resistance of the PCM layer dominates to the extent that the resistances of the tube wall and the tube side film are negligible. Thus,

$$q = \frac{2\pi k_{PCM} L \Delta T}{\ln\left(\frac{r_o + x_s}{r_o}\right)} \quad (2)$$

These equations are combined to eliminate x_s .

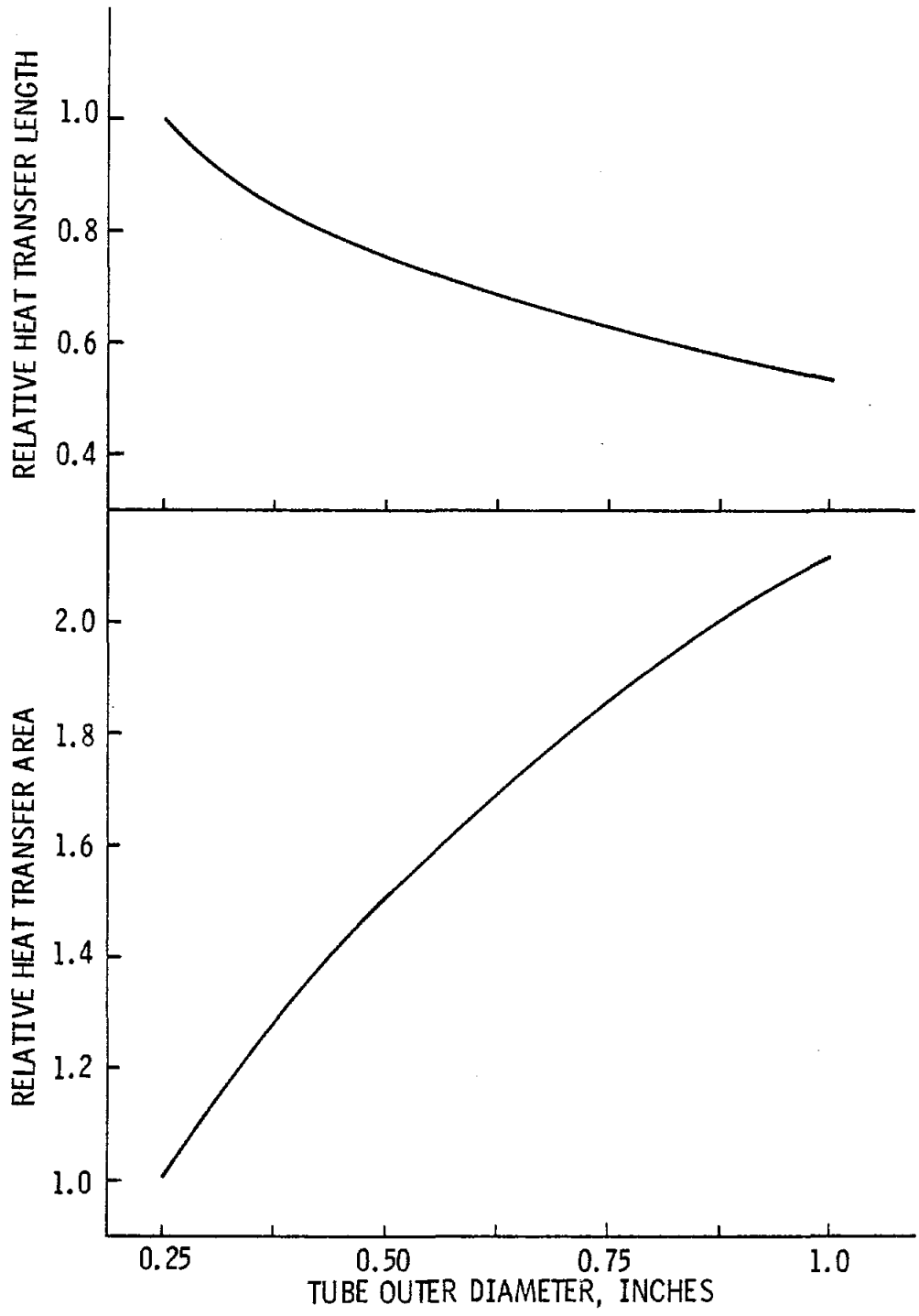
$$q = 4\pi k_{PCM} L \Delta T \left[\ln\left(1 + \frac{Q}{\pi r_o^2 \rho H_L F_{PCM} L}\right) \right]^{-1} \quad (3)$$

The resultant equation is evaluated numerically to determine the total length of tube required for a given service.

For a 6.35 mm (0.25") tube O.D., a required heat transfer length of 4.496×10^5 m (1.475×10^6 ft) and a total heat transfer area of 8970 m² (96552 ft²) are obtained. These results reflect an 80% utilization factor based on the C&W operational experience.

The variation of total tube length and heat transfer area with tube diameter is shown on Figure III-1. As can be readily seen, the required heat transfer length decreases with increasing tube diameter, with 25.4 mm (1.0") tubes requiring about half the length of a 6.35 mm (0.25") tube. The required heat transfer area, however, also increases directly with tube diameter which overwhelms the decrease in the length. Consequently, the area increases with tube diameter, with a 25.4 mm (1.0") tube having approximately twice the area of the 6.35 mm (0.25") tube. With heat exchanger costs directly proportional to tube surface area, the tube selection decision is driven to the smallest tube diameter.

Figure III-1
REQUIRED HEAT TRANSFER LENGTH AND AREA
AS FUNCTION OF TUBE O. D.



The mass of PCM is the amount required to store and liberate the 148 MWh capacity through the latent heat. With the 80% utilization factor, 2.43×10^6 kg (5.35×10^6 lb) of the sodium hydroxide/sodium nitrate eutectic is required.

The liquid phase requires a containment volume of 1350 m^3 ($47,780 \text{ ft}^3$). Employing the standard tank established in the groundrules and described in Appendix XI, 7.7 tanks are required. This tankage allows for approximately 5% of the tank volume to serve as ullage.

When the PCM is completely solidified the level is 3.25 m (10.7 ft) above the tank bottom. The interior width of the tank that allows a horizontal tube run as part of a serpentine tube (Sketch 1 in Appendix I) is approximately 3.35 m (11 ft). With a 5.1 cm (2.0 in) spacing between the horizontal runs of the serpentine approximately 253 m (830 ft) of tubing can be placed in a single tube or a nesting of serpentine tube. Sketch 1 shows a nesting of eight tubes. The effective internal width for tube bundles is 11.8 m (38.6 ft). Placing the nested tube assemblies on a 5.1 cm (2.0 in) spacing will allow 232 assemblies to be inserted in each tank. The 7.7 tanks fulfill the heat transfer area requirements.

The heat transfer area based on the simplified method is compared to the results of a preliminary optimization (Appendix IV) using computer program TESST. The simplified model based on the worst-case condition was found to be very conservative. The preliminary optimization with computer code showed a reduction of about 35% in the amount of PCM and a reduction of about 25% in the heat transfer area, compared to the simplified approach. The major reduction in the amount of PCM is due to the way the passive TES system operates. The vertical thermocline uses a large amount of sensible heat both in liquid and solid states of PCM.

The simplified method can be benchmarked against the results of the preliminary optimization study. The amount of PCM was found to be 1.6×10^6 kg (3.53×10^6 lb) which indicates a 1.213 utilization factor relative to latent heat only. Using this in equation (3) a total heat transfer length

of 3.402×10^5 m (1.116×10^6 ft) is required for the 6.35 mm (0.25") O.D. tube. This is almost exactly the result from the optimization study presented in Appendix IV. If the utilization factor can be applied to other tube sizes, then the optimized design using 15.9 mm (0.625") O.D. tubes would be approximately 2.294×10^5 m (7.52×10^6 ft) of heat transfer length and 1.6×10^6 kg (3.53×10^6 lb) of PCM. This is expected to be very close to the bare tube version corresponding to the final design presented in Section 5.0 of the main text.

APPENDIX IV

A PRELIMINARY OPTIMIZATION OF THE TUBE INTENSIVE CONCEPT

The preliminary optimization of the tube-intensive concept was performed with computer code TESST (Appendix V) developed by Comstock and Wescott for the performance and cost evaluation of passive tube-intensive TES concepts. This code has been modified to analyze a system charged and discharged by water/steam.

The code is an analytical program rather than a design program. It requires a specific unit design as input and calculated performance of that unit is the output. The program can be used for design by analysis of a large matrix of design options and separate parametric evaluation of the output.

The TES subsystem is part of a complete solar energy system. Since this system is not completely specified (see Section 3.1) the operating conditions of the solar collector field are specified to provide saturated steam at 288°C (550°F) with a flow rate proportional to a daily solar cycle (Figure 3.1-1). The inlet and outlet conditions of the solar collector field were set at 550°F saturated water and 550°F saturated steam, respectively, and the flow calculated. A part of this flow meets the constant demand and the remaining goes to the TES subsystem for charging the unit. This is shown schematically on Figure IV-1.

The input to the TES subsystem during the charging cycle is thus specified, but the output conditions of the charging fluid depend on the size of the unit. Moreover, the variable insolation of the solar-TES system makes it impractical to set fixed output conditions. If the TES unit is too large, considerable subcooling of water and PCM is expected. If the unit is too small, the opposite would be true. Therefore, the charging capacities of the TES units over a range of design options would be different.

During discharge 232°C (450°F) saturated water is supplied to the TES unit to supplement the collector field output to the demand or to supply the

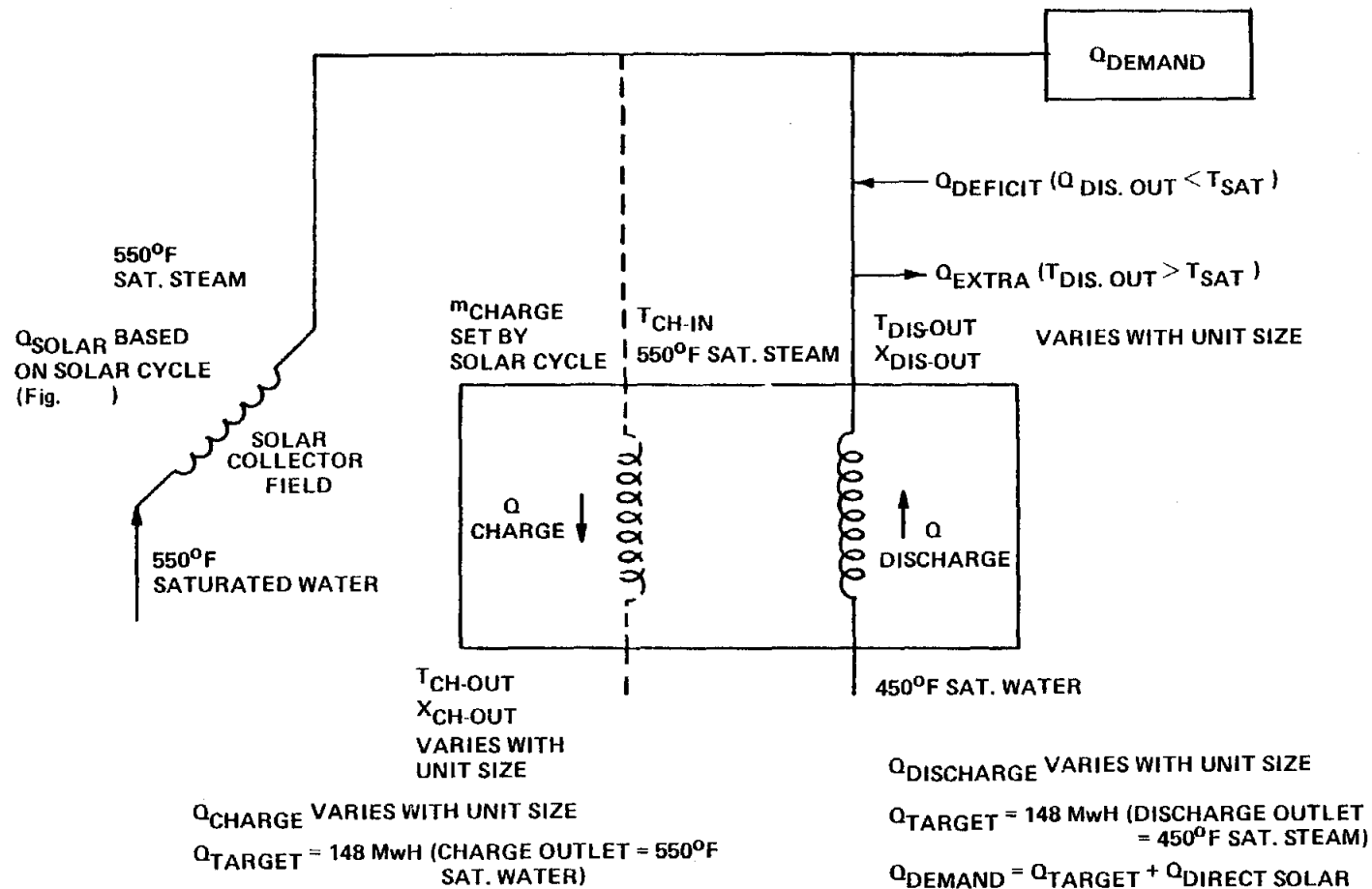


Figure IV-1
SCHEMATIC EXPLANATION OF TERMS USED IN TES OPTIMIZATION

demand completely. As in the case of charging, the outlet conditions of the discharging steam also depend on the size of the unit. If the outlet temperature exceeds the target conditions of saturated vapor, the amount of energy in this superheated steam is termed extra and it is energy no longer available in storage. If the outlet is a wet steam mixture, energy must be supplied to bring the condition to the target saturation state. This supplementary energy is termed a deficit energy.

The first approach to preliminary optimization is therefore based on comparing various units having the same input. The units having inputs of less than 148 MWh will require supplementary energy. The optimum design is selected based on the minimum total cost of major TES components and the cost of this deficit energy.

The second approach to preliminary optimization is based on the comparison of various units having the same net useful discharge. The optimum design is selected on the basis of the minimum total cost of major TES components plus the cost of deficit energy. This approach takes into account the performance of the TES unit in meeting the target discharge conditions.

The two optimization procedures are explained below with notations, assumptions, and figures.

INPUT DATA USED FOR OPTIMIZATION

Tube O.D., inch	0.25
Tube thickness, inch	0.025
Length of each tube, ft	100
Cost of PCM, \$/lb	0.165
Cost of tank (13'x13'x40'), \$/tank	63,000
Cost of tube bundle, \$/ft ²	12.0
Cost of deficit power, \$/10 ⁶ Btu Capitalized at 15%	4.90

A Figure of Merit (FOM) is defined as a measure of the TES design ability to satisfy the design requirements.

$$\begin{aligned}
 \text{FOM} &= \frac{Q_{\text{discharge}}}{Q_{\text{demand}}} \\
 &= \frac{Q_{\text{discharge}}}{Q_{\text{discharge}} - Q_{\text{extra}} + Q_{\text{deficit}}}
 \end{aligned}$$

Note that a FOM > 1.0 means that the TES unit is too big and discharges superheated steam (Q_{extra}). A FOM < 1.0 would mean that the TES unit is too small and to discharge quality steam, requires supplementary energy.

A series of calculations using TESST were conducted in which the amount of PCM varied between $1.2\text{-}2.4 \times 10^6$ kg ($2.64\text{-}5.29 \times 10^6$ lbm) and the total heat transfer length ranged from $2.44\text{-}5.36 \times 10^5$ m ($8.0 \times 10^5\text{-}1.76 \times 10^6$ ft). The results are shown on Figures IV-2 and IV-3 as a function of the total energy charged into storage. For a constant energy input ($x = \text{constant}$) a series of sizes is obtained, and a total cost including deficit energy costs to the target 148 MWh level is calculated. These results are shown on Figures IV-4 and IV-5 as a function of amount of PCM and total tube length for constant storage capacity.

Figures IV-6 and IV-7 show the variation of the figure of merit for the same range in the quantity of PCM and the number of tubes. Using these two figures, a series of unit sizes are obtained for a constant FOM, and the cost of each unit calculated in accordance with the input groundrules. The results are presented in Figures IV-8 and IV-9. These latter curves show the variation of the total cost of major components for various values of constant FOM.

The optimum design parameter from Figures IV-4, IV-5, IV-8 and IV-9 are as follows:

Total amount of PCM	1.6×10^6 kg
Total amount of Tubes	11200

TES OPTIMIZATION BASED ON NET INPUT

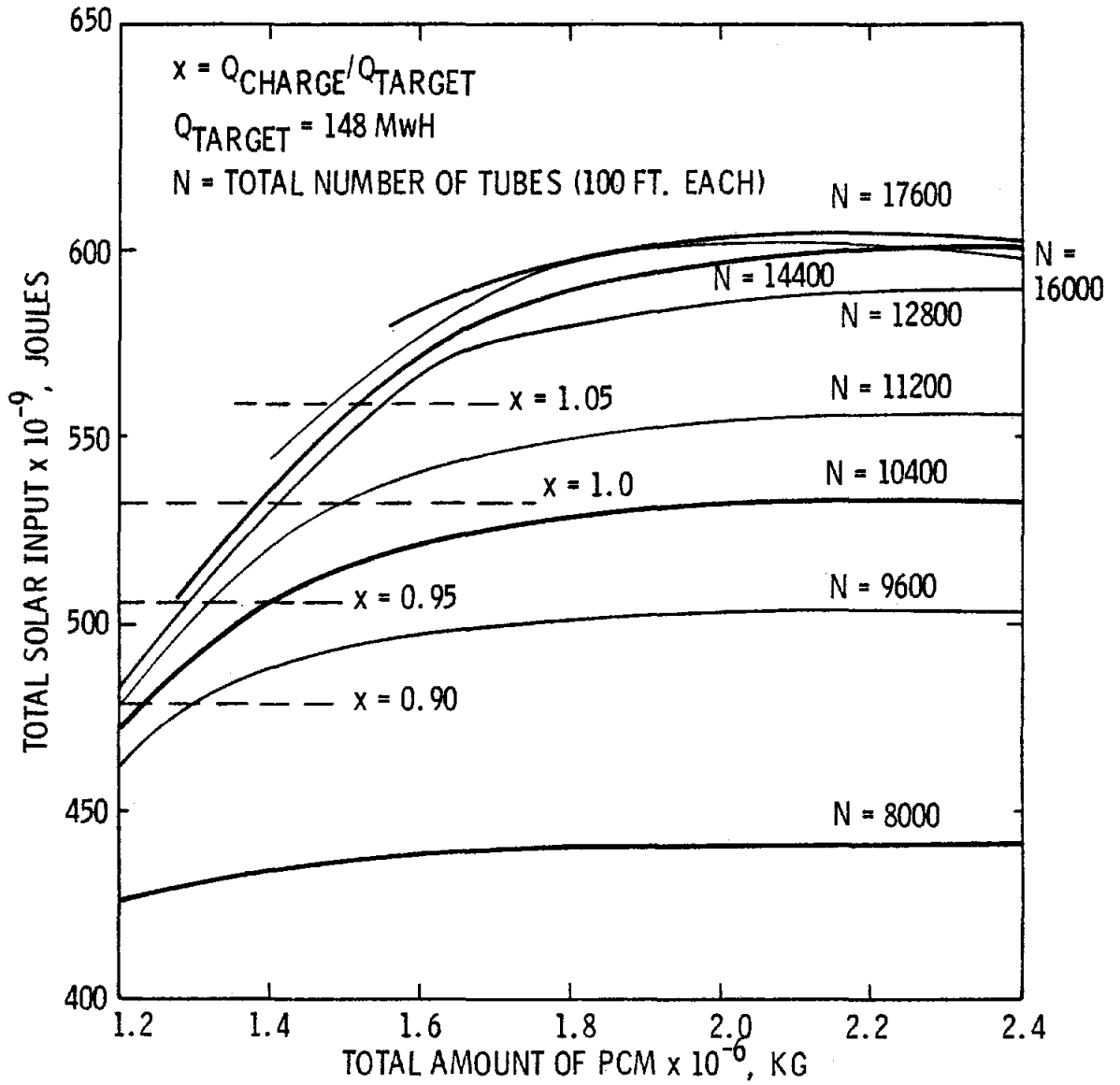


Figure IV-2
 VARIATION OF TOTAL SOLAR ENERGY INPUT
 WITH AMOUNT OF PCM

TES OPTIMIZATION BASED ON NET INPUT

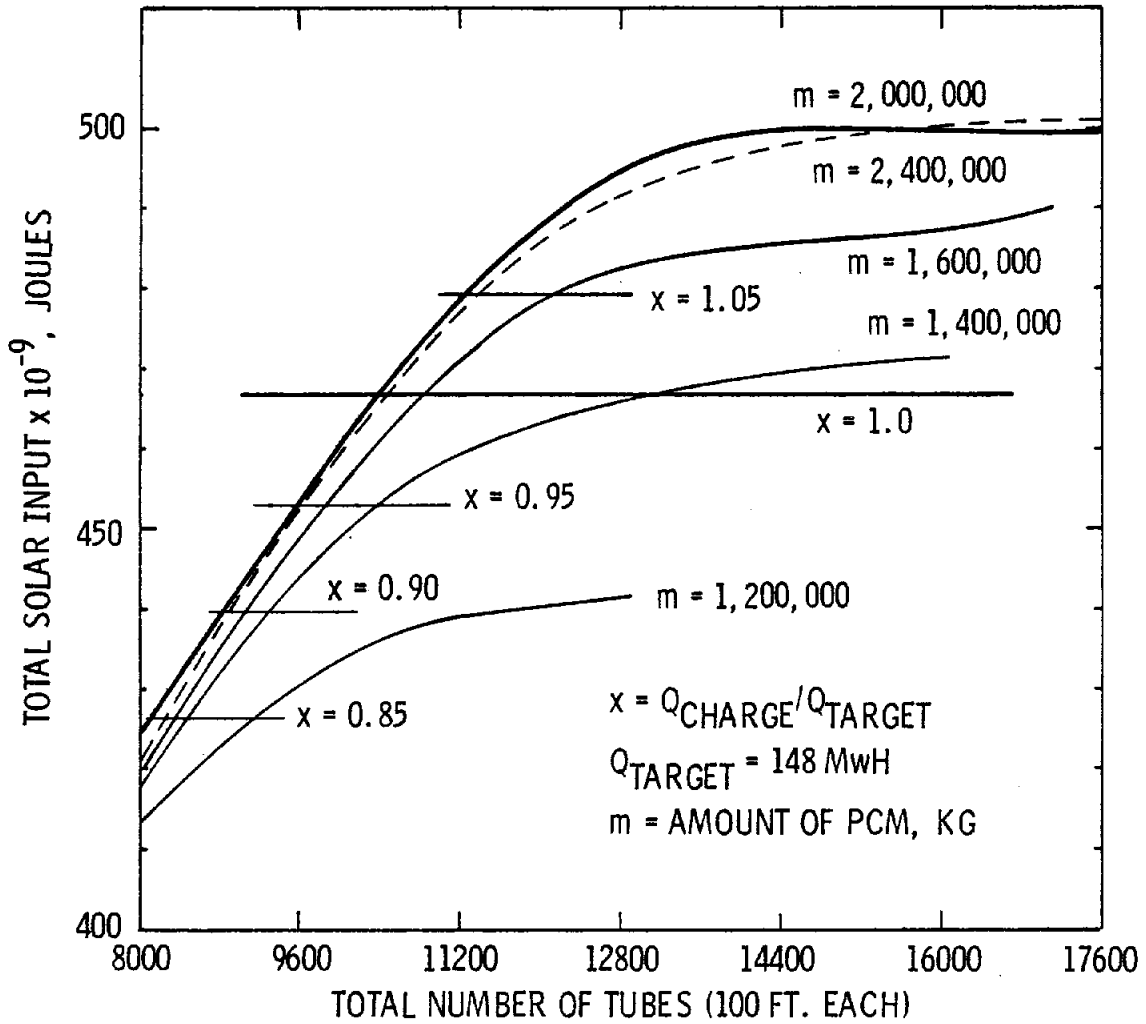


Figure IV-3
 VARIATION OF TOTAL SOLAR ENERGY INPUT
 WITH NUMBER OF TUBES

TES OPTIMIZATION BASED ON NET INPUT

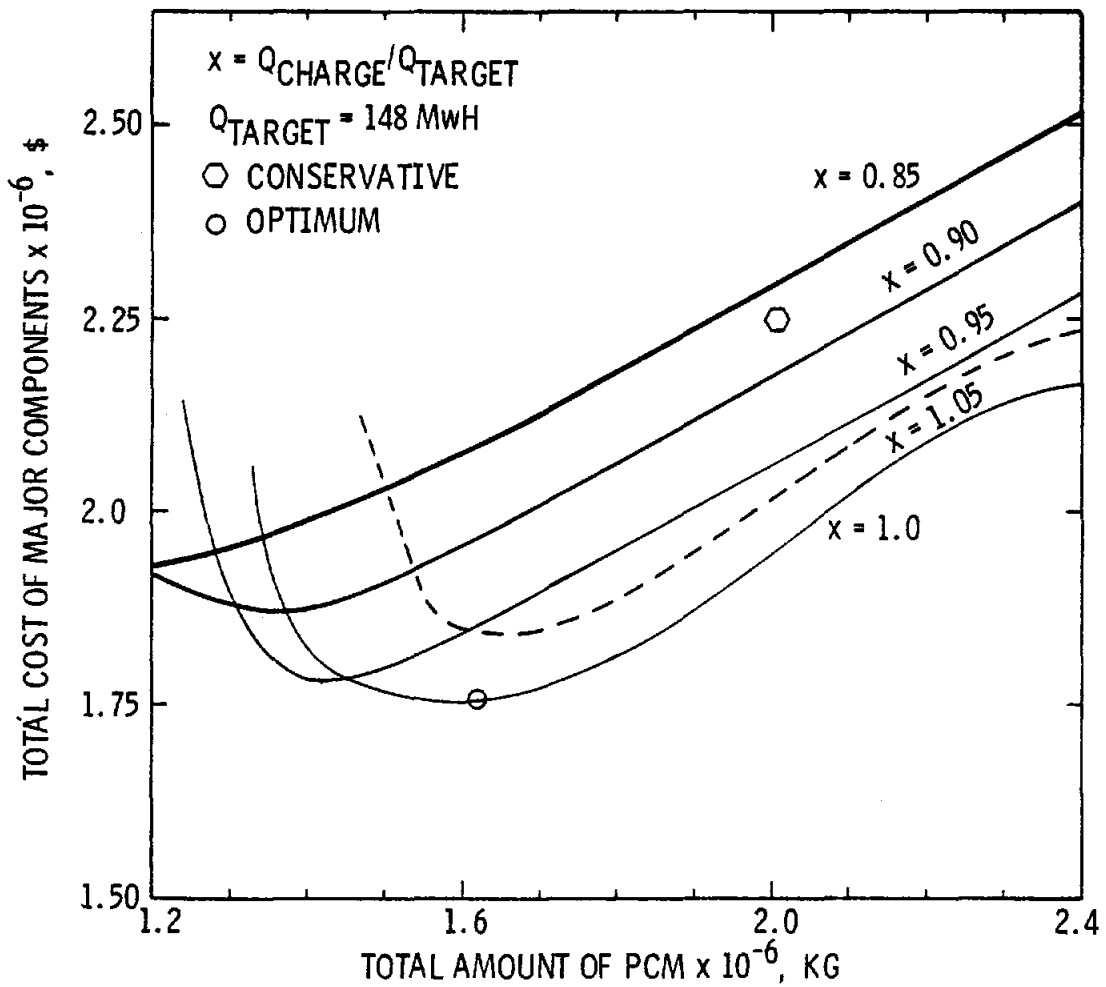


Figure IV-4
 VARIATION OF TOTAL COST OF MAJOR COMPONENTS
 WITH CHARGING CAPACITY AND AMOUNT OF PCM

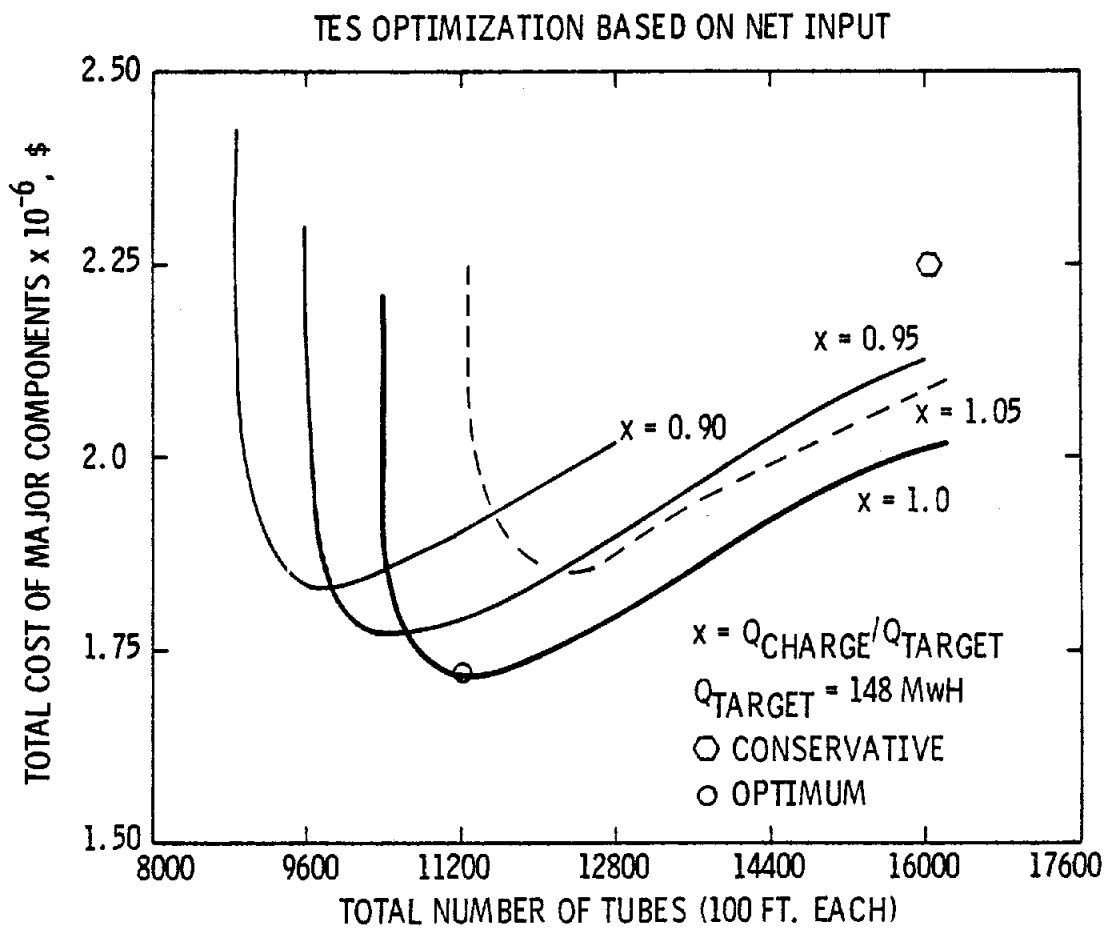


Figure IV-5
 VARIATION OF TOTAL COST OF MAJOR COMPONENTS
 WITH CHARGING CAPACITY AND NUMBER OF TUBES

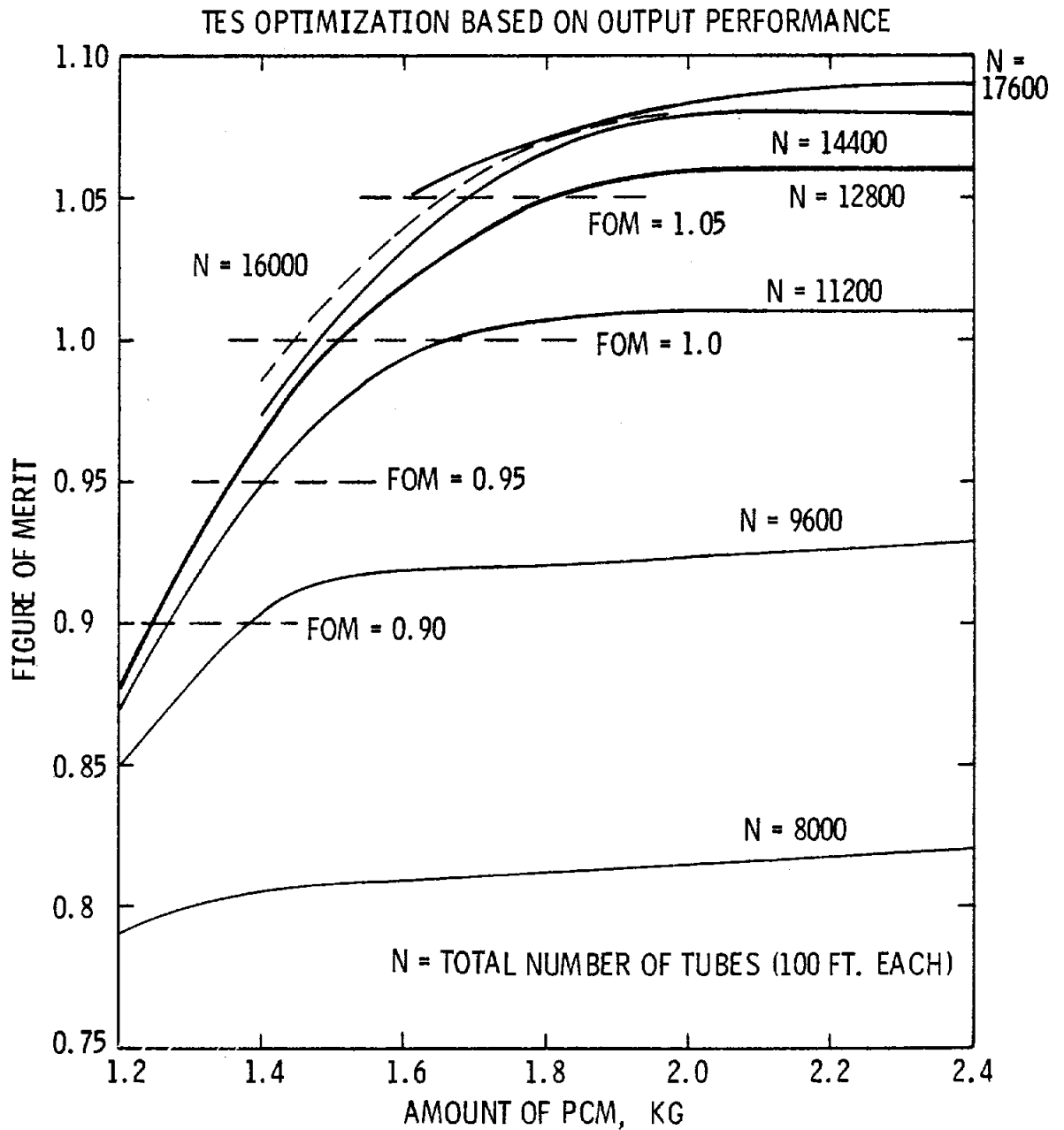


Figure IV-6
 VARIATION OF FIGURE OF MERIT (FOM) WITH AMOUNT OF PCM

TES OPTIMIZATION BASED ON OUTPUT PERFORMANCE

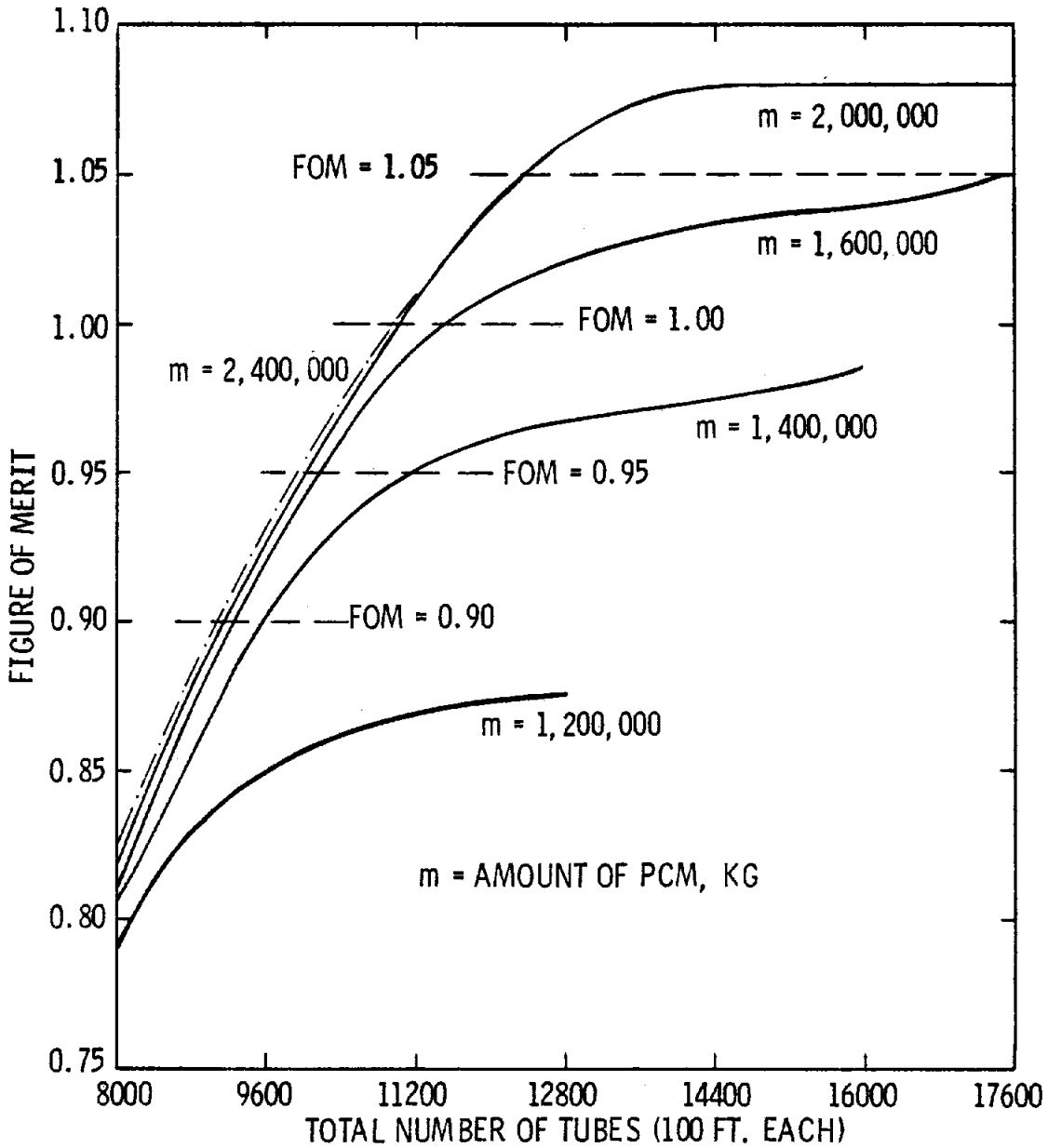


Figure IV-7
 VARIATION OF FIGURE OF MERIT (FOM) WITH NUMBER OF TUBES

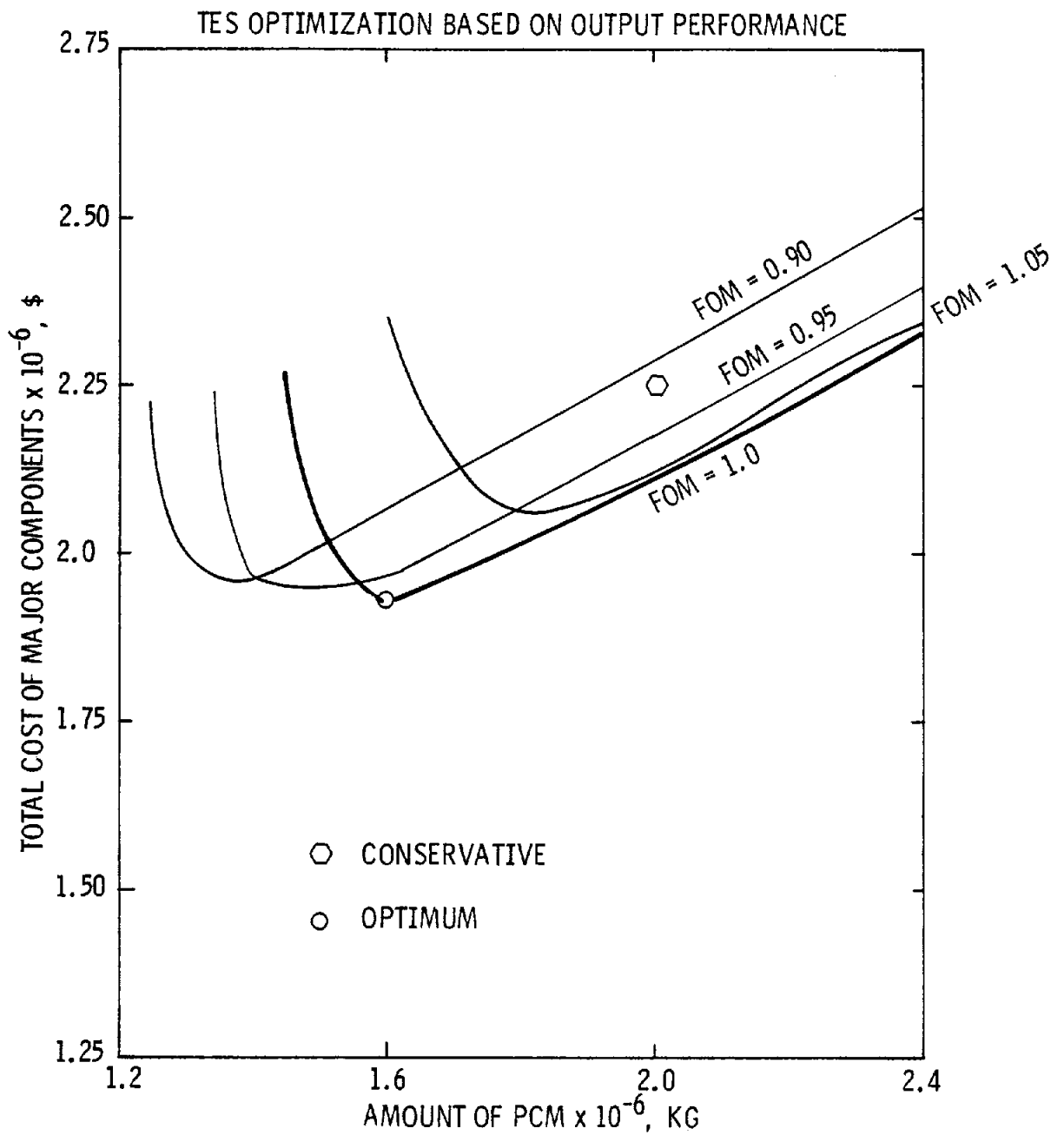


Figure IV-8
 VARIATION OF TOTAL COST OF MAJOR COMPONENTS
 WITH FIGURE OF MERIT (FOM) AND AMOUNT OF PCM

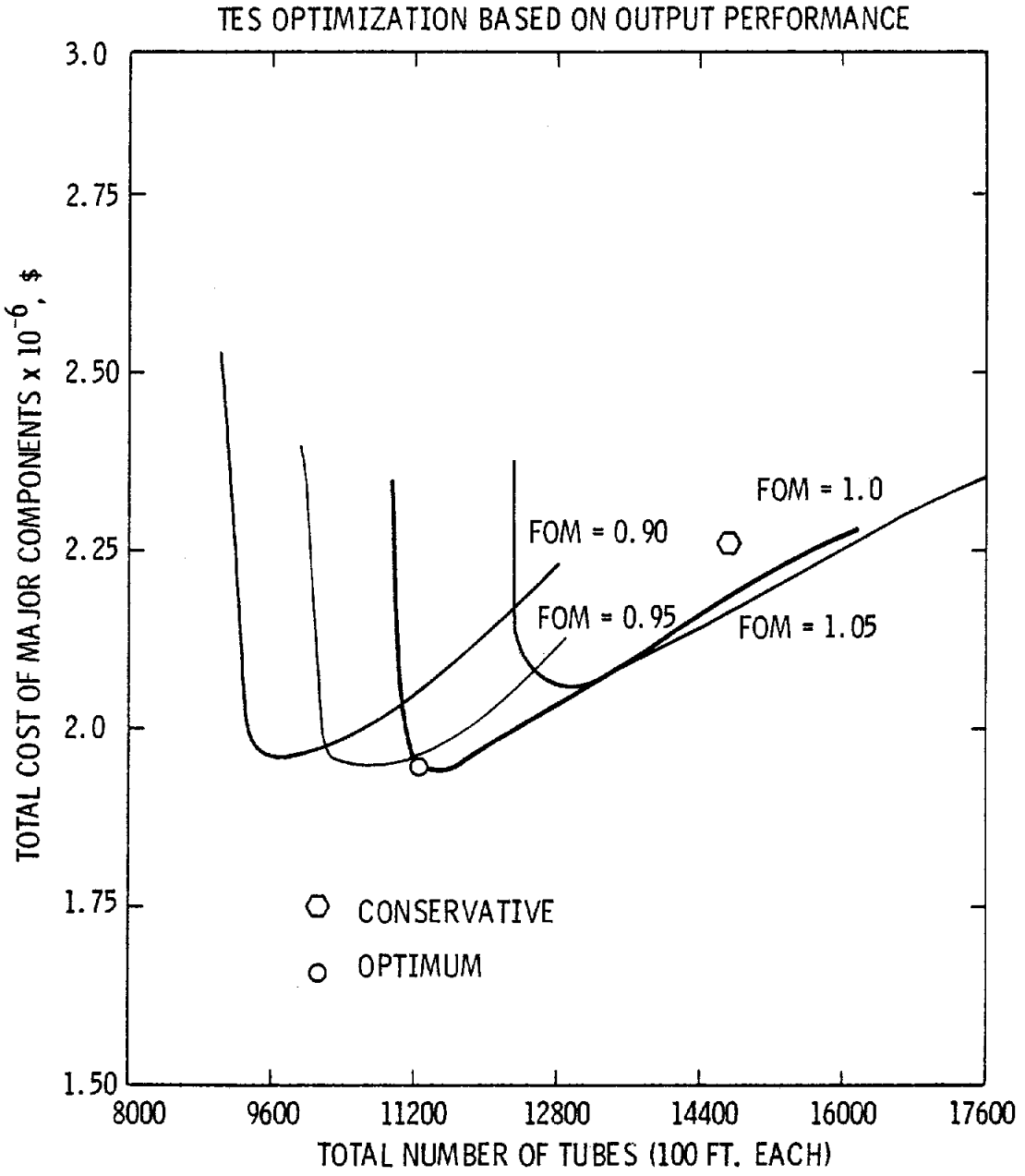


Figure IV-9
 VARIATION OF TOTAL COST OF MAJOR COMPONENTS
 WITH FIGURE OF MERIT (FOM) AND NUMBER OF TUBES

Each of Figures IV-4, IV-5, IV-8 and IV-9 also show the amount of PCM and the number of tubes, as obtained from a conservative simplified procedure explained in Appendix III.

In each of these figures, the sharp rise in cost on the left side of the optimum point is due to a large increase in one design parameter as the other parameter decreases. The slow rise in cost on the right side of the optimum point suggests only a small decrease in one design parameter as the other parameter increases. These figures also suggest that the optimum TES design would have $Q_{\text{CHARGE}} = 148 \text{ MWh}$ (Or FOM = 1). If the unit is too big, the extra capacity will be wasted. If the unit is too small, the cost of deficit power will be higher than that associated with a bigger unit.

APPENDIX V
COMPUTER PROGRAM TESST

The primary analytical tool used in the performance evaluation and unit optimization has been the computer program TESST. The earlier version of this program is fully explained in Reference (1). The program calculates the thermal and hydraulic performance for a specific design through its daily duty cycles. Calculations are performed for a number of cycles so that equilibrium is achieved from an initial, input-uniform PCM temperature. The detailed model of the TESS is coupled to a very simple model of the solar collector field in that the output of the storage is input to the collectors. The insolation heat rates and a uniform boiler or process demand are specified. The unit is charged when the insolation heat rates and a uniform boiler or process demand are specified. The unit is charged when the insolation exceeds the demand and discharged for the remaining of the specified operation time. The thermal analysis is performed during the overnight period to determine heat loss and temperature redistribution within the PCM.

The storage unit is modeled as a vertical cylinder with the numerical elements being horizontal slices, each of which is assumed to be at uniform temperature. In this way, a step-wise temperature gradient is calculated which approaches a smooth curve as the number of elements increases. The computed temperature of each element is taken to be the midpoint temperature for purposes of axial conduction calculations and plotting of the output.

A heat balance is made around each element consisting of three components:

- ... the axial conduction from one element to the next consisting of conduction through the PCM, through the tubes, and through the vessel wall;
- ... the conduction to the environment which is primarily conduction loss through the thermal insulation; and
- ... the heat transfer between the heat transfer fluid and the PCM.

The last component is, of course, set equal to zero when no heat transfer fluid is flowing. The rates of heat flow by these modes are multiplied by the time step and summed; a net energy change per element is computed; and the new temperature is found from PCM properties.

Since the focus of this study has been the TES subsystem, decoupled from the solar collector field and the process, it was necessary to decouple the collectors and the TES unit on the computer model. Consequently, constant input and output conditions to the collector are specified. The charging steam/flow rate is then calculated depending on the insolation heat rate specified.

This code, which was developed for single-phase heat transfer medium, was modified to analyze a system charged and discharged by water/steam. The major modifications include:

- Heat transfer coefficients for laminar and turbulent film condensation in the charge mode.
- Heat transfer coefficients for wet and dry wall conditions and superheated steam regime in the discharging mode.
- Corresponding pressure drop calculations for two-phase flow in charge/discharge mode.
- Static flow stability analysis in the discharge mode in which the discharge steam flow is systematically through the tubes for a fixed PCM temperature profile and the pressure drop of the steam/water is calculated. The analysis is fully discussed in Section 5.5.3.

The heat transfer enhancement with the use of extended surfaces was independently studied as discussed in Section 3.4.2. The effect of these extended surfaces on heat transfer rates were simulated in the code TESST by an augmented value of PCM thermal conductivity. After a trial and error approach, a factor of 10 was established.

The final performance evaluation was performed with the code TESST using the conductivity enhancement factor of 10 and with the final selected design options as described in Section 5.

APPENDIX VI

HEAT TRANSFER ENHANCEMENT

The initial sizing and cost estimates have indicated that approximately 45% of the component costs for the tube-intensive concept is due to the large heat transfer surface requirements. A drastic reduction in the amount of heat transfer tubing can be achieved by methods of heat transfer augmentation such as fins or PCM conductivity enhancement (6, 7). Not only could the net cost of the heat exchanger be reduced, but improved reliability would also be achieved by reducing the probability of tube leaks. A study was performed to examine the heat transfer in a local unit cell surrounding a tube during the discharge process. A simple two-dimensional, finite difference computer program (FREEZE) was written to measure the heat rate into the tube and the freezing of the PCM over the discharge process. The program was used to evaluate various methods of heat transfer enhancement suggested in the literature (6, 7). Based on this initial effort, which was conducted in parallel to the concept selection phase, a design concept was developed and incorporated into the final conceptual design. The geometry of this design was simulated in FREEZE, and the results of the calculation used to size the heat transfer bundle.

This appendix is broken into three sections. The first describes the initial analysis results. This is followed up by the evaluation of the selected design for augmented heat transfer. Finally, the computer program FREEZE is described.

1.0 EVALUATION OF METHODS OF HEAT TRANSFER ENHANCEMENT

The methods of heat transfer augmentation include conductivity enhancement, achieved by mixing a small volume fraction of high conductivity material such as steel or aluminum into the PCM. Analytical and experimental studies reported in References (6) and (7), have considered aluminum and steel wools and an aluminum honeycomb (Duocel)

attached to the tubes. The results indicate that the latter method shows promise. Conductivity enhancement studies here reflect various volumetric additions of the Duocel. Extended heat transfer surfaces, to provide a high conductivity path from the remote regions of the PCM to the tubes, have also been considered in References (6) and (7). Various configuration of fins and screens (See Figure 3.4.2-1) have been considered. For these methods, a range of tube diameters from 6.35 mm to 25.4 mm (0.25" to 1.0") has been considered.

Since the FREEZE code employs an entirely rectangular grid, the discharge heat transfer tube surface is also modeled as a rectangle. The dimensions are selected to match the exposed area of the actual tube. Initially, the PCM is all liquid at the melting temperature (260°C, 500°F), and the tube wall temperature is stepped to the discharge steam temperature (232°C, 450°F) and maintained there. As time marches heat is transferred to the tube and a freeze wave (a solid-liquid boundary) propagates through the PCM. Calculations were performed for a four-hour period.

Typical propagation patterns of the freeze waves are shown in Figure VI-1 for a 1.0" tube on a 4.0" square array. The quadrant shown is a symmetrical section of the unit cell surrounding the tubes. (See Figure 3.4.2-1.) The bare tube case does not include any PCM conductivity enhancement. Steel is employed for the fins in the two-fin and four-fin configurations. The effect of the high conductivity paths through the PCM is readily seen in terms of the amount of PCM frozen in a given time span. Improvements can still be made if conduction paths from the remote corners of the unit cell to the tube or the main fins are provided. Screens or thin plates could serve in this capacity.

Figure VI-2 shows typical histories for the tube heating rate. The specific curves correspond to the three cases presented in Figure VI-1. For a given time into discharge, the heat transfer rates are certainly higher with larger numbers of conductivity paths. However, referring back to the previous figure, at the same time, the total amount of PCM frozen and, consequently, the total heat removed, is also greater with the high degree of finning. It should be noted that sensible heat of

Figure VI-1
FREEZE FRONT PROGRESSION
1.0" TUBE O.D., 4" SQUARE ARRAY

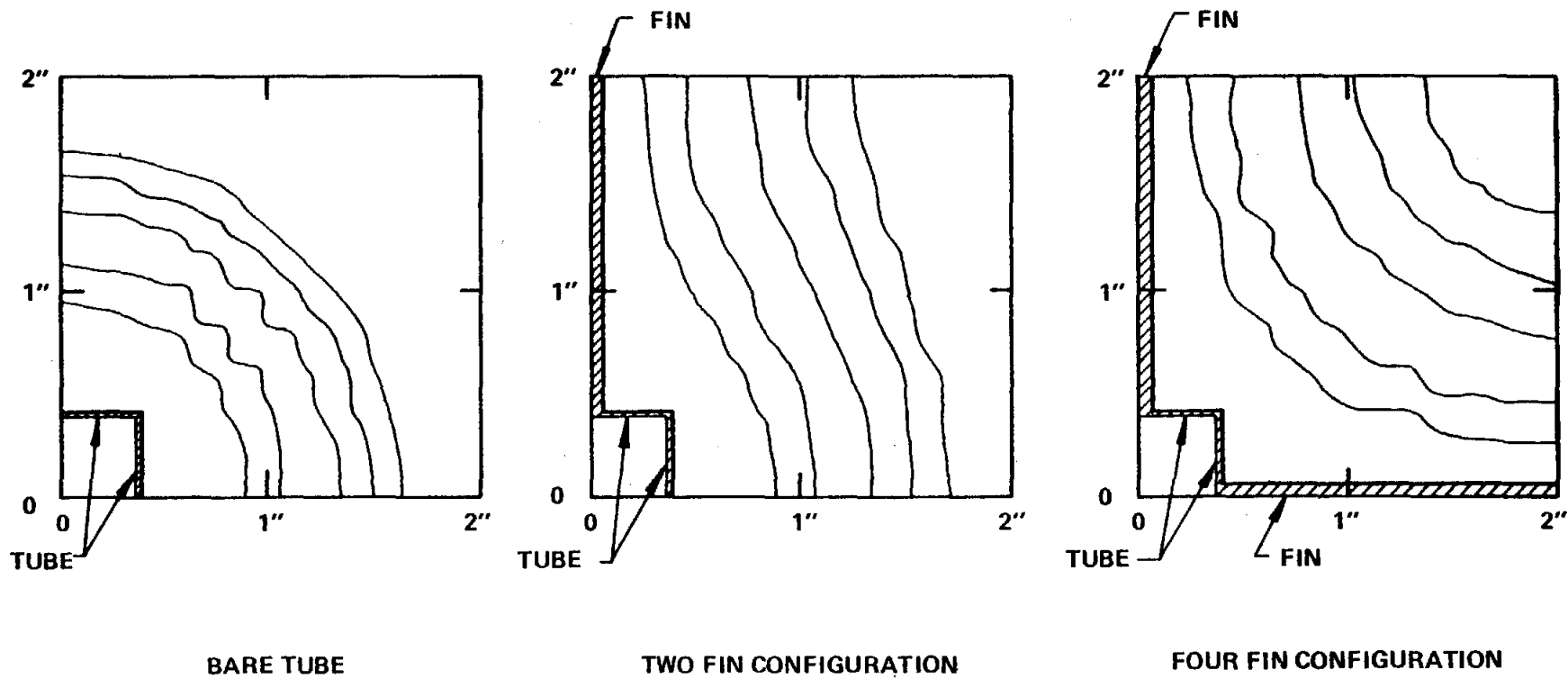
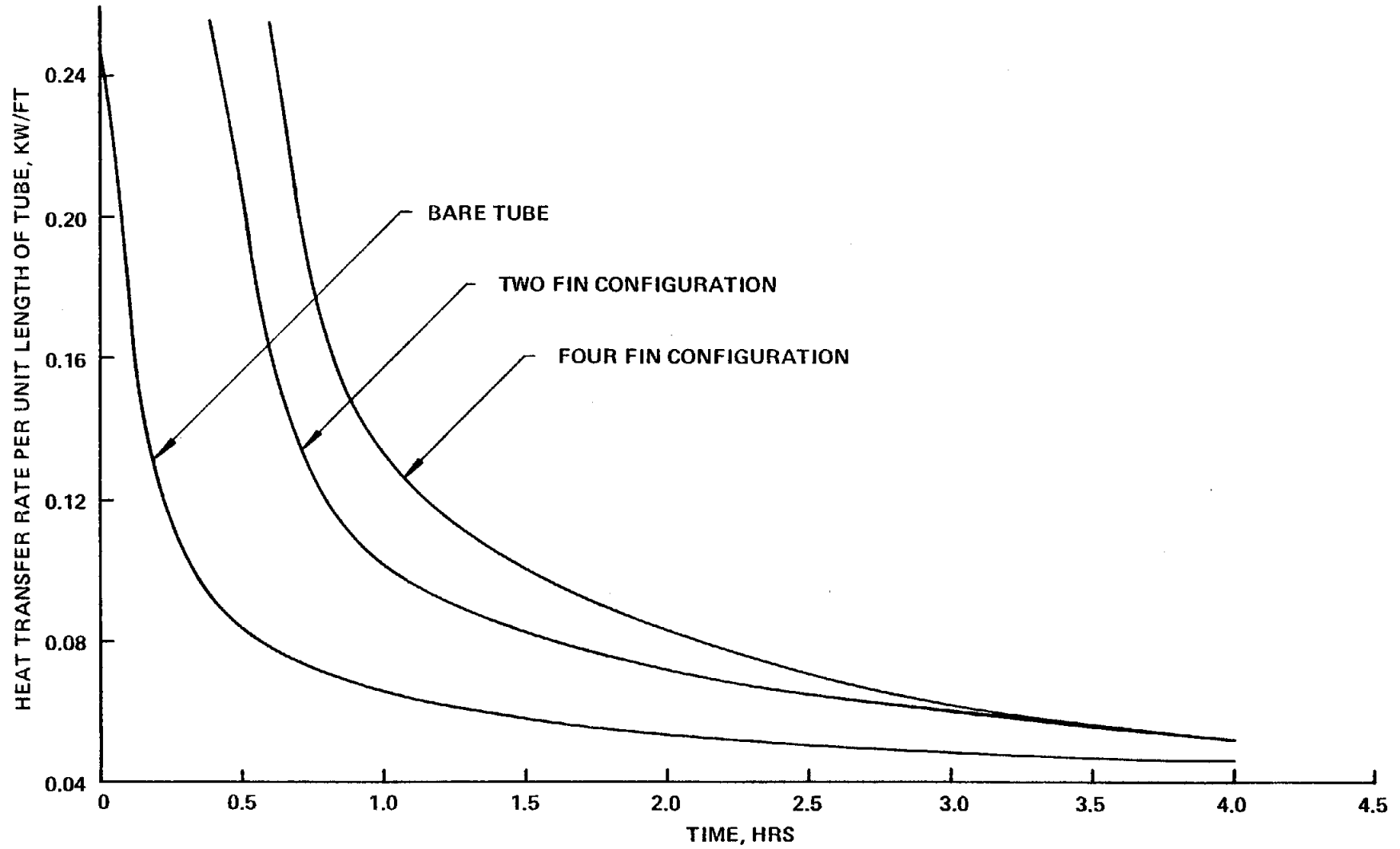


Figure VI-2

TUBE LINEAR HEAT RATE DURING DISCHARGE

1.0" OD TUBE, 4.0" SQUARE ARRAY



the solid phase contributes about 4 to 7% to the total heat removal. There is no sensible heat available from the liquid phase due to the initial conditions.

To compare the configurations, a common basis is needed. The current design effort requires that a target storage capacity and a peak discharge rate be satisfied simultaneously. A design point is defined at the time when the ratio of the integrated heat rate to the heat rate equals the ratio of the target storage capacity (148 MWh) to the discharge rate (30 MW), i.e., 4.93 hours. At this condition the tube length calculated by dividing the instantaneous heat rate into the target value satisfies both the storage capacity and discharge rate requirements. Owing to the different heat rate histories of each case, this design point occurs at different times from the start of the discharge problem. To insure a minimum amount of PCM, the freeze fraction in the unit cell should near unity at the design point; if not, there is a waste of PCM and the case should be recalculated for a smaller tube spacing.

A series of calculations was conducted with variation of fin and tube configurations and sizes. Most of the calculations were performed for a 0.25" O.D. tube, since the tube-intensive design during the concept selection phase employed this tube size. Tube sizes of 0.50" and 1.00" O.D. with and without finning were also considered. Tube spacings of 4" x 4" were used in the majority of cases. The effect of reduced spacing was considered for the 0.25" O.D. tube with fins. The results of this study are summarized in Table VI-1. Total tube length is based on a 30 MW heat rate. The tubes are assumed to be 100 feet long. No attempt was made at this stage of the evaluation to optimize a given tube size and configuration.

TABLE VI-1
CHARACTERISTICS OF HEAT TRANSFER ENHANCEMENT
METHODS AT THE DESIGN POINT

	<u>Number of Tubes</u>	<u>Spacing</u>	<u>Freeze Fraction</u>
<u>I. 0.25" O.D.</u>			
a. Bare Tube	12346	4"x4"	0.220
b. 3% Duocel	3497	4"x4"	0.701
c. 4% Duocel	3175	4"x4"	0.900
d. 5% Duocel	2616	4"x4"	0.895
e. 5% Duocel 10 Mils, PCM Contact Resistance	2844	4"x4"	0.828
f. Finned (1/16" Thick Fins)			
1. Two Fins	6160	4"x3"	0.609
2. Two Fins	7112	3"x3"	0.682
3. Four Fins	4552	4"x4"	0.617
4. Four Fins	5992	3"x3"	0.839
g. Screens			
1. Without Connecting Plate	4292	4"x4"	0.520
2. With Connect- ing Plate	2822	4"x4"	0.728
<u>II. 0.50" O.D.</u>			
a. Bare Tube	8982	4"x4"	0.278
b. Finned (4-1/16" Thick Fins)	4354	4"x4"	0.824
<u>III. 1.00" O.D.</u>			
a. Bare Tube	6623	4"x4"	0.478
b. Finned (1/8" Thick Fins)			
1. Two Fins	4491	4"x4"	0.543
2. Four Fins	4335	4"x4"	0.756

Use of the reticulated aluminum ("Duocel") (7) conductivity enhancement shows the greatest potential for reduced number of tubes. The presence of a small contact resistance between the PCM-filled Duocel and the tube does not change the results significantly.

The use of screens or fins (or the equivalent) also results in a significant reduction in the number of tubes. The finning concepts considered are radial fins, 180° (2 fins) or 90° (4 fins apart). The relative benefit (bare tube vs. finned) of fins appears to decrease with increasing tube diameter. The screening concepts considered are basically an extension of the fin concepts. Additional thin parallel plates are inserted between the tubes to approximate many screens. This was analyzed with and without a connecting plate perpendicular to the screens, providing a thermal short circuit to the tube. This configuration is equivalent to parallel banks of two-fin tubes with screens inserted between them. As can be seen from Table VI-1, the greatest benefit is gained simply by adding screens between the tubes. A smaller but significant additional benefit is obtained with the connecting plate. The relative benefit of screens is also expected to decrease with tube diameter. Simple use of larger tube diameter without heat transfer enhancement reduces the tube requirement relative to the 0.25" O.D., but this reduction is fairly modest compared to other concepts. All the cases show potential for a significant reduction in the number of tubes. However, all the concepts represent corresponding increases in material requirements and/or complexity. This may preclude the use of a concept due to excessive cost or fabrication problems.

The cases shown in Table VI-1 were analyzed for the most part on a 4" x 4" tube spacing. Many of the cases, in particular those for the bare tube and some of the finned cases, have freeze fractions that are fairly small. This implies that a significant fraction of the PCM volume is "wasted", and a tighter spacing is possible without severely penalizing performance. This can be seen by comparing the 3" x 3"- and 4" x 4"-0.25" four-fin tube cases. A tighter spacing reduces the PCM requirements and may result in lower overall cost. Tube bundle sizing calculations were performed for bare tubes based on the results given in Table VI-1. Spacing was determined by allowing the freeze waves

around the tubes to just touch at the design point, i.e., the freeze fraction for all diameters is 0.768 at their respective spacings. The results of this are shown in Figure VI-3.

These calculations indicate that the spacing requirement for a 0.50" tube is not significantly greater than that of a 0.25" O.D. tube. However, since the total tube length (number of tubes) is less for an 0.50" tube relative to the 0.25", the total PCM volume is reduced. This accounts for the minimum in the PCM volume as a function of tube diameter. These results indicate that there may be a lowest cost configuration with a tube O.D. greater than 0.25", taking into account both the tube and PCM costs.

Sizing calculations were also performed for the two-fin tubes for 0.25" and 1.0" tubes. The results are summarized in Table VI-2. Spacing perpendicular to the fins is dictated by the freeze wave thickness. Note that reducing the fin length (0.25" O.D., "long" vs. "short" fin case) increased the number of tubes required but reduced the PCM volume and increased the volume utilization (freeze fraction). However, the fins drastically increased the total surface area and consequently the required metal.

Figure VI-3
EFFECT OF TUBE DIAMETER ON TES
SIZE FOR BARE TUBES

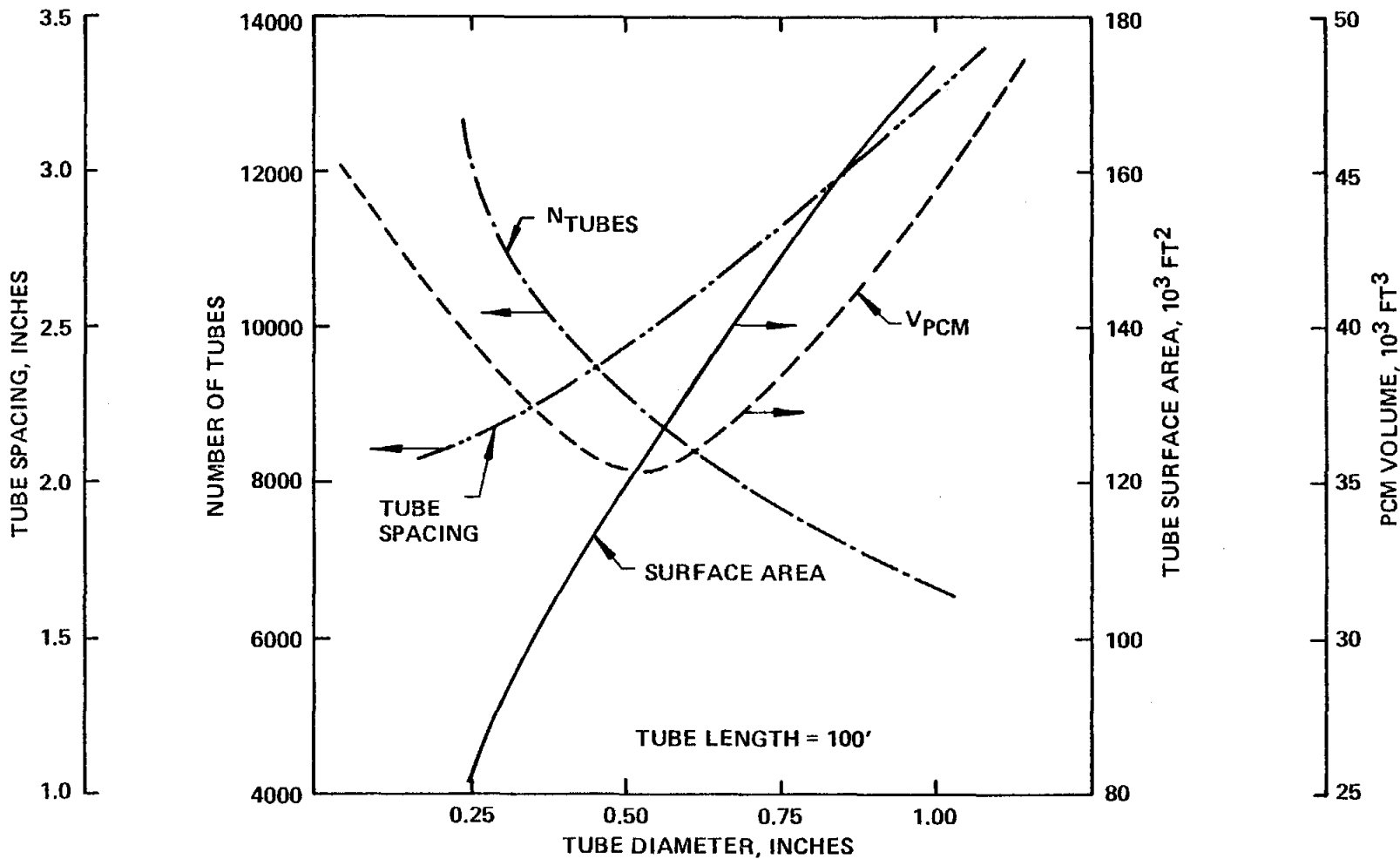


TABLE VI-2
RESULTS OF SIZING CALCULATIONS
FOR DOUBLE FINNED TUBES

	<u>Number of Tubes</u> [†]	<u>Freeze Fraction</u>	<u>Spacing</u>	<u>Surface Area (ft²)</u>	<u>PCM Volume (ft³)</u>
I. <u>0.25" O.D.</u>					
a. Bare Tube	12346	0.768	2.15 x 2.15"	80800	39360
b. Long Fin	6160	0.735	4.0 x 2.5"	418910	41565
c. Short Fin	7112	0.859	3.0 x 2.4"	370215	34950
II. <u>1.00" O.D.</u>					
a. Bare Tube	6623	0.768	3.25" x 3.25"	173380	44010
b. Long Fin	4491	0.740	4.0" x 3.0"	332770	34280

[†]100 ft Tubes Assumed

2.0 EVALUATION OF THE SELECTED CONCEPT

The fin and screen calculations described in the previous section indicate that effective and efficient heat transfer is achieved when high conductivity paths are provided in two directions relative to the tube. Based on this, a simple fin configuration which lends itself to relatively easy fabrication and bundle assembly was conceived. This concept is shown in Figure VI-4. The analysis of the concept considered variations in tube spacing (Dimensions X and Y in Figure VI-4) and spacing between channels (Dimension Z). Both aluminum and steel channels were evaluated.

The freeze pattern around the channel is a three-dimensional problem; however, as a simple three-dimensional tool was unavailable, the problem was broken up into two parts. The problem was analyzed as if the surface which is formed by the tubes and flange surfaces of the channel were a slab at a uniform temperature. This allowed the effect of the y- and z-spacing to be analyzed using the two dimensional FREEZE model. This is shown in Figure VI-5b. The average heat flux in the y-direction at the design point is then calculated. These results are summarized on Table VI-3 along with the freeze fraction.

If the flange surface along the x-direction were truly isothermal, the entire surface would see the same heat flux (see Figure VI-5a). This would result in a uniformly thick freeze wave progressing in the y-direction away from the flanges. However, in reality the surface is not isothermal. There is a "fin effectiveness" associated with the flanges, and the freeze layer will decrease in thickness with distance away from the tubes. This implies that the heat flux is not uniform in the x-direction, and the effective heat transfer area is somewhat less than the total flange surface area. This "effectiveness" (f) was estimated by comparing the actual freeze fraction of a tube with radial fins 180° apart to that which would be obtained if the fins were isothermal, all for a given unit cell. This was done for several fin lengths and materials (steel and aluminum). The effectiveness of steel fins was found to vary from 0.97 to 0.78 for x-spacings of 3.5" to 6.0" respectively. For an aluminum fin with a 6.0" x-spacing, the effectiveness was found to be 0.90. The results are summarized on Table VI-3.

FIGURE VI - 4

REFERENCE HEAT TRANSFER ENHANCEMENT CONCEPT

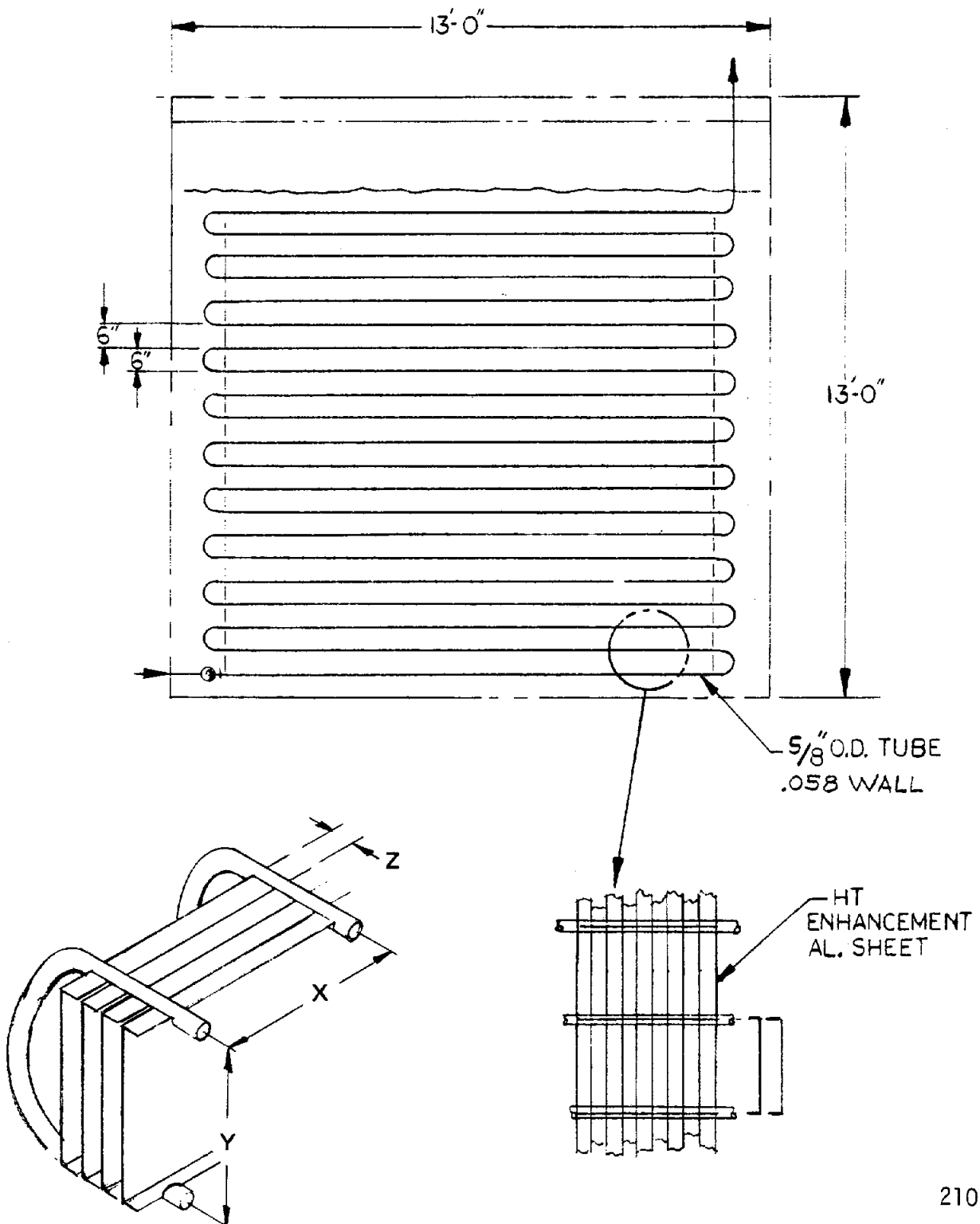


Figure VI-5
MODEL OF HEAT TRANSFER ENHANCEMENT CONCEPT

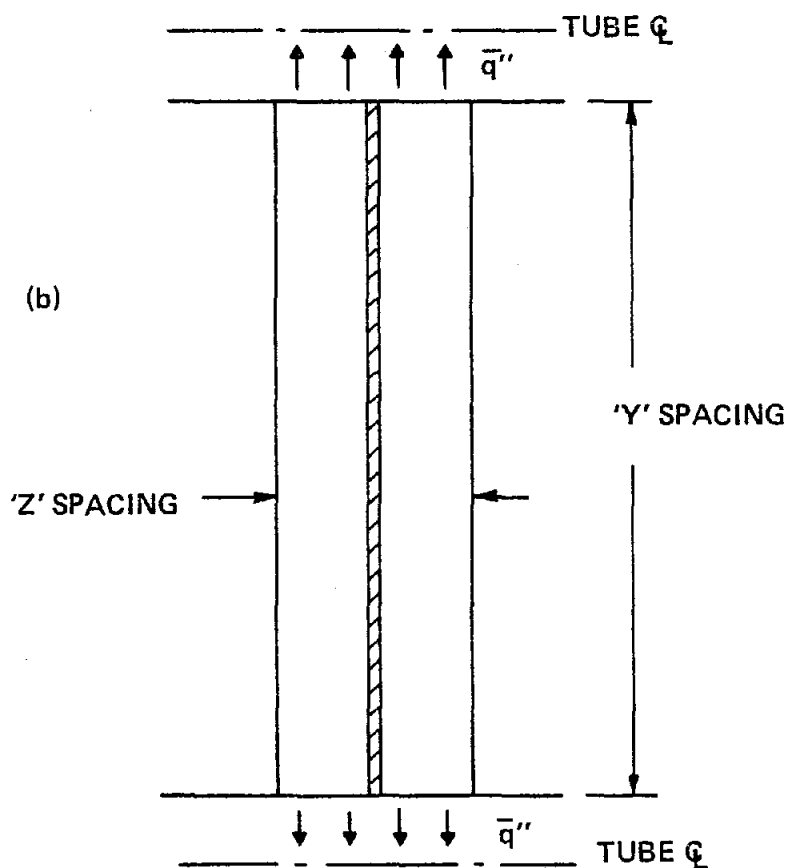
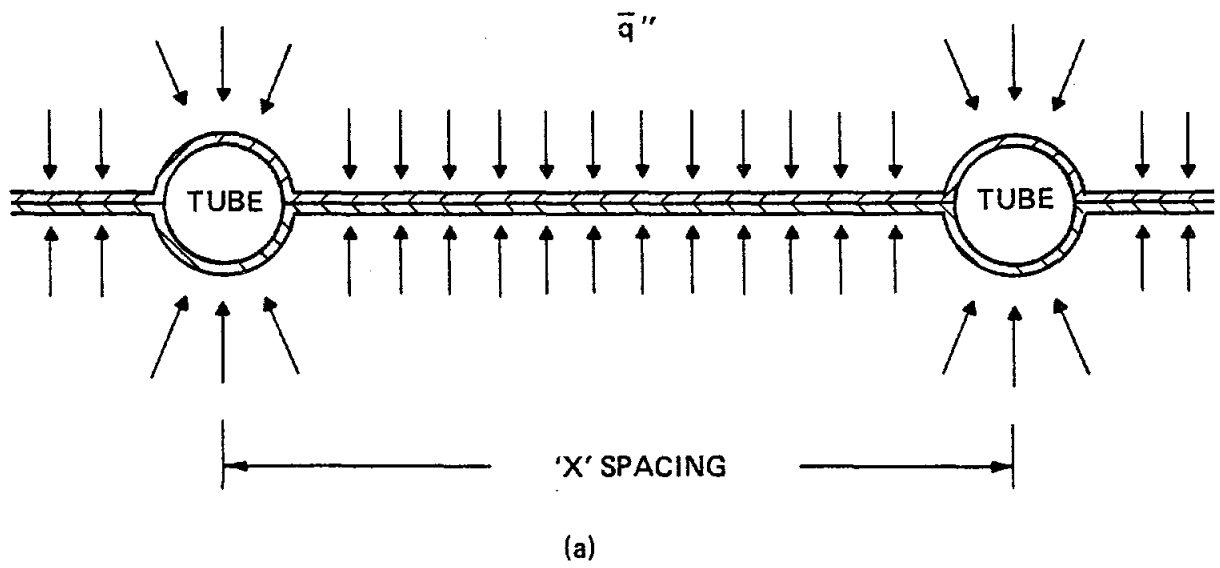


TABLE VI-3
SUMMARY OF RESULTS
CHANNEL CONCEPT

I. RESULTS FOR AXIAL (y-) SPACING OF TUBES

	<u>Heat Flux</u> <u>Btu</u> <u>hr · ft²</u>	<u>Freeze</u> <u>Fraction</u> <u>(F)</u>
A. <u>STEEL</u>		
a. 3/4" Plate Spacing		
(1) 3.5"	450	0.993
(2) 4.0"	492	0.963
b. 1" Plate Spacing		
(1) 4.0"	441	0.923
(2) 6.0"	459	0.599
B. <u>ALUMINUM</u>		
a. 1/2" Plate Spacing		
(1) 6.0"	853	1.000
b. 3/4" Plate Spacing		
(1) 4.0"	616	1.000
(2) 6.0"	816	0.990

II. RESULTS FOR HORIZONTAL (x-) SPACING OF TUBES

		<u>Effectiveness</u> <u>(f)</u>
a. STEEL	x = 3.5"	0.97
	4.0"	0.89
	6.0"	0.78
b. ALUMINUM	x = 6.0"	0.90

The effectiveness thus calculated was used to adjust the heat transfer area. This, combined with the average heat flux (\bar{q}''), obtained from the FREEZE calculations, was used to obtain the required tube length.

$$L_{\text{tube}} = \frac{30 \text{ MW}}{\bar{q}'' [2(P-d)f + \pi d - 4\delta_f]}$$

where P = x-spacing

d = tube O.D.

f = effectiveness

δ_f = channel web thickness = 1/32"

The channel section fin heat transfer enhancement concept results in a drastic reduction in the tubing requirement. Use of bare tubes would require approximately 824,200 ft of tubing to obtain the required discharge heat rate and capacity. Reduction in required tube length by up to a factor of 6 is possible with the channel concept.

Variations in the tube spacing (in the x- and y-directions) from 3.5" to 6", and channel spacing (z-direction) from 1/2" to 1" were considered. Steel and aluminum channels were considered. A 1/32" thickness was assumed. These calculations showed aluminum to be superior to the carbon steel for a given geometrical configuration with respect to reduction in tube length. Aluminum channels required from 25 to 60% less enhanced tubing than corresponding steel channels. In addition, the use of aluminum results in higher freeze fractions and thus, better volume utilization of the PCM.

The tube spacing in the y-direction appears to have little effect on the tube length required. This is true except when the PCM is essentially completely frozen, at which point the sensible heat of the solid PCM dictates. The reduction in required tube length is found to increase almost linearly with increasing x-spacing for a given y-spacing. This is a direct result of the increasing effective heat transfer area. The metal surface perpendicular to the tube in the y-direction transfers the heat away from the spaces between the tubes to the flanges which form the top and bottom of the channel. These flanges act like radial fins and

conduct the heat to the tube. Thus, the controlling heat transfer area is that of the flange, which increases with increasing x spacing.

Tube spacing of 6" x 6" with aluminum channels gives a good compromise between heat transfer and structural concerns. Spacings beyond this may not be practical from a structural standpoint, and give diminishing heat transfer benefits. The channel spacing (z-dimension) does not have a large impact on the heat transfer characteristics. Reducing the channel spacing from 1" to 3/4" results in 10% reduction in tube length. Further reduction to 1/2" results in only an additional 5% reduction. This spacing, however, increases the required number of channels by 50%. A channel spacing of 3/4" would give a good compromise between heat transfer requirements and material needs.

Aluminum channels with 6" x 6" tube spacing and 3/4" channel spacing require 130,000 feet of enhanced tube length for an end-of-discharge heat rate of 30 MW. PCM freeze fractions of the order of 90% or better could reasonably be expected.

An alternate enhancement concept is shown in Figure VI-6. This configuration gives benefits equivalent to the channel concept, provides positive placement of the heat transfer surfaces, and helps insure good contact with the tubes. This concept is, however, considerably more complicated than the channel and would undoubtedly be more costly. Note that the important feature of this configuration is that, like the channel, a means is provided to conduct the heat away from the spaces between the tubes to a large effective heat transfer area. This again allows for a much shorter tube length.

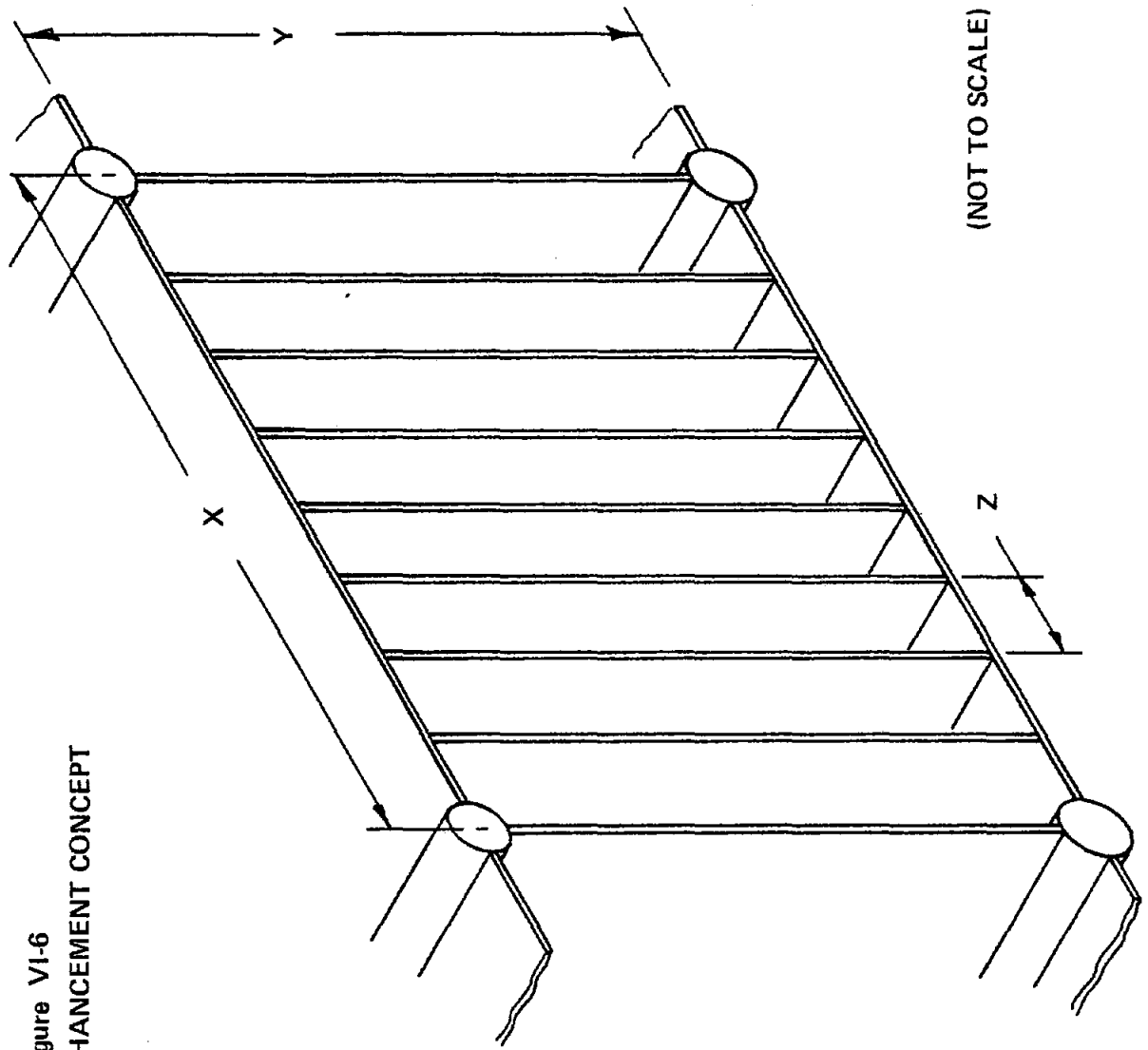


Figure VI-6
ALTERNATE ENHANCEMENT CONCEPT

3.0 DESCRIPTION OF FREEZE MODEL

General Description

The general setup of the FREEZE model is shown in Figure VI-7. A rectangular cell with a square tube approximating the circular tube is used. Note that neither the cell nor the elements need to be symmetric. All elements are assumed to be phase change material (PCM) unless otherwise specified. The properties assumed are $\rho = 130 \text{ lbm/ft}^3$, $C_p = 0.45 \text{ Btu/lbm } ^\circ\text{F}$, and $Q_L = 118 \text{ Btu/lbm}$. The conductivity of the PCM can be specified arbitrarily to account for uniform conductivity enhancement. Elements can be specified to be metal and the properties are input for each metal element.

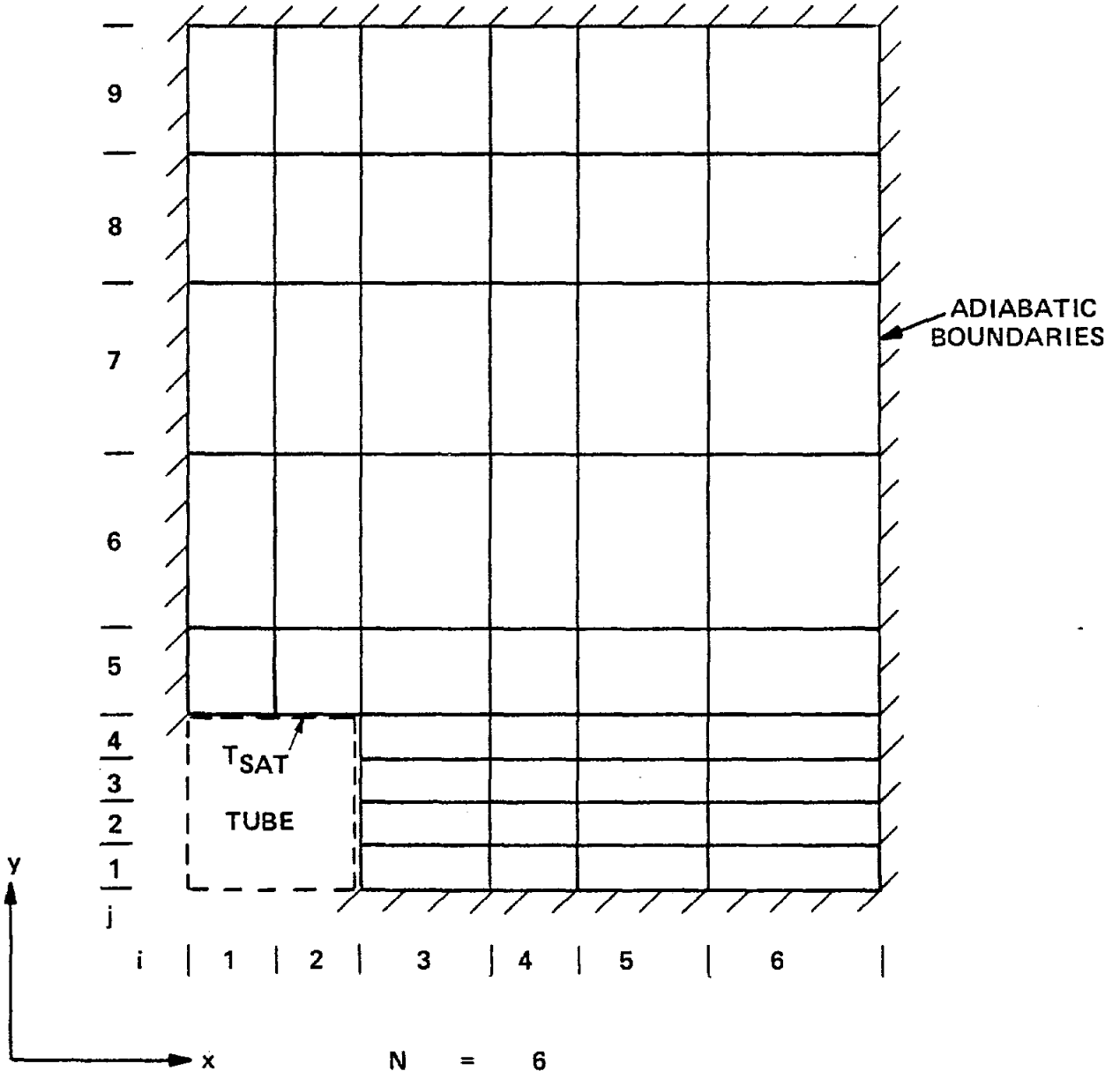
Difference Equations

The governing difference equations are obtained by considering the net heat conducted in or out of an element. The heat conducted from an element to another is put in the form:

$$\dot{q}_{1-2} = \frac{A \Delta T_{1-2}}{R_{1-2}}$$

where A is the area normal to the center of elements 1-2 and R_{1-2} is the thermal resistance between the element centroids. The difference equation for a general element and some representative examples of special cases are given below (see Figure VI-8 for the geometry). The $k_{i,j}$'s are the thermal conductivities of the elements. All equations are per unit depth of material.

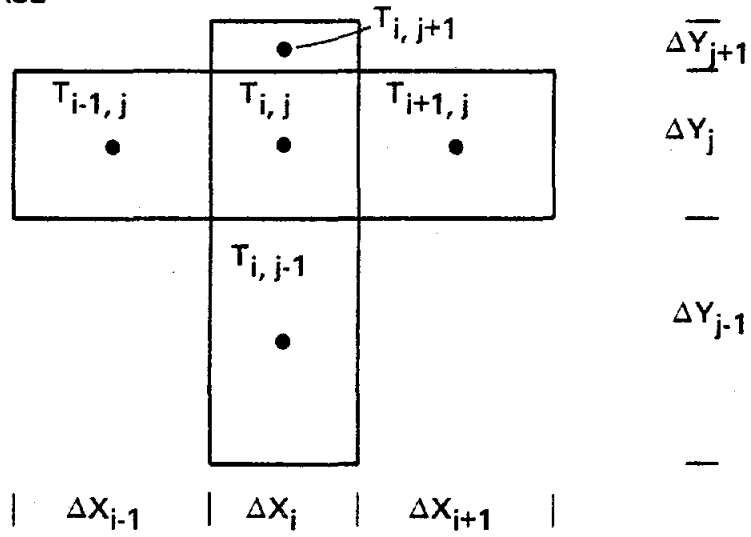
Figure VI-7
 EXAMPLE OF FREEZE MODEL SETUP



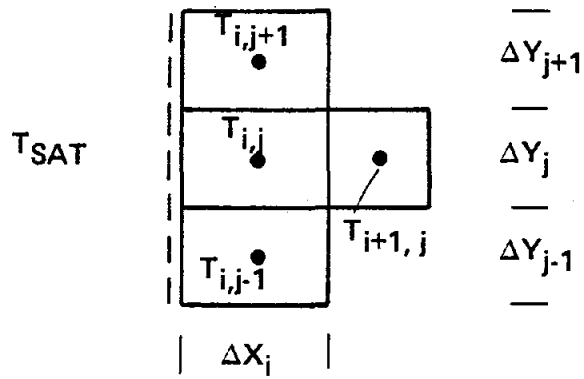
N = 6
 NT = 2
 K = 9
 KT = 4

Figure VI-8
 EXAMPLE OF DIFFERENT REGIONS IN MODEL

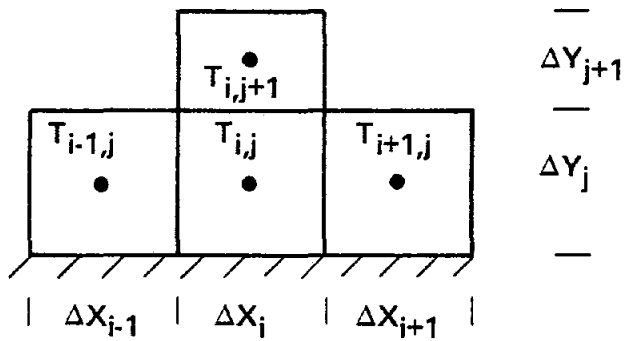
A-2a GENERAL CASE



A-2b NEAR TUBE



A-2c NEAR ADIABATIC BOUNDARY



a. General Case (Figure VI-8a)

$$\begin{aligned} \dot{q}_{NET} = & \frac{\Delta Y_j (T_{i+1,j}^n - T_{i,j}^n)}{\left(\frac{\Delta X_{i+1}}{2 k_{i+1,j}} + \frac{\Delta X_i}{2 k_{i,j}} \right)} + \frac{\Delta Y_{i-} (T_{i-1,j}^n + T_{i,j}^n)}{\left(\frac{\Delta X_{i-1}}{2 k_{i-1,j}} + \frac{\Delta X_i}{2 k_{i,j}} \right)} \\ & + \frac{\Delta X_i (T_{i,j+1}^n - T_{i,j}^n)}{\left(\frac{\Delta Y_{j+1}}{2 k_{i,j+1}} + \frac{\Delta Y_j}{2 k_{i,j}} \right)} + \frac{\Delta X_i (T_{i,j-1}^n + T_{i,j}^n)}{\left(\frac{\Delta Y_{i-1}}{2 k_{i,j-1}} + \frac{\Delta Y_j}{2 k_{i,j}} \right)} \end{aligned}$$

b. Near Tube (Figure VI-8b)

$$\begin{aligned} \dot{q}_{NET} = & \frac{\Delta Y_j (T_{sat} - T_{i,j}^n)}{\left(\frac{\Delta X_i}{2 k_{i,j}} + R_c \right)} + \frac{\Delta Y_j (T_{i+1,j} - T_{i,j})}{\left(\frac{\Delta X_{i+1}}{2 k_{i+1,j}} + \frac{\Delta X_i}{2 k_{i,j}} \right)} \\ & + \frac{\Delta X_i (T_{i,j+1}^n - T_{i,j}^n)}{\left(\frac{\Delta Y_{j+1}}{2 k_{i,j+1}} + \frac{\Delta Y_j}{2 k_{i,j}} \right)} + \frac{\Delta X_i (T_{i,j-1}^n - T_{i,j}^n)}{\left(\frac{\Delta Y_{j-1}}{2 k_{i,j-1}} + \frac{\Delta Y_j}{2 k_{i,j}} \right)} \end{aligned}$$

where R_c is a resistance term which can include

- a) contact resistance between tube and PCM
- b) resistance of tube wall
- c) tube side film resistance

c. Near Adiabatic Boundary (Figure VI-8c)

The expression for q_{NET} is similar to that of the general case except the term representing conduction from the (i,j) element to, in this case the (i,j-1) element, is deleted since no heat is transferred across this face.

The "n" superscript refers to the n^{th} time step, and q_{NET} is being computed for the $n+1$ time step. Thus q_{NET} is known.

Determination of Temperature

The total heat removed at the $n+1$ time step is calculated for each PCM element

$$Q_{TOTAL_{i,j}} = \sum_{X=1}^n \dot{q}_{NET_{i,j}} \Delta\theta$$

and is compared to the latent heat in the element. A freeze fraction $Z_{i,j}$ is determined for each element.

$$Z_{i,j} = \frac{|Q_{TOTAL_{i,j}}|}{(\rho_{i,j})(\Delta X_i)(\Delta Y_j) Q_L}$$

where Q_L = latent heat of fusion

The absolute value sign is used since Q_{TOTAL} will be negative.

If $Z_{i,j}$ is ≥ 1.0 , the element is assumed to be a slurry at the melt temperature, T_{melt} , thus

$$T_{i,j}^{n+1} = T_{\text{melt}}$$

If element is already totally frozen (if $z_{i,j} \geq 1.0$, set = 1.0) or the element is a metal element (and $Z = 1.0$ by definition), the heat conducted is set equal to the change in heat stored, thus:

$$\left. \frac{\partial q}{\partial \theta} \right|_{\text{STORED}_{i,j}} = \dot{q}_{\text{NET } i,j}$$

$$(\rho_{i,j} C_{p \ i,j}) (\Delta X_i) (\Delta Y_j) \frac{(T_{i,j}^{n+1} - T_{i,j}^n)}{\Delta \theta} = \dot{q}_{\text{NET } i,j}$$

$$T_{i,j}^{n+1} = T_{i,j}^n + \dot{q}_{\text{NET}} \Delta \theta / (\rho_{i,j} C_{p \ i,j}) (\Delta X_i) (\Delta Y_j)$$

This is a pure explicit method. As such it has stability constraints on the mesh size and time step. In general, if the dimensionless parameters Fo_x, Fo_y, Fo_{xy} are each ~ 0.25 there will not be stability problems.

$$Fo_x = \frac{\alpha_{i,j} \Delta \theta}{(\Delta X_i)^2}$$

$$Fo_y = \frac{\alpha_{i,j} \Delta \theta}{(\Delta Y_j)^2}$$

$$Fo_{xy} = \frac{\alpha_{i,j} \Delta \theta}{(\Delta X_i) (\Delta Y_j)}$$

$$\alpha_{i,j} = \frac{k_{i,j}}{\rho_{i,j} C_{p i,j}}$$

Recommendation for Future Work

Use of the FREEZE code during this study has pointed out some limitations which should be addressed if the code is to be used to any great extent in the future. The most important and restrictive limitation is that of the stability criteria. Currently a time step of 0.5 sec. is used in the code. Even with such a short time step, stability problems arise for high conductivity elements. Stability requirements limit the mesh size or, require a shorter time step or adjusted properties (primarily C_p). The mesh size is often specified by the configuration to be analyzed and may be difficult to change. A reduced time step greatly increases computer time which is excessive at present (~150 seconds for a 16 x 16 element mesh run for 4 hours). Changing properties to obtain stability introduces further error, which is not easily quantified, into the calculations. Possible solutions to this would be use of a better, more sophisticated explicit method (such as the DuFort-Frankel method) which has less severe stability constraints, or use of a fully implicit scheme (always stable) using an efficient matrix solver. The methods would allow the mesh size and time step to be specified independently and, since the time step would undoubtedly be greatly increased, computer time could most likely be reduced. It may also be appropriate to generalize the boundary conditions so that a configuration which is not a simple square tube array might be analyzed.

Input Guide to FREEZE

<u>Card No.</u>	<u>Column</u>	<u>Variable</u>	<u>Format</u>	<u>Description</u>
1	1-80	TITLE	20A4	Case Description
2	1-5	N	15	Number of X increments
	6-10	NT	15	Number of X increments within the tube dia.
	11-15	K	15	Number of Y increments
	16-20	KT	15	Number of Y increments within the tube dia.
3	1-5	IPRINZ	15	Print option for the element freeze fractions 0 - No freeze fraction printout 1 - Element freeze fraction printed for each time interval
	6-10	IPRINT	15	Print option for the element centroid temperatures 0 - No temperature printout 1 - Element centroid temperatures printed at each time interval
4	1-10	ETIME	F10.2	Total time of analysis (hr). Must be in increments of 10 min.
5	1-80	DX(I) I=1,N	8F10.5	Size of increments in 'X' Direction, N inputs (in)
6	1-80	DY (J) J=1,K	8F10.5	Size of increments in 'Y' Direction, K inputs (in)
7	1-10	COND	F10.5	Thermal conductivity of the PCM material, (Btu/hrft - °F)
8	1-5	METAL	15	Number of metal elements
9	If METAL = 0, Skip Card Set 9, METAL Sets of Input			
	1-5	N1	15	Metal element 'X' index
	6-10	K1	15	Metal element 'Y' index
	11-20	IKAY	F10.5	Metal element thermal conductivity (Btu/hrft °F)
	21-30	CSUBP	F10.5	Metal element specific heat (Btu/lbm°F)
	31-40	DENS	F10.5	Metal element density (lbm/ft ³)
10	1-10	RC	F10.5	Contact resistance between freeze layer and tube (°F/Btu/hr ft ²)

This code is available as FREEZELG, CY=1, ID=FRETZ

```

1 PROGRAM FREEZE(INPUT,OUTPUT,TAPES=INPUT,TAPE6=OUTPUT)
COMMON/PROP/TK(80,80),CP(80,80),RHO(80,80),IFLAG(80,80),FUSION
COMMON/DIM /DX(80),DY(80),N,NT,K,KT
COMMON/HEAT/T(80,80),Z(80,80),QTOTAL(80,80),TMELT,TSAT,RC,DTHETA,
5 DTHETA,T1(80,80)
COMMON/GROSS/FROZE,QDOT,IPRINZ,IPRINT
COMMON/TIME1/ETIME,TITLE(20)
DATA RHO/6400*130./
DATA CP/6400*0.45/
10 DATA IFLAG/6400*1/
DATA FUSION,TSAT,TMELT/118.0,450.0,500.0/
DATA T1/6400*500.0/
DATA T/6400*500.0/
DATA Z/6400*0.0/
15 DATA QTOTAL/6400*0.0/
10 READ(5,100) (TITLE(K),N1,20)
IF(ENF(5),NE,0) STOP
CALL INPUT
C... ALL PROPERTIES ARE INITIALLY SET EQUAL TO THOSE
20 C... OF THE PCM EXCEPT THE CONDUCTIVITY.
C... A 0.5 SEC TIME STEP IS USED.
DTHETA = 0.5
THETA = 0.0
ETIME = ETIME*60./10.
25 NTIME = IFLX(ETIME)
C... CHECK FOR STABILITY
CALL STABLE
CALL FRAC
CALL QDOT
30 CALL OUTPUT
DO 30 N2 = 1,NTIME
DO 20 N1 = 1,1200
THETA = THETA + DTHETA/60.
C... CALCULATE TEMPERATURES AND LOCAL FREEZE FRACTIONS
35 CALL TEMP
20 CONTINUE
C... SUMMARY AFTER TEN MINUTES
C... TOTAL PCM FREEZE FRACTION CALCULATED ALONG
C... WITH PURE HEAT RATE
40 CALL FRAC
CALL QDOT
CALL OUTPUT
30 CONTINUE
GOTO 10
45 100 FORMAT(20A4)
END

```

SYMBOLIC REFERENCE MAP (R=3)

ENTRY POINTS	DEF LINE	REFERENCES
47 - FREEZE	1	

```

1 SUBROUTINE INPUT
COMMON/DIM /DX(80),DY(80),N,NT,K,KT
COMMON/PROP/TK(80,80),CP(80,80),RHO(80,80),IFLAG(80,80),FUSION
COMMON/HEAT/T(80,80),Z(80,80),QTOTAL(80,80),TMELT,TSAT,RC,DTHETA,
5 DTNETA,TI(80,80)
COMMON/CROSS/FROZE,QUIT,IPRINZ,IPRINT
COMMON/TIME1/ETIME,TITLE(20)
WRITE(6,400) (TITLE(K),K=1,20)
READ(5,100) N,NT,K,KT
10 WRITE(6,500) N,NT,K,KT
READ(5,100) IPRINZ,IPRINT
WRITE(6,1100) IPRINZ,IPRINT
READ(5,200) ETIME
WRITE(6,1300) ETIME
15 READ(5,200) (DX(I),I=1,N)
WRITE(6,600) (DX(I),I=1,N)
DO 10 I=1,N
10 DX(I) = DX(I)/12.0
READ(5,200) (DY(J),J=1,K)
20 WRITE(6,700) (DY(J),J=1,K)
DO 20 J=1,K
20 DY(J) = DY(J)/12.0
READ(5,700) GOND
WRITE(6,1200) GOND
25 DO 40 J=1,80
DO 30 I=1,80
TK(I,J) = GOND
30 CONTINUE
40 CONTINUE
30 READ(5,100) METAL
WRITE(6,800) METAL
IF(METAL.EQ.0) GOTO 60
WRITE(6,850)
WRITE(6,900)
35 DO 50 I=1,METAL
READ(5,300) NI,K1,TKAY,CSURP,DENS
WRITE(6,300) NI,K1,TKAY,CSURP,DENS
TK(NI,K1) = TKAY
40 CP(NI,K1) = CSURP
RHO(NI,K1) = DENS
IFLAG(NI,K1) = 0
50 CONTINUE
60 READ(5,200) RC
WRITE(6,1000) RC
45 100 FORMAT(5I5)
200 FORMAT(8F10.5)
300 FORMAT(2I5,3F10.5)
400 FORMAT(1H1,20A4//)
500 FORMAT(20H N NT K KT, /415/)
50 600 FORMAT(12H DX(I),I=1,N,/(8F10.5))
700 FORMAT(12H DY(J),J=1,K,/(8F10.5))
800 FORMAT(28H NUMBER OF METAL ELEMENTS = ,I3/)
850 FORMAT(35H PROPERTIES OF METAL ELEMENTS,NI,K1)
900 FORMAT(40H NI K1 TKAY CSURP DENSITY /)
55 1000 FORMAT(21H CONTACT RESISTANCE = ,F10.5/)
1100 FORMAT(20H IPRINZ IPRINT, /2110/)
1200 FORMAT(50H PHASE CHANGE MATERIAL (PCM) THERMAL CONDUCTIVITY, /,61H

```

ALL OTHER PROPERTIES ARE THOSE OF THE REFERENCE PCM MATERIAL, /F10,
15)

60 ~~1300-FORMAT(25H-END-OF-TIME-PERIOD,HR =, /F10,2/)~~

RETURN
END

SYMBOLIC REFERENCE MAP (P=3)

ENTRY POINTS	DEF LINE	REFERENCES									
1 INPUT	1	61									
VARIABLES	SN	TYPE	RELOCATION	REFS		REFS	REFS	REFS	REFS	REFS	REFS
422 COND		REAL		REFS	24	27	DEFINED	23			
14000 CP		REAL	ARRAY PROP	REFS	3	DEFINED	39				
427 CSUBP		REAL		REFS	37	39	DEFINED	36			
430 DENS		REAL		REFS	37	40	DEFINED	36			
45403 THETA		REAL	HEAT	REFS	4						
0 DX		REAL	ARRAY DIM	REFS	2	16	18	DEFINED	15	18	
120 DY		REAL	ARRAY DIM	REFS	2	20	22	DEFINED	19	22	
0 ETIME		REAL	TIME	REFS	7	14	DEFINED	13			
0 FROZE		REAL	GROSS	REFS	6						
62000 FUSTON		REAL	PROP	REFS	5						
420 I		INTEGER		REFS	15	16	2*18	27	DEFINED	15	16
					17	26	35				
45400 IFLAG		INTEGER	ARRAY PROP	REFS	3	DEFINED	41				
3 IPRINT		INTEGER	GROSS	REFS	6	12	DEFINED	11			
2 IPRINZ		INTEGER	GROSS	REFS	6	12	DEFINED	11			
421 J		INTEGER		REFS	19	20	2*22	27	DEFINED	19	20
					21	25					
242 K		INTEGER	DIM	REFS	2	8	10	19	20	21	
					8	9	DEFINED				
243 KT		INTEGER	DIM	REFS	2	10	DEFINED	9			
425 KI		INTEGER		REFS	37	38	39	40	41		
					36						
423 METAL		INTEGER		REFS	31	32	35	DEFINED	30		
240 N		INTEGER	DIM	REFS	2	10	15	16	17		
					9						
241 NT		INTEGER	DIM	REFS	2	10	DEFINED	9			
424 NI		INTEGER		REFS	37	38	39	40	41		
					36						
1 QOUT		REAL	GROSS	REFS	6						
31000 QTOTAL		REAL	ARRAY HEAT	REFS	4						
45402 RC		REAL	HEAT	REFS	4	44	DEFINED	43			
31000 RHO		REAL	ARRAY PROP	REFS	3	DEFINED	40				
0 T		REAL	ARRAY HEAT	REFS	4						
45404 THETA		REAL	HEAT	REFS	4						
1 TITL		REAL	ARRAY TIME	REFS	7	8					
0 TK		REAL	ARRAY PROP	REFS	3	DEFINED	27	38			
426 TKAY		REAL		REFS	37	38	DEFINED	36			
45400 TMELT		REAL	HEAT	REFS	4						
45401 TSAT		REAL	HEAT	REFS	4						
45405 TI		REAL	ARRAY HEAT	REFS	4						
14000 Z		REAL	ARRAY HEAT	REFS	4						

```

1 SUBROUTINE STABLE
COMMON/DIM Z(OX(A0),OY(A0),N,NT,K,KT)
COMMON/PROP/TK(A0,A0),CP(A0,A0),RHO(A0,A0),IFLAG(A0,A0),FUSION
5 COMMON/HEAT/T(A0,A0),Z(A0,A0),QTOTAL(A0,A0),TMELT,ISAT,RC,DTHETA,
1 THETA,TI(A0,A0)
COMMON/GROSS/FROZE,NOOT,IPRINZ,IPRINT
C... THIS SUBROUTINE CHECKS FOR NUMERICAL STABILITY
FNPI(I,J) = DX(I+1)/DX(I)*TK(I,J)/TK(I+1,J) + 1.0
FNMI(I,J) = -DX(I-1)/DX(I)*TK(I,J)/TK(I-1,J) + 1.0
10 FKPI(I,J) = DY(J+1)/DY(J)*TK(I,J)/TK(I,J+1) + 1.0
FKMI(I,J) = -DY(J-1)/DY(J)*TK(I,J)/TK(I,J-1) + 1.0
FOX(I,J) = TK(I,J)*DTHETA/(RHO(I,J)*CP(I,J)*DX(I)**2*3600.)
FOY(I,J) = TK(I,J)*DTHETA/(RHO(I,J)*CP(I,J)*DY(J)**2*3600.)
15 FCX(I,J) = RC/OX(I)*TK(I,J)*2. + 1.
FCY(I,J) = RC/OY(J)*TK(I,J)*2. + 1.
NTI = NT+1
KTI = KT+1
FX = 0.0
FY = 0.0
20 DO 200 J=1,K
DO 100 I=1,N
10 CONTINUE
IF(J.GE.KTI) GOTO 10
IF(I.LE.NT) GOTO 100
25 IF(I.NE.1.AND.I.NE.NT1.AND.I.NE.N) GOTO 15
IF(I.EQ.1) FX = FOX(I,J)/FNPI(I,J)
IF(I.EQ.NT1) FX = FOX(I,J)*(1./FNPI(I,J)+1./FCX(I,J))
IF(I.EQ.N) FX = FOX(I,J)/FNMI(I,J)
GOTO 16
30 15 FX = FOX(I,J)*(1./FNPI(I,J)+1./FNMI(I,J))
16 IF(J.NE.1.AND.J.NE.KTI.AND.J.NE.K) GOTO 20
IF(J.EQ.1) FY = FOY(I,J)/FKPI(I,J)
IF(J.EQ.KTI) FY = FOY(I,J)*(1./FKPI(I,J)+1./FCY(I,J))
IF(J.EQ.K) FY = FOY(I,J)/FKMI(I,J)
35 GOTO 30
20 FY = FOY(I,J)*(1./FKPI(I,J)+1./FKMI(I,J))
30 CHECK = FX + FY
IF(CHECK.GT.0.5) GOTO 300
40 100 CONTINUE
200 CONTINUE
GOTO 500
300 WRITE(6,400) I,J
400 FORMAT(37H STABILITY CRITERIA VIOLATED AT I,J =,2I5)
STOP
45 500 CONTINUE
RETURN
END

```

SYMBOLIC REFERENCE MAP (R=3)

ENTRY POINTS	DEF. LINE	REFERENCER
1 STABLE	1	46


```

1 SUBROUTINE TEMP
COMMON/DIM /DX(80),DY(80),N,NT,K,K1
COMMON/PROP/TK(80,80),CP(80,80),RHO(80,80),IFLAG(80,80),FUSION
COMMON/HEAT/T(80,80),Z(80,80),QTOTAL(80,80),TMELT,TSAT,RC,DTHETA,
5 DTHETA,T1(80,80)
COMMON/GROSS/FROZE,QUOT,IPRINZ,IPRINT
C... THIS SUBROUTINE CALCULATES THE TEMPERATURE AND FREEZE
C... FRACTION DISTRIBUTION AT EACH POINT IN TIME
KT1 = KT + 1
10 DO 200 J=1,K
DO 100 I=1,N
IF(J.GE.KT1) GOTO 10
IF(I.LE.NT) GOTO 100
15 QNET = QHF(I,J)
IF(IFLAG(I,J).NE.1) Z(I,J) = 1.0
IF(Z(I,J).GE.1.0) GOTO 20
QTOTAL(I,J) = QTOTAL(I,J) + QNET
ABQ = ABS(QTOTAL(I,J))
HLATE = DX(I)*DY(J)*RHO(I,J)*FUSION
Z(I,J) = ABQ/HLATE
C... ELEMENTS WHICH ARE NOT COMPLETELY FROZEN ARE ASSUMED
C... TO BE AT THE MELTING TEMPERATURE
T(I,J) = TMELT
25 IF(Z(I,J).GE.1.0) Z(I,J) = 1.0
GOTO 100
20 T(I,J) = T1(I,J) + QNET/(CP(I,J)*RHO(I,J)*DX(I)*DY(J))
100 CONTINUE
200 CONTINUE
30 DO 400 J = 1,K
DO 300 I = 1,N
IF(J.GE.KT1) GOTO 250
IF(I.LE.NT) GOTO 300
250 CONTINUE
35 T1(I,J) = T(I,J)
300 CONTINUE
400 CONTINUE
RETURN
END
    
```

SYMBOLIC REFERENCE MAP (R=1)

ENTRY POINTS	DEF LINE	REFERENCES
1 TEMP	1	38

VARIABLES	SN	TYPE	RELLOCATION	REFS	21	DEFINED	19
115 ABQ		REAL		REFS	3	27	
14400 CP		REAL	ARRAY PROP	REFS	4		
45803 DTHETA		REAL		REFS	2	20	27
0 DX		REAL	ARRAY DIM	REFS	2	20	27
120 DY		REAL	ARRAY DIM	REFS	6		
0 FROZE		REAL	GROSS	REFS	3	20	
62000 FUSION		REAL	PROP	REFS			

```

1 FUNCTION-QUE (I,J)
COMMON/DIM /DX(80),DY(80),N,NT,K,KT
COMMON/PROP/TK(80,80),CP(40,80),RHI(80,80),IFLAG(80,80),FUSION
COMMON/HEAT/T(80,80),Z(80,80),Q(TOTAL(80,80),TMELT,TSAT,RC,DTHETA,
5 ITHETA,TI(80,80)
COMMON/GROSS/FROZE,GOOT,IPRINZ,IPRUI
RNPI(I,J) = -2.*DY(J)*(TI(I+1,J) - TI(I,J))/(DX(I+1)/TK(I+1,J) + DX
1(I)/TK(I,J))
RNM1(I,J) = -2.*DY(J)*(TI(I-1,J) - TI(I,J))/(DX(I-1)/TK(I-1,J) + DX
10 1(I)/TK(I,J))
RKPI(I,J) = -2.*DX(I)*(TI(I,J+1) - TI(I,J))/(DY(J+1)/TK(I,J+1) + DY
1(J)/TK(I,J))
RKMI(I,J) = -2.*DX(I)*(TI(I,J-1) - TI(I,J))/(DY(J-1)/TK(I,J-1) + DY
15 1(J)/TK(I,J))
RFX(I,J) = DY(J)*(TSAT - TI(I,J))/RC + DX(I)/TK(I,J)/2.)
RFCY(I,J) = DX(I)*(TSAT - TI(I,J))/RC + DY(J)/TK(I,J)/2.)
NT1 = NT + 1
KT1 = KT + 1
C... THIS SUBROUTINE CALCULATES THE NET HEAT CONDUCTED
20 C... INTO EACH ELEMENT
QCNDX = 0.0
QCNDY = 0.0
IF(I.NE.1.AND.I.NE.NT1.AND.I.NE.N) GOTO 5
IF(I.EQ.1) QCNDX = RNPI(I,J)
25 IF(I.EQ.NT1.AND.J.GE.KT1) GOTO 5
IF(I.EQ.NT1) QCNDX = RNPI(I,J) + RFX(I,J)
IF(I.EQ.N) QCNDX = RNM1(I,J)
GOTO 6
5 QCNDX = RNPI(I,J) + RNM1(I,J)
30 6 IF(J.NE.1.AND.J.NE.KT1.AND.J.NE.K) GOTO 10
IF(J.EQ.1) QCNDY = RKPI(I,J)
IF(J.EQ.KT1.AND.I.GE.NT1) GOTO 10
IF(J.EQ.KT1) QCNDY = RKPI(I,J) + RFCY(I,J)
IF(J.EQ.K) QCNDY = RKMI(I,J)
35 GOTO 20
10 QCNDY = RKPI(I,J) + RKMI(I,J)
20 QCND = QCNDX + QCNDY
QUE = QCND*DTHETA/3600.
RETURN
40 END
    
```

SYMBOLIC REFERENCE MAP (R=3)

ENTRY POINTS	DEF LINE	REFERENCES
4 QUE	1	30

VARIABLES	SN	TYPE	DECLARATION	RELOCATION	REFS						
14400 CP		REAL	ARRAY	PROP	REFS	3					
45403 DTHETA		REAL		HEAT	REFS	4	38				
0 DX		REAL	ARRAY	DIM	REFS	2	2*24	3*26	2*27	4*29	31 2*33
						34	2*36				
120 DY		REAL	ARRAY	DIM	REFS	2	24	2*26	27	2*29	2*31 3*33
						2*34	4*36				

```

1 SUBROUTINE FRAC
COMMON/DIM /DX(80),DY(80),N,NT,K,KT
COMMON/PROP/TK(80,80),CP(80,80),RHO(80,80),IFLAG(80,80),FUSION
COMMON/HEAT/T(80,80),Z(80,80),QTOTAL(80,80),TMELT,TSAT,RC,DTHETA,
5 DTHETA,TI(80,80)
COMMON/GROSS/FROZE,QUIT,IPRINZ,IPRINT
C... THIS ROUTINE CALCULATES THE TOTAL
C... PCM FREEZE FRACTION
10 SUMZ = 0.0
SUMA = 0.0
KT1 = KT + 1
DO 200 J=1,K
DO 100 I=1,N
15 IF(J,GF,KT1) GOTO 10
IF(I,LE,NT) GOTO 100
10 CONTINUE
XFLAG = FLUAT(IFLAG(I,J))
SUMZ = SUMZ + DX(I)*DY(J)*XFLAG*Z(I,J)
SUMA = SUMA + DX(I)*DY(J)*XFLAG
20 100 CONTINUE
200 CONTINUE
FROZE = SUMZ/SUMA
RETURN
END
    
```

SYMBOLIC REFERENCE MAP (K=3)

ENTRY POINTS	DEF LINE	REFERENCES
1 FRAC	1	23

VARIABLES	SN	TYPE	RELOCATION	REFS					
14400 CP		REAL	ARRAY	PROP	REFS	3			
45403 DTHETA		REAL		HEAT	REFS	4			
0 DX		REAL	ARRAY	DIM	REFS	2	18	19	
120 DY		REAL	ARRAY	DIM	REFS	2	18	19	
0 FROZE		REAL		GROSS	REFS	6	DEFINED	22	
62000 FUSION		PFAL		PROP	REFS	3			
46 I		INTEGER			REFS	15	17	2*18	19
45400 IFLAG		INTEGER	ARRAY	PROP	REFS	3	17		DEFINED
3 IPRINT		INTEGER		GROSS	REFS	6			
2 IPRINZ		INTEGER		GROSS	REFS	6			
45 J		INTEGER			REFS	14	17	2*18	19
242 K		INTEGER		DIM	REFS	2	12		DEFINED
243 KT		INTEGER		DIM	REFS	2	11		
44 KT1		INTEGER			REFS	14	DEFINED	11	
240 N		INTEGER		DIM	REFS	2	13		
241 NT		INTEGER		DIM	REFS	2	15		
1 QUIT		REAL		GROSS	REFS	6			
31000 QTOTAL		REAL	ARRAY	HEAT	REFS	4			
45402 RC		REAL		HEAT	REFS	4			
31000 RHO		REAL	ARRAY	PROP	REFS	3			
43 SUMA		REAL			REFS	19	22	DEFINED	10
42 SUMZ		REAL			REFS	18	22	DEFINED	9

```

1 SUBROUTINE QDDT
COMMON/DIM /DX(80),DY(80),N,NT,K,KT
COMMON/PROP/TK(80,80),CP(80,80),RHO(80,80),IFLAG(80,80),FUSION
5 COMMON/HEAT/T(80,80),Z(80,80),QTOTAL(80,80),TMELT,TSAT,RC,DTHETA,
1 THETA,T1(80,80)
COMMON/GROSS/FROZE,QDDT,IPRIN7,IPRINT
C... THIS ROUTINE CALCULATES THE TUBE
C... HEAT RATE - PER FOOT OF TUBE
QDDT = 0.0
10 NT1 = NT + 1
KT1 = KT + 1
DO 50 I=1,NT
QDDT = QDDT + DX(I)*(T(I,KT1) - TSAT)/(DY(KT1)/2./TK(I,KT1) + RC)
50 CONTINUE
15 DO 60 J=1,KT
QDDT = QDDT + DY(J)*(T(NT1,J) - TSAT)/(DX(NT1)/2./TK(NT1,J) + RC)
60 CONTINUE
QDDT = QDDT/3412.*4.
C... MULTIPLY BY 4 TO OBTAIN HEAT RATE OF WHOLE TUBE
20 RETURN
END
    
```

SYMBOLIC REFERENCE MAP (R=3)

ENTRY POINTS	DEF LINE	REFERENCES				
1 QDDT	1	20				
VARIABLES	SN	TYPE	RELICATION	REFS		
14400 GP	REAL	ARRAY	PROP	REFS	3	
45403 DTHETA	REAL		HEAT	REFS	4	
0 DX	REAL	ARRAY	DIM	REFS	2	13 16
120 DY	REAL	ARRAY	DIM	REFS	2	13 16
0 FROZE	REAL		GROSS	REFS	6	
62000 FUSION	REAL		PROP	REFS	3	
57 I	INTEGER			REFS	3*13	DEFINED 12
45400 IFLAG	INTEGER	ARRAY	PROP	REFS	3	
3 IPRINT	INTEGER		GROSS	REFS	6	
2 IPRIN7	INTEGER		GROSS	REFS	6	
60 J	INTEGER			REFS	3*16	DEFINED 15
242 K	INTEGER		DIM	REFS	2	
243 KT	INTEGER		DIM	REFS	2	11 15
56 KT1	INTEGER			REFS	3*13	DEFINED 11
240 N	INTEGER		DIM	REFS	2	
241 NT	INTEGER		DIM	REFS	2	10 12
55 NT1	INTEGER			REFS	3*16	DEFINED 10
1 QDDT	REAL		GROSS	REFS	6	13 16 18 DEFINED 9 13
31000 QTOTAL	REAL	ARRAY	HEAT	REFS	4	
45402 RC	REAL		HEAT	REFS	4	13 16
31000 RHO	REAL	ARRAY	PROP	REFS	3	
0 T	REAL	ARRAY	HEAT	REFS	4	13 16
45404 THETA	REAL		HEAT	REFS	4	
0 TK	REAL	ARRAY	PROP	REFS	3	13 16

231

```

1      SUBROUTINE OUTPUT
      COMMON/DIM /DX(80),DY(80),N,NT,K,KT
      COMMON/PROP/TH(80,80),CP(80,80),PHI(80,80),IFLAG(80,80),FUSION
5      COMMON/HEAT/T(80,80),Z(80,80),QTOTAL(80,80),TMELT,TSAT,RC,DTHETA,
      THETA,TI(80,80)
      COMMON/GROSS/FROZE,QUOT,IPRINZ,IPRINT
      WRITE(6,100) THETA
      KT1 = KT + 1
      NT1 = NT + 1
10     IF(IPRINZ.EQ.0) GOTO 30
      WRITE(6,200)
      DO 20 J=1,K
      IF(J.LE.KT1) GOTO 10
      WRITE(6,300) (Z(I,J),I=1,N)
15     GOTO 20
      10 WRITE(6,300) (T(I,J),I=NT1,N)
      20 CONTINUE
      30 IF(IPRINT.EQ.0) GOTO 60
      WRITE(6,400)
      DO 50 J=1,K
      IF(J.LE.KT1) GOTO 40
      WRITE(6,700) (T(I,J),I=1,N)
      GOTO 50
      40 WRITE(6,700) (T(I,J),I=NT1,N)
25     50 CONTINUE
      60 WRITE(6,500) FROZE.
      WRITE(6,600) QUOT
100    FORMAT(/11H TIME,MIN.=,F10.2/)
200    FORMAT(36H-FREEZE FRACTIONS,7(I,J),I=1,N,J=1,K/)
30     FORMAT(10F10.4)
400    FORMAT(/47H-CENTROID TEMPERATURES,T(I,J),I=1,N,J=1,K,DEG-F/)
500    FORMAT(/25H-FRACTION OF PCM FROZEN =,F10.4)
600    FORMAT(/40H-TURE HEAT RATE (PER FT. OF TURE),KW/FT.=,F10.4)
700    FORMAT(10F10.2)
35     RETURN
      END

```

SYMBOLIC REFERENCE MAP (R=3)

ENTRY POINTS	DEF LINE	REFERENCES
1 OUTPUT	1	35

VARIABLES	SN	TYPE	RELOCATION	REFS						
14400 CP		REAL	ARRAY	PROP	REFS	3				
45403 DTHETA		REAL		HEAT	REFS	4				
0 DX		REAL	ARRAY	DIM	REFS	2				
120 DY		REAL	ARRAY	DIM	REFS	2				
0 FROZE		REAL		GROSS	REFS	6	26			
62000 FUSION		REAL		PROP	REFS	3				
206 I		INTEGER			REFS	14	16	22	24	DEFINED 14 16
						22	24			
45400 IFLAG		INTEGER	ARRAY	PROP	REFS	3				
3 IPRINT		INTEGER		GROSS	REFS	6	14			

APPENDIX VII

PRELIMINARY SIZING OF THE CHUBB BOILER TANK

The preliminary sizing of the Chubb Boiler Tank Concept has been based largely on Reference (5) in order to incorporate the results and recommendations from the on-going development program. The layout of this TES subsystem is shown on Sketch 2 in Appendix I. The charging heat exchanger is submerged in a liquid pool of the intermediate heat transfer fluid located at the bottom of the containment tank. The condensing steam within the tubes vaporizes this working fluid, which rises and then condenses on cans containing the PCM, thus charging the system. During discharge, the working fluid in the liquid phase is sprayed onto the PCM cans. The energy claimed from storage vaporizes the working fluid, which rises to the top of the containment tank where the discharge heat exchanger is located. The vapor condenses in the tubes, producing saturated steam within the tubes.

Heat Transfer Fluid

To provide reasonable temperature differences between steam and the heat transfer fluid in the charging and discharging heat exchangers and between heat transfer fluid and the PCM, the vaporization pressures of the heat transfer fluid must be appropriately set. The selected temperature for vaporizing the heat transfer fluid during charging is approximately halfway between the charging steam temperature and the PCM melting temperature: 274°C (525°F). For the condensation of the fluid on the discharge exchanger tube surface, a similar decision was made: 246°C (475°F).

The selection of heat transfer fluid was based on the operating temperature requirement. The biphenyl was selected because of near-atmosphere operational pressure for the operating temperature range of $246\text{-}274^{\circ}\text{C}$ ($475\text{-}525^{\circ}\text{F}$). The boiling point variation of pure biphenyl from Reference (43) is as follows:

<u>Boiling Point</u>		<u>Pressure</u>	
<u>°C</u>	<u>°F</u>	<u>kPa</u>	<u>psia</u>
246	475	82.8	12.0
256	492	101	14.7
274	525	150	21.7

Consequently, the tank operates between a slight vacuum pressure level to a slightly pressurized level.

As noted in the main text, water vapor has a very strong effect on the biphenyl vaporization curves. Consequently, a small amount of water vapor present, perhaps due to tube leaks, could require an operating pressure level as high as 1.03 MPa (150 psia).

The required quantity of biphenyl was scaled from Reference (5) on the basis of heat transfer rates. The design employs 1750 kg (3850 lb) of biphenyl for a peak heat transfer rate of 150 kW. Scaling to 30 MW would require 3.5×10^5 kg (7.7×10^5 lb), or 112,000 gal. To compensate for scaling effects and to provide an optimistic cost estimate, a 50,000 gal inventory of biphenyl was established.

Phase Change Material

The PCM is encapsulated in cans which are not vented to the open atmosphere. Consequently, the sodium metaborate eutectic must be used. The cans may or may not be vented to the local biphenyl environment. Reference (5) has discussed a concept in which all the encapsulating cans are interconnected and vented to the atmosphere. However, that approach is unattractive due to the very large number of cans required.

A mass of 1.94×10^6 kg (4.28×10^6 lb) of PCM is required to store the 148 MWh of thermal energy, assuming 100% utilization and taking no credit for any solid or liquid phase sensible heat. This requires 1080 m^3 ($38,200 \text{ ft}^3$) to contain the PCM in the liquid phase.

The PCM containers used in this sizing study are standard cans recommended by Reference (5): 10.2 cm (4") in diameter, 46.2 cm (18.2") high, and 0.18-0.30 mm (7-12 mils) thick. Each can encloses 3.75 liters (0.132 ft³) thus 289,550 cans are required for the PCM inventory.

The operating experience with this system has shown that there is a tendency for the heat transfer fluid to condense inside the can if it is vented. This may require that the can be sealed from the biphenyl environment. There are no data on the behavior of the metaborate under these circumstances. However, no problems are anticipated since the metaborate is chemically extremely stable. Operation with sealed cans in a pressurized environment at 1.03 MPa (150 psia) would require a can thickness of 1.52-1.65 mm (60-65 mils). This is based on the ASME B&PV Code, Section VIII sizing procedure for external pressure and allowable stress characteristics of carbon steels. An alternate approach would be to pressurize the can to approximately 1.03 MPa (150 psia) so that there is very little operating pressure differential across the can. For this case the ASME code requires a 0.51 mm (20 mil) wall thickness for the can.

Containment Tank

The preliminary sizing of containment tanks of other concepts has been based on modular rectangular tank of 13' x 13' x 40" dimensions. However, for the pressurized or vacuum containment required of the boiler tank, a large cylindrical tank was selected.

Setting the cans on an equilateral triangular spacing, the most compact arrangement is achieved. The number of cans that are stacked vertically dictates the number of cans to be arranged in the cross section, which in turn dictates the inner diameter of the tank. Tank geometry as a function of the number of cans stacked is shown on Table VII-1.

The tank height also includes the height of the charging and discharging heat exchangers. The design of these components, described below, requires additional height, which also depends on the vessel diameter. Table VII-1 shows a broad summary of diameter vs. total height which includes the stacked cans and the charging and discharging heat exchangers.

TABLE VII-1

PRELIMINARY TANK SIZING

<u>Number of Cans Stacked</u>	<u>Number of Cans In One Row</u>	<u>Height of Stacked Cans (Ft)</u>	<u>Tank Diameter (Ft)</u>
6	48258	9.1	77
7	41364	10.62	71.5
8	36194	12.13	66.94
9	32172	13.65	63.13
10	28955	15.17	59.90
11	26323	16.68	57.13
12	24129	18.2	54.7
13	22273	19.7	52.6
14	20682	21.23	50.7
15	19303	22.75	48.9

The height of the tank depends on the height of charging and discharging heat exchangers below and above the stacked cans. A rough estimate of compact packing of these heat exchangers resulted in 3 possible overall tank sizes.

<u>Diameter (Ft)</u>	<u>Height (Ft)</u>
80	14
60	21
50	35

To reduce heat losses and the amount and the cost of insulation, the surface area of the tank should be minimum for the volume contained. This requires that height equals diameter, if losses at the bottom of the tank are considered; and that height equals the tank radius, if the bottom heat losses are neglected. Thus a height-to-diameter ratio in the range 0.5-1.0 is desirable to minimize heat losses and required insulation. A diameter of 15.2 m (50') and a height of 10.7 m (35') were selected for preliminary tank size.

To span the range of possible operating pressures the boiler tank thickness was sized for both vacuum and high pressure levels. Design pressures of 1.03 MPa (150 psia) internal and 34 kPa (5 psia) external were established. The tank configuration, consisting of a vertical cylinder with ellipsoidal heads, was sized to Section VIII of the ASME B&PV code. Paragraph UG-27 was used to size the thickness of the cylindrical part of the shell.

SA-515 material was assumed for an allowable stress of 1.03 MPa (15 ksi) and a joint efficiency of 1.0. Paragraph UG-28 was used to analyze the thickness of the cylindrical part of the shell under external pressure. Figure UG-28, Appendix V of the code was used to calculate the thickness of the cylindrical shell subjected to the external pressure. Paragraphs UG-32 and UG-33 were used to size the thickness of the ellipsoidal head. For vacuum operation the tank wall is 15.9 mm (0.625") and the ellipsoidal head is 22.2 mm (0.875"). Under pressure operation the thickness must be much larger: 82.6 mm (3.25") for both the cylindrical shell and the ellipsoidal head. The tank weights are 1.466×10^6 lb for the thick wall pressure vessel and 3.4×10^5 lb for the vacuum vessel.

Charging Heat Exchanger

During charging, heat transfer to the biphenyl is assumed to be saturated pool boiling. The entire 13.9°C (25°F) between the condensing steam and boiling biphenyl is assumed across the biphenyl. From Reference (44), heat fluxes on the order of 12.6 kW/m^2 ($4000 \text{ Btu/hr}\cdot\text{ft}^2$) are characteristic for biphenyl. These conditions indicate a film coefficient of $0.90 \text{ kW/m}^2\cdot^{\circ}\text{C}$ ($160 \text{ Btu/hr}\cdot\text{ft}^2\cdot^{\circ}\text{F}$) is appropriate.

It is possible to increase the nucleate pool boiling heat transfer coefficient by surface treatment. However, for the preliminary sizing, an overall heat transfer coefficient of $0.85 \text{ kW/m}^2\text{C}$ ($150 \text{ Btu/hr}\cdot\text{ft}^2\text{F}$) is used. For the 30 MW charging rate, a heat transfer area of 2540 m^2 ($27,300 \text{ ft}^2$) is required. Using a 6.35 mm (0.25") O.D. tube formed into a helical coil with a 30.5 m (100 ft) length for the basic tube bundle configuration, 4200 coil tubes are required. If seven tubes are headered together for a basic tube bank, 600 tube banks are required.

Discharge Heat Exchanger

For biphenyl condensation to cause the boiling of steam, an overall heat transfer coefficient of $1.70 \text{ kW/m}^2\text{C}$ ($300 \text{ Btu/hr}\cdot\text{ft}^2\text{F}$) is reasonable. For a 30 MW discharge rate across a 14°C (25°F) temperature difference, 1270 m^2 ($13,650 \text{ ft}^2$) of heat transfer area are required. Again using a tube 6.35 mm (0.25") O.D. and 0.635 mm (0.025") thick, formed into a helical coil 30.5 m (100 ft) long, 2085 coils are required.

Other Equipment

The other equipment required for this concept include:

- Biphenyl Purification System
- Glycol Start-up Loop
- Biphenyl Spray Pump for Discharge Cycle
- Hexagonal Cages to hold Cans
- Piping with Trace Heaters for Biphenyl Transport
- Load Bearing and Loose Insulation

These items were not examined for cost evaluation but an estimate was scaled from Reference (5).

APPENDIX VIII

PRELIMINARY SIZING OF MACROENCAPSULATION OF PCM CONCEPT

The preliminary sizing of this concept is similar to that of the Chubb boiler tank concept (Appendix VII). It was realized very early in the sizing that the major (overwhelming) cost components in this concept are the pressure vessels. Therefore, the major emphasis was placed on the quick estimate of the pressure vessel sizing and cost. The concept is shown on Sketch 2 of Appendix I.

Phase Change Material

The PCM is encapsulated in hermetically sealed cans, or long closed tubes. The requirements are the same in Appendix VII, thus 1.94×10^6 kg (4.28×10^6 lb) of the sodium metaborate must be encapsulated. This requires 1080 m^3 ($38,200 \text{ ft}^3$) to contain the PCM in the liquid phase.

PCM Cans

Instead of using short cans as in the Chubb boiler tank, long tubes closed at two ends were selected for simplicity. To encapsulate the PCM, 12,250 tubes 10.2 cm (4.0") in diameter and 11.6 m (38') high are required.

The encapsulating tubes are subjected to an external steam pressure of 1200 psi. The thickness of the tube depends on the net operating pressure. If sodium metaborate salt can be pressurized, the most economical solution would be to pressurize the tubes to a maximum operating pressure of 8.3 MPa (1200 psia).

The thickness of the tubes was calculated according to ASME B&PV Code, Section VIII procedure for internal and external pressure. The results indicate a required thickness of 8.1 mm (0.32"). If the cans are pressurized so the net external pressure is 5.5 MPa (800 psi), then a 6.4 mm (0.25") thickness would be required. Pressurizing to 8.3 MPa (1200 psi) reduces the thickness to 3.8 mm (0.15"). It should be noted that the cans are not a major cost component in this concept.

Containment Tank

The preliminary sizing of containment tanks of other concepts has been based on a modular rectangular tank, 13'x13'x40'. However, for the pressure vessel of this concept, a modular tank of 4.0-m (13 ft) diameter and 12-m (40 ft) length was selected. Due to a very high pressure, a large, field fabricated tank is not economical for this concept.

The thickness of the pressure vessel was calculated to satisfy the ASME B&PV Code, Section VIII. For a design pressure of 8.3 MPa (1200 psi), the minimum thickness of the tank is 18 cm (7 in).

The number of pressure vessels required was calculated from the total number of tubes to be enclosed. The containment cans are set in an equilateral-triangular arrangement to maximize the number of cans per pressure vessel. Within the 3.6-m (11.8-ft) inner tank diameter, 927 cans are enclosed. Thus, slightly over 14 pressure vessels are needed.

APPENDIX IX

DIRECT CONTACT SYSTEMS USING PCM DROP INTERMEDIATE HEAT EXCHANGER

PCM Drop Heat Exchanger

Two widely different intermediate fluids were considered: one, a liquid metal; the other, an oil. Both are shown on Table IX-1. As compared with oils, the liquid metals are characterized by high density, low specific heat, high thermal conductivity, high viscosity, and low Prandtl numbers. The density of the liquid metal is higher than that of the PCM, causing the PCM drops to rise while solidifying; the reverse is the case for oils. The consideration of two such fluids demonstrates the effects of an extreme range of properties of the intermediary fluid.

The subsystem configurations for the two concepts under consideration are shown in Sketch 3. The temperature relation between the elements is shown by Figure IX-1, which is a simplification neglecting any sensible heat absorbed or delivered by the PCM or by the charging or discharging steam. The fluid loop represents one pass of the liquid through the system. At maximum discharge rate, the intermediate fluid enters the heat exchanger at 462.5°F and leaves at 487.5°F, providing a temperature swing of 25°F and a log mean temperature difference of 22.8°F in both cases.

The maximum discharge rate of 30 MW (102×10^6 Btu/hr) and the specific heat of the fluid determine its maximum flow rate. At lower thermal discharge rates, the fluid flow would be maintained at the maximum rate, and the PCM flow rate modulated as required. This will maintain uniform heat transfer conditions in the heat exchanger, and avoid controls which would be needed to modulate the fluid flow. During reduced discharge, the temperature swing of the fluid will, of course, be lower.

The discharge heat exchanger is a conventional shell-and-tube type with the fluid on the shell side and the steam generated in the tubes.

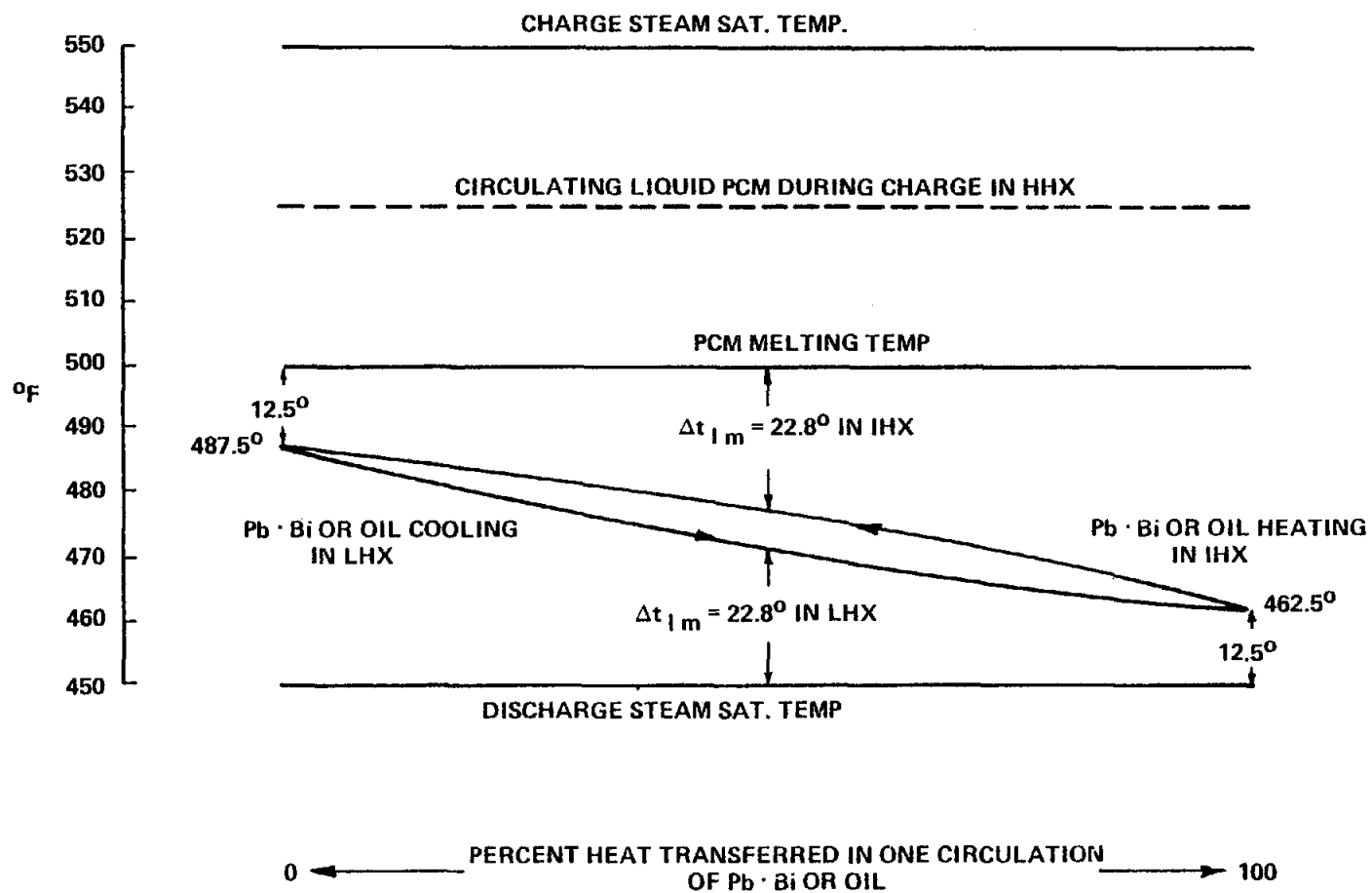
TABLE IX-1

PROPERTIES OF Pb·Bi EUTECTIC ALLOY AND BIPHENYL AT 500⁰F

(Ref.45 and Ref.46)

	Units	Pb·Bi Alloy		Biphenyl	
Density	kg/m ³ (lbm/ft ³)	10.4 x 10 ³	(650)	830	(51.8)
Specific heat	J/kg·°C (Btu/lbm·°F)	146	(.035)	2.51 x 10 ³	(0.60)
Thermal conductivity	W/(m·°C) (Btu/hr·ft·°F)	10.1	(5.81)	106 x 10 ⁻³	(0.061)
Viscosity	$\frac{N \cdot s}{m^2}$ (lbm/ft·hr)	2.00 x 10 ⁻³	(4.84)	203 x 10 ⁻⁶	(0.49)
Prandtl number		.029		4.82	

Figure IX-1
 DIRECT CONTACT WITH
 Pb · Bi OR OIL - PCM DROPLET INTERMEDIATE HX



The charging heat exchanger consists of banks of horizontal finned tubes with a few vertical tubes extending to the top to provide an expansion path to the top for the liquid PCM during melting. This component is identical to the one used in the mechanical scraper systems; the calculations are not reported here.

At the beginning of the charging period, most of the PCM will be in solid form. Any liquid will be in the interstices between the solid drops, and any excess will be at the top. It is expected that the solid PCM drops will adhere to each other forming a coherent mass and that, when melting occurs, a liquid-filled cavity will be formed around the heat exchanger, with heat being transferred from the tubes to the solid PCM surface by thermal convection of the liquid. This has been observed in the Thermbank Electric Water Heater (42), which uses a similar PCM but bare tube heaters.

In the intermediate heat exchanger, the fluid flows upward and the PCM drops rise (liquid metal) or fall (oil) relative to the fluid. The net upward velocity of the drop is the vector sum of the fluid and the drop velocities. The heat exchanger is so sized that the dwell time of the drop in the heat exchanger is sufficient to completely solidify the drop, transferring its latent heat and some sensible heat to the fluid. The sizing of the intermediate heat exchanger is based on the results presented in Reference (2).

The terminal velocity, v_t , of the drop relative to the fluid is given by

$$v_t = \left[\frac{4g}{3} \left| \frac{\rho_f - \rho_L}{\rho_f} \right| \times \frac{D}{C_d} \right]^{.5} \quad (1)$$

where D = drop diameter

ρ_f = fluid density

ρ_L = liquid PCM density

C_d = drag coefficient of the drop

g = acceleration due to gravity

C_d can be found from correlations vs. the drop Reynolds number (Re) (47). It has a fairly uniform value of 0.4 for Re in the range 10^3 to 10^5 , where the Re is calculated using the drop diameter, the drop velocity, the liquid PCM density and the fluid viscosity.

The time, t , required for the drop to solidify is given by (2):

$$t = \frac{a \rho_s C_{Pf}}{3B} \left\{ \frac{a}{k_s \varphi} \left[\frac{1}{2} \ln \frac{\left(\frac{\varphi^2 - \varphi + 1}{(\varphi + 1)^2} \right)}{\left(\frac{\varphi^2 - \alpha \varphi + \alpha^2}{(\varphi + \alpha)^2} \right)} + \sqrt{3} \left[\tan^{-1} \left(\frac{2 - \varphi}{\sqrt{3} \varphi} \right) - \tan^{-1} \left(\frac{2\alpha - \varphi}{\sqrt{3} \varphi} \right) \right] \right. \right. \\ \left. \left. + \left(\frac{1}{h} - \frac{a}{k_s} \right) \ln \frac{A+B}{(A+B\alpha^3)} \right\} \quad (2)$$

where

$$A = \frac{C_{Pf}(T_m - T_{fo})}{\lambda} + \left(\frac{\dot{m}_s}{\dot{m}_f} \right) \left(\frac{\rho_s}{\rho_L} \right)$$

$$B = - \left(\frac{\dot{m}_s}{\dot{m}_f} \right) \left(\frac{\rho_s}{\rho_L} \right)$$

$$\varphi = (-1) \left(\frac{A}{-B} \right)^{1/3}$$

$$\alpha = \left(1 - \frac{\rho_L}{\rho_s} \right)^{1/3}$$

and

- a = bubble outside radius
- C_{pf} = specific heat of carrier fluid
- h = outside film heat transfer coefficient
- k_s = thermal conductivity of solid salt
- \dot{m}_f = mass flow rate of carrier fluid
- \dot{m}_s = mass flow rate of salt
- T_m = salt melt temperature
- T_{fo} = carrier fluid outlet temperature (hot)
- ρ = salt density (s = solid, L = liquid)
- λ = salt latent heat of fusion

The average surface heat transfer coefficient, h, of the drop which is required in Equation 2 is obtained from (35):

$$h = \frac{k_f}{D} \left[.97 + K (Re)^{.5} \right] Pr^{.3} \quad (3)$$

- where k_f = thermal conductivity of fluid
- Pr = fluid Prandtl number, and
- K = .30 for liquid metal, and
.68 for oil

The time for the drop to solidify was obtained by first calculating v_t using $C_d = 0.4$. Re was then determined and if $Re < 10^3$, the correlation present on Reference (47) was used to estimate a new value of C_d . The calculations were repeated until a convergence was obtained. With the final Re value, the film coefficient and the time for solidification were calculated.

In order to size the PCM drop heat exchanger, a cylindrical shape with diameter = height was used. The residence time of the drop is given by the height and the absolute velocity of the drop. The latter is the combination of the fluid velocity and the drop velocity relative to the

fluid. The velocity of the fluid is obtained from the continuity equation, the total mass flow having already been determined by the discharge rate and selected fluid ΔT .

$$t = \frac{\ell}{v_t + V_f} = \frac{\text{Vol}}{A v_t + \left(\frac{m_f}{\rho_f}\right)} = \frac{\pi/4 \ell^3}{\pi/4 \ell^2 v_t + \left(\frac{m_f}{\rho_f}\right)} \quad (4)$$

where $V_d = \text{net velocity of drop} = v_t \pm V_f$

The velocity of the drop relative to the fluid is added when the drop rises in the fluid (liquid metal), and subtracted when it sinks (oil). For a given drop size, iteration with Equation (1) yields the drop velocity and Equation (2) yields the required drop time. Equation (3) is used to determine the cylindrical tank dimensions and consequently the volume.

By this method, the heat exchanger volume was determined in terms of drop size as the variable parameter. The results are given in Table IX-2 and IX-3, and Figures IX-2 and IX-3 for both the liquid metal and the oil.

For drops of equal size, the drop solidification time in oil is significantly longer than in liquid metal, reflecting the higher conductivity of the latter and the higher surface heat transfer coefficient of the drop in the metal. The terminal velocity of the drop is slightly higher in the oil than in the metal, the higher density difference in the metal being more than offset by its higher viscosity. The most significant difference as shown on Figure IX-2 is the relation between drop diameter and heat exchanger volume. This results from the fact that the net velocity of the drop is $(V_f + v_t)$ in the metal, but $(V_f - v_t)$ in the oil; as $v_t \rightarrow V_f$, the residence time in the heat exchanger $\rightarrow \infty$.

TABLE IX-2

Pb·Bi - PCM DROP HX SUMMARY

<u>Drop Dia.</u>	<u>Drop Velocity*</u>	<u>Drop Re</u>	<u>Drop Coefficient</u> $\left(\frac{\text{Btu}}{\text{hr} \cdot \text{ft}^2 \cdot \text{°F}} \right)$	<u>Time to Solidify</u>	<u>Fluid Velocity</u>	<u>Net Drop Velocity</u>	<u>HX Height</u>	<u>HX Vol.</u>
(in)	(ft/sec)			(sec)	(ft/sec)	(ft/sec)	(ft)	(ft ³)
.024	.345	333	6475	.331	8.1	8.44	2.84	17.99
.036	.462	823	6411	.667	4.98	5.44	3.62	37.3
.048	.597	1155	5606	1.15	3.28	3.88	4.46	69.7
.0625	.686	1728	5180	1.87	2.21	2.90	5.43	125.7
.100	.862	3472	4494	4.55	.95	1.82	8.27	444.
.125	.970	4890	4230	6.95	.57	1.54	10.7	962.
.250	1.37	13800	3490	26.5	---	---	---	---

* Relative to the fluid

TABLE IX-3

OIL - PCM DROP HX SUMMARY

<u>Drop Dia.</u>	<u>Drop Velocity re Fluid</u>	<u>Drop Re</u>	<u>Drop Coefficient</u> $\left(\frac{\text{Btu}}{\text{hr} \cdot \text{ft}^2 \cdot ^\circ\text{F}} \right)$	<u>Time to Solidify</u>	<u>Fluid Velocity</u>	<u>Net Drop Velocity</u>	<u>HX Height</u>	<u>HX Vol.</u>
(in)	(ft/sec)			(sec)	(ft/sec)	(ft/sec)	(ft)	(ft ³)
.024	.359	273	597	1.37	3.16	2.80	3.83	44.10
.036	.538	614	581	2.26	2.45	1.91	4.35	64.65
.048	.694	1057	564	3.31	2.10	1.41	4.70	81.5
.0625	.792	1567	524	4.89	1.82	1.03	5.05	93.
.100	1.003	3182	461	10.03	1.53	.53	5.50	131.
.125	1.12	4444	434	14.21	1.50	.38	5.55	134.
.250	1.585	12568	362	47.6	1.69	.11	5.235	113.

Figure IX-2
TIME TO SOLIDIFY PCM DROP vs PCM DROP DIAMETER

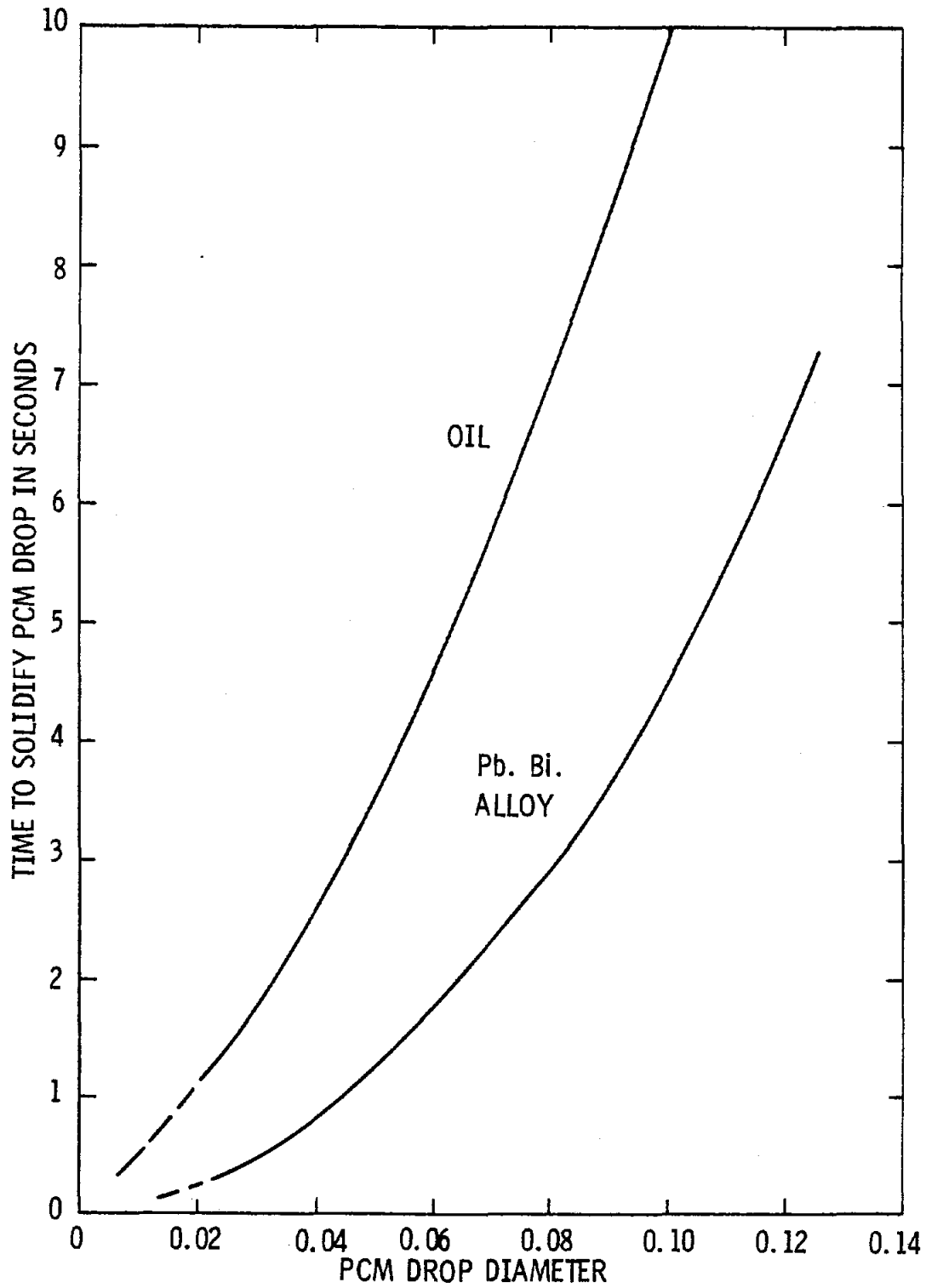
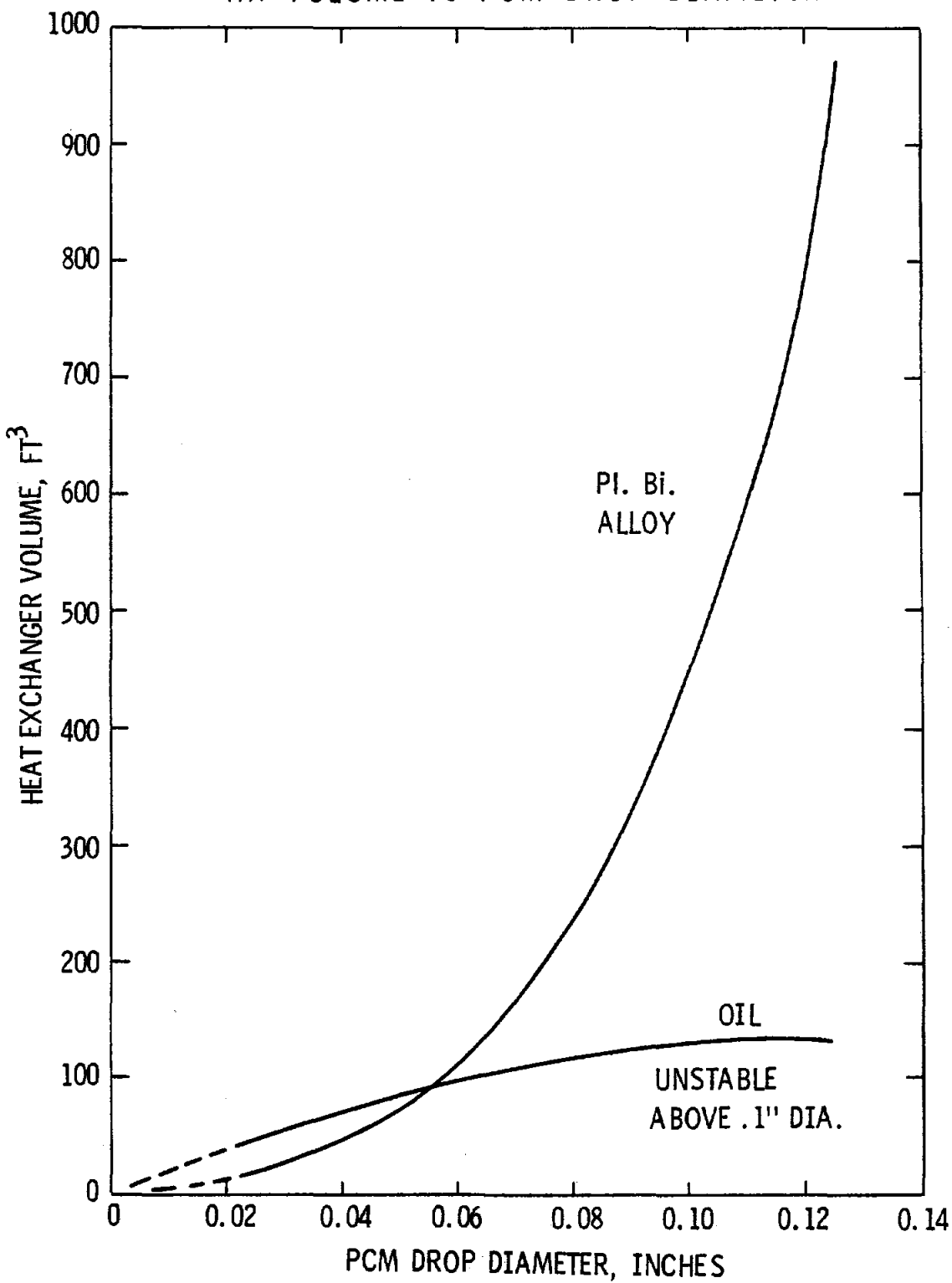


Figure IX-3
HX VOLUME vs PCM DROP DIAMETER



The separation of the solid PCM from the fluid becomes easier and less costly as the drop size increases. Therefore, a drop size of 1/16" was selected for both fluids for use in the concept analysis.

PCM Drop Separators for Direct Contact Systems

A separator is required to remove the solidified drops of PCM from the fluid. When the fluid is oil, the drops are carried out of the intermediate heat exchanger with the oil. In this case, a continuous centrifugal separator could be used. If the system were to be modularized, using eight modules, the flow rate of the PCM through each of 8 separators is 109×10^3 lb/hr. The oil flow rate is approximately 2000 gal/min.

Using the methods given in Reference (47), it was estimated that 24" diameter bowls, rotating at 3000 rpm could be used, and that bowl lengths totalling 25 feet would be required for each module. Carbon steel is a suitable material. The cost for separation equipment for the oil system was estimated to be \$250,000. The cost is assumed to be representative of the equipment whether the system uses a single component or 8 modules.

In the case of liquid metal, the PCM drops rise in the fluid. This lends itself to a simpler separation method, but one for which off-the-shelf equipment is not available. The method which has been proposed (2) suggests causing the fluid and solidified PCM to flow into a separator where the PCM drops would rise to a free surface of the fluid from which they could be removed for conveying to the PCM storage tank. This could be done by a relatively simple mechanism which would require little power. It is estimated that after the necessary development, a mechanism to handle the total flow of 868×10^3 lb/hr of PCM might be produced at a cost of \$100,000.

PCM Containment Tank

The PCM containment tanks are the same for both liquid metal and oil concepts. As discussed in Section 3.2, for fine spherical drops of solid PCM a high packing density can be expected. Consequently, a volume utilization of 95% was assumed for these concepts. For the 148 MWh capacity assuming

only the latent heat (no sensible heat) contributions, 2.04×10^6 kg (4.506×10^6 lb) of PCM occupying 3740 m^3 ($40,200 \text{ ft}^3$) in the liquid state are required. Allowing for a reasonable ullage, a 12.7-m (41.5-ft) diameter tank with height equal to diameter was selected.

The tank wall thickness was sized to the ASME B&PV code, Section VIII. The membrane stress in the tank supports the hydrostatic load. Allowable stress intensities typical for carbon steels were used: 103 MPa (15,000 psi). To take advantage of the fact that the load is hydrostatic, the tank is built up of 1.8-m (6-ft) high plates. Consequently, the wall thickness can vary with height. The results are shown on Table IX-4. The resulting tank weight is 1.347×10^6 lb.

TABLE IX-4

TANK DESIGN FOR PCM DROP CONCEPTS

<u>Course</u>	<u>Height</u>		<u>Plate Thickness</u>	
	<u>m</u>	<u>(ft)</u>	<u>mm</u>	<u>(in)</u>
1 Bottom	1.82	(6)	15.9	(5/8)
2	3.66	(12)	15.9	(5/8)
3	5.46	(18)	12.7	(1/2)
4	7.32	(24)	11.1	(7/16)
5	9.1	(30)	9.5	(3/8)
6	10.9	(36)	6.35	(1/4)
7 Top	12.7	(42)	6.35	(1/4)

Discharge Heat Exchanger for PCM Drop Direct Contact Systems

The discharge heat exchangers in the PCM-drop direct contact systems exchange heat between the oil or liquid-metal intermediate heat transfer fluid and the saturated water at 450°F, to produce saturated steam at that temperature. Only the latent heat of vaporization of the water was considered in the sizing of the heat exchangers.

The heat exchanger for each fluid was sized by calculating the average surface heat transfer coefficients for the boiling water and the fluid, and an overall heat transfer coefficient, for a shell-and-tube heat exchanger in which the steam flows through the tubes.

The film coefficient for the two-phase flow of water in the tubes may be related to the coefficient of the liquid phase flowing alone, by the Lockhart and Martinelli parameter. The film coefficient for the liquid phase is given by the Dittus-Boelter equation. This equation can also be used for the saturated liquid and saturated steam flows. These equations and all associated empirical parameters are presented in Reference (40).

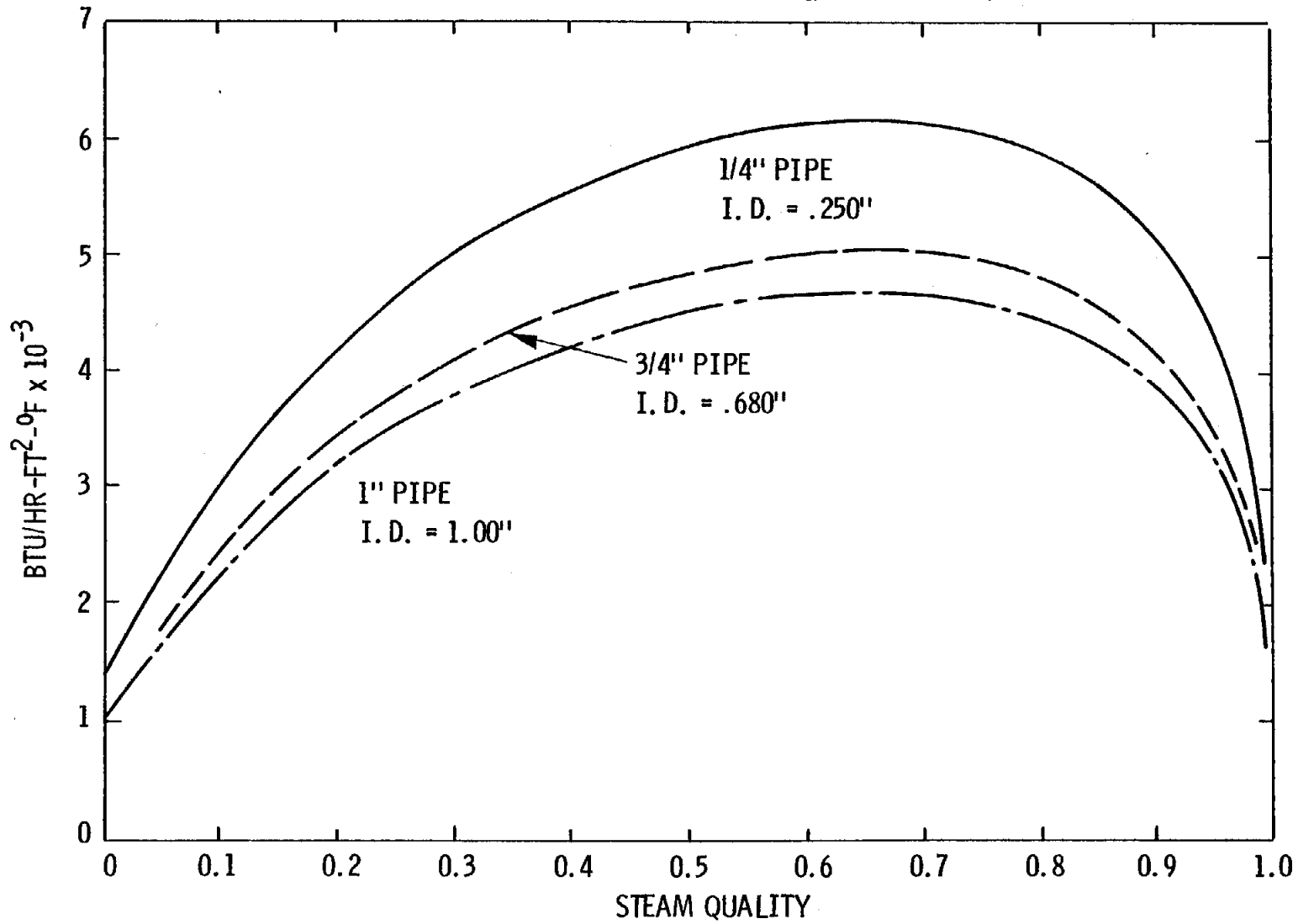
A velocity of 100 ft/sec for the saturated steam was established as a reasonable representative value for steam generators. Based on this, a mass velocity of 3.27×10^5 lbm/hr·ft² is obtained. For this condition, the two phase film coefficient was calculated as a function of steam quality for tube inside diameters of 1.0, 0.680, and 0.250 inches. The results are shown on Figure IX-4. The 0.68-inch tube was taken as the basis for heat exchanger sizing because it is the smallest tube size which would be practical in large heat exchangers. The average coefficient for the 0.680-in-diameter tube is 4075 Btu/hr·ft²·°F.

The shell-side coefficient was estimated by treating the tube bundle as a tube bank, with the tubes in triangular spacing, which minimizes the shell volume and the fluid inventory. A single pass of the fluid through the tube bank was assumed.

Figure IX-4

TWO PHASE HEAT TRANSFER COEFF. - SAT. WATER AT 450°F

$G = 327 \times 10^3 \text{ LB/HR-FT}^2$ (STEAM VEL. = 100 FT/SEC)



The film coefficient for the liquid metal, h_m , was calculated from the Rickard correlation (45).

$$\frac{h_m D}{k_f} = 4.03 + 0.228 \left[\frac{D G_{\max}}{M_f} Pr \right]^{0.67}$$

For the oil (biphenyl), the coefficient, h_o , was determined from (Ref. 45):

$$\frac{h_o D}{k_f} = .33 \left[\frac{D G_{\max}}{\mu_f} Pr \right]^{0.6} Pr^{1/3}$$

In these correlations the characteristic dimension is the tube outer diameter. The maximum value of the mass velocity occurs in the minimum gap between the tubes. Values of 4.68×10^6 lb/hr·ft² and 3.73×10^5 lb/hr·ft² were used for the liquid metal and oil, respectively, reflecting an assumed maximum velocity of 2 ft/sec.

The overall coefficient includes the effect of the steam film, the fluid film, the tube wall, and internal and external fouling resistances.

In the liquid metal case, a thermal resistance for the steam side of 0.001 hr·ft²·°F/Btu was used, and no resistance was used for the metal side because the liquid metal system will be protected from oxidation by an inert or reducing cover gas. The film coefficients are so high in this heat exchanger that the fouling resistance represents about 60% of the total resistance to heat flow.

In the oil system both internal and external fouling resistance were each taken as 0.001. In this case, the total fouling effect is about 60% of the total resistance. If the best boiler water treatment tech-

niques can be applied to the feed water for the heat exchanger, the fouling on the water side could be largely eliminated, with a proportionate decrease in heat exchanger size and cost, and a substantial reduction in the fluid inventory and cost.

The heat transfer area and total length of the 0.75" O.D. tubes is determined from the peak discharge rate (30 MW), the LMTD of the heat exchanger (22.8°F), and the overall heat transfer coefficient calculated above. A triangular array of tubes was used to get the most compact size. Interaction between tube length and number of tubes, the heat exchanger diameter, and the height were determined, to calculate the fluid inventory.

The results for the two fluids are shown on Table IX-5. Table IX-6 summarizes the inventories of the intermediary fluid on the drop heat exchanger, the discharge heat exchanger, and the inter-connecting piping. The latter component was sized to be as tight as could reasonably be expected.

TABLE IX-5

DISCHARGE HEAT EXCHANGER CHARACTERISTICS FOR PCM DROP SYSTEMS

		<u>Pb·Bi Eutectic</u>	<u>Oil, Biphenyl</u>
<u>Tube Side</u> (450 ⁰ F Saturated water, two phase flow in 0.680" I.D. tube)			
G_{max}	(lb/hr·ft ²)	327x10 ³	327x10 ³
V_{max}	(sat. vapor) (ft/sec.)	100	100
h_{tp}	(at max. flow) (Btu/hr·ft ² · ⁰ F)	See Fig.IX-4	See Fig.IX-4
h_{tp}	avg, x=0 to x=1 (Btu/hr·ft ² · ⁰ F)	4075	4075
Surface (inside)	(ft ²)	7.32x10 ³	23.4x10 ³
<u>Tube Bundle</u>			
Number of tubes		2213	8000
Tube length	(ft)	18.7	16.4
Total tubing	(ft)	41.35x10 ³	131x10 ³
Tube O.D.	(inch)	0.75	0.75
Tube pitch	(inch)	1.10	0.90
<u>Shell Side</u>			
Volumetric fluid flow	(gal/min)	22.8x10 ³	16.4x10 ³
h	(Btu/hr·ft ² · ⁰ F)	3530	348
U	(Btu/hr·ft ² · ⁰ F)	614	192
G_{max}	(lb/hr·ft ²)	4.68x10 ⁶	3.73x10 ⁵
<u>Fluid Inventory</u>			
Volume	(ft ³)	187	252
Wt.	(lb)	121x10 ³	13.1x10 ³

TABLE IX-6

HEAT TRANSFER FLUID INVENTORY

	<u>Pb·Bi Eutectic</u>		<u>Oil (Biphenyl)</u>	
	<u>(ft³)</u>	<u>(lbm)</u>	<u>(ft³)</u>	<u>(lbm)</u>
PCM Drop Heat Exchanger	330	215,000	130	6,730
Pipe Volume	253	164,500	182	9,430
Discharge Heat Exchanger	187	121,600	252	13,050

APPENDIX X

Direct Contact Systems Using an Intermediate Heat Transfer Fluid

This concept depends upon the compatibility of the PCM and the intermediary fluid. No data have been found on long-term chemical stability of the PCMs and fluids which meet the requirements of this study. However, short-term tests (1) have shown that a NaOH-NaNO₃ mixture having 8% NaNO₃ did not oxidize a mixture of terphenyls, in the absence of air, at 320°C (608°F). With this background, fluids such as the terphenyls and biphenyl were considered to be possibilities, with the reservation that if this concept were to be selected for development, the compatibility must first be investigated.

For purposes of the present analysis, it was assumed that with any organic fluid, some thermal degradation would occur during the lifetime of the equipment. Therefore, a purification system would remove insolubles and high boiling polymerization products, and vent low boiling products, including water vapor, with makeup as required.

Biphenyl has been thoroughly characterized as a heat transfer fluid for nuclear reactors and power plants (46), including purification systems for removing gases and high-boiling thermal degradation products.

The concept involves elements for which little or no experience is available for guidance in estimating the system cost or design. The solidification of the PCM at the oil-PCM interface is expected to require about five times as much surface as is available over the cross section of factory-fabricated modular tanks of rail-transportable dimensions. The use of a large field-erected tank with height-to-diameter ratios between 0.5 and 1.0 would not improve the situation. It is thought that the surface might be augmented as needed by means of high velocity oil jets impinging on the interface. The physical shape and the size of the solid PCM particles produced at the interface are unpredictable. If the particles are very fine and of very irregular shape, they might settle slowly and form a solid mass with a large

liquid-filled interstitial volume. When the solid mass builds up to the oil interface, no further heat can be withdrawn with the result that the liquid in the interstices cannot be solidified. As shown in Section 3.2, the interstitial volume in a mass of fine irregularly shaped particles can, in some circumstances, be as high as 90% of the total volume. In the present analysis the PCM utilization factor was taken to be 0.58. Before any future development of this concept, these areas would require research.

A characteristic of the concept is that the PCM can store and deliver sensible heat in the liquid phase, but after the liquid has been cooled to the PCM melting point (or the lower end of the solid-liquid range, if any), the PCM mass operates isothermally because solid and liquid co-exist throughout. The PCM cannot be cooled below its melting point and no sensible heat contained in the solid can be delivered.

The charging heat exchanger for both concept variations consists of banks of horizontal finned tubes with a few vertical tubes extending to the top to provide a PCM expansion path during melting. This component is identical to the mechanical-scraper charging heat exchanger, so the calculations are not presented here.

Reflux Oil Intermediate Heat Exchanger

A schematic of this concept is shown on Sketch 4 in Appendix I. The temperature relationship among the components is shown on Figure X-1 where, for simplicity, only the latent heats were considered. In order to have reasonable heat exchanger sizes, the ΔT 's between steam and PCM were split evenly for the oil intermediary. Properties of biphenyl shown on Figure X-2 indicate a slight vacuum operation is required.

The sizing of the reflux oil heat exchanger requires a knowledge of the heat flux which will be obtained when the oil, assumed to be biphenyl, boils on the surface of the PCM, which is solidifying as heat is withdrawn by the oil. No experimental data has been found for this case, nor does any of the commonly used correlations apply. A value which

might be typical of the heat flux for pool boiling of oil is 50,000 Btu/hr.ft² for $\Delta T = 100^\circ\text{F}$ (48). The ΔT has been fixed at 25°F, and therefore the expected heat flux is 12,000 Btu/hr.ft².

Figure X-1
DIRECT CONTACT
REFLUX OIL INTERMEDIATE HX

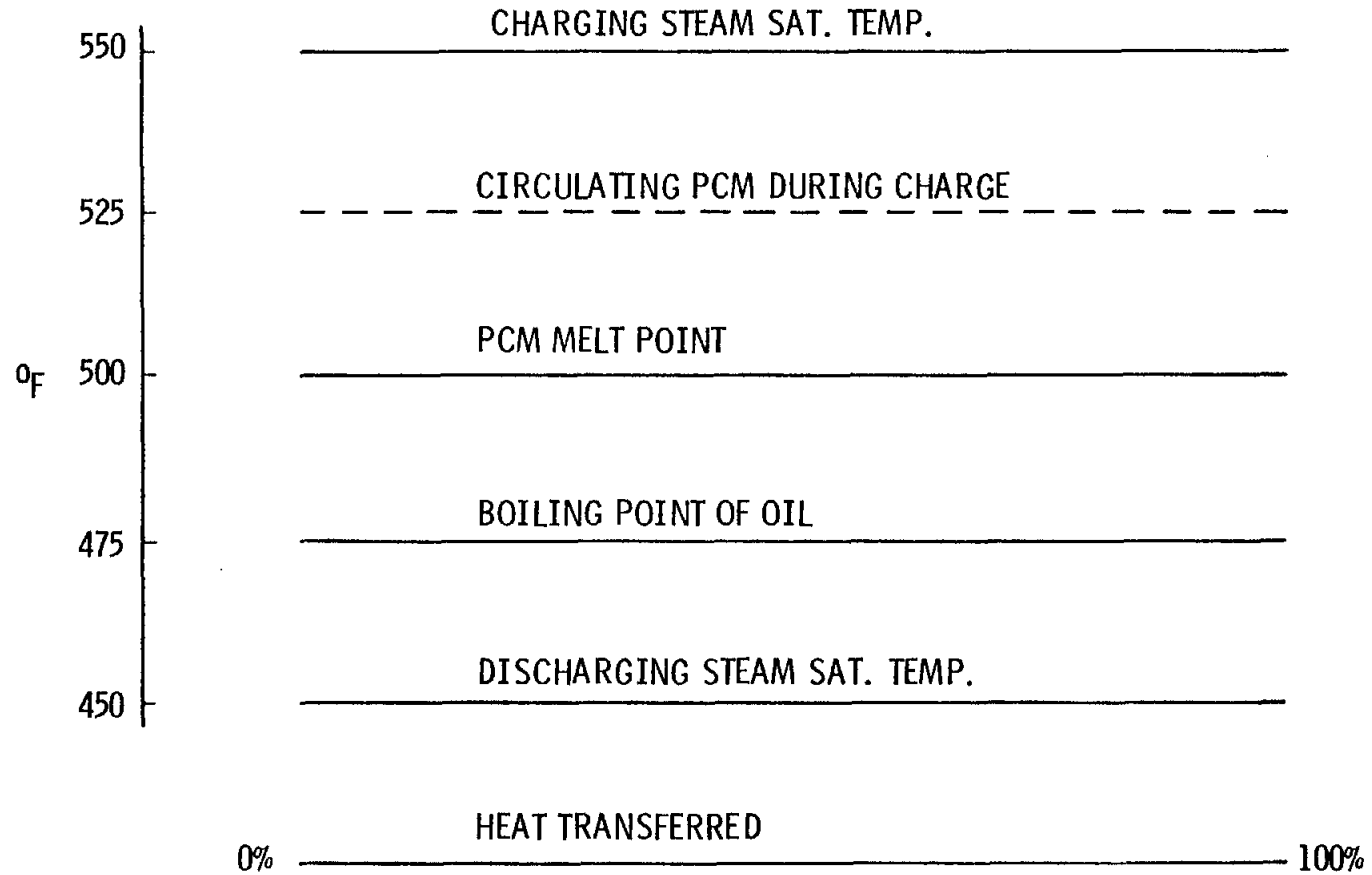
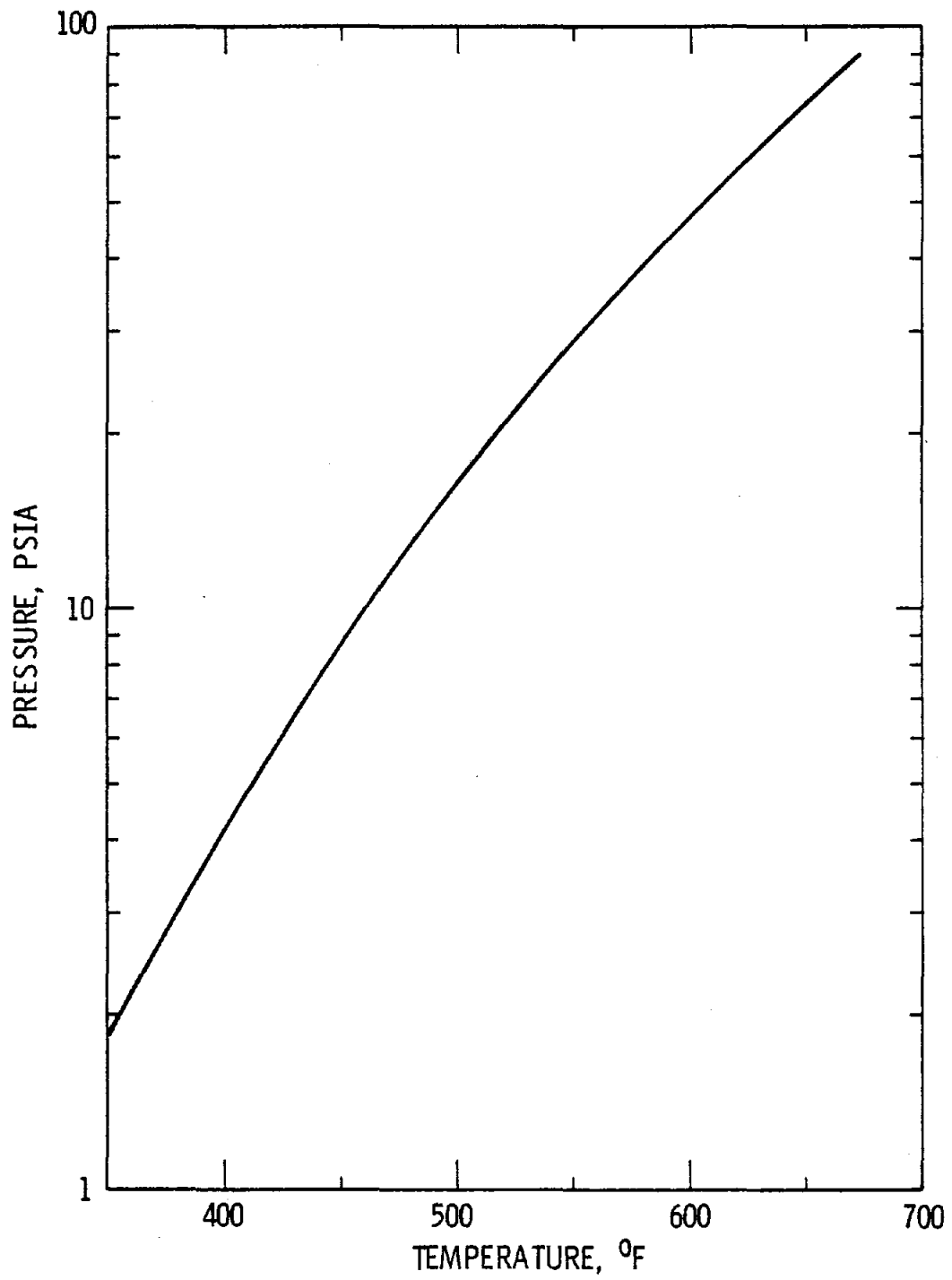


Figure X-2
VAP. PRESS. OF BIPHENYL FROM MONSANTO CHEM. Co.
"ORGANIC COOLANT DATA BOOK" 1958



In the required 10 module tanks, each 13x13x41.8 feet, the available PCM surface is $1.69 \times 10^3 \text{ ft}^2$. To meet the maximum discharge rate of 30 MW ($102.4 \times 10^6 \text{ Btu/hr}$), with a heat flux of 12,000 Btu/hr·ft requires $8.54 \times 10^3 \text{ ft}^2$, or five times that available. The system of high pressure oil jets impinging on the PCM surface is expected to provide the required surface "amplification."

The discharge heat exchanger consists of a tube bank of 3/4" O.D. by 0.680" I.D. tubing. The internal mass flow rate and internal two phase heat transfer coefficient are taken to be the same as for the PCM drop discharge heat exchangers described in Appendix IX.

The coefficient for the condensing oil, h_o , was calculated from the correlation (49)

$$h_o = 0.728 \left[1 + 0.2 \frac{c \Delta T}{h_{fg}} (n-1) \right] \left[\frac{g \rho (\rho - \rho_v) k^3 h_{fg}}{n D \mu \Delta T} \right]^{.25}$$

using properties of Table X-1 for biphenyl, a temperature difference of 25°F between the boiling water and the condensing oil, and $n = 15$ layers of tubes in the tube bank. This yielded the value $h_o = 224 \text{ Btu/hr}\cdot\text{ft}^2\cdot^\circ\text{F}$, which is within the expected range (48).

The overall coefficient of $156 \text{ Btu/hr}\cdot\text{ft}^2\cdot^\circ\text{F}$ was calculated using fouling resistances of $.001 \text{ hr}\cdot\text{ft}^2\cdot^\circ\text{F}/\text{Btu}$ each for the steam and oil sides of the tube, in addition to the film conductances of the steam and oil and the tube wall thermal resistances. The heat transfer surface of $26.2 \times 10^3 \text{ ft}^2$ is required to meet the 30 MW rate through the 25°F ΔT . The corresponding length of 0.75 in tubing is 147,000 feet. This can be arranged in a tube bank of seven layers, which occupies approximately 0.7 feet of height in a modular tank.

Since this system must operate in a slight vacuum, the use of the standard rectangular tanks may be questionable. These banks were designed to lie flat and not upended as in this case. Using them in the

TABLE X-1

PROPERTIES OF BIPHENYL AT 500°F

		<u>Oil</u> <u>(Biphenyl) *</u>
ρ_f	lb/ft ³	51.8
μ_f	lb/hr·ft	.49
Pr		4.82
k_f	Btu/hr·ft·°F	.061
C_p	Btu/lb·°F	.60

* Reference 46

selected orientation is required by the coverage of the discharge heat exchanger. The standard modular tank should, however, provide representative costs. The module dimensions and number of modules were based on the total volume requirements, which were determined to be as follows:

... PCM to store 148 MWh (505×10^6 Btu), at a PCM utilization factor of 0.58 occupies 67.1×10^3 ft³.

... The discharge HX, in a triangular array, with a pitch 1.5 times the diameter occupies 1.12×10^3 ft³.

... A volume of 1.34×10^3 ft³ is allowed to accommodate the oil jets and associated piping.

... The total tankage volume is 70.6×10^3 ft³.

This total volume can be contained in 10 modules, 13'x13' in area and 41.8' in height, which are of a size that can be preassembled and transported by rail.

The oil circulation rate to support the maximum discharge rate of 30 MW is 975.2×10^3 lbm/hr, based on a latent heat of vaporization of 105 Btu/lb. The pumping power, assuming 100 psi pressure drop through the jets, and efficiency of 0.9, is 112 kW (150 hp), an insignificant parasitic loss.

These characteristics are summarized on Table 3.4.7-1 in the main text.

The purification system must remove thermal degradation products such as high and low boiling substances and solids. Purification techniques for organic coolants used in nuclear reactors and power plants can be applied. In addition, the purification system must be capable of removing water which might result from very small leaks in the heat

exchangers, or which might be present initially in the oil. Small concentrations of water cause large increases in the vapor pressure of biphenyl, as shown on Figure 3.4.3-2 of the main text.

Circulating Oil Intermediate Heat Exchanger

The circulating oil system is similar to the reflux oil system with respect to the quantity of PCM, the charge heat exchanger, and the PCM containment tanks. The differences lie in the method of using the oil, and in the discharge heat exchanger. The temperature relationships among the components are shown in the main text, Figure 3.5.2. The oil circulation rate necessary to meet the maximum discharge rate of 30 MW based on a temperature change of 25°F is 6.8×10^6 lb/hr.

The jet agitator system will need a pressure of about 100 psi, which requires 790 kW (1060 hp) for a 90% pumping efficiency. Pump cost is estimated at \$400/horsepower giving a pump cost of \$424,000, plus an allowance of \$25,000 for the piping assembly.

The pressure drop associated with the jets dissipates across the jet orifices, and the high pressure is not felt by the tank.

The discharge heat exchanger consists of a tube bundle of the same dimensions as that used in the PCM drop-oil system described in Appendix IX and listed on Table IX-4. The cost, however, is based on the tube bundle without the shell at \$12/ft², for a cost of \$281,000.

The oil inventory consists of the volume in the space above the PCM when fully charged, plus the change in volume of the PCM at the fully discharged state. The PCM density when liquid is approximately 110 lb/ft³, and 130 lb/ft³ when solid. This accounts for a volume change of 6.0×10^3 ft³. This volume of oil moves in and out of the tanks during a thermal cycle. The volume which remains in the tanks is 2.55×10^3 ft³. The total inventory is 8.55×10^3 ft³, or 443×10^3 lb; at \$1.45/lb, the oil inventory cost is \$642,000.

The PCM tankage requirement is the same as for the reflux system, viz., ten modules of square cross-section, 13' x 13' in area and 41.8 feet in height. A similar tank 36 feet in height is required as an oil reservoir.

APPENDIX XI

MECHANICAL SCRAPER SYSTEMS

This appendix presents the basic sizing calculation results for both mechanical scraper systems: the vertical drum with external rotating scraper and the horizontal rotating drum with fixed scrapers. These two concepts span the range of possible design configurations. The major features of these designs are the containment tank, the scraper modules which serve as the discharging heat exchanger, and the charging heat exchanger. The scraper modules include the drums, the scrapers and the associated driving motors and linkages. The horizontal rotating drum system also requires a PCM pump. The designs are shown on Sketches 5 and 6 in Appendix I.

Both mechanical concepts best employ a rectangular tank configuration, for volume utilization and mechanical operation. The height of the tank in the vertical scraper concept is limited to a reasonable limit on the height of the scraper module. A rectangular cross section would provide the best distribution per scraper module. The horizontal scraper is best with a rectangular cross section for uniformity of volume utilization. The width of the tank is limited by the deflection of the drum. Thus, a rectangular containment tank was selected. The tank was selected as a reference for the study and was also employed with the tube intensive concept, the microencapsulation concept using a porous carrier, and the initial design of the direct contact heat exchanger systems.

Containment Tanks

The outer envelope for shop-fabricable, rail-shippable tank was established as 4 m (13 ft) wide and 12 m (40 ft) long (see Section 3.1). The hydrostatic head of the PCM loads the walls of the tank. The walls are reinforced with vertical tee sections which are 20 cm (8 in) deep, 15 cm (6 in) wide, and spaced 61 cm (24 in) around the tank on the insides. The walls and bottom are made from 12.7 mm (0.5 in) carbon steel plate. The tank top is 6.35 mm (0.25 in)-thick plate. In the case of the

horizontal mechanical scraper concept, tee sections welded to the cover plate position the fixed scraper to the rotating drum.

The sizing of the structural components conform to Section VIII of the ASME B&PV code. Allowable stress intensities were taken from Table UC-S-23 for carbon steel. Each section of the tank wall was modeled as an unequally wide flange beam. The maximum bending in the beam is related to the hydrostatic loading (37) and from this, the stress on the beam is determined. A 1.14 shape factor is used to relate the bending stress allowable to the tensile allowable in the code. The thickness of the plate is established to sustain the bending at the center of the plate between two tee sections.

The tank is set on Foamglas insulation which has a compressive strength of 690 kPa (100 psia) (39). The combined weight of the tank, internals, and PCM exerts a distributed load of approximately 69 kPa (10 psi) for an uneven support of the tank. The roof of the tank can sustain a 3 kPa (60 lb/ft²) load as per the AISC code.

The amount of PCM and number of tanks required depend directly on the volume utilization. Honeywell (34) in their mechanical scraper design effort experimentally determined a heat recovery factor of 60%. This value reflects both a volume utilization and the effective latent heat for the off-eutectic salt mixture. The operation of the Honeywell scraper involved only partially frozen PCM in order to maintain a more easily removed slush from the scraped surfaces and to avoid freezing of the scraper, a common scraper problem. This mode of operation is used for the current application; an off-eutectic mixture sodium hydroxide/sodium nitrate is employed. A very optimistic 90% volume utilization was used for the initial sizing. This is judged to be very high; 75% is a more realistic value. However, the 90% factor will yield the most optimistic component sizes and serves as an upper bound. For the 60% recovery factor, 3.23×10^6 kg (7.13×10^6 lb) of PCM occupying 1812 m^3 ($64,000 \text{ ft}^3$) in the liquid phase is required to provide the 148 MWh capacity. With the upper bound on the utilization, 2.13×10^6 kg (4.7×10^6 lb) of PCM occupying 1190 m^3 ($42,000 \text{ ft}^3$) in the liquid phase is required.

The available volume for each of the modular containment tanks is 182 m^3 ($6,420 \text{ ft}^3$). This allows for the volume occupied by the internal tank structure, for the heat transfer equipment, and for a minimum ullage 15 cm (6 in) high. Consequently, the number of tanks required to contain the PCM is 10 for the representative heat recovery factor and 7 for the very optimistic utilization value.

Discharging Heat Exchanger

One of the main problems with latent heat TES systems is that the solidification of the PCM on the heat transfer surface greatly inhibits the heat transfer. Consequently, a large amount of exchanger surface is required. The scraper concepts physically remove this insulating layer of PCM and maintain high heat transfer rates throughout the discharge process. The discharge heat exchanger is composed of scraper modules, each of which is a 15 cm (6 in)-diameter drum with a 6.35 mm (0.25 in)-thick wall through which the discharging steam flows. In the case of the vertical scraper concept, the charging steam is also passed through the scraper module.

A heat transfer surface area requirement of 470 m^2 ($5,100 \text{ ft}^2$) was estimated for the discharge process. This is based on an overall heat transfer coefficient of $2.27 \text{ kW/m}^2 \cdot ^\circ\text{C}$ ($400 \text{ Btu/hr} \cdot \text{ft}^2 \cdot ^\circ\text{F}$) and a 28°C (50°F) temperature difference between the steam and the PCM. The overall thermal conductance reflects boiling steam within the drum, heat conduction through the carbon steel drum wall, and heat conduction through a small layer of PCM which exists because of clearance requirements and average layer buildup between sweeps of the scraper. The effort reported in Reference (3) employed a slightly more optimistic value of $2.84 \text{ kW/m}^2 \cdot ^\circ\text{C}$ ($500 \text{ Btu/hr} \cdot \text{ft}^2 \cdot ^\circ\text{F}$). For the required heat transfer area 300 scraper modules are needed. This applies to both vertical and horizontal concepts.

The power required to turn the scrapers or augers was calculated first on the basis of the motor size in the Honeywell (34) design. Roughly, 1.7 kW/m^2 ($.21 \text{ hp/ft}^2$) of heat transfer area would be required to turn the scrapers or augers, or a total of 798 kW (1070 hp) for the current application. For a scraper operation of approximately 5 hr per day, this parasitic energy approximately 5% of the rated capacity.

An additional calculation was performed, based on the shear force of 550 kPa (80 psi) (3) required to scrape the PCM from the surface of the drum during optimum operating conditions. A PCM rate of solidification of 0.13 mm/s (.005 in/s) and a 60 RPM drum or scraper speed were assumed. The power required to rotate the scrapers/augers for the entire system is 64 kW (86 hp) or 0.14 kW/m^2 . ($.017 \text{ hp/ft}^2$). The former value was used for estimating equipment and parasitic power requirements.

The power required to operate the liquid pump for the horizontal scraper concept was sized by accounting for the head difference of the PCM and the pressure drop in the piping. This power requirement was almost negligible, 4.3 kW (5.8 hp) for the entire system.

Charging Heat Exchanger

The mechanical scraper concept reduces the heat transfer requirement for discharge to such a low level that the charging process is controlling. For the horizontal scraper, the scraper cannot provide any charging since it is located outside the PCM. The vertical scraper does provide some charging, approximately 17%. A finned tube heat exchanger was selected for the charging heat exchanger. The charging steam flows within a 25 mm (1") Scd 40 pipe with 3.2 mm (0.125") thick fins, 12.7 mm (0.5") high. The spacing between fins is 32 mm (0.125").

The heat transfer rate per unit length of finned tube is estimated at 2.28 kW/m (2380 Btu/hr·ft). This is based on 28°C (50°F) temperature difference between steam and PCM, and an overall heat transfer coefficient including condensing steam within the tubes, tube wall thermal resistance, natural circulation between the liquid PCM and the solid-liquid interface. Standard film coefficients and methods for handling extended surface heat transfer were taken from Reference (49). For the peak charging rate of 30 MW, 13100 m (42,900 ft) of tubing is required, providing 3840 m² (41,300 ft²) of heat transfer surface, including the area of the fins. This must be used for the horizontal scraper concept.

The vertical scraper concept has a reduced requirement since the submerged scrapers provide heat transfer. The natural convection from the scraper wall controls the heat transfer between the condensing steam and the PCM. The 474 m^2 ($5,100 \text{ ft}^2$) of scraper area provides 5 MW of the required charging rate. Thus, the charging heat exchanger must be 10,800 m (35,400 ft) long with total heat transfer area of $317,000 \text{ m}^2$ ($34,300 \text{ ft}^2$) to provide the remaining 25 MW of the peak charging rate design target.

APPENDIX XII
OIL/ROCK SENSIBLE HEAT STORAGE BENCHMARK

The design and sizing of the oil/rock storage system is described in this appendix. The basic approach and assumptions used are described below. A general description of the system and component sizes are given in the body of the report and will not be repeated here. The system configuration is shown on Figure 3.5-1. The following assumptions and design parameters were used:

1. The system is based on the Barstow oil/rock system but resized to temperature range and storage requirements given in Section 3.1.
2. A single shell-and-tube heat exchanger is used for both charging and discharging.
3. Oil/rock volume fractions are 0.25, and 0.75 (50), respectively.
4. Maximum oil velocity is 3.96m/sec (13 ft/sec) (50).
5. There is a single field erected storage tank with a 0.67 aspect ratio (50).
6. A system total pressure drop of .24 MPa (35 psi) is assumed.
7. An overall heat transfer coefficient of $0.568 \text{ kW/m}^2 \cdot ^\circ\text{C}$ ($100 \text{ Btu/hr} \cdot \text{ft}^2 \cdot ^\circ\text{F}$) is used. This value is conservative and is based on information in Reference (50).
8. A pump/motor efficiency of 85% is assumed as a representative value.
9. 122 m (400 feet) of schedule 40 pipe is assumed for a reasonable representation.
10. Two utilization factors are considered, 60% and 80%, to bound the system sizes.

11. Heat exchange pinch points of 5.6°C (10°F), 8.3°C (14°F), and 13.9°C (25°F) are considered. (See Figure 3.5-2.)

Pertinent design data and approach to sizing are summarized on Table XII-1 and are briefly described below.

1. Heat Exchanger

Based on a charging/discharging rate of 30 Mwt and the given overall heat transfer coefficient and temperature pinch points, the total heat transfer surface area is calculated. Since these sizing calculations are used in defining a cost benchmark, detailed design of the heat exchanger and other components was not undertaken.

As the pinch point increases, the required heat transfer surface area decreases. However, for a given storage capacity this will result in the need for a larger storage volume. Thus, one is presented with a trade-off between heat exchanger area and storage volume. This issue is resolved by comparing the cost of the two. From a cost standpoint, the system using the largest heat exchanger and smallest storage volume will be the cheapest. A 5.6°C (10°F) pinch point is judged to be the lowest reasonably practicable. The heat exchanger and storage tank size as a function of pinch point is given on Table XII-2.

2. Storage Tank

Based on the inlet and exit conditions on the Caloria side of the heat exchanger and the physical properties of Caloria and rock (see Table XII-1), the storage volume required for 148 MWh is calculated. To take into account the efficiency of this storage system, two utilization factors are considered: 0.6 and 0.8. The utilization factor is defined as the ratio of the theoretical storage volume required to the actual storage volume required. A utilization factor of 0.8 is considered optimistic; 0.6 is considered to be conservative. These values were selected based on a review of Reference (50). Tank dimensions corresponding to the minimum costs are: for the 60% UF, a 24.7 m (81 ft)

diameter and 16.8 m (55 ft) height; and a 22.5 m (74 ft) diameter and 15.2 m (50 ft) height for the 80% utilization.

The tank wall thickness is sized to Section VIII of the ASME B&PV Code. Allowable membrane stress intensities were back calculated from the Barstow tank design presented in Reference (50). The nature of the hydrostatic load allows a reduction in required wall thickness up the height of the tank. To take advantage of this, the tank is constructed of 1.8 m (6 ft)-high plate steel. Consequently, the allowable wall thickness can vary accordingly. The results are shown on Table XII-3. The tank weights are 504,000 lb and 438,000 lb for the 60% and 80% UF, respectively.

3. Piping

The mass flow rate of Caloria was determined from the heat exchanger steam and oil conditions. Using this information along with a maximum Caloria flow rate of 3.9 m/sec. (13 ft/sec), the piping inner diameter was determined. This value was then increased to the nearest schedule 40 pipe size.

4. Pump

The pump/motor is based on an overall system ΔP of .24 MPa (35 psi). A review of Reference (50) revealed that the largest contributor to pressure drop is the heat exchanger, which contributes approximately .14 MPa (20 psi). Therefore, a total system pressure drop of .24 MPa (35 psi) is believed to be representative.

TABLE XII-1
OIL/ROCK DESIGN DATA

1. Heat Exchanger

- Overall Heat Transfer Coeff. = $0.578 \text{ kW/m}^2 \cdot ^\circ\text{C}$
($100 \text{ Btu/hr}\cdot\text{ft}^2\cdot^\circ\text{F}$)
- 3 Pinch Points Examined - 5.6, 8.3, and 13.9°C (10, 15, and 25°F)
- Charging/discharging Rate - 30 Mwt
- Steam Conditions
 - . Charging: Sat. Vapor to Sat. Liquid at 7.20 MPa, 287.8°C
(1045 psi, 440°F)
 - . Discharging: Sat. Liquid to Sat. Vapor at 2.92 MPa, 232.2°C
(423 psi, 450°F)
- Log Mean Temp. Differences Based on Oil/Steam Temperature Profiles Shown on Figure 3.5-2.

2. Storage Tank

- 0.67 Aspect Ratio Used
- Oil/Rock Volume Fractions - 0.25/0.75
- Caloria Properties: $C_p = 2.76 \text{ kJ/kg}\cdot^\circ\text{C}$ ($0.66 \text{ Btu/lb}\cdot^\circ\text{F}$)
 $\rho = 6.90 \text{ kg/m}^3$ (43 lb/ft^3)
- Rock Properties: $C_p = 1.00 \text{ kJ/kg}\cdot^\circ\text{C}$ ($0.24 \text{ Btu/lb}\cdot^\circ\text{F}$)
 $\rho = 2660 \text{ kg/m}^3$ (166 lb/ft^3)
- Utilization Factors: 60% and 80%
- Tank Thickness Requirements Described in Table XII-3

3. Piping

- 400 ft of Sch. 40 Piping
- Pipe Diameter Based on Caloria Velocity Limit of 3.96 m/sec (13 ft/sec)
- Pipe Diameter Calculated, then Increased to Nearest Standard Size

4. Pump/Motor

- 85% Efficiency Assumed
- System $\Delta P = 0.24 \text{ MPa}$ (35 psi) Assumed

TABLE XII-2
HEAT EXCHANGER AND STORAGE VOLUME SIZE AS A FUNCTION OF PINCH POINT

<u>Pinch Point</u> <u>°C(°F)</u>	<u>Heat Transfer Area</u> <u>m²(ft²)</u>	<u>Storage Volume by</u> <u>Utilization Factor</u>	
		<u>60%</u> <u>m³(ft³)</u>	<u>80%</u> <u>m³(ft³)</u>
5.6 (10)	2612 (28,120)	8058(284,500)	6043(213,400)
8.3 (15)	2738 (23,600)	9709(325,200)	6907(243,900)
13.9 (25)	2067 (22,250)	12,890(455,200)	9669(341,400)

TABLE XII-3

A. OIL/ROCK CONTAINMENT TANK, 60% UF

<u>Course</u>	<u>Height</u>		<u>Plate Thickness</u>	
	<u>m</u>	<u>ft</u>	<u>cm</u>	<u>in</u>
1 Bottom	1.82	(6)	38.1	(1 1/2)
2	3.66	(12)	33.3	(1 5/16)
3	5.46	(18)	30.2	(1 3/16)
4	7.32	(24)	25.4	(1)
5	9.1	(30)	20.6	(13/16)
6	10.9	(36)	15.9	(5/8)
7	12.7	(42)	12.7	(1/2)
8	14.6	(48)	11.1	(7/16)
9 Top	16.68	(55)	6.35	(1/4)

B. OIL/ROCK CONTAINMENT TANK, 80% UF

<u>Course</u>	<u>Height</u>		<u>Plate Thickness</u>	
	<u>m</u>	<u>ft</u>	<u>mm</u>	<u>in</u>
1 Bottom	.61	(2)	31.7	(1 1/4)
2	2.4	(8)	28.6	(1 1/8)
3	4.3	(14)	23.8	(1 5/16)
4	6.1	(20)	20.6	(13/16)
5	7.9	(26)	15.9	(5/8)
6	9.7	(32)	12.7	(1/2)
7	11.6	(38)	11.1	(7/16)
8	13.4	(44)	6.35	(1/4)
9 Top	15.2	(50)	6.35	(1/4)

UNLIMITED RELEASE

INITIAL DISTRIBUTION:

Division of Thermal and Mechanical Energy Storage Systems
U.S. Department of Energy
MS 6B025 Room 1G-100
Forrestal Building
Washington, D. C. 20585
Attn: M. Gurevich
S. Strauch
J. H. Swisher

Division of Solar Thermal Energy Systems
U.S. Department of Energy
600 E Street N.W., Room 419
Washington, D.C. 20585
Attn: G. W. Braun
K. Cherian
M. U. Gutstein
J. E. Rannels

Dr. Maxine Savitz
Deputy Asst. Secretary for Conservation
Conservation and Renewable Energy
U.S. Department of Energy, CE-10
1000 Independence Avenue, SW
Washington, D. C. 20585

Special Programs Division
Albuquerque Operations Office
U.S. Department of Energy
P. O. Box 5400
Albuquerque, NM 87115
Attn: D. Krenz
D. Plymale

San Francisco Operations Office
U.S. Department of Energy
1333 Broadway
Oakland, CA 94612
Attn: D. Elliott
R. W. Hughey

Aerospace Corporation
2350 El Segundo Blvd.
El Segundo, CA 90009
Attn: P. Mathur
L. R. Sitney

Babcock and Wilcox Company
P. O. Box 1269
Lynchburg, VA 24505
Attn: R. Wright

C. Grosskreutz
Black & Veatch
P. O. Box 8405
Kansas City, MO 64114

Comstock & Wescott, Inc.
Cambridge, MA 02138
Attn: B. M. Cohen
R. E. Rice

E. Y. Lam
Bechtel National, Inc.
P. O. Box 3965
50 Beale
San Francisco, CA 94119

W. Moen
Boeing Engineering and Construction Co.
P. O. Box 3707
Seattle, WA 98124

Combustion Engineering
1000 Prospect Hill Road
Windsor, CT 06095
Attn: G. Allen (2)
G. di Lauro (2)

Electric Power Research Institute
P. O. Box 10412
3412 Hillview Ave.
Palo Alto, CA 94303
Attn: J. Bigger
T. R. Schneider

M. Nadler
Solar Thermal Systems
Exxon Enterprises, Inc.
P. O. Box 592
Florham Park, NJ 07932

R. J. Zoschak
Foster Wheeler Corporation
12 Peach Tree Hill Road
Livingston, NJ 07039

S. A. Schartz
General Electric Company
One River Road
Schenectady, NY 12345

J. Alario
Grumman Aerospace Corporation
Bethpage, NY 11714

J. J. Jimeney
Gibbs & Hill, Inc.
393 Seventh Avenue
New York, NY 10001

Jet Propulsion Laboratory
4800 Oak Grove Dr.
Pasadena, CA 91103
Attn: J. Becker
R. Manvi

F. L. Harris
Kaiser Engineers
P. O. Box 23210
Oakland, CA 94623

Martin Marietta Corporation
Box 179
Denver, CO 80201
Attn: T. Heaton
T. Tracey

R. P. Dawson
McDonnell Douglas
5301 Bolsa Ave.
Huntington Beach, CA 92647

Solar Energy Research Institute
1536 Cole Blvd.
Golden, CO 80401
Attn: R. Copeland
B. P. Gupta
R. Ortiz (Library)
C. Wyman

M. Sparks, 1
A. Narath, 4000; Attn: J. H. Scott, 4700
G. E. Brandvold, 4710
T. B. Cook, 8000; Attn: D. M. Olson, 8100
A. N. Blackwell, 8200

W. E. Alzheimer, 8120
B. F. Murphey, 8300; Attn: D. M. Shuster, 8310
G. W. Anderson, 8330
W. Bauer, 8340

R. L. Rinne, 8320; Attn: C. T. Yokomizo, 8326
L. Gutierrez, 8400; Attn: R. A. Baroody, 8410
R. C. Wayne, 8430
D. E. Gregson, 8440
C. M. Tapp, 8460

C. S. Selvage, 8450
P. J. Eicker, 8451
A. C. Skinrood, 8452
S. E. Faas, 8453 (17)
C. T. Schafer, 8453

W. G. Wilson, 8453
Publications Division, 8265, for TIC (27)
Publications Division, 8265/Technical Library Processes Division, 3141
Technical Library Processes Division, 3141 (3)
M. A. Pound, 8214, for Central Technical Files (3)